Dear Sir/Madam

Following my email regarding The Wildlife Trusts response to the Examiner's questions, please find attached the following papers referenced in our response:

- Reference 5: Lucke, K., U. Seibert, P.A. Lepper and M-A. Blanchet. 2009. Temporary shift in masked hearing thresholds in a harbour porpoise (Phocoena phocoena) after exposure to seismic airgun stimuli. Journal of the Acoustical Society of America, 125:4060 – 4070
- Reference 6: Faulkner, R.C., Farcas, A. & Merchant, N.D.(2018). Guiding principles for assessing the impact of underwater noise. Journal of Applied Ecology. 1–6.

In addition, the following document was also request which I have attached (Q2.2.71):

- Heinänen, S. & Skov, H 2015. 'The identification of discrete and persistent areas of relatively high harbour porpoise density in the wider UK marine area'. JNCC Report No.544 JNCC, Peterborough

Kind regards

Tania

Tania Davey
Living Seas Sustainable Development Officer
The Wildlife Trusts
Tel: 01507 528388

Banovallum House
Manor House Street
Horncastle
Lincolnshire
LN9 5HF

Stay in touch with The Wildlife Trusts across the UK. **Find us on our website, Twitter, Facebook and Instagram**
Royal Society of Wildlife Trusts, The Kiln, Waterside, Mather Road, Newark, Nottinghamshire NG24 1WT. Registered Charity Number 207238

PRACTITIONER'S PERSPECTIVE

Journal of Applied Ecology BRITISH ECOLOGICAL SOCIETY

Guiding principles for assessing the impact of underwater noise

Rebecca C. Faulkner [iD] | Adrian Farcas [iD] | Nathan D. Merchant [iD]

Noise & Bioacoustics Team, Cefas, Lowestoft, Suffolk, UK

Correspondence
Rebecca C. Faulkner
Email: rebecca.faulkner@cefas.co.uk

Handling Editor: Manuela González-Suárez

1 | INTRODUCTION

Underwater noise pollution poses a global threat to marine life and is a growing concern for policymakers and environmental managers. Evidence is mounting of noise-induced habitat loss, heightened physiological stress, masking of biologically important sound (e.g. for communication, predator/prey detection), auditory injury, and in extreme cases, direct or indirect mortality (Popper et al., 2014; Southall et al., 2007). Initial studies focused on charismatic megafauna (particularly marine mammals), but in recent years effects have been discovered in other taxa and at lower trophic levels, including various fish species (Popper et al., 2014), functionally important marine crustaceans (Solan et al., 2016) and zooplankton (McCauley et al., 2017).

Projected growth in the blue economy is expected to bring an expansion in noise-generating activities, notably the construction of offshore wind turbines and other marine infrastructure, geophysical surveys using seismic airguns or sub-bottom profilers, sonar usage and vessel traffic. With increasing awareness of the potential cumulative impact of these and other activities on marine ecosystems, managers are faced with tough choices over how best to alleviate pressure on the marine environment from multiple stressors and industrial sectors. Unlike other marine pollutants such as microplastics or persistent organic pollutants, underwater noise is ephemeral and quickly disperses in the environment. If effective, interventions to reduce noise pollution could lead to a rapid easing of this pressure on acoustically sensitive organisms.

Current measures to manage underwater noise pollution largely involve requiring environmental impact assessments (EIAs) for major inshore and offshore projects, in accordance with legislation for protected species or habitats (e.g. EU Habitats Directive, US Marine Mammal Protection Act). If acoustically sensitive species may be present and potentially harmful noise levels are expected, modelling is carried out to estimate the possible extent of adverse effects. On this basis, regulators may grant or decline consent, or require additional mitigatory action to be taken. However, many EIAs for underwater noise do not apply scientifically credible methods, and regulators often lack the expertise to critically assess consent applications (Farcas, Thompson, & Merchant, 2016). Furthermore, while in some northern European countries noise abatement technologies are being routinely deployed (e.g. for pile driving of offshore wind farms in Germany, Denmark, Norway, Sweden and the Netherlands), in other jurisdictions it is rare for the effect of reducing technologies to be assessed (and consequently recommended or required as a condition of consent), and the consideration of cumulative effects remains inadequate (Willsteed, Gill, Birchenough, & Jude, 2017; Wright & Kyhn, 2015).

Our purpose in this article is to set out clear guiding principles for assessing the impact of underwater noise, providing developers, regulators and policymakers with a robust, science-based framework to address this emerging threat. Based on our experience of advising these stakeholders and of conducting assessments, we identify shortcomings in current practice (and suggest remedies), and propose concrete steps to improve the compatibility of individual EIAs with cumulative effects
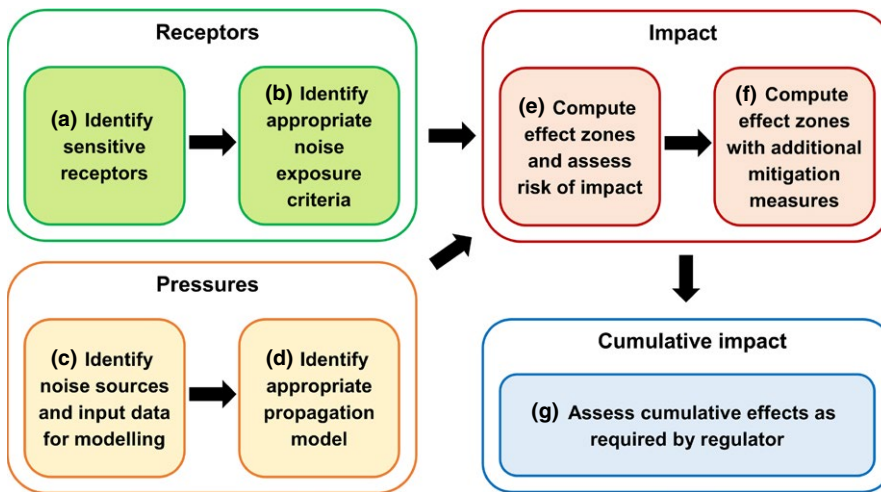
FIGURE 1 Proposed EIA workflow for underwater noise. Each stage is addressed in a corresponding section in the text [Colour figure can be viewed at wileyonlinelibrary.com]

assessments. We also promote an adaptive approach to EIA which enables regulators to consider the benefits of additional noise reduction measures, rather than the assessment being presented as a fait accompli. Our aim is to encourage more rigorous and informative assessments, and to help orient newcomers to this rapidly evolving area.

2 | THE EIA PROCESS

Each stage in the EIA process for underwater noise (Figure 1) involves making choices which critically affect the outcome of the assessment. In summary, acoustically sensitive species (receptors) are first "scoped in" to the assessment (Figure 1a), and corresponding noise exposure criteria are identified which specify thresholds for different types of effect (Figure 1b). Then, significant noise sources from the project are scoped in (Figure 1c), and used to derive input parameters for a noise propagation model which predicts the extent and magnitude of noise levels at the site (Figure 1d). "Effect zones" are then derived by combining the noise model predictions with the noise exposure criteria (Figure 1e), yielding predicted areas where the thresholds for different effects are exceeded. Though seldom done in practice, the risk reduction achieved by applying additional noise reduction technologies may then be modelled (Figure 1f), and the developer may be required to lead or participate in a cumulative effects assessment which includes other planned developments (Figure 1g). In the following sections, we discuss the challenges and pitfalls of the EIA process at each stage, and make recommendations for best practice.

2.1 | Receptors

2.1.1 | Identify sensitive receptors

The first step is to identify receptors that have the potential to be affected by anthropogenic noise (Figure 1a). Detailed knowledge is required about the project area, including the spatial and temporal distribution of species and their seasonal sensitivities (e.g. known spawning and nursery grounds or migratory routes). Receptors

that are "scoped in" should include acoustically sensitive species protected under environmental legislation and other relevant species (e.g. identified as important for conservation, ecological, or economic reasons). Although many EIAs primarily focus on marine mammals and (to a lesser extent) fish and sea turtles, marine crustaceans and elasmobranchs are also sensitive to noise and vibration, and should be scoped in where relevant (Hawkins & Popper, 2017). Information on acoustic sensitivity should be derived from the scientific literature to identify at-risk species.

In considering species sensitivity to sound, it is important to note that sound has two components: sound pressure and particle motion. Similarly to other mammals, marine mammals primarily sense sound pressure. Although some fish species are able to detect sound pressure indirectly, fish and aquatic invertebrates primarily sense particle motion (Nedelec, Campbell, Radford, Simpson, & Merchant, 2016). At present, there are no noise exposure criteria for particle motion, and current criteria (even for species which only sense particle motion) are based solely on sound pressure (Popper et al., 2014). Furthermore, the modelling of particle motion is not common practice and warrants further research (Farcas et al., 2016). As such, the scope for including particle motion in routine assessments is currently limited, although instrumentation and techniques for particle motion measurement and analysis are becoming more widely available (Nedelec et al., 2016).

2.1.2 | Identify appropriate noise exposure criteria

The next step is to identify appropriate noise exposure criteria (also termed impact criteria or noise thresholds ; Figure 1b). Such criteria define sound levels at which various severities of response are expected, e.g. mortality, Permanent Threshold Shift (PTS; permanent loss of hearing sensitivity) and Temporary Threshold Shift (TTS; e.g. Southall et al., 2007; Lucke, Siebert, Lepper, & Blanchet, 2009; Popper et al., 2014; National Marine Fisheries Service, 2016). Criteria for marine mammals typically require the application of a frequency weighting to account for the frequency sensitivity of hearing for the species or species group (National Marine Fisheries Service, 2016; Southall et al., 2007; Tougaard, Wright, & Madsen, 2015).

In selecting noise exposure criteria, assessments should refer to the latest set of widely applied and peer-reviewed criteria available. For example, currently the most relevant marine mammal criteria are those developed by the U.S. National Oceanic and Atmospheric Administration (NOAA) to reflect recent advances in the field (National Marine Fisheries Service, 2016). These provide acoustical thresholds for the onset of TTS and PTS in marine mammals in response to impulsive and continuous (non-impulsive) sound. At present, the most relevant criteria for fish are those published by Popper et al. (2014). These criteria provide quantitative thresholds for TTS, recoverable injury and mortality in fish in response to several impulsive sound sources, and qualitative guidance for continuous sources. There is currently insufficient data to establish noise criteria for marine invertebrates (Popper et al., 2014). However, studies conducted thus far have revealed a range of negative effects from noise (e.g. Solan et al., 2016), and assessments should draw on this literature where relevant.

While these noise exposure criteria provide thresholds for auditory impairment, they do not quantitatively address behavioural responses. Behavioural effects are particularly difficult to assess, since they are highly dependent on behavioural context (Ellison, Southall, Clark, & Frankel, 2012; Popper et al., 2014) and responses may not scale with received sound level (Gomez et al., 2016). Consequently, there is considerable uncertainty in assessing the risk of behavioural responses, and the application of simplistic sound level thresholds for behaviour should be avoided. Recent studies have considered more sophisticated approaches to quantify the risk of behavioural responses, for example through dual criteria based on dose-response curves for proximity to the sound source and received sound level (Dunlop et al., 2017). Approaches based directly on the "distance of effect" reported for insitu behavioural studies (e.g. Merchant, Faulkner, & Martinez, 2017) can also be used as an empirical estimate of the risk of behavioural responses (Gomez et al., 2016), provided that the sound level of the noise source in the cited study is not substantially exceeded in the assessment scenario.

One common pitfall in the application of noise exposure criteria is inconsistency between the acoustic metric modelled to predict risk and the acoustic metric defining the exposure threshold (and auditory weighting if applicable). Impulsive noise criteria are generally defined using zero-to-peak sound pressure level (SPL), peak-to-peak SPL or cumulative sound exposure level (SEL), while non-impulsive criteria use cumulative SEL or the rms (root mean square) SPL. Since it is not possible to convert directly between these units, it is critical that predictions of noise levels arising from the activity are made using the same units as the threshold to be applied.

2.2 | Pressures

2.2.1 | Identify noise sources and input data for modelling

To assess the validity of noise exposure predictions made using modelling, regulators need to know that: (i) all relevant noise sources have been scoped in; (ii) appropriate source levels for these noise sources have been estimated using units which are consistent with the threshold criteria; and (iii) sufficient and appropriate data are available to parameterise the noise propagation model.

When identifying which noise sources should be scoped in, all potential sources should initially be considered. These include lower intensity noise sources, increased vessel activity, dredging and drilling. If these are subsequently scoped out, clear justification should be provided based on published literature, such as source levels for the activities and acoustic sensitivities of the receptors.

Once the source(s) have been identified, the predicted source level(s) should be stated, providing detail of how the source level was derived (i.e. from published literature or using a source model), and any associated uncertainty. As highlighted in section 2.1.2, the source level should be expressed using the same acoustical metric as the noise exposure criteria.

In addition to the source level, evidence of appropriate environmental data for the model is required, including the bathymetry, sediment characteristics of the seabed, sea surface and water column properties, and ambient noise levels. Where possible, uncertainty in these parameters should be incorporated into the assessment. Inadequate input data can result in misleading noise exposure predictions; these factors are considered in more detail in Farcas et al. (2016).

2.2.2 | Identify appropriate propagation model

Many sound propagation loss models are available, ranging from sophisticated numerical models to simplistic models based on spreading laws. No single model is applicable to all environments and acoustic frequencies (see Farcas et al. (2016) for more detailed discussion). The choice of model primarily depends on: (i) water depth; (ii) frequency range of sound to be modelled; and (iii) whether the environment varies considerably with range from the source. To ensure confidence in the modelling, models should be validated with field measurements of sound propagation. Common shortcomings at this stage in the assessment include the application of models which are not appropriate for the environment, insufficient model validation and inadequate description of the model (often the case when contractors use proprietary models).

2.3 | Impact

2.3.1 | Compute effect zones and assess risk of impact

By combining noise model predictions with the noise exposure criteria, "effect zones" are derived (see Figure 2). These zones show the predicted areas where the thresholds for different effects are exceeded. The risk of impact can then be assessed by overlaying effect zones on species densities and/or known (seasonal) habitat (e.g. fish spawning areas).

The effect zones predicted can be strongly influenced by the noise exposure criteria used (Figure 2a), whether animals are assumed
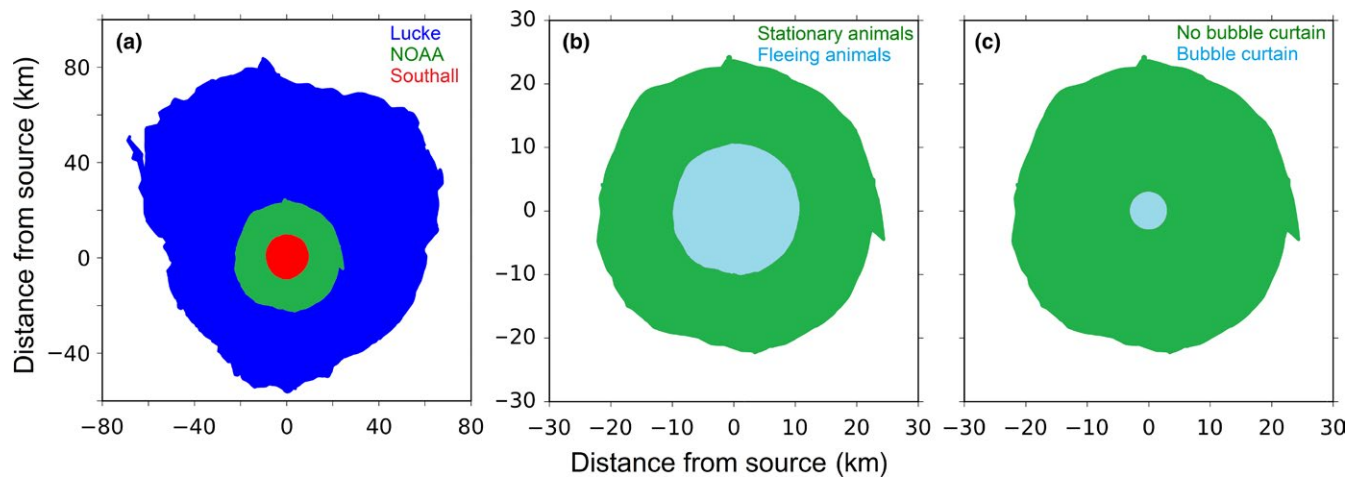
FIGURE 2 Illustrative comparison of TTS effect zones for harbour porpoise *Phocoena phocoena exposed to pile driving*: (a) when using different noise exposure criteria: Southall et al. (2007); NOAA (National Marine Fisheries Service, 2016) and Lucke et al. (2009); (b) with/without fleeing animal assumption, NOAA criteria; (c) with/without bubble curtain, NOAA criteria. The model parameters used are detailed in the Supporting Information [Colour figure can be viewed at wileyonlinelibrary.com]

to flee from the source at the onset of disturbance (Figure 2b) and whether noise abatement measures are implemented to reduce risk (Figure 2c).

Guidelines for selecting appropriate criteria are provided in section 2.1.2, and regulators should be aware that criteria selection can be a major factor in determining the assessment outcome (Figure 2a), since they may differ in their noise exposure thresholds and any frequency weightings applied.

Assumptions of fleeing animal behaviour in the estimation of effect zones are controversial, since animals may be motivated to remain in the affected area (e.g. due to prey availability or mating opportunities) despite harmful noise exposure. On the other hand, assuming for the purposes of the assessment that animals remain stationary, including close to the source, for extended periods (some criteria use a 24-hr period for cumulative exposure) may be considered unrealistic. The assumptions underlying such models, particularly probability of fleeing, swim speed and flight path, will strongly influence the size of the effect zones predicted (Figure 2b), and these parameters should be given careful consideration by developers and regulators to ensure that risk is not underestimated.

2.3.2 | Compute effect zones with additional mitigation measures

The most direct and comprehensive way to mitigate the risk of acoustic impact on marine species is to reduce the amount of noise pollution emitted at source (noise abatement). For pile driving, alternative piling technologies such as vibratory piling and continuous flight auger (CFA) piling may reduce noise levels emitted (though see Graham et al., 2017). There are also several noise reduction technologies available, such as big bubble curtains and acoustic barriers that are integrated into the piling rig (e.g. IHC Noise Mitigation System), which are now being routinely deployed in German waters. The application of these technologies reduces the effect zones predicted

for auditory injury (Figure 2c), and has been demonstrated to reduce the distance at which harbour porpoise are displaced from pile driving activities (Dähne, Tougaard, Carstensen, Rose, & Nabe-Nielsen, 2017). Nevertheless, in many countries it is rare for such technologies to be required by regulators, and the reduction in effect zones that would be achieved through their use is not typically modelled as part of the assessment process. We recommend that modelling the effect of noise abatement technologies is required by regulators of noise-generating activities, so that regulators are informed of the risk reduction options available. This is particularly important for the assessment of cumulative impact from multiple activities (see next section), where regulators need to be informed of the measures available to reduce cumulative risk for specific populations and habitats.

Although noise abatement technologies are uncommon in some countries, less direct mitigation measures are often applied. Standard mitigation measures include spatiotemporal restrictions on activities to avoid sensitive habitats and times of year. Such restrictions will often be the most cost-effective mitigation solution for seasonally occurring species, provided accurate and up-to-date species distribution data are available. Additionally, in situ measures may be taken (e.g. JNCC, 2017), such as soft-start procedures (also known as "ramp up"), whereby the source level is gradually increased (with the intent to displace animals before harmful levels are reached), and the establishment of a surveillance zone in which a marine mammal observer will monitor visually and/or acoustically for marine mammals prior to and during the activity. However, these in situ measures have been criticised as arbitrary and evidence for their efficacy is lacking (Wright & Cosentino, 2015). Some developers have also used acoustic deterrent devices (ADDs) to displace animals prior to the activity, with the intent of reducing the risk of auditory injury. Use of ADDs introduces additional acoustic disturbance, and the extent of marine mammal displacement from ADDs may exceed the range of displacement from the activity itself if

noise abatement measures are applied (Dähne et al., 2017). As such, use of ADDs should be considered carefully in the context of the proposed activity.

2.4 | Cumulative impact

2.4.1 | Assess cumulative effects as required by regulator

Impacts from individual projects do not occur in isolation, but form part of the cumulative pressure exerted on marine ecosystems by human activity. To assess the cumulative impact of multiple human activities, environmental managers are increasingly requiring (or are themselves carrying out) cumulative effects assessments (CEAs) for underwater noise, often based on data gleaned from individual EIAs. This highlights the need for consistency in the methods and metrics used in individual EIAs. EIA-based CEAs led by developers of individual projects have clear shortcomings when compared to CEAs led by government agencies on a regional and strategic level (Willsteed et al., 2017). Nevertheless, this approach remains the preferred option in many jurisdictions. Developers conducting these EIAs and CEAs should consider it in their interests to promote coherence in EIA methodologies, since this reduces the uncertainty (and therefore the risk of declined consent) in resulting CEAs. Similarly, regulators and government agencies conducting CEAs should specify clear requirements at the EIA stage to ensure that assessments at the project level can feed into a consistent cumulative assessment.

In the case of impulsive noise, many regulators now require licensed activities to be reported to national noise registries, which in turn feed into international registries used in region-scale assessments of impulsive noise activity and its associated risks (Merchant et al., 2017). There is great potential for these reporting and assessment mechanisms to be integrated into the regulatory process as forward-looking management tools for cumulative effects assessment and marine spatial planning, and to meet the requirements of legislative frameworks such as the EU Marine Strategy Framework Directive (MSFD). These registries could also serve as vehicles for the much-needed standardisation of data reported to regulators within the EIA process.

3 | CONCLUSIONS

Scientific understanding of the impacts of underwater noise pollution is advancing rapidly and the potential for widespread effects on marine fauna is increasingly clear. Both developers and regulators have a responsibility to address this risk by ensuring that the potential impacts of noise-generating activities are appropriately assessed and mitigated for. Nevertheless, at present many EIAs for underwater noise do not apply appropriate methods and lack reference to the best available science. The guiding principles set out here provide a basis for the more consistent, evidence-based approach that is required to conduct meaningful EIAs and to inform larger-scale risk assessments. We hope these guidelines will empower regulators, developers and stakeholders to raise the standard of EIA practice, leading to better informed regulatory decisions which support sustainable management of underwater noise pollution.

AUTHORS' CONTRIBUTIONS

R.C.F. and N.D.M. conceived the ideas and led the writing of the manuscript; A.F. carried out the modelling for Figure 2. All authors contributed critically to the drafts and gave final approval for publication.

DATA ACCESSIBILITY

Data have not been archived because this article does not contain data.

ORCID

Rebecca C. Faulkner http://orcid.org/0000-0003-1791-934X

Adrian Farcas http://orcid.org/0000-0002-3320-8428

Nathan D. Merchant http://orcid.org/0000-0002-1090-0016

REFERENCES

Dähne, M., Tougaard, J., Carstensen, J., Rose, A., & Nabe-Nielsen, J. (2017). Bubble curtains attenuate noise from offshore wind farm construction and reduce temporary habitat loss for harbour porpoises. *Marine Ecology Progress Series*, *580*, 221–237. https://doi.org/10.3354/meps12257

Dunlop, R. A., Noad, M. J., McCauley, R. D., Scott-Hayward, L., Kniest, E., Slade, R., ... Cato, D. H. (2017). Determining the behavioural dose response relationship of marine mammals to air gun noise and source proximity. *Journal of Experimental Biology*, *220*, 2878–2886. https://doi.org/10.1242/jeb.160192

Ellison, W. T., Southall, B. L., Clark, C. W., & Frankel, A. S. (2012). A new context-based approach to assess marine mammal behavioral responses to anthropogenic sounds. *Conservation Biology*, *26*, 21–28. https://doi.org/10.1111/j.1523-1739.2011.01803.x

Farcas, A., Thompson, P. M., & Merchant, N. D. (2016). Underwater noise modelling for environmental impact assessment. *Environmental Impact Assessment Review*, *57*, 114–122. https://doi.org/10.1016/j.eiar.2015.11.012

Gomez, C., Lawson, J. W., Wright, A. J., Buren, A. D., Tollit, D., & Lesage, V. (2016). A systematic review on the behavioural responses of wild

marine mammals to noise: The disparity between science and policy. *Canadian Journal of Zoology*, *94*, 801–819. https://doi.org/10.1139/cjz-2016-0098

Graham, I. M., Pirotta, E., Merchant, N. D., Farcas, A., Barton, T. R., Cheney, B., … Thompson, P. M. (2017). Responses of bottlenose dolphins and harbor porpoises to impact and vibration piling noise during harbor construction. *Ecosphere*, *8*, e01793. https://doi.org/10.1002/ecs2.1793.

Hawkins, A. D. & Popper, A. N. (2017). A sound approach to assessing the impact of underwater noise on marine fishes and invertebrates. *ICES Journal of Marine Science: Journal du Conseil*, *74*, 635–651. https://doi.org/10.1093/icesjms/fsw205

JNCC. (2017). *JNCC guidelines for minimising the risk of injury to marine mammals from geophysical surveys*. Aberdeen, UK: Joint Nature Conservation Committee.

Lucke, K., Siebert, U., Lepper, P. A., & Blanchet, M.-A. (2009). Temporary shift in masked hearing thresholds in a harbor porpoise (*Phocoena phocoena*) after exposure to seismic airgun stimuli. *The Journal of the Acoustical Society of America*, *125*, 4060–4070.

McCauley, R. D., Day, R. D., Swadling, K. M., Fitzgibbon, Q. P., Watson, R. A., & Semmens, J. M. (2017). Widely used marine seismic survey air gun operations negatively impact zooplankton. *Nature Ecology & Evolution*, *1*, 195.

Merchant, N. D., Faulkner, R. C., & Martinez, R. (2017). Marine noise budgets in practice. *Conservation Letters*. https://doi.org/10.1111/conl.12420

National Marine Fisheries Service. (2016). *Technical guidance for assessing the effects of anthropogenic sound on marine mammal hearing: Underwater acoustic thresholds for onset of permanent and temporary threshold shifts*. U.S. Dept. of Commer. NOAA. NOAA Technical. Memorandum, NMFS-OPR-55, 178 p

Nedelec, S. L., Campbell, J., Radford, A. N., Simpson, S. D., & Merchant, N. D. (2016). Particle motion: The missing link in underwater acoustic ecology. *Methods in Ecology and Evolution*, *7*, 836–842. https://doi.org/10.1111/2041-210X.12544

Popper, A. N., Hawkins, A. D., Fay, R. R., Mann, D. A., Bartol, S., Carlson, T. J., … Tavolga, W. N. (2014). *ASA S3/SC1.4 TR-2014 Sound exposure guidelines for fishes and sea turtles: A technical report prepared by ANSI-Accredited Standards Committee S3/SC1 and registered with ANSI*. American National Standards Institute.

Solan, M., Hauton, C., Godbold, J. A., Wood, C. L., Leighton, T. G., & White, P. (2016). Anthropogenic sources of underwater sound can modify how sediment-dwelling invertebrates mediate ecosystem properties. *Scientific Reports*, *6*, 20540.

Southall, B., Bowles, A., Ellison, W., Finneran, J. J., Gentry, R., Greene, C. R. J., … Tyack, P. (2007). Marine mammal noise-exposure criteria: Initial scientific recommendations. *Aquatic Mammals*, *33*, 411–521.

Tougaard, J., Wright, A. J., & Madsen, P. T. (2015). Cetacean noise criteria revisited in the light of proposed exposure limits for harbour porpoise. *Marine Pollution Bulletin*, *90*, 196–208.

Willsteed, E., Gill, A. B., Birchenough, S. N. R., & Jude, S. (2017). Assessing the cumulative environmental effects of marine renewable energy developments: Establishing common ground. *Science of the Total Environment*, *577*, 19–32.

Wright, A. J., & Cosentino, A. M. (2015). JNCC guidelines for minimising the risk of injury and disturbance to marine mammals from seismic surveys: We can do better. *Marine Pollution Bulletin*, *100*, 231–239.

Wright, A. J., & Kyhn, L. A. (2015). Practical management of cumulative anthropogenic impacts with working marine examples. *Conservation Biology*, *29*, 333–340.

BIOSKETCH

Rebecca Faulkner is the primary scientific advisor on underwater noise to regulatory bodies in England and Wales, and has extensive experience of assessing the impacts of noise on aquatic life.

Adrian Farcas is a senior scientist responsible for modelling underwater noise for EIAs and in advisory work for UK Government.

Nathan Merchant is a principal scientific advisor on underwater noise to the UK Department for Environment, Food & Rural Affairs (Defra), co-convenor of the OSPAR Intersessional Correspondence Group on Noise, and a member of the European Technical Group on Noise, which advises on the implementation of the EU MSFD.

Temporary shift in masked hearing thresholds in a harbor porpoise (*Phocoena phocoena*) after exposure to seismic airgun stimuli

Klaus Lucke and Ursula Siebert
Forschungs- und Technologiezentrum Westküste, Christian-Albrechts-Universität zu Kiel, 25761 Büsum, Germany

Paul A. Lepper
Department of Electronic and Electrical Engineering, Advanced Signal Processing Group, Loughborough University, Loughborough LE11 3TU, United Kingdom

Marie-Anne Blanchet
Fjord & Baelt, Margrethes Plads 1, 5300 Kerteminde, Denmark

An auditory study was conducted to derive data on temporary threshold shift (TTS) induced by single impulses. This information should serve as basis for the definition of noise exposure criteria for harbor porpoises. The measurements of TTS were conducted on a harbor porpoise by measuring the auditory evoked potentials in response to amplitude-modulated sounds. After obtaining baseline hearing data the animal was exposed to single airgun stimuli at increasing received levels. Immediately after each exposure the animal's hearing threshold was tested for significant changes. The received levels of the airgun impulses were increased until TTS was reached. At 4 kHz the predefined TTS criterion was exceeded at a received sound pressure level of 199.7 dB_{pk-pk} re 1 μPa and a sound exposure level (SEL) of 164.3 dB re 1 μPa^2 s. The animal consistently showed aversive behavioral reactions at received sound pressure levels above 174 dB_{pk-pk} re 1 μPa or a SEL of 145 dB re 1 μPa^2 s. Elevated levels of baseline hearing sensitivity indicate potentially masked acoustic thresholds. Therefore, the resulting TTS levels should be considered masked temporary threshold shift (MTTS) levels. The MTTS levels are lower than for any other cetacean species tested so far.

I. INTRODUCTION

Anthropogenic sound resulting from shipping, industrial and military activities and many other sources has led to a substantial increase in the underwater background noise in the oceans over the past decades (Hildebrand, 2004). The North and Baltic Seas are among the most intensively used and consequently noisiest marine areas (OSPAR Commission, 2000). Seismic surveys are one of the most prominent contributors to the overall noise budget in these areas, as in almost all oceans. Consequently, these surveys moved into the focus of interest of scientists as well as policy makers due to the intensity of the emitted sounds and spatiotemporal scale of these activities. Seismic surveys are conducted covering vast areas while searching for hydrocarbon deposits—in the central North Sea the most recent campaign was conducted at the Doggerbank area in spring/summer 2007. The total source level of airgun arrays used as sound source during these surveys depends on size, number, and timing of the individual airguns. With source levels ranging from 225 to 255 dB re 1 μPa$_{peak}$ (Richardson *et al.*, 1995), seismic surveys are routinely conducted continuously over several weeks, with repetition rates of several signals per minute.

The acoustic emissions produced during these programs may reach intensities with a potential of causing a variety of effects in the marine fauna at considerable distances—from behavioral reactions (McCauley *et al.*, 2000; Tougaard *et al.*, 2003) and potential stress to physiological effects (Finneran *et al.*, 2002), injury (McCauley *et al.*, 2003), and possibly death (Ketten *et al.*, 1993).

Most odontocete species are known to produce, and be sensitive to, sound (see review in Richardson *et al.*, 1995; Wartzok and Ketten, 1999). They are represented in the central and southern North Sea, the Baltic Sea, and especially in German waters by the harbor porpoise (*Phocoena phocoena*) as the only resident cetacean species. Harbor porpoises have a very acute sense of hearing underwater (Andersen, 1970; Kastelein *et al.*, 2002) and have been shown to use echolocation to find their prey (Busnel *et al.*, 1965) as well as for spatial orientation and navigation underwater (Verfuß *et al.*, 2005). Their acoustic sense has evolved to be their likely dominant sense vital to their survival. Any impairment or damage to their auditory system may have deleterious consequences for the affected individuals.

Auditory studies on terrestrial animals have shown that the exposure to intense impulsive sounds could exceed the tolerance of their auditory system and lead to an increased

hearing threshold (Ahroon *et al.*, 1996; Kryter, 1994; Yost, 2000). Such a noise-induced threshold shift (TS) can either be temporary (TTS) or permanent (PTS), depending on the hearing system's capacity for recovery once the sound has ceased. A similar cause-effect relationship has been found in odontocetes as TTS has been demonstrated in bottlenose dolphins (*Tursiops truncatus*) and belugas (*Delphinapterus leucas*) (Schlundt *et al.*, 2006; Finneran *et al.*, 2002; Nachtigall *et al.*, 2003, 2004) after exposure to intense intermittent or continuous noise. The TTS data obtained so far indicated that the energy flux density [i.e., the acoustic energy over time or sound exposure level (SEL)] of a signal can be used in combination with a maximum peak pressure to determine noise exposure criteria for marine mammals. As SEL is calculated by integrating the squared pressure over a standard unit of time, the duration of a signal plays an important role with regard to TTS. It is still unclear whether the dose-response function follows an "equal-energy rule" in marine mammals, but in the absence of specific data it can be used as a first-order approximation, as pointed out by Southall *et al.* (2007).

Based on these TTS data, a peak pressure of 224 dB$_{peak}$ re 1 μPa and a SEL of 195 dB re 1 μPa^2 s were initially proposed as noise exposure criteria for mid-frequency cetaceans (e.g., bottlenose dolphins and belugas) for exposures to pulsed sounds (Ketten and Finneran, 2004). With the noise exposure criteria proposed by Southall *et al.* (2007), the focus of marine mammal policy has shifted toward PTS and the onset of behavioral disruption. They proposed appropriate interim noise exposure criteria for all toothed whale species based on the dose-response functions found in the two cetacean species tested for their TTS limit so far (see above). The relevant PTS level for single impulses is set for all toothed whale species to a peak pressure of 230 dB$_{peak}$ re 1 μPa and a SEL of 198 dB re 1 μPa^2 s. A criterion for SEL has also been set for the first time for multiple exposures to impulsive sounds, which are likely to lead to a reduced tolerance of the auditory system (Ahroon *et al.*, 1996). This threshold (198 dB re 1 μPa^2 s) is identical to the SEL criteria for single impulses. The subjects from former TTS studies are categorized as mid-frequency cetaceans with the main energy of their echolocation clicks and their range of best hearing sensitivity <100 kHz. Harbor porpoises, in contrast, are categorized as high-frequency cetaceans (Ketten, 2000; Southall *et al.*, 2007), with a best hearing sensitivity at frequencies above 100 kHz (Andersen, 1970; Kastelein *et al.*, 2002) and an energy maximum of their echolocation signals in the range 110–140 kHz (Verboom and Kastelein, 1995). There are no TTS data available for this species, or for any other high-frequency cetacean species. These differences in their acoustic and auditory characteristics may also be reflected in differences in the overall tolerance of their auditory systems to intense noise. Accordingly, a transfer of the first-order approximated auditory dose-response function to the harbor porpoise could be questionable. The same applies to an application of the noise exposure criteria proposed by Southall *et al.* (2007) to assess effects of pile driving impulses on harbor porpoises (as generated, e.g., during the construction of wind turbines).
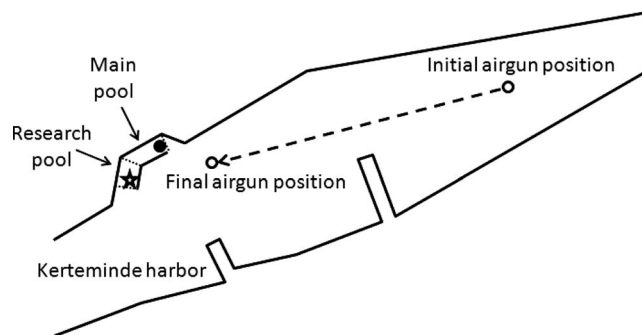

FIG. 1. Schematic overhead view of the experimental setup. Symbols indicate the approximate position of the harbor porpoise during the exposures to the airgun impulses in the main pool (filled circle), its position during the hearing tests (star), and the initial as well as the final location of the airgun (open circles) within the harbor of Kerteminde.

To base the assessment of acoustic effects of impulsive noise on species-specific data, a dedicated TTS study was conducted on one harbor porpoise. A key element for the planned study was access to a harbor porpoise trained to participate in experiments so that the experiments could be conducted under controlled conditions and definitive information on the dose-response function gathered. The aim of this acoustic study was to define the tolerance limit of the auditory system of the harbor porpoise to single impulsive sounds. Such data would enable regulatory agencies to define "zones of impact" (Richardson *et al.*, 1995) around the construction sites. At the same time, such data could be applied as a more robust baseline in the definition of noise exposure criteria for other high-frequency cetacean species [see outline by Southall *et al.* (2007)].

II. METHODS

A. Subject and facility

A male harbor porpoise held under human care in the Fjord & Bælt Centre (F&B) in Kerteminde, Denmark was chosen as subject for the studies. This animal, named *Eigil*, was estimated to be between 9 and 10 years old, with a length of 143 cm and an average weight of 40 kg in 2005 when the study began. A comprehensive medical record of all treatments exists for Eigil for almost his entire life. He was held in this facility with two female harbor porpoises at that time. The older female was pregnant twice during the study period from 2005 until 2007 and gave birth to a female calf right after the end of the studies in summer 2007. The design of the auditory experiments was altered due to the pregnancies and thus they are relevant for discussion of the results.

The animals were held together at the F&B in a semi-natural outdoor pool of 30×20 m^2 and an average depth of 4 m. Their enclosure stretches along the entrance from the Baltic Sea to a small fjord on one side of the busy fishing harbor of Kerteminde. It has a natural sea bottom and solid walls of concrete and steel on the two long sides. It is separated from the harbor on its narrow ends by nets, thereby providing a constant water exchange with the Baltic Sea (Fig. 1).

J. Acoust. Soc. Am., Vol. 125, No. 6, June 2009

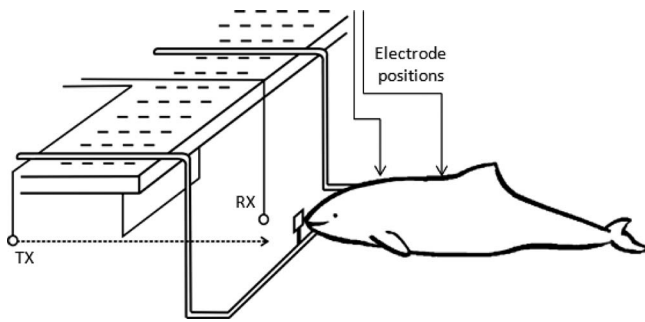Lucke *et al.*: Threshold shift in a harbor porpoise   4061

FIG. 2. Schematic plot of the research setup for the AEP measurements with the animal positioning itself at 1.5 m water depth in front of its underwater station and with its body in a straight line with the sound path of the incoming AEP stimuli. The direct sound path is indicated by a dashed line between sound source (TX) and monitoring hydrophone (RX) and the animal's position.

The enclosure is divided into two compartments ("main pool" and "research pool"), allowing separation of the animals for experiments. A floating pen ($4.5 \times 4.5 \times 1.5$ m^3) in the research pool was wrapped with sound absorbing foam, providing an acoustic shelter for the two females during the planned exposures to intense sound in the later stage of the study.

All experiments were conducted with Eigil, who was separated temporarily from the two females to avoid behavioral or acoustic interference between the animals during the research. Eigil was trained to accept the electrodes that were attached to his head and back with suction cups and to dive on command to an underwater station at 1.5 m water depth. The training method used was based on operant conditioning and positive reinforcement (Pryor, 1984; Ramirez, 1999). No food deprivation was used during these experiments. He stationed himself actively at the setup with his rostrum touching a 4×4 cm^2 polyvinylchloride (PVC) plate in front of the sound transducers (Fig. 2) for the hearing tests. He stayed there for 100 s on average until he was called back to the surface by the trainer to receive reinforcement. This experimental sequence was called a "send." A complete research session was comprised of four sends on average. The number of research sessions per day depended on weather conditions and varied between one and four during the study period with an average of two sessions, ideally one in the morning and one in the afternoon.

B. Study design

The study was divided into two modules: The first consisted of measurements of the animal's absolute hearing thresholds over almost its entire functional frequency spectrum, thus providing a baseline for the second module, a tolerance test of the animal's hearing. This TTS test was designed to follow the same procedural structure as the experiments conducted by Finneran et al. (2002). The animal's hearing thresholds were measured in half octave steps over ~5.5 octaves with the lower-frequency limit set by the methodological parameters of the auditory evoked potential (AEP) stimulation. The threshold measurements were repeated several times at three selected frequencies (representing the low, mid-, and high frequencies of its functional

hearing range) to measure normal variation. This would subsequently allow definition of a frequency-specific TTS criterion.

C. Measurement of auditory sensitivity (AEP method)

The measurement of AEPs (AEP method) was chosen to measure the hearing thresholds in the harbor porpoise as it allows a comparatively rapid data acquisition and is non-invasive. For this reason the technique has been widely adopted in human patients and is also used for screening newborns (Hall, 2006). This technique is based on the presentation of acoustic stimuli, which will generate neuronal potentials in the acoustic system upon perception of these stimuli (Picton, 1987). Two surface electrodes are placed on the animal's skin using suction cups—one near the blowhole and the other near the dorsal fin—to record the neural responses evoked within the auditory system (Supin et al., 2001). These potentials are generated within neuronal nuclei at different positions in the auditory system, thereby forming an electric field, which can be detected and recorded even on the skin surface. AEPs are useful for measuring the functioning of the auditory system and examining important aspects of auditory processing. To distinguish these comparatively small electric potentials from the overall neuronal activity—i.e., electric activity of the animal's musculature, other sensory inputs, etc.—the acoustic test stimuli are presented at a high repetition rate. By coherently averaging the evoked potentials (e.g., more than 500 AEPs), non-acoustic neuronal signals and incoherent acoustic signals not associated with the acoustic stimuli are reduced or eliminated.

A refined methodological approach is based on the use of rhythmic sound modulations. By sinusoidally modulating the amplitude of carrier tone or sound pulse sequence, it is possible to elicit a neuronal response, which includes a specific frequency component correlated with the modulation frequency used. This effect occurs because the auditory system is capable of following the envelope of a sinusoidal signal and producing corresponding neuronal potentials, called an envelope-following response (EFR). By applying a fast-Fourier transformation (FFT) analysis, the modulation frequency component can be identified and quantified. The resulting amplitude of the EFR represents the energy content of the neuronal response at the given modulation frequency. The strength of this EFR can simultaneously be taken as a relative measure for the perception of the carrier frequency of the amplitude-modulated (AM) signal. At each frequency, the stimuli were presented in decreasing intensity, starting at a clearly audible level, until a (neuronal) response was no longer detected. The resulting data were statistically tested for significance by using an F-test to identify EFRs from arbitrarily occurring noise at the given AM frequency (cf. Finneran et al., 2007).

D. Sound generation and data acquisition

The animal's hearing was tested at frequencies between 4 and 160 kHz with sinusoidally amplitude-modulated (modulation rate: 1.2 kHz; duration: 25 ms) signals as AEP stimuli. The signals were of 25 ms duration with a modula-
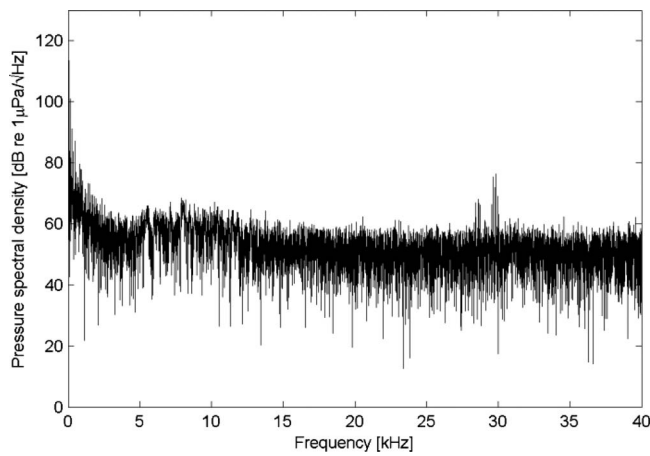
FIG. 3. Background noise level (plotted as pressure spectral density) recorded in the research pool at F&B during quiet conditions. (Analysis carried out on a 2.62 s sequence sampled at 400 kS/s using a Hanning window. The 0.38 Hz FFT bin size was then normalized to a 1 Hz power spectral density band.)
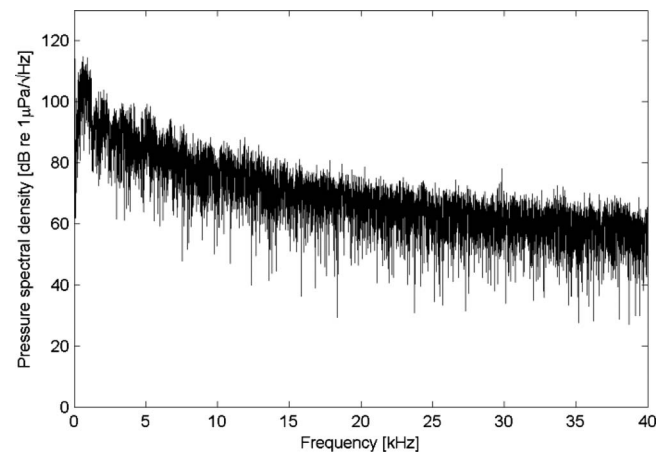

FIG. 4. Background noise level (plotted as pressure spectral density) recorded in the research pool at F&B recorded at the same position as in Fig. 2 during noisy conditions. (Analysis carried out on a 2.62 s sequence sampled at 400 kS/s using a Hanning window. The 0.38 Hz FFT bin size was then normalized to a 1 Hz power spectral density band.)

tion depth of factor 1. A custom-made software application was used to program all acoustic stimuli transmitted to elicit the AEPs during the hearing threshold tests. The signal generation system consisted of a data acquisition card (National Instruments DAQ 6062 E) and two function generators (Thurlby Thandar TG 230 and Agilent 33220A—with the first triggering the latter). At frequencies between 4 and 8 kHz all signals were amplified by a power amplifier PA 100E (Ling Dynamic Systems Ltd., Royston, UK) and transmitted via an underwater transducer USRD J-9. At higher frequencies a power amplifier Brüel&Kjaer 2713 was used to amplify the signals. Due to differences in their transmit response and the geometry of the pool, five different sound transducers had to be used to transmit the acoustic stimuli during the AEP tests: Signals at 4 and 8 kHz were transmitted via an underwater transducer USRD J-9, at 16 and 80 kHz via a Reson TC 4033, at 22.4 kHz via a SRD Ltd. 4 in. ball hydrophone, at 44.8 kHz via a SRD HS70, and all remaining frequencies were transmitted via a SRD HS150 hydrophone. All transmitted and received signals were constantly observed in real time at an oscilloscope and recorded for post-analysis via a monitoring hydrophone (Reson TC 4014) and a preamplifier (Etec B1501) for received level, signal quality, and undesired signal artifacts using software packages SEAPRODAQ (Pavan *et al.*, 2001) and custom software LU-DAQ. The evoked potentials were fed into a custom-built input station consisting of an amplifier (20 dB gain) and an optical separation unit (including 20 dB gain). Additionally, the signals were band-pass filtered (high-pass frequency: 300 Hz, low-pass frequency: 10 kHz, NF Electronic Instruments FV-665) to avoid artifacts. Each sequence of 500 successive potentials was averaged and displayed online as well as stored for post-hoc analysis.

The background noise in Kerteminde harbor is dominated by shipping noise from a variety of boat traffic ranging from recreational and small fishing boats passing the enclosure to fishing boats turning into the unloading area on the opposite side of the harbor and supply vessels for a nearby island (see comparison: Figs. 3 and 4). The background noise

was thus dominated by low-frequency noise at varying levels and frequencies, depending on the size, speed, and activity of the respective boats.

E. Sound exposure procedure

A TS was defined as a difference of twice the standard deviation from the average hearing threshold at the particular frequency applied. The TTS criterion of 6 dB as proposed by Southall *et al.* (2007) was used as a second, frequency-independent criterion in this study. The tolerance of the animal's auditory system was then tested by first exposing the animal to a sound impulse as a fatiguing stimulus and then immediately re-measuring the hearing threshold. Any reduction in the animal's hearing sensitivity exceeding the preset TTS criteria would be regarded as evidence of an actual TS. Subsequent measurements of the animal's hearing threshold at the affected frequency would provide information about the recovery function of the auditory system.

The animal's hearing sensitivity was tested at three frequencies (4, 32, and 100 kHz) separately for TTS at a given exposure level of the fatiguing stimulus; i.e., only one hearing frequency was tested after each exposure. As long as the hearing threshold was shown to remain within its normal variation at all three frequencies, the subsequent exposure level of the fatiguing stimulus would be elevated and this procedure repeated until a TS is detected. This precautionary approach was chosen to avoid any risk of permanent hearing loss.

Various metrics have been used for both peak and energy amplitude, hearing threshold, spectral level, and spectral density, many discussed by Madsen (2005). A summary of calculation methodology is given below. Where possible, reported units are provided in formats used in other relevant studies to allow comparison with previous results.

For a specific pulse, the peak-to-peak pressure ($P_{\text{pk-pk}}$) was calculated. Since the peak may have a negative pressure, the peak-to-peak pressure is equivalent to the sum of the magnitudes of the peak positive and peak negative pressures.

J. Acoust. Soc. Am., Vol. 125, No. 6, June 2009

Lucke *et al.*: Threshold shift in a harbor porpoise   4063

Peak pressure is defined as the maximum magnitude of peak positive or peak negative pressure. The value is expressed as the peak-to-peak sound pressure level (SPL) in dB re 1 μPa. This is calculated from

$$\text{SPL}_{\text{pk-pk}} = 20 \log \left[\frac{P_{\text{pk-pk}}}{P_0} \right]$$

where P_0 is the reference pressure of 1 μPa (peak-to-peak).

The SEL for a single pulse is the integral of the square of the pressure waveform over the duration of the pulse using a 90% energy criterion. The duration of the pulse is defined as the region of the waveform containing the central 90% of the energy of the pulse. Given by

$$E_{90} = \int_{t_5}^{t_{95}} p^2(t) dt$$

The value is then expressed in dB re 1 μPa^2 s and is calculated from

$$\text{SEL} = 10 \log \left[\frac{E_{90}}{E_0} \right]$$

where E_0 is the reference value of 1 μPa^2 s, t_5 is the time of a 5% increase in energy for the total pulse energy, and t_{95} is the time of 95% of the total energy of the pulse. The pulse duration is therefore defined as the time taken from 5% to 95% of the total pulse energy.

The root mean square (rms) pressure was calculated by taking the square root of the average of the square of the pressure waveform over the duration of the pulse, again using a 90% energy criteria, with the pulse duration defined as above. This is given as

$$P_{\text{rms}} = \sqrt{\frac{1}{T_{90}} \int_{t_5}^{t_{95}} P^2(t) dt}$$

F. Sound source for the fatiguing stimulus

A small sleeve airgun (20 in^3) was used as sound source to produce the fatiguing sound stimuli during the second module. This device was pressurized with nitrogen at a pressure of 137 bar (2000 psi) and was operated at a depth of 2 m (i.e., in mid-water) from a small inflatable boat (source boat) in Kerteminde harbor at varying positions between the F&B and the eastern exit of the harbor area. The exact position of the source boat was determined by GPS, and this information, along with time, weather conditions, and other relevant information on the sound source, was documented for further analysis. An intensive calibration of the airgun had been conducted prior to the study using calibrated hydrophones at the receiving position at the F&B to predict the received levels of the airgun stimuli as a function of its distance to the receiving position in the main pool at the F&B.

The sudden release of pressure from the airgun during a "shot" results in an oscillating air bubble, which projects a short (less than 50 ms), intense impulse (Fig. 5) into the water and across adjacent boundaries (ground wave; audibility of airgun shot in air). The main acoustic energy of this
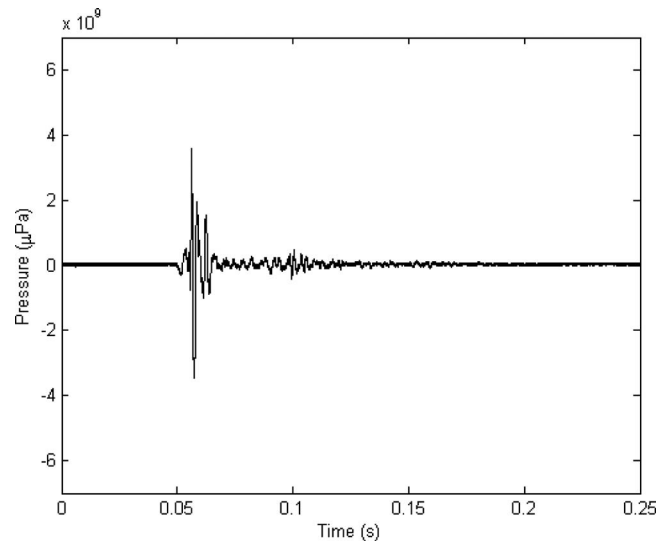

FIG. 5. Time domain representation of an airgun impulse. The airgun was fired at 2 m water depth in Kerteminde harbor and the impulse was recorded at a distance of 14 m to the receiving hydrophone.

impulse is centered below 500 Hz but considerable energy can also be detected up to above 20 kHz, well above background noise in quieter periods (Fig. 6).

Both high- and low-frequency components of the airgun emissions are likely to be attenuated over greater distance in a waveguide. The pulse recorded at the closest range from the airgun to the receiving position used in this study (shown in Fig. 6) therefore has the broadest observed spectrum and was felt to represent the worst case with regard to the potential auditory effects.

Prior to each airgun shot, the two female harbor porpoises were separated into the sound-insulated floating pen. Their general behavior and breathing rates were observed for the period of the sound exposure and compared with baseline data previously obtained under normal conditions. Eigil remained in the main pool. A receiving hydrophone was positioned at 1.5 m water depth at a position at the narrow end of
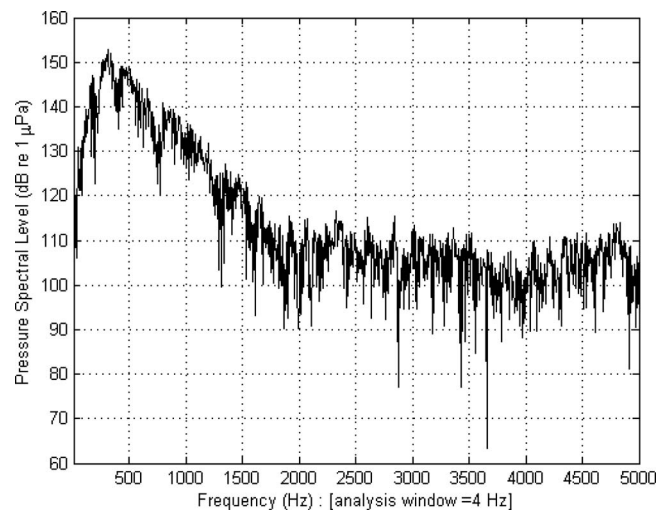

FIG. 6. Frequency spectrum analysis of the recorded airgun impulse (Fig. 4) showing the pressure spectral level (dB re 1 μPa). The frequency spectrum is plotted in hertz, and the spectrum levels are based on a 4 Hz analysis band.
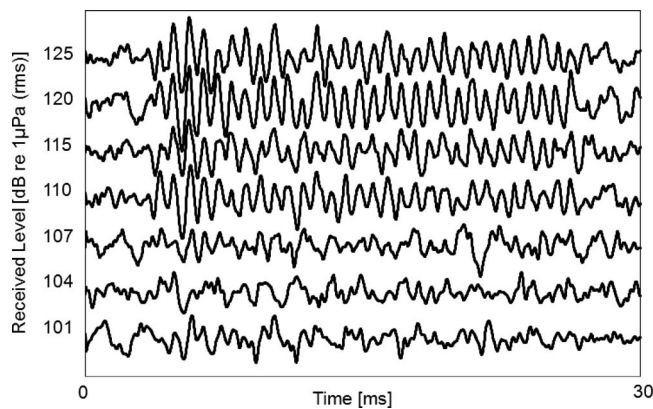
Lucke *et al.*: Threshold shift in a harbor porpoise

FIG. 7. Examples of EFRs in a harbor porpoise in response to acoustic stimulation with AM signals (averaged over 500 presentations); sampling duration was 30 ms, carrier frequency was 100 kHz, modulation rate was 1.2 kHz, and modulation depth was factor 1. Received levels descended from 125 dB re 1 μPa (rms) in 5-dB steps to 110 dB re 1 μPa (rms) and then in 3-dB steps to 101 dB re 1 μPa (rms).
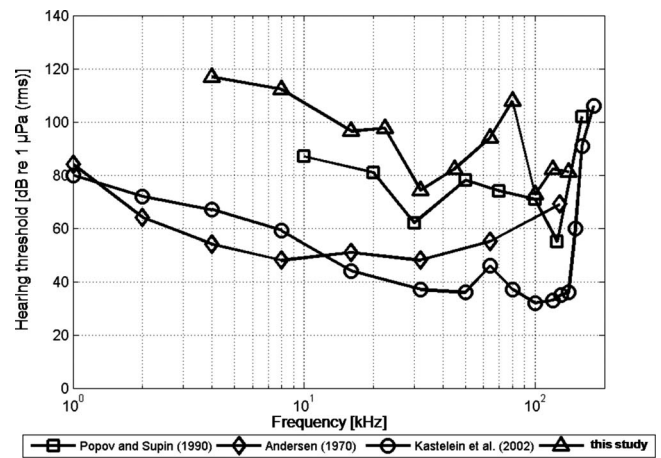

FIG. 8. Harbor porpoise hearing threshold data from different studies. The triangles represent the threshold values achieved in this study. Data from another AEP study (Popov and Supin, 1990) as well as from two behavioral auditory studies (Andersen, 1970; Kastelein *et al.*, 2002) are given for comparison.

the pool facing the eastern exit of Kerteminde harbor. This position had proven to receive the most intense signals during the airgun calibration. The airgun was triggered as soon as Eigil was within approximately 1 m of the receiving hydrophone with his body fully underwater. Control experiments were repeatedly made by conducting the complete procedure except for the exposure to the fatiguing stimulus. The animal's behavior was monitored and video recorded for further analysis. Immediately after each exposure to the fatiguing stimulus, the animal was then led into the research pool where the AEP setup was located. The post-exposure AEP measurements began less than 4 min after the exposure and typically were concluded within 12 min. Within this period his hearing sensitivity could be determined at a single frequency. During this second module, Eigil's hearing sensitivity was tested at 4, 32, and 100 kHz. These frequencies were chosen as representative frequencies for the low, mid-, and high ranges of the animal's functional hearing spectrum.

III. RESULTS

A. Hearing threshold

Eigil's baseline audiogram was determined based on the AEP measurements (Fig. 7) at frequencies between 4 and 140 kHz. At the highest frequency tested, 160 kHz, no AEP responses were detected. The measurements of Eigil's auditory sensitivity at the remaining frequencies resulted in elevated thresholds compared to hearing data published for other harbor porpoises (Fig. 8).

The shape of Eigil's hearing curve with its two minima at the mid- and high-frequency ranges is in good accordance with the previously published data. However, a clear rise in threshold was measured compared to data obtained by Kastelein *et al.* (2002) in a behavioral hearing study, with the maximum difference at 80 kHz. At the higher frequencies Eigil's threshold values are still elevated by 10–20 dB, but the difference is not as pronounced compared to the thresholds obtained by Andersen (1970). Compared to the results from the AEP study by Popov and Supin (1990), Eigil's thresholds are elevated by roughly 10 dB. The mean hearing

thresholds at 4, 32, and 100 kHz, respectively, were at 116.9, 74.2, and 72.7 dB re 1 μPa (rms). Based on the variation of the hearing thresholds measured during the first module, the TTS criteria were defined as 122.9 dB re 1 μPa (rms) at 4 kHz, 79.0 dB re 1 μPa (rms) at 32 kHz, and 85.7 dB re 1 μPa (rms) at 100 kHz.

B. TTS tests

Over a period of 4.5 months, Eigil was exposed to a total of 24 airgun impulses. The received peak pressure of the pulses ranged from 161.2 dB$_{pk-pk}$ re 1 μPa to 202.2 dB$_{pk-pk}$ re 1 μPa, with an acoustic energy (SEL) ranging from 140.5 dB re 1 μPa^2 s to 167.2 dB re 1 μPa^2 s. These levels were achieved using source ranges between 150 and 14 m from the animal's position during the exposure.

1. Threshold shifts

A TTS was first measured after Eigil had been exposed to an airgun impulse at a peak pressure of 200.2 dB$_{pk-pk}$ re 1 μPa with corresponding SEL of 164.5 dB re 1 μPa^2 s. The TS was measured when the animal hearing was tested after the exposure for its sensitivity at 4 kHz. Since this TS was only 1.8 dB above the predefined TTS criterion, the exposure was repeated several days later with a received peak pressure level of 202.1 dB$_{pk-pk}$ and a SEL of 165.5 dB re 1 μPa^2 s. The resulting TS at 4 kHz was 9.1 dB above the TTS criterion and hence a clear support of TTS. Another verification of this effect was achieved 2 days later, after an exposure at a peak pressure level of 201.9 dB$_{pk-pk}$ re 1 μPa with a SEL of 165.8 dB re 1 μPa^2 s, when Eigil's hearing revealed a TS at 4 kHz of 15 dB (Fig. 9). No significant elevation of hearing threshold at 32 kHz was observed at a comparable exposure level to the 4 kHz test case. The received energy was similar to the 4 kHz case, but a slightly lower received peak-to-peak pressure was observed (Fig. 10). No statistical change in hearing sensitivity was observed after an exposure to similar source levels

J. Acoust. Soc. Am., Vol. 125, No. 6, June 2009

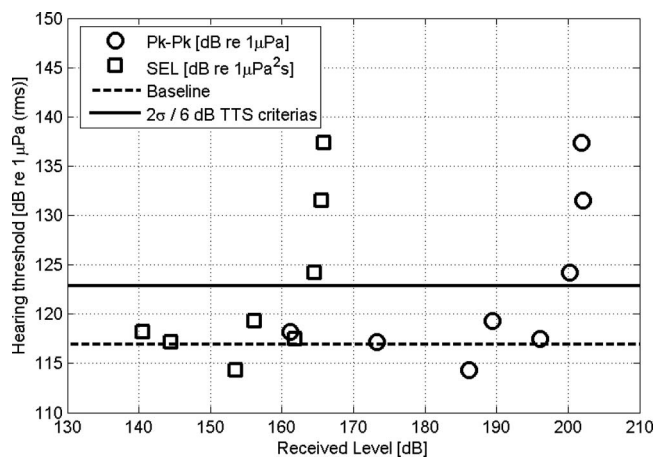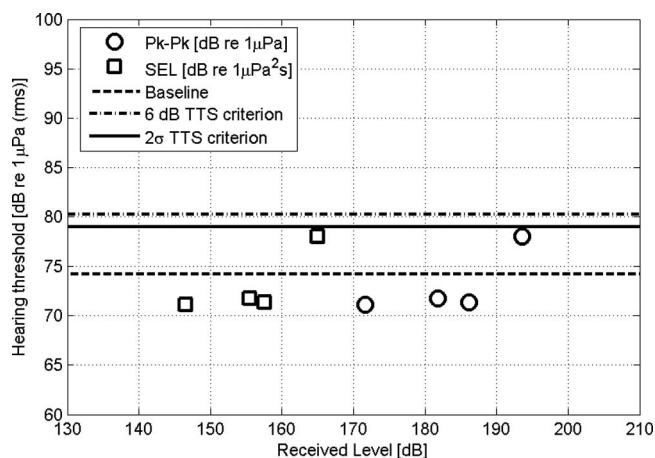Lucke *et al.*: Threshold shift in a harbor porpoise   4065

FIG. 9. Hearing threshold at 4 kHz for a harbor porpoise after exposure to airgun stimuli (i.e., post-exposure) at different received levels plotted in relation to the animal's pre-exposure hearing sensitivity. Each post-exposure hearing threshold is plotted twice—circles indicating the received peak-to-peak pressure of the fatiguing stimuli and squares the equivalent received SELs of the same exposure impulses. The dashed line represents the normal hearing threshold and the solid line the two TTS criteria used for comparison (which are identical at 4 kHz). Symbols above the solid line indicate a TS of hearing threshold.
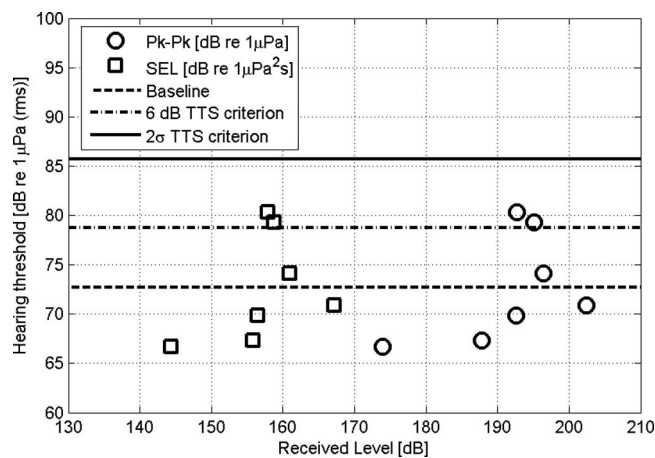

FIG. 11. Hearing threshold at 100 kHz for a harbor porpoise after exposure to airgun stimuli (i.e., post-exposure) at different received levels plotted in relation to the animal's pre-exposure hearing sensitivity. Each post-exposure hearing threshold is plotted twice—circles indicating the received peak-to-peak pressure of the fatiguing stimuli and squares the equivalent received SELs of the same exposure impulses. The dashed line represents the normal hearing threshold. The other lines (dotted-dashed line and solid line) indicate the two different TTS criteria used for comparison; symbols above both these lines indicate a temporary shift of hearing threshold.

for the 100 kHz test case—as regards both received peak pressure and energy (Fig. 11). It should be noted that the airgun source itself creates less energy at the mid- and high-frequency ranges than at 4 kHz.

2. Recovery

An important factor for the assessment of this noise-induced effect is the recovery of the animal's auditory system. After the first clear TS had been measured, a series of AEP measurements was conducted over the following days to follow the further development of Eigil's hearing sensitivity at the affected frequency. 178 min after the initial exposure his hearing had recovered only partially from its TS. It

was reduced by 2.9 dB but still being elevated above the TTS criterion. Eigil's sensitivity at 4 kHz improved by 3.5 dB, 269 min post-exposure but only by another 1.4 dB, 29 h post-exposure (Fig. 12).

Assuming a linear recovery from TTS, the animal's hearing sensitivity would have reached the TTS criterion level again in 12 h for the 202.1 dB exposure. However, a log-fitted curve provides a better fit to the data (i.e., the highest regression coefficient) for calculating Eigil's auditory recovery function. By applying this function the animal's hearing sensitivity would have recovered back to the level of the TTS criterion in 55.0 h.

FIG. 10. Hearing threshold at 32 kHz for a harbor porpoise after exposure to airgun stimuli (i.e., post-exposure) at different received levels plotted in relation to the animal's pre-exposure hearing sensitivity. Each post-exposure hearing threshold is plotted twice—circles indicating the received peak-to-peak pressure of the fatiguing stimuli and squares the equivalent received SELs of the same exposure impulses. The dashed line represents the normal hearing threshold. The other lines indicate the two different TTS criteria used for comparison.
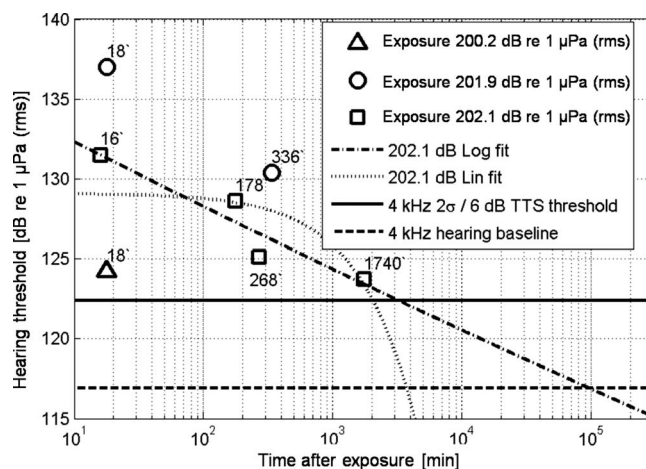

FIG. 12. Recovery function of a harbor porpoise's hearing threshold at 4 kHz after sound-induced TSs. Hearing thresholds measured subsequent to the exposures after different times (given in minutes next to the symbols) are indicated by different shapes for every exposure to the fatiguing stimulus. The recovery function for the exposure at 202,1 dB re 1 μPa (rms) is indicated by the diagonal and curved lines. The dashed line represents the normal hearing threshold and the solid line the two TTS criteria used for comparison (which are identical at 4 kHz).

3. Behavioral reactions

Eigil showed no behavioral reaction during the first exposures when he was exposed to a received pressure level of less than 174 dB_{pk-pk} re 1 μPa or a SEL of 145 dB re 1 μPa^2 s. At higher received levels, the animal showed repeatedly a typical aversive reaction at the time of the sound exposure and behavioral avoidance in the direction of the location of the source. Subsequently the animal avoided approaching the exposure station prior to further exposures as well as during control experiments. It should be noted that the exposure station was deliberately placed at a point of maximum received level within the total available enclosure. After a TTS had been documented and confirmed, the received levels were not raised any higher and no further trials were conducted.

Because one of the female harbor porpoises was pregnant during the exposure period, special measures were taken to protect her and the other animals from unnecessary sound exposures. Both females were kept in a sound-insulated pool and their behavior was continuously monitored during the sound exposures. None of them showed any obvious behavioral reactions during the airgun experiments. The attenuation of the airgun impulses inside their pool was at the order of 30–40 dB lower than at the exposure station. Correspondingly, the two females were never exposed to peak-to-peak pressure levels of more than 160 dB re 1 μPa.

IV. DISCUSSION

The TSs documented in this study represent the first data of its kind for harbor porpoises. Up to now all assessments of potential effects of anthropogenic sounds on harbor porpoises had to be made based on data from other odontocete species, or even terrestrial animals. Thus, the results of this study provide the first reliable information for the harbor porpoise for airgun (or impulse) exposures. These data, and more from future studies, could serve as a basis not only for defining noise exposure criteria for this species but also for deriving group-specific noise exposure criteria for all high-frequency cetaceans. The TS levels for the harbor porpoise differ strongly from data on the bottlenose dolphin or the beluga. This study provides more empirical data for high-frequency echolocating species than was available for Southall *et al.* (2007). Thus, the authors suggest that the proposed thresholds should be adapted accordingly.

The analysis of the animal's observed behavioral reactions to the fatiguing stimuli for the first time provides quantitative clues of a behavioral threshold in harbor porpoises. The fact that Eigil was swimming away from the location of the sound source after exposure to the airgun stimulus but not in control experiments infers avoidance or flight behavior. In a free-ranging animal this reaction might have lasted over a longer period of time than observed in Eigil, who calmed down and was back under behavioral control of the trainers after a few seconds when he was sent to subsequent hearing tests. It also remains questionable whether or not the level of 174 dB_{pk-pk} re 1 μPa pressure or a SEL of 145 dB re 1 μPa^2 s can be applied as threshold limit for behavioral reactions to impulsive sounds in harbor porpoises

in general as Eigil was rewarded for tolerating the intense sound exposures and reactions might occur even at lower levels. It seems more likely that this limit varies individually and may be context-specific. So far, the only available data on behavioral reactions of harbor porpoises to impulsive sound have come from observations during the construction of wind turbines at Horns Rev, Denmark (Tougaard *et al.*, 2003) where at a distance of up to 15 km a movement directed away from the sound source was observed in the animals. In the BROMMAD study (Gordon *et al.*, 2000), by contrast, no obvious behavioral reactions were observed in free-ranging harbor porpoises in response to airgun exposures at an estimated received level of 176 dB_{0-pk} re 1 μPa. In this context, the results of the present study constitute the first behavioral threshold in harbor porpoises that was measured under controlled acoustic conditions. The resulting data may be used as a first indication of a threshold range for behavioral reactions of harbor porpoises. The disturbing nature of this sound to harbor porpoises at the given intensities is emphasized by the avoidance behavior observed in Eigil prior to exposures after the exposure level had passed his behavioral threshold for the first time. The fact that Eigil was actively avoiding the monitoring hydrophone showed that he was sensitized. It was a lasting effect as he showed no signs of habituation during the remaining exposures.

The rate of recovery from TTS slowed during recovery period, suggesting a log-correlation in the recovery function. These first data would suggest that recovery rates are different between harbor porpoises and the previously tested mid-frequency cetaceans. The latter usually recover within minutes or, at a maximum, within 2 h from a comparable amount of TS (Finneran *et al.*, 2002; Nachtigall *et al.*, 2003, 2004). Such a slow recovery of the harbor porpoise's hearing sensitivity would also indicate that the third exposure to the airgun stimulus at levels over 200 dB re 1 μPa (received level, RL of 201.9 dB re 1 μPa) may have been premature as the TS was not yet fully recovered. The documented shift of 15 dB above the TTS criterion therefore could then be considered as a cumulative effect from the two consecutive exposures. The level for onset of TTS should accordingly be calculated based on the first two TS values, i.e., a peak-to-peak pressure of 199.7 dB_{pk-pk} re 1 μPa and a SEL of 164.3 dB re 1 μPa^2 s. These levels depend of course on the TTS criterion chosen and would be altered accordingly. Nevertheless, due to the comparatively strong variability within the experimental conditions, a frequency-specific definition of the TTS criterion for this type of fatiguing stimuli seems most appropriate.

The AEP method is the only available method to conduct comparable studies on wild animals. Those studies are relevant to validate the results from a single captive animal in a larger number of animals at a later stage. The results of this study show, on the one hand, that the AEP method can be successfully applied for auditory studies on harbor porpoises even if the animals are unrestrained like Eigil, who was actively swimming and free to leave the experiments at any time. His constant movement during the experiments, on the other hand, caused strong myogenic potentials, which

were recorded along with the auditory potentials during the experiments. These myogenic potentials are strong enough to raise the overall neuronal noise level of the recorded potentials. Any masking of the lowest levels of the auditory potentials by other electrophysiological signals, such as the myogenic potentials, could obscure the real lower end of the regression line, hence leading to a zero-crossing of the regression at a higher threshold value. Consequently the resulting hearing threshold would be elevated.

Probably the most prominent factor that may have influenced the hearing thresholds is the level of background noise in Kerteminde harbor. It is most likely that this broadband noise masked perception of the AEP stimuli by Eigil. A similar effect has been found in auditory studies in humans (Parker *et al.*, 1976) and also in harbor porpoises (Lucke *et al.*, 2007). Acoustic events, such as boats passing at close distance to the research station, were avoided during the experiments by pausing the session. Nevertheless, it was impossible to conduct the experiments at a consistently low level of background noise. As these conditions varied within each research session, and with extreme noise events excluded, one may assume that roughly the same overall noise conditions applied for all sessions.

Despite these physical factors affecting the baseline hearing thresholds, the results may also reflect a genuine hearing deficit that Eigil either developed due to an unnoticed infection of his auditory system or as a result of previously unmonitored exposure to intense sound or a long-term exposure to sounds, e.g., from the nearby harbor. However, it can be ruled out that the elevated thresholds are the result of ototoxic drugs as Eigil is known to have never received such treatments. An age-related hearing deficit is also unlikely as it usually only occurs at high frequencies. The elevated baseline hearing thresholds stretch over both the high and low frequencies. Further aspects leading to error in estimation of Eigil's hearing threshold are the comparatively conservative statistical analysis of the resulting EFR data (F-test) and the use of AEP stimuli, which are likely to be shorter than the auditory integration time of the animal's hearing system.

As a consequence of this physiological and physical masking, the measured baseline hearing thresholds cannot be regarded as absolute but should be defined as masked thresholds, and, accordingly, the documented TSs have to be regarded as masked temporary threshold shifts. The presence of masking noise may have reduced the amount of TTS measured, as indicated by TTS studies on humans (Humes, 1980) and chinchillas (Ades *et al.*, 1974), simulating a pre-exposure reduction in hearing sensitivity. Nevertheless, the onset level of TTS itself, as defined in this study, is likely to be unaffected by the masking noise (Finneran *et al.*, 2005; Southall *et al.*, 2007), presumably due to its comparatively low acoustic energy in comparison to the intense airgun stimuli.

Whether the differences in TTS levels between harbor porpoises and the marine mammal species tested so far are species-specific or representative of the functional hearing groups, as defined by Southall *et al.* (2007), remains unclear. More harbor porpoises, as well as other high-frequency toothed whale species, need to be tested to elucidate this correlation. As for terrestrial animals (Henderson, 2008), the large difference in acoustic tolerance in toothed whales is likely to be attributable to the physical differences in the conductive apparatus rather than to systematic differences in the inner ear. Anatomical differences in the fine structure of the inner ear (Wartzok and Ketten, 1999; Ketten, 2000) and correlated differences in stiffness of the basilar membrane could account for a lower acoustic tolerance to intense sounds in harbor porpoises compared to the toothed whale species tested so far. Moreover, differences in metabolic processes in the inner ear could potentially mediate the high TTS growth rate as well as the long recovery time in harbor porpoises. In the absence of more detailed information it may be valid to generalize and describe this correlation best by means of a mass dependency in the dose-response function for acoustic effects in toothed whales, as documented by Ketten (2006) for the effects of blast impacts.

The TTS data defined in this study are applicable as baseline for the assessment of all activities that go along with the emission of short, impulsive sounds with regard to harbor porpoises. This includes seismic surveys as well as piling construction, both of which show strong acoustic commonalities despite the complexity of their sound emissions. Underwater explosions, however, should be treated separately in this context due to their specific acoustic characteristics of the shock wave, which may yield strong auditory effects irrespective of the peak pressure or energy of the impulse.

Seismic surveys, piling operations, and several other anthropogenic activities at sea involve the repeated emission of intense impulses at varying repetition rates (e.g., 10–15 s interval for seismic surveys and 2–30 s interval for piling). Marine mammals in the vicinity of these operations will consequently be exposed to multiple impulses. While the TTS values determined in this study apply only to a single exposure to a pulsed signal, the auditory effects will accumulate with repeated exposures to such signals if the interval between subsequent exposures is shorter than the recovery time of the hearing system. So far there is no information available on the underlying summation procedure for marine mammals. For harbor porpoises it seems unlikely that they will stay in the area of such intense sound emissions. Nevertheless, if these operations are started without sufficient time for animals to leave the area where received levels will be above or near the TTS levels (as determined in this study), there is an increased risk of TTS or even PTS. The comparatively high TTS growth factor, in combination with the slow recovery rate, worsens this scenario drastically for harbor porpoises compared to mid-frequency odontocetes.

The results emphasize the need for dedicated studies on the cumulative effects of multiple exposures.

ACKNOWLEDGMENTS

Ades, H. W., Trahiotis, C., Kokko-Cunningham, A., and Averbuch, A. (**1974**). "Comparison of hearing thresholds and morphological changes in the chinchilla after exposure to 4 kHz tones," Acta Oto-Laryngol. **78**, 192–206.

Ahroon, W. A., Hamernik, R. P., and Lei, S.-F. (**1996**). "The effect of reverberant blast waves on the auditory system," J. Acoust. Soc. Am. **100**, 2247–2257.

Andersen, S. (**1970**). "Auditory sensitivity of the harbour porpoise *Phocoena phocoena*," *Investigations in Cetacea* (G. Pilleri, Bern), Vol. **2**, pp. 255–259.

Busnel, R. G., Dziedzic, A., and Andersen, S. (**1965**). "Rôle de l'impédance d'une cible dans le seuil de sa détection par le système sonar du marsouin *P. phocaena* (Role of the target strength on the detection threshold by the sonar system of the harbour porpoise)," C.R. Séances Soc. Biol. **159**, 69–74.

Finneran, J. J., Carder, D. A., Schlundt, C. E., and Ridgway, S. H. (**2005**). "Temporary threshold shift (TTS) in bottlenose dolphins (*Tursiops truncatus*) exposed to mid-frequency tones," J. Acoust. Soc. Am. **118**, 2696–2705.

Finneran, J. J., Houser, D. S., and Schlundt, C. E. (**2007**). "Objective detection of bottlenose dolphin (*Tursiops truncatus*) steady-state auditory evoked potentials in response to AM/FM tones," Aquat. Mamm. **33**, 43–54.

Finneran, J. J., Schlundt, C. E., Dear, R., Carder, D. A., and Ridgway, S. H. (**2002**). "Temporary shift in masked hearing thresholds in odontocetes after exposure to single underwater impulses from a seismic watergun," J. Acoust. Soc. Am. **111**, 2929–2940.

Gordon, J., Freeman, S., Chappell, O., Pierpoint, C., Lewis, T., and MacDonald, D. (**2000**). "Investigations of the effects of seismic airguns on harbour porpoises: Experimental exposures to a small source in inshore waters," in *Behavioural and Physiological Responses of Marine Mammals to Acoustic Disturbance (BROMMAD)*, edited by D. Thompson (University of St. Andrews, St. Andrews, UK).

Hall, J. W., III (**2006**). *New Handbook for Auditory Evoked Responses* (Allyn and Bacon, Boston, MA).

Henderson, D. (**2008**). "Creation for noise standards for man: 50 years of research," Bioacoustics **17**, 10–12.

Hildebrand, J. (**2004**). "Sources of anthropogenic sound in the marine environment," International Policy Workshop on Sound and Marine Mammals, London, UK, 28–30 September.

Humes, L. E. (**1980**). "Temporary threshold shift for masked pure tones," Audiology **19**, 335–345.

Kastelein, R. A., Bunskoek, P., Hagedoorn, M., and Au, W. W. L. (**2002**). "Audiogram of a harbour porpoise (*Phocoena phocoena*) measured with narrow-band frequency-modulated signals," J. Acoust. Soc. Am. **112**, 334–344.

Ketten, D. R. (**2000**). "Cetacean Ears," in *Springer Handbook of Auditory Research*, edited by W. W. L. Au, A. N. Popper, and R. R. Fay (Springer, New York, NY), Vol. **12**, pp. 43–108.

Ketten, D. R. (**2006**). "Experimental measures of blast and acoustic trauma in marine mammals," Final Report, Office of Naval Research.

Ketten, D. R., and Finneran, J. J. (**2004**). "Noise exposure criteria: Injury (PTS) criteria," Presentation at the Second Plenary Meeting of the Advisory Committee on Acoustic Impacts on Marine Mammals, Arlington, VA.

Ketten, D. R., Lien, J., and Todd, S. (**1993**). "Blast injury in humpback whale ears: Evidence and implications," J. Acoust. Soc. Am. **94**, 1849–1850.

Kryter, K. D. (**1994**). *The Handbook of Hearing and the Effects of Noise* (Academic, New York).

Lucke, K., Lepper, P. A., Hoeve, B., Everaarts, E., van Elk, N., and Siebert, U. (**2007**). "Perception of low-frequency acoustic signals by a harbour porpoise (*Phocoena phocoena*) in the presence of simulated offshore wind turbine noise," Aquat. Mamm. **33**, 55–68.

Madsen, P. T. (**2005**). "Marine mammals and noise: Problems with root mean square sound pressure levels for transients," J. Acoust. Soc. Am. **117**, 3952–3957.

McCauley, R. D., Fewtrell, J., Duncan, A. J., Jenner, C., Jenner, M.-N., Penrose, J. D., Prince, R. I. T., Adhitya, A., Murdoch, J., and McCabe, C. (**2000**). "Marine seismic surveys: Analysis and propagation of air-gun signals and effects of air-gun exposure on humpback whales, sea turtles, fishes and squid," Report on research conducted for The Australian Petroleum Production and Exploration Association.

McCauley, R. D., Fewtrell, J., and Popper, A. N. (**2003**). "High intensity anthropogenic sound damages fish ears," J. Acoust. Soc. Am. **113**, 638–641.

Nachtigall, P. E., Pawloski, J. L., and Au, W. W. L. (**2003**). "Temporary threshold shifts and recovery following noise exposure in the Atlantic bottlenose dolphin (*Tursiops truncatus*)," J. Acoust. Soc. Am. **113**, 3425–3429.

Nachtigall, P. E., Supin, A. Ya., Pawloski, J. L., and Au, W. W. L. (**2004**). "Temporary threshold shifts after noise exposure in the bottlenose dolphin (*Tursiops truncatus*) measured using auditory evoked potentials," Marine Mammal Sci. **20**, 673–687.

OSPAR Commission (**2000**). "Quality Status Report 2000, Region II–Greater North Sea," OSPAR Commission, London.

Parker, D. E., Tubbs, R. L., Johnston, P. A., and Johnston, L. S. (**1976**). "Influence of auditory fatigue on masked pure-tone thresholds," J. Acoust. Soc. Am. **60**, 881–885.

Pavan, G., Manghi, M., and Fossati, C. (**2001**). "Software and hardware sound analysis tools for field work," *Proceedings of the 2nd Symposium on Underwater Bio-Sonar and Bioacoustic Systems*, Proc. I.O.A., Vol. **23**, pp. 175–183.

Picton, T. W. (**1987**). "Evoked potentials, auditory, human," in *Encyclopedia of Neuroscience*, Vol. **1**, edited by G. Adelmann (Birkhäuser, Boston).

Popov, V. V., and Supin, A. Ya. (**1990**). "Electrophysiological studies of hearing in some cetaceans and manatee," in *Sensory Abilities of Cetaceans: Laboratory and Field Evidence*, edited by J. A. Thomas and R. A. Kastelein (Plenum, New York), pp. 405–415.

Pryor, K. (**1984**). *Don't Shoot the Dog: The New Art of Teaching and Training* (Bantam Books, New York).

Ramirez, K. (**1999**). *Animal Training: Successful Animal Management Through Positive Reinforcement* (Shedd Aquarium, Chicago, IL).

Richardson, W. J., Greene, C. R., Jr., Malme, C. I., and Thomson, D. H. (**1995**). *Marine Mammals and Noise* (Academic, San Diego, CA).

Schlundt, C. E., Dear, R. L., Carder, D. A., and Finneran, J. J. (**2006**). "Growth and recovery of temporary threshold shifts in a dolphin exposed to midfrequency tones with durations up to 128 s," J. Acoust. Soc. Am. **120**, 3227.

Southall, B. L., Bowles, A. E., Ellison, W. T., Finneran, J. J., Gentry, R. L., Greene, C. R., Jr., Kastak, D., Ketten, D. R., Miller, J. H., Nachtigall, P. E., Richardson, W. J., Thomas, J. A., and Tyack, P. L. (**2007**). "Marine mammal noise exposure criteria: Initial scientific recommendations," Aquat. Mamm. **33**, 411–414.

Supin, A. Ya., Popov, V. V., and Mass, A. (**2001**). *The Sensory Physiology of Aquatic Mammals* (Kluwer, Boston, MA).

Tougaard, J., Carstensen, J., Henriksen, O. D., Skov, H., and Teilmann, J. (**2003**). "Short-term effects of the construction of wind turbines on harbour porpoises at Horns Reef," Technical Report No. HME/362-02662, TechWise A/S, Hedeselskabet, Roskilde.

Verboom, W. C., and Kastelein, R. A. (**1995**). "Acoustic signals by harbour

J. Acoust. Soc. Am., Vol. 125, No. 6, June 2009

Lucke *et al.*: Threshold shift in a harbor porpoise   4069

porpoises (*Phocoena phocoena*)," in *Harbour Porpoises—Laboratory Studies to Reduce Bycatch*, edited by P. E. Nachtigall, J. Lien, W. W. L. Au, and A. J. Read (De Spil, Woerden, The Netherlands), pp. 1–39.

Verfuß, U. K., Miller, L. A., and Schnitzler, H.-U. (**2005**). "Spatial orientation in echolocating harbour porpoises (*Phocoena phocoena*)," J. Exp. Biol. **208**, 3385–3394.

Wartzok, D., and Ketten, D. R. (**1999**). "Marine mammal sensory systems," in *Biology of Marine Mammals*, edited by J. E. Reynolds III and S. A. Rommel (Smithsonian Institution Press, Washington, London), pp. 117–175.

Yost, W. A. (**2000**). *Fundamentals of Hearing: An Introduction* (Academic, New York).

JNCC Report
No: 544

The identification of discrete and persistent areas of relatively high harbour porpoise density in the wider UK marine area

Stefan Heinänen, Henrik Skov

March 2015

Summary

This report provides the results of detailed analyses of 18 years of survey data in the Joint Cetacean Protocol (JCP) undertaken to inform the identification of discrete and persistent areas of relatively high harbour porpoise (*Phocoena phocoena*) density in the UK marine area within the UK Exclusive Economic Zone (EEZ). This identification is needed for the fulfilment of obligations required by the EU Habitats Directive.

Although JCP comprises the largest collation of standardised survey data on harbour porpoise (in total at least 545 distinct surveys from ship and aircraft) the different 'Management Units' (MUs, division of populations of a particular species into smaller units based on ecological evidence and/or divisions used for the management of human activities) have received a variable survey coverage over the 18 years. As a consequence, many areas have been surveyed only over a few years, making reliable projected estimates of yearly distributions a challenging task. The study addressed these challenges by developing distribution models statistically. The models are capable of predicting seasonal and yearly mean densities (number of animals per unit area) by integrating survey-specific information with annual and seasonal data on environmental conditions, using space-time statistical 'smoothing' methods for periods of several years.

The distribution models were, to a large degree, based on a hydrodynamic model framework consisting of both a 2D model (currents) and a 3D model (water column structure). Post-processing methods were used to transform hydrodynamic variables into dynamic habitat predictors for the distribution models. Data on concentrations of prey to harbour porpoises are not available for the entire EEZ area in the required fine spatial scale (5km). Therefore, physical oceanographic properties of currents, water masses, and the seafloor that enhance the probability for harbour porpoises of encountering prey within the range of their preferred habitats were used as habitat variables (predictor variables). Anthropogenic disturbance predictors have been included in the form of mean shipping intensity at the resolution required.

The model results indicate that the sampled densities of harbour porpoises are influenced by both oceanographic and anthropogenic pressure variables. Water depth and hydrodynamic variables seem to have an influence on the distribution both in the Celtic and Irish Seas, and in the North Sea MUs. The response to water depth in the Celtic and Irish Sea regions shows a preference for shallower areas, while the responses in the North Sea region show two peaks during summer; one at 40m and one at 200m depth. Surface salinity is an influential water mass descriptor in relation to predicting the presence of the animals in the North Sea, and reflects avoidance of estuarine water masses. In the North Sea, the stability of the water column in terms of temperature differences is the most important determinant of the density of harbour porpoise occurrence during summer. This response displays similar patterns to water depth, with two peaks: one at the interface between mixed and stratified waters (tidal mixing front), and another peak at high values of stratification (typically found in deeper areas).

Eddy activity modelled by the hydrodynamic model is an important dynamic predictor variable in the Celtic/Irish Sea and North Sea, and current speed is also an important predictor in the Celtic/Irish Sea. The coarseness of surface sediments seems to play a major role for the presence and density of porpoises in all three management units. The model results also indicate a negative relationship between the number of ships and the distribution of harbour porpoises in the Celtic/Irish Sea and the North Sea, but not in north-west Scottish waters.

The identification of discrete and persistent areas of relatively high harbour porpoise density in the wider UK marine area

The yearly predictions of the summer and winter distribution of harbour porpoises reflect the relationships with the physical conditions and shipping traffic as well as with the time and location of the observations. Analyses of the persistence of high density areas integrated evaluations of the number of years high densities were predicted for an area, with evaluations of the degree of recent high densities as predicted by the distribution models.

Due to the uneven survey effort over the modelled period, the uncertainty in modelled distributions vary to a large extent. The uncertainty of the modelled density estimates as visualised by the patterns of relative standard errors indicates robust model predictions in most parts of St. George's Channel, Irish Sea and Welsh coastal waters, in all shelf waters of the North Sea north of the Channel and in most parts along the north-west Scottish coast. However, model uncertainties are particularly high during winter as well as offshore off north-west Scotland and in the Celtic Sea. To avoid identification of modelled high-density areas that do not reflect the patterns of observed densities, only areas with three or more years of survey effort were included in the ultimately devised set of persistent high-density areas.

The identified persistent high density areas are:

- Three coastal areas off west Wales (Pembrokeshire and Cardigan Bay), and north-west Wales (Anglesey, Lleyn Peninsula), and part of the Bristol Channel (Camarthen Bay)
- Smaller areas north of Isle of Man (winter) and on the Northern Irish coast near Strangford Lough
- Western Channel off Start Point, Cornwall (summer)
- North-western edge of Dogger Bank (summer)
- Inner Silver Pit
- Offshore area east of Norfolk and east of outer Thames estuary (winter)
- Smith Bank, Outer Moray Firth (summer)
- Coastal areas off north-west Scotland, including the Minches and eastern parts of the Sea of Hebrides.

The identification of discrete and persistent areas of relatively high harbour porpoise density in the wider UK marine area

Persistent high-density summer
Persistent high-density winter
Persistent high-density summer and winter
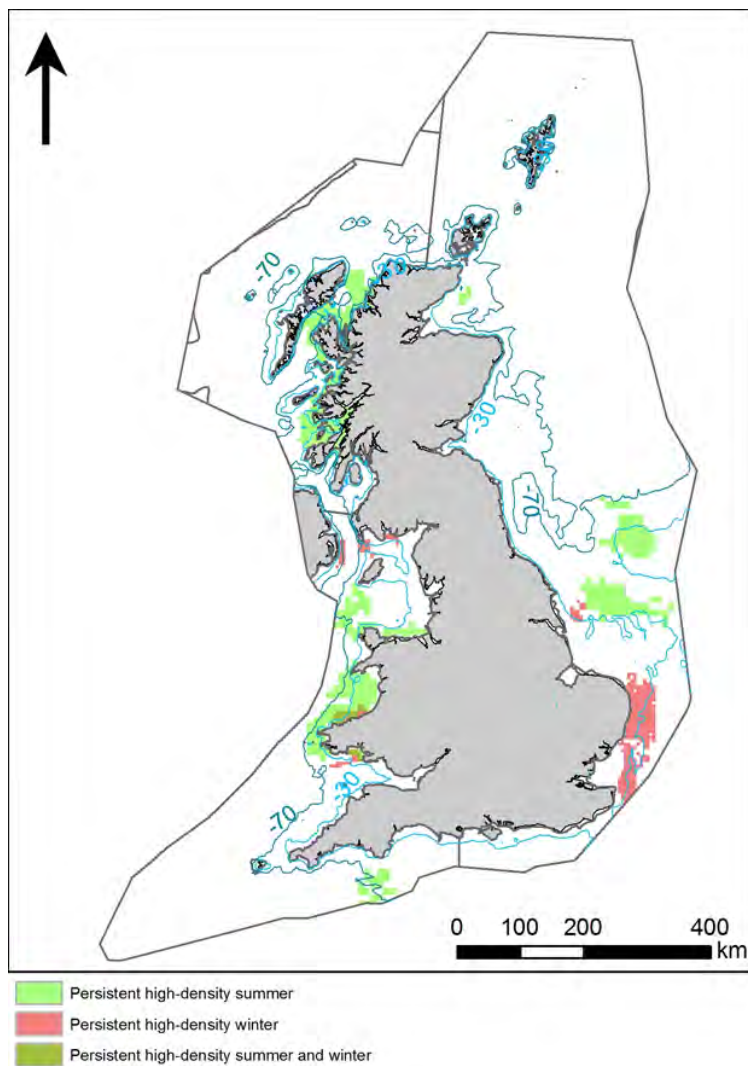
Map showing selected persistent high-density areas of harbour porpoise with survey effort from three or more years, as derived from the statistical manipulations used in the present report.

The following areas were also identified as persistent high-density areas, but due to less than three years of survey effort they were not included in the above list:

•   Parts of high density zone between western edge of Dogger Bank and Norfolk coast, including both the Inner and Outer Silver Pit areas
•   Offshore area north of Shetland
•   Edge of the Norwegian Trench
•   Shelf edge off south-west Cornwall.

Contents

List of abbreviations

AIS	Automatic Identification System
AUC	Area Under the Curve (of a receiver operating characteristic curve)
BGS	British Geological Survey
Dev. Exp.	Deviance Explained
EEZ	Exclusive Economic Zone
F	Relative strength of predictor variable in model
GAM	Generalized Additive Model
GAMM	Generalized Additive Mixed Model
JCP	Joint Cetacean Protocol
MGCV	Mixed GAM Computation Vehicle supplied with R for generalized additive modelling
MU	Harbour porpoise Management Unit
P	Approximate statistical significance of the smooth terms (variables) included in the model
PSU	Practical Salinity Units
R	Statistical software package 'R'
SAC	EU Special Area of Conservation
SCANS	Small Cetaceans in the European Atlantic and North Sea
SNCB	Statutory Nature Conservation Body
Z	Chi-square test statistic

1   Introduction

For the further development of the UK's Natura 2000 network, a network of nature protection areas established under the EU Birds[1] and Habitats Directive[2], identification of discrete and persistent areas of relatively high harbour porpoise (*Phocoena phocoena*) density is required for the UK marine area out to the 200 nautical miles limit. This report provides the results of detailed analyses of the Joint Cetacean Protocol (JCP) undertaken to inform this identification.

Following the requirements of the Habitats Directive in relation to Special Areas of Conservation (SACs) for the Directives' 'Annex II' species, sites will be proposed for the Natura 2000 network only where there is a clearly identifiable area representing the physical and biological factors essential to their life and reproduction. Although a number of SACs have been identified for which harbour porpoise is listed for Natura, it has been difficult to clearly identify important sites for this species. Under Article 4 of the EU Habitats Directive, the UK has a number of sites graded D[3] for the species (34) and one site graded C (Skerries & Causeway, Northern Ireland), but no areas have been graded as either A or B.

Realising the difficulties in implementing criteria for designation of SACs for the species based on absolute estimates (corrected for missed animals) of density and abundance, the focus of the study was on determination of discrete areas of relatively high and persistent harbour porpoise density in UK waters. The JCP data set represents the largest collated cetacean database in the world with results from a wide range of surveys. However, the data remains patchy, fragmented and often uneven, leaving many uncertainties, and a unified understanding of harbour porpoise distribution in the three management units has not so far been achieved. The environmental factors governing distribution of the species in UK waters, for example, have not been conclusively identified, and this has impaired on the possibility to define 'good' porpoise habitats. Adding to this, due to the spatio-temporal patchiness of the survey effort, determination of the persistence over time of areas of high densities of harbour porpoises has been very difficult.

This study addressed these challenges by developing statistical distribution models capable of predicting seasonal and yearly mean densities in the three management units (MUs) (see Figure 1) between 1994 and 2011 using the environmental specifics in the management units. The models were developed using the JCP data set in combination with spatial and temporal explicit oceanographic data as well as static data on topography and anthropogenic pressures. The JCP at-sea observation data set (no land-based data included) comprises 39 data sources with data from at least 545 distinct survey platforms (ships and aircraft) representing over 1.1 million km of survey effort (distance over which surveying was carried out).

The database made available to this analysis consisted of standardised effort and corrected densities of harbour porpoises aggregated into transect segments roughly 10km long (Paxton *et al.* 2012). Densities of observed animals had been corrected for distance, perception (animals missed by observers) and availability (animals missed due to diving behaviour) bias. The production of standardised corrected densities across the wide range of survey platforms and methods rests on a number of assumptions regarding comparability of search efforts and detection functions.

---

[1] See http://eur-lex.europa.eu/LexUriServ/LexUriServ.do?uri=OJ:L:2010:020:0007:0025:EN:PDF
[2] See http://www.central2013.eu/fileadmin/user_upload/Downloads/Document_Centre/OP_Resources/HABITAT_DIRECTIVE_92-43-EEC.pdf
[3] SACs are graded from A to D based on national population within the site based on the proportion of the national population within the site. See http://ec.europa.eu/environment/nature/legislation/habitatsdirective/docs/standarddataforms/notes_en.pdf

1.1   Scope of Work

The main aim of the modelling study is to determine whether there are *clearly identifiable and persistent areas of relatively high harbour porpoise density* (number of animals per unit area). The term 'clearly identifiable' has been taken to mean that the area can be delineated from the surrounding (neighbouring) waters by, for example, *an elevated abundance on a regular basis and over a reasonable period of time*. In addition, the strength of the evidence increases with the degree to which higher densities have occurred recently.

In order to produce models for harbour porpoise density by MUs using the JCP data, they need to take into account the following considerations:

1.   Initially, areas where there has been insufficient temporal observation effort will need to be identified and mapped. Any persistent areas of high density identified through the modelling that correspond to areas with insufficient temporal data will not be considered during the present analysis. Such areas are, however, reported as they will, be used to provide an indication of where surveys could potentially be focused in the future.

2.   It is recognised that fitting the model to the entire dataset is too computationally burdensome. Therefore, for the analysis, the dataset needs to be divided into a series of subsets. The three harbour porpoise Management Units (MUs) proposed by the SNCBs were therefore adopted for the present analysis. These are the Celtic and Irish Sea MU, North Sea MU and West Scotland MU (Figure 1).

3.   The sightings data need to be standardised by the characteristics of the observational effort and (relative) abundance data generated, taking effort extent into account.

4.   Spatio-temporal models need to be fitted to these abundance data for the appropriate subsets, using similar methods to those employed in Paxton *et al.* (2012). One difference, however, is that a greater focus is given to capturing small-scale spatial, but relatively long-term temporal, density variations. The choice of model selected needs to identify significant environmental covariates.

5.   The predictions from the spatio-temporal models are then examined for persistent areas of high density between years, using a variety of techniques. An exploration of available methods for the delineation of such areas needs to be undertaken and the most appropriate method used, with a justification provided.

6.   Analysis needs to be undertaken on the entire sea area for management unit, but resulting maps need to be masked to only display the results within the UK limits. This should allow boundary effects (higher uncertainty close to the boundaries) to be taken into account.

7.   The relationship between estimated abundance within these areas and size of area need to be examined, to determine if there are nonlinearities such that a high proportion of data about overall abundance can be captured within a relatively small area. The models need also to include information on the variability over time of these areas (seasonally and inter-annually as appropriate).
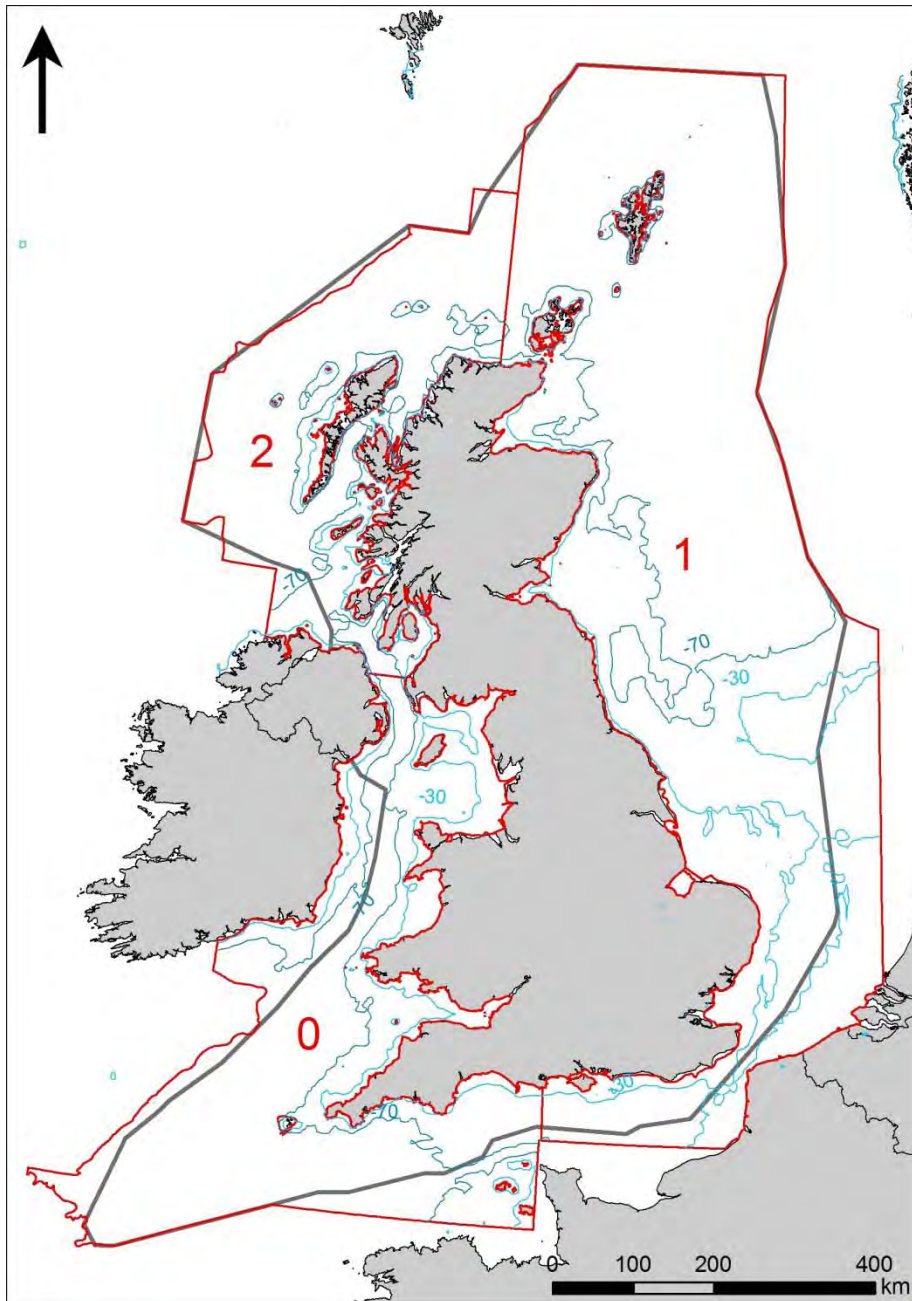
Figure 1. UK management units (0-2; 0 Celtic/Irish Sea, 1 North Sea, 2 West Scottish Waters) for harbour porpoise (red colour) and the mask used for presentation of model results (black line). The 30m and 70m depth contours are indicated.

2 Methods

2.1 Overview of analytical approach

An overview of the model design is given in Figure 2, which outlines the different phases of the analyses undertaken to produce this report. The model design began with a hydrodynamic model framework consisting of a 2D model producing time-series information about water currents and associated variables, and a 3D model producing time-series information about water-mixing regimes and associated variables. Post-processing methods were used to devise and define dynamic-habitat predictors and distribution models covering the summer (April-September) and winter (October-March) seasons. The chains were also used to derive statistical harbour porpoise densities to the predictor variables.

To be able to accurately describe the distribution of marine mammals over time it is necessary to take account of the actual oceanographic components realised during each observation; i.e. currents, oceanographic fronts, water temperature, salinity, water mixing as well as the anthropogenic pressure components, as for example disturbance from ship traffic. Without taking into account these characteristics, distribution models of marine mammals will be unlikely to resolve the true variation in the distribution of the animals. A way to derive in-situ oceanographic factors is by linking observations to numerical 3-dimensional hydrodynamic models. 3D hydrodynamic models enable mapping of locations, timing and movement of salinity fronts, eddies and upwelling which enhance the probability of prey detection for marine mammals. These features are driven by daily and seasonal variations in weather, tidal cycles, freshwater run-off cycles from land and major current systems. They are key differentiators in the marine landscapes, and thereby the associated biodiversity. The hydrodynamic model set-up is described in Appendix 1.

The fourth step, spatio-temporal modelling, is the crucial step of this study. In this step, the corrected densities of harbour porpoises were modelled as a response to the spatio-temporal dynamics of habitat features and shipping density. Data on concentrations of prey to harbour porpoises are not available for the entire EEZ area at the required fine spatial scale. Therefore, physical properties of the habitat that enhance the probability of harbour porpoises encountering prey offer the best predictors (Skov *et al.*, 2014). The temporal variation in the physical environment has been extracted from the hydrodynamic model based on both time and location to the species observations. Anthropogenic disturbance predictors have been included in the form of mean shipping intensity. This approach has allowed for prediction of the distribution of the harbour porpoises in space and time.

Generalized Additive Models (GAMs) were chosen as the basis for spatio-temporal modelling due to the suitability of GAMs for this type of data because they can deal with non-linear relationships, non-normally distributed errors, and over-dispersions. The JCP survey data displays a significant amount of over-dispersion due to an excess of zeros (absences), which is often called 'zero inflation' (Martin *et al.* 2005). After testing several model designs (see section 4.2), the zero-inflation has been dealt with by modelling the distribution in two-steps: (1) a probability part (fitted with a binomial distribution) and (2) a positive part, where all zeros are excluded (fitted with a gamma distribution). These types of models are in the literature usually called 'hurdle models' or 'delta-gamma models' (Stefánsson 1996, Heinänen *et al.* 2008). The predictions of both steps are then combined to produce the final density models.

Despite aggregation and standardisation, the JCP data s*et al*so displays a degree of spatial and temporal autocorrelation that undermines the assumption of independence if it cannot be explained by the included environmental variables. Thus, residuals have been checked for autocorrelation, and the need for extending the GAMs to generalized additive mixed models (GAMMs) has been assessed (Zuur *et al.* 2009).
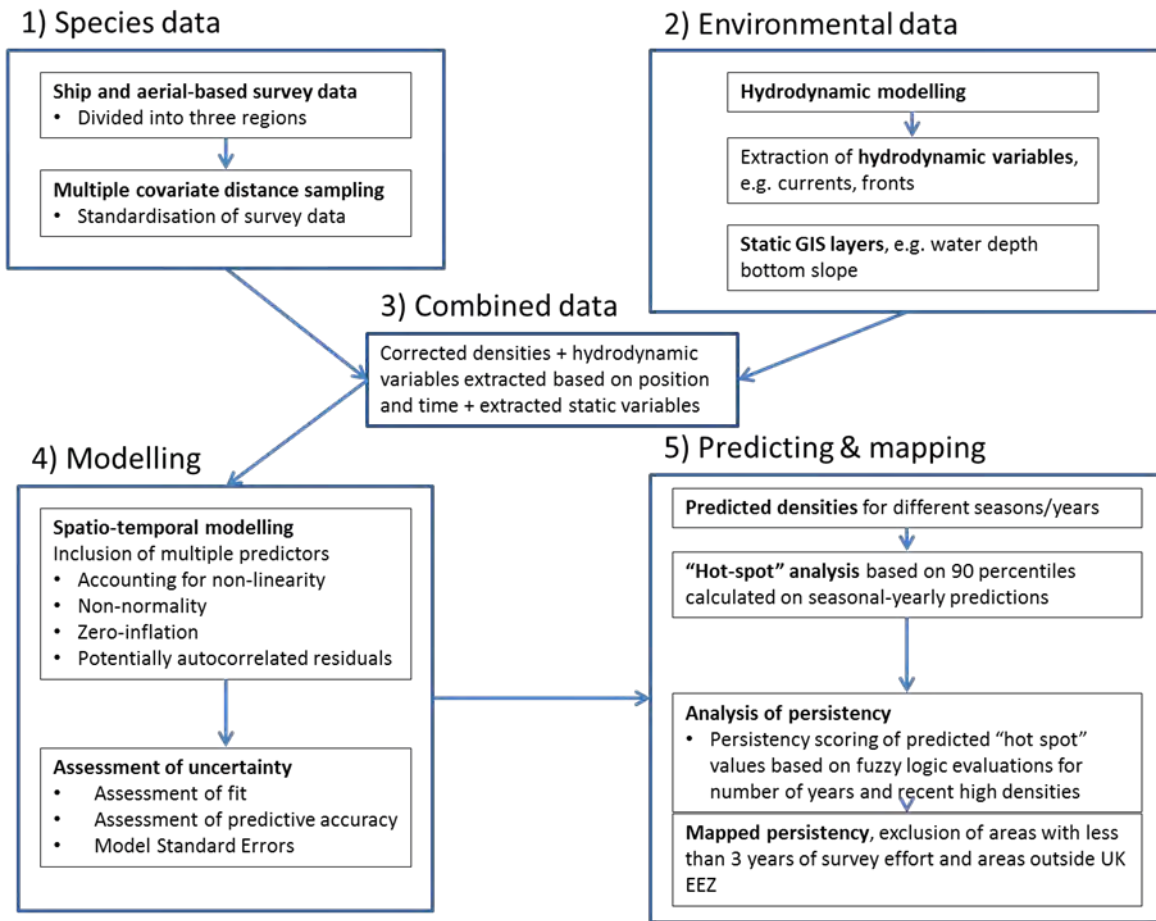
1) Species data

Ship and aerial-based survey data
- Divided into three regions

Multiple covariate distance sampling
- Standardisation of survey data

2) Environmental data

Hydrodynamic modelling

Extraction of **hydrodynamic variables**, e.g. currents, fronts

Static GIS layers, e.g. water depth bottom slope

3) Combined data

Corrected densities + hydrodynamic variables extracted based on position and time + extracted static variables

4) Modelling

Spatio-temporal modelling
Inclusion of multiple predictors
- Accounting for non-linearity
- Non-normality
- Zero-inflation
- Potentially autocorrelated residuals

Assessment of uncertainty
- Assessment of fit
- Assessment of predictive accuracy
- Model Standard Errors

5) Predicting & mapping

Predicted densities for different seasons/years

"Hot-spot" analysis based on 90 percentiles calculated on seasonal-yearly predictions

Analysis of persistency
- Persistency scoring of predicted "hot spot" values based on fuzzy logic evaluations for number of years and recent high densities

Mapped persistency, exclusion of areas with less than 3 years of survey effort and areas outside UK EEZ

Figure 2. The different working steps of the study.

2.2 Standardised JCP data on densities of harbour porpoise

The JCP data standardised to transect segments of equal length on densities of harbour porpoise were provided by JNCC. The data included 40 data sources covering a period of 18 years between 1994 and 2011 and cover the entire UK EEZ. Effort data were supplied as segments; the majority of the survey segments were approximately 10km long, however segments of both small and larger size were included. Sightings data were supplied as corrected abundance per segment. Details of the corrections applied to sightings to account for distance, perception and availability bias are given by Paxton *et al*. (2012). The data for 2011 mainly covered an international survey of the Dogger Bank area. The corrections applied to the 2011 data are similar to the corrections listed by Paxton *et al*. (2012). The data were split into the three Management Units (MUs; Figure 1). The majority of the survey effort segments were approximately 10km long, however segments of both smaller and larger sizes were included.

Only sightings and effort collected in sea state 2 or less were included. The yearly distribution of effort is shown in Appendix 2. In the Celtic/Irish Sea MU for most years in the period a comparable amount of effort is included in the database for the western Channel, Celtic Sea, St. George's Channel and the Irish Sea. A proportionally larger effort was made during the SCANS surveys in 1994 and 2005 (Hammond *et al*. 2002, 2013). In the coastal areas of the western Channel, Wales and western Irish Sea most survey effort has been undertaken after 2000. In contrast, in MU 1, the North Sea, there was a shift in the distribution of effort took place in 2003. With the exception of the SCANS survey in 1994, the whole area south of a line between Flamborough Head and the northern flanks of the Dogger Bank had virtually no effort before 2003. Yet, from 2003 to 2011 the southern part of the management unit has

received much effort on account of baseline surveys related to offshore wind energy development schemes. Survey effort in MU 2, north-west of Scotland, has been focused on inshore west coast areas and the Minches, and these parts have received a relatively even amount of effort spread over the period. The offshore areas west of the Hebrides were only surveyed in 1994 and 2007. The majority of the data collected in this area was only in summer.

2.3   Development of predictor variables

Studies on the biological oceanography of marine top predators have documented that the fine-scaled geographical distribution of these animals is correlated with hydrographic fronts, upwelling and eddies, exhibiting spatial dynamics and oscillations at different frequencies (Schneider 1982, Kinder *et al.* 1983, Skov & Prins 2001, Camphuysen *et al.* 2006). So, by statistically relating the hydrodynamic variables to the observed distribution of harbour porpoise, the development of distribution models will be possible which both accurately describe discrete areas of concentration of the species, and which captures the year-to-year and seasonal variation in the location of these areas on account of the temporal changes in the regional physical oceanography.

A prerequisite for the dynamic predictors to be useful in predictive modelling is their availability as GIS data layers covering the entire model area during the whole survey period. The selection of predictors is based on experience from modelling harbour porpoise distribution in the German Bight (Skov & Thomsen 2008, Skov *et al.* 2014).

The model results from the German Bight highlighted the importance of frontal features, rather than parameters reflecting structures and processes at a large scale like water masses and currents. In the oceanographic context of UK waters, these structures may be grouped as follows:

1.   Horizontal high-frequency fronts;
2.   Semi-permanent up-/down-welling cells;
3.   Semi-permanent eddies.

The processes responsible for the increased predictability and probability of prey to marine predators at certain hydrographic fronts in the horizontal as well as vertical planes have been explained by their persistent occurrence (Schneider 1982, Kinder *et al.* 1983, Skov & Prins 2001, Camphuysen *et al.* 2006). For this project, variables were selected that reflect conditionally stable processes and structures. These variables essentially comprise horizontal fronts and eddies. High-frequency horizontal fronts build between currents and water masses which are controlled by either tides and/or discontinuities in bottom topography. On the UK shelf, tidal mixing fronts marking the boundaries between stratified and mixed water column forms a particularly significant effect with strong influences on biological productivity (Pingree & Griffiths 1978, Nielsen *et al.* 1993, Pedersen 1994).

Plume fronts develop where river discharges form strong gradients in salinity towards more-saline offshore water masses. Discontinuities of bottom topography, including extensions of islands and headlands on larger landmasses, can interact with strong currents to generate semi-permanent fronts and eddies with enhanced local biological productivity (Camphuysen *et al.* 2006). Another striking frontal feature in the UK EEZ is the fronts which develop where water masses from the deeper parts of the North Atlantic propagates across the shelf break driven by oceanic currents and tides. Shelf-break fronts and associated mixing and eddies support high densities of marine life at all trophic levels (Schneider & Hunt 1982, Mann & Lazier 1991).

The patterns created by tidal currents were expected to be small scale, while patterns created by changes in mixing regimes and water density were expected to be large scale. Therefore

the following habitat predictor variables were computed as seasonal-yearly means: current speed, current gradient and eddy activity (see Figures 4 and 5, Table 1), whereas the following variables were computed as seasonal means across years: difference between top and bottom temperature and surface salinity (see Figures 5 and 6, Table 1). The parameter 'current gradient' or frontal strength was developed from the UK 2D flow model by calculating the local gradient ($|dU/dx|+|dV/dy|$) in horizontal current from the eastern and northern current components (U and V) (Table 1). The horizontal eddy activity abs($|dV/dx|-|dU/dy|$) was similarly calculated to represent the local 'eddy potential', with absolute values of anticlockwise and clockwise eddies (Table 1). In the two expressions dx and dy indicate the horizontal grid spacing in the east and north direction, respectively. Patterns in mixing regimes were calculated by differences between top and bottom temperatures, while patterns in estuarine impact were calculated from surface salinity using computed values from the UK 3D flow model.

Static, topographic predictors have also been shown before to be useful for describing the distribution of pelagic species. Water depth (see Figure 7, Table 1) was included as a predictor using the model bathymetry used in the UK 2D flow model. As the processes potentially enhancing the probability of prey encounter are expected to be associated with the slopes of sea floor discontinuities (Skov *et al.* 2014) the slope of the seabed was included as a static variable (Figure 7). The slope was calculated based on water depth using the standard slope tool in ArcGIS 10.1 software.

Recent modelling activities in the German Bight suggest that coarseness of surface sediments is an important predictor of harbour porpoise abundance (Skov *et al.* 2014). For inclusion of surface sediments in the distribution models, the DigSBS dataset from the British Geological Survey at the scale of 1:250,000 was used (Cooper *et al.* 2010). In order to cover the entire inshore part of the NNW Scottish Waters MU the EUSeaMap (EMODnet geology) version of the BGS data was used (Cameron & Askew 2011). This data set has been produced to describe regional patterns in surface geology determined from a range of remotely sensed and physical ground truthing data. The method has been critically assessed and is deemed fit for purpose by specialists within the BGS.

The sediment classifications are primarily based on particle size analysis (PSA) of both surface sediment samples and the uppermost sediments taken from shallow cores. Sediments are classified according to the modified Folk scale (Folk 1954). This classification divides sediments into 15 classes, according to the proportions of sand, gravel and mud present. It is based on the weight percentages of Gravel, particles with an average diameter larger than $-1\emptyset$ (2mm); Sand, particles with an average diameter between $-1\emptyset$ (2mm) and $4\emptyset$ (63μm), and Mud, particles with an average diameter smaller than $4\emptyset$ (63μm). A modified Folk triangle classification has been used based on the gravel percentage and the sand to mud ratio. In areas where many samples are taken in close proximity it is possible that several sea-bed sediment types are present, for example in an area of sediment waves the surface sediment type may differ between the crests and troughs of the sediment wave. In these cases, the most commonly sampled sediment type is used to define the mapped area. The modified Folk classes were split into four classes:

1. Muddy
2. Sandy
3. Gravelly (gravel > 5%)
4. Hard bottom

Focal statistics in ArcGIS Spatial Analyst were then used to calculate the mean of these classes within a range of three or five grid cells (15 or 25km). Both were assessed and 15km had a better explanatory ability in Irish Sea–Celtic Sea and sea areas north-west of Scotland and were therefore used, whereas 25km was used in the North Sea (see Figure 6, Table 1). The use of mean values calculated at this coarse scale as a predictor variable was justified by

the need to represent the general characteristics (degree of coarseness) of the surface sediments of the model domain.

The mean density of shipping was included as a pressure variable, as its intensity has been shown by Skov *et al.* (2014) to influence harbour porpoise distribution negatively in the German Bight. Data on ship traffic in the UK EEZ were derived by Anatec Ltd. using their ShipRoutes database (see Figure 8, Table 1). ShipRoutes is a shipping route database developed to assist in identifying shipping passing in proximity to proposed offshore developments such as oil and gas sites, wind farms and dredging areas. The database was developed in two main phases:

• Movements Analysis: The number of movements per year on routes passing through western European waters was estimated by analysing a number of data sources including port callings data and voyage information obtained directly from Ship Operators. It is noted that ShipRoutes excludes the movements of 'non-routine traffic' such as fishing vessels, military vessels, tugs, dredgers, cruise ships, offshore wind farm construction traffic, recreational craft and anchored vessels.
• Routeing Analysis: The routes taken by ships between ports were obtained from several data sources, including:
- Offshore installation, standby vessel and shore-based survey data (radar and Automatic Identification System (AIS) data).
- Satellite tracking of ships.
- Passage plans obtained from Ship Operators.
- Consultation with ports and pilots.
- Admiralty charts and publications.
(Note: routes are generally defined up to the entrances to estuaries, rivers and port approach channels rather than all the way to berth.)

The movements and routeing information was combined to create the ShipRoutes database containing all the shipping routes passing through western European waters, with each route having a detailed distribution of shipping levels and characteristics. The variation in shipping density has been estimated over the 5km model grid by calculating the number of ships per year passing through each cell based on the ShipRoutes data. The calculation is illustrated in Figure 3.
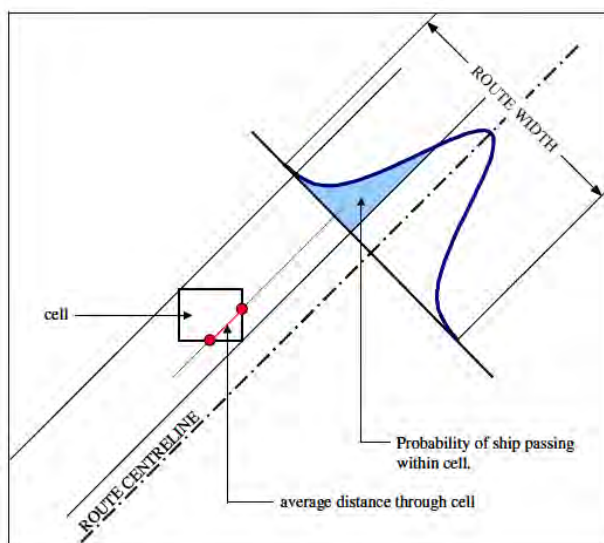
Figure 3. Calculation of Density of Ships passing through a 5km grid cell.

Table 1. List of predictor variables included in the initial prediction models.

Mean density of ships	Description	Rationale for inclusion
Water depth	Static – metres below mean sea level	Key topographic feature
Seabed relief	Static - slope (in degrees from horizontal) of sea floor	Interaction with frontal dynamics which concentrate prey
Densities of ships	Static - mean number of ships/year	Disturbance
Coarseness of sediments	Static - continuous variable (index) describing degree of coarseness of sediments	Key topographic feature which concentrate prey
Surface salinity	Mean seasonal surface salinity (psu) averaged across years	Water mass characteristics
Temperature difference (surface-bottom)	Mean seasonal difference between surface and bottom temperature (C°) averaged across years	Mixing regime, dynamics related to tidal mixing fronts
Current speed	Seasonal-yearly mean of magnitude of horizontal current speed (m/s) integrated over the whole water column	Hydrodynamic structure determining variation in prey availability
Current gradient	Seasonal-yearly mean of horizontal gradient of currents (m/s/m depth) integrated over the whole water column	Hydrodynamic structure concentrating prey
Eddy potential	Seasonal-yearly mean of eddy activity measured as the local vorticity (m/s/m depth) integrated over the whole water column	Hydrodynamic structure concentrating prey
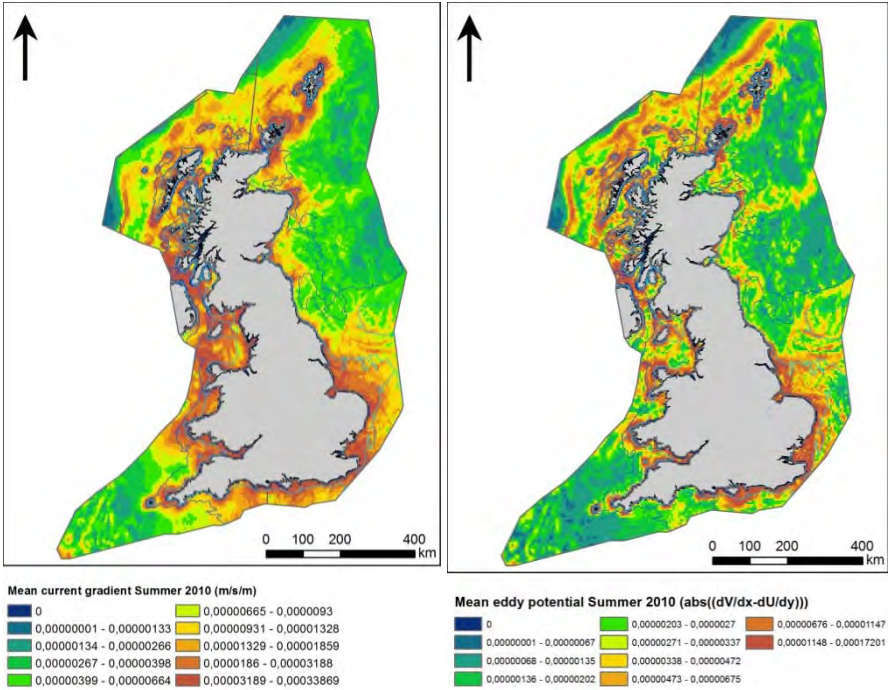
Figure 4. Examples of seasonal mean current gradient (2010) for the summer season and mean eddy activity (2010) for the summer season used as predictor variables.

.
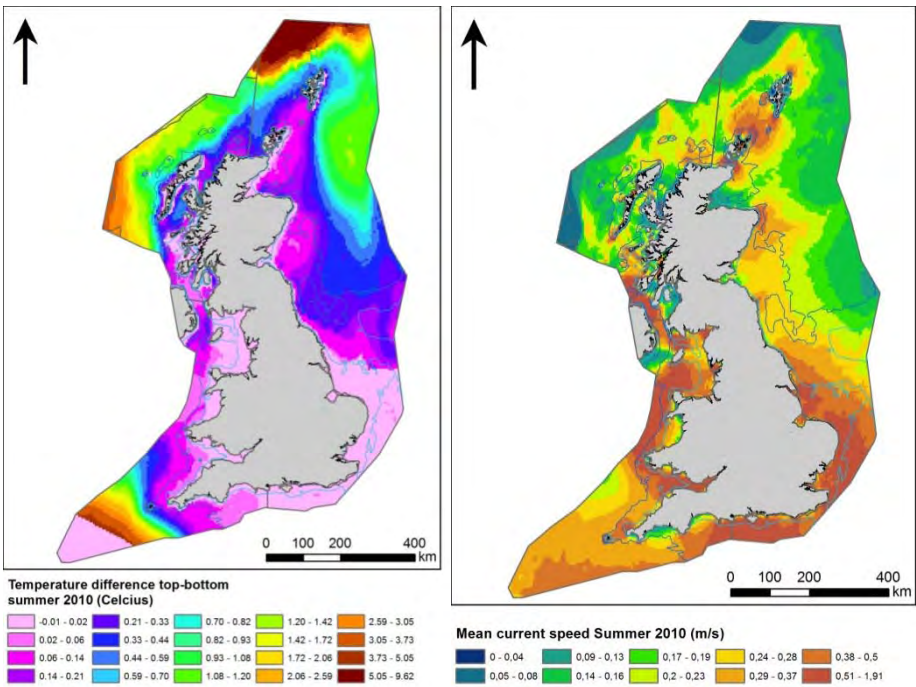
Figure 5. Mean temperature difference between surface and bottom for the summer season and an example of seasonal mean current speed (2010) for the summer season used as predictor variables.

Surface Sediments (Grain size index)

1 - 1,86	2,01 - 2,08	2,41 - 2,6	3,01 - 4
1,87 - 1,98	2,09 - 2,21	2,61 - 2,79	
1,99 - 2	2,22 - 2,4	2,8 - 3	

Surface salinity Summer 2010 (PSU)

0.21 - 29.83	32.04 - 33.01	34.12 - 34.39	34.67 - 34.81	35.09 - 35.22
29.83 - 31.07	33.01 - 33.70	34.39 - 34.53	34.81 - 34.95	35.22 - 35.36
31.07 - 32.04	33.70 - 34.12	34.53 - 34.67	34.95 - 35.09	35.36 - 35.50
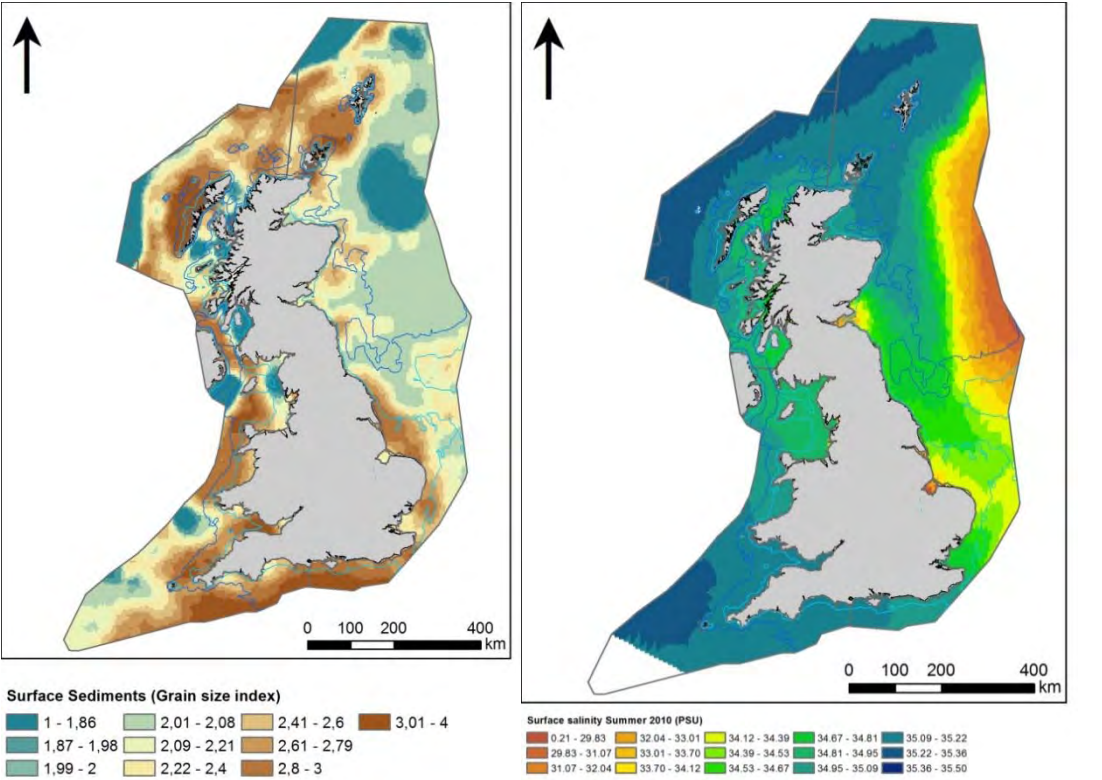
Figure 6. Mean surface salinity (summer) and Index of surface sediment particle size used as a predictor variables.

Water depth (Meters)

-4.453,78 - -1.694,8	-909,01 - -297,85	-158,15 - -123,23	-88,3 - -53,39	-35,91 - -18,46
-1.694,79 - -909,02	-297,84 - -158,16	-123,22 - -88,31	-53,38 - -35,92	-18,45 - -1

Slope of seabed (Degrees)

0	0,035 - 0,067	0,136 - 0,202	0,304 - 0,471	0,808 - 1,581
0,001 - 0,034	0,068 - 0,135	0,203 - 0,303	0,472 - 0,807	1,582 - 8,579
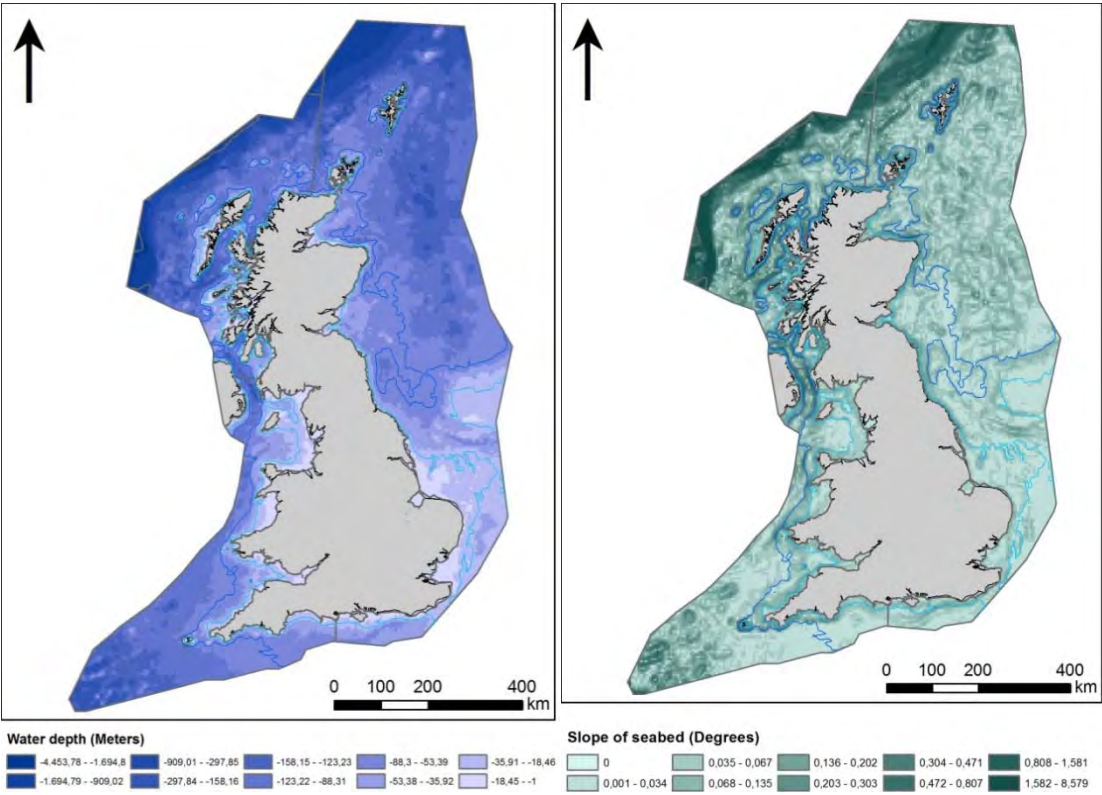
Figure 7. Bathymetry and slope of sea floor used as predictor variables

Number of ships per year

0	795 - 1.191	3.178 - 4.765	16.678 - 101.254
1 - 397	1.192 - 1.985	4.766 - 8.339
398 - 794	1.986 - 3.177	8.340 - 16.677
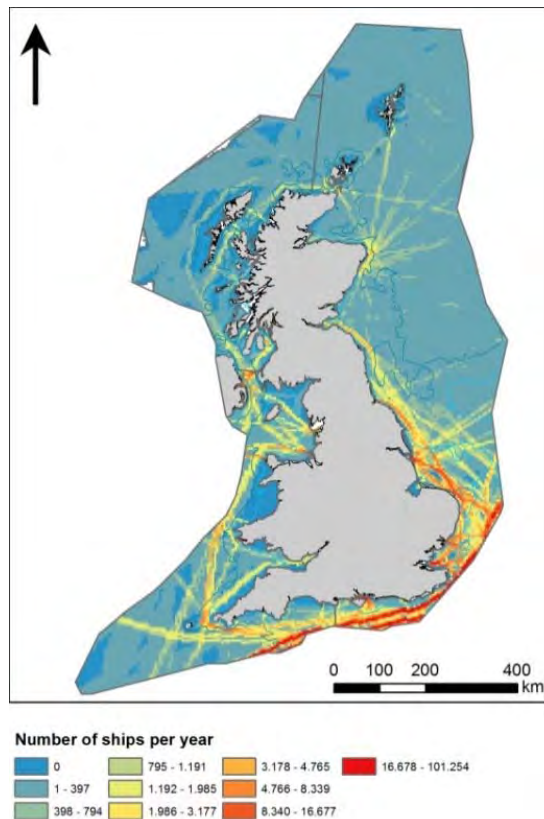
Figure 8. Ship density (number of ships per year) used as a predictor variable.

2.4 Integration of densities and predictor variables

Before model fitting, the standardised and corrected densities of harbour porpoises (response variable) were combined with the dynamic and static environmental variables based on position (midpoint of each segment) and time. Current speed, current gradient and absolute vorticity were extracted based on yearly, seasonal means. Because of the patchy, 'small-scale nature', of the vorticity the mean (combined mean of all years and season) of vorticity was calculated within a range of 15km using focal statistics in ArcGIS 10.1. This was undertaken to better match the scale in the response variable.

Long-term mean seasonal values (2008-2010) of surface salinity and temperature differences were extracted and the static variables water depth, bottom slope, sediments and shipping intensity were also further extracted to the survey data. As the length of the segments in the survey data differed, a segment length was used as a predictor variable in the binomial models (see model description below) to account for the fact that the probability of observing a porpoise increases with effort. The, X and Y coordinates (Easting and Northing) were also used as predictor variables to account for some of the variance not explained by the environmental variables.

The data were grouped into a summer and winter season. It was decided to use two seasons as it has been shown in other studies that harbour porpoises change their distribution patterns particularly between these two seasons (Gilles *et al.* 2009, Sveegard *et al.* 2011).

2.5   Selection and fitting of distribution models

By using species distribution models (also called 'habitat models') it is possible to relate observed species distribution to a set of predictor variables (Franklin 2009, Elith & Leathwich 2009). This approach is used to overcome uneven sampling and to be able to predict the distribution in areas that are not surveyed. The processes shaping the distribution of marine mammals, including harbour porpoises, are highly complex. As the relationships between the observed species and the measured environmental predictors are typically non-linear, the semi-parametric modelling algorithm of generalized additive models (GAM, Hastie & Tibshirani 1990) was used. GAMs are widely used (e.g. Guisan *et al.* 2002), and have been shown to perform well in comparisons with other methods (e.g. Moisen & Frescino 2002, Elith *et al.* 2006). Formulation of the GAM can be written as (Franklin 2009):

$$g\big(E(Y)\big) = LP = \hat{\beta}_0 + \sum_{j=1}^{p} X_j \, f_j + \varepsilon,$$

where the expected value of Y, E(Y), is linked to the linear predictor, LP, with a link function, g(). The predictor variables, X, each with a smooth function f are combined to produce the linear predictor (LP), $\hat{\beta}_0$ is the coefficient and ε the error term. The method has previously been successfully applied for estimation of harbour porpoise densities from transect survey data (Hammond *et al.* 2013). By extending the GAM to a mixed model it is possible to include random factors and correlation structures to account for non-independences in the response variable (Zuur *et al.* 2009). We assessed the use of a GAMM using a variable resembling survey transects (concatenation of survey, vessel and day) as a random factor to account for the potential non-independency induced by the transect survey design.

2.5.1   Model fitting

Because of 'zero inflation', an excess of zeros in the data set (Potts & Elith 2006), the GAM models were fitted using a two-step approach, a hurdle model (also called a delta model). The first step in the delta model consisted of a presence/absence part, fitted with a binomial error distribution (with a logit link). In the second, positive part, all the zeros were excluded (Le Pape 2004, Potts & Elith 2006) and the density (response variable) was fitted with a gamma error distribution with a log link (Stefánson 1996). The two model parts were thereafter combined by multiplying the predictions of both model parts. The associated standard error was calculated by using the formula for the variances of the product of two random variables (Goodman 1960), which has also been used by others (Clark *et al.* 2009, Webley *et al.* 2011).

There are other options for modelling overdispersion including negative-binomial, quasipoisson or Tweedie models. These models are capable of handling overdispersion but not necessarily zero inflation which is a special case of overdispersion. Potts & Elith (2006) showed that negative binomial models were incapable of accounting for zero inflation, when compared to hurdle models. Zero inflated models are another group of models that can handle zero inflation and also deal with false zeroes (Martin *et al.* 2005). As the JCP data set is severely zero inflated (Figure 9) the hurdle model was chosen (which assumes that the zeroes are true zeroes) as it has been shown to be successful by others (see e.g. Potts & Elith 2006). The hurdle model is useful as it accounts for both zero inflation and overdispersion, and enables fitting the binomial and positive model parts to different environmental variables. This is advantageous as different processes might be important for explaining presence and abundance (Potts & Elith 2006).

The models were fitted in the statistical software package R, version 3.0.2 (R Core Team 2013) and the package 'mgcv' (Wood 2006) using thin plate regression splines. Thin plate regression splines are useful for fitting smooth functions of multiple variables of noisy data

without having to define knot locations (Wood 2006). This type of smoother is therefore suitable for fitting the JCP data to the continuous environmental variables, as well as for fitting interactions between e.g. Easting and Northing as they are on the same scale. Tensor product smoothers, for example, would be beneficial if interactions between variables of different scales were to be fitted (Wood 2006). The degree of smoothing in the 'mgcv' package is chosen automatically based on generalized cross validation (Wood 2006). The default dimension (k = maximum degrees of freedom for each smooth function) is ten for single covariate smooth functions. To avoid overfitting the GAMs, smooth functions for each of the variables were limited to five (k=5). Granadeiro *et al.* (2004), for example, used a maximum of four degrees of freedom. The smoothing of the interaction term between X and Y coordinates was limited to 20 (k=20).
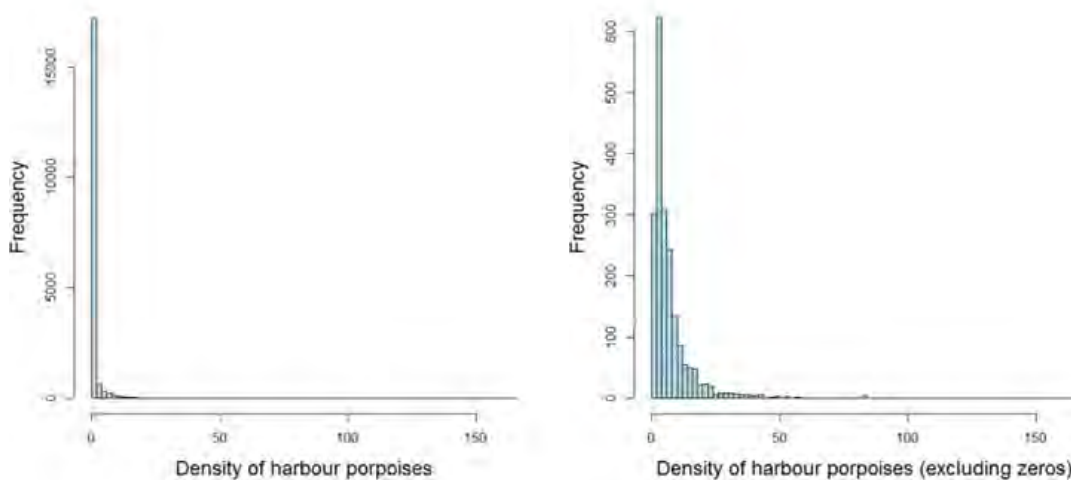
Figure 9. Example of 'zero inflation' in the Celtic/Irish Sea MU during summer (to the left). The data is still overdispersed when all zeroes are excluded (right graphic) which makes the hurdle model with a gamma error distribution (for the positive part) suitable as modelling approach. Frequency represents number of transect segments.

An initial full model including all environmental variables, chosen prior to the modelling, was first fitted. The model was further refined in lines with the recommendations by Wood and Augustin (2002). Uninfluential variables were dropped, (if the estimated degree of freedom for the variable was close to one while the confidence band included zeroes everywhere and the UBRE/GCV score decreased when the variable was removed). Variables contributing very little to the model fit (little change in UBRE/GCV score; Wood & Augustin 2002) and variables displaying ecologically meaningless responses (based on expert judgement) were also removed (Austin 2002, Wintle *et al.* 2005). Variables assumed to be ecologically important, and therefore important for extrapolation (particularly reducing over predictions in un-surveyed areas) were occasionally retained in the model although they were not significant. The variable selection procedure can therefore be described as a combination of a statistical and an ecological knowledge based approach.

Since highly correlated variables can result in exclusion of important variables, inaccurate model parameterisation and decreased predictive accuracy (Graham 2003, Heikkinen *et al.* 2006), the pairwise Pearson's correlation between the predictor variables was checked. Because the correlation was lower than 0.75 for all pairs of variables, all variables were considered for inclusion in the models.

2.5.2　Model diagnostics uncertainty and predictive ability

The fit of the GAM models was assessed based on deviance (variance) explained by the model. Diagnostic plots, normality and homogeneity of variance (homoscedasticity) of the residuals as well as observed against fitted values were assessed (Zuur *et al.* 2009). Model residuals were assessed for spatial autocorrelation using a variogram (Zuur *et al.* 2012).

The uncertainty about the predictions was assessed using point-wise standard errors for the function estimate of the models. The relative standard error (proportional error) was calculated by dividing the combined model standard errors (described above, which are default outputs from the predict.gam function in the mgcv package) by the model predictions. The relative standard error was mapped to define areas of higher uncertainty (based on the function estimates of the models).

The predictive accuracy of each model was evaluated using a 10-fold cross validation approach where the data was randomly grouped into 10 groups of which one of the groups was left out for testing and the rest for fitting. The same procedure was repeated for all groups and the mean of the evaluation statistics was calculated. The binomial model was tested using Area Under the Curve (AUC; 1 means perfect discriminative ability and 0.5 means no better than random) and the combined density predictions were evaluated using Spearman's rank correlation (Pearce & Ferrier 2000, Potts & Elith 2006). According to Sweet's (1988) classification 0.60-0.70 indicates poor discriminative ability, 0.70-0.80 fair, 0.80-0.90 good and >0.90 excellent.

2.6　Spatio-temporal modelling approach

To be able to fit models capable of showing both temporal and spatial changes based on the JCP data is challenging as the data are very patchy in both time and space. Therefore, four different modelling approaches were assessed and evaluated. Based on the evaluations, the best performing model (model 3) was subsequently used in the analyses of persistent high-density areas.

All four model approaches have been based on different models for each management unit and all models are two-step (hurdle) models. Below they are listed starting with the most 'environment driven' model adding more geographic and temporal influence in ascending order:

1)　A GAM using environmental variables only as predictors (important to note that environmental variables are also correlated with coordinates and should therefore also be considered as spatial, however without a temporal predictor). The idea behind this model setup is that the model tries to explain and predict the areas with highest porpoise densities based on the relationship to the environmental variables, using all of the survey data available (environmental data extracted on a yearly basis). The only temporal variation in the model predictions are due to variations in the environmental variables, as it can be assumed that the survey data cannot provide reliable information on temporal variation because of its extremely fragmented nature.

2)　Same as above divided into three different GAMs for the following time periods 1994-1999, 2000-2005 and 2006-2011. The premise here is that because the distribution of porpoises might have changed over a longer time period, different models were fitted for periods with relatively equal spatial sample coverage.

3)　A GAM with a three-way interaction term between coordinates (X and Y) and the three or five (for the Celtic/Irish Sea MU during summer) time periods as a factor variable, in addition to the environmental variables used in method 1 and 2. The idea behind this modelling method is the same as above, however an interaction with coordinates was added

15

to be able to account for some of the geographical variation not accounted for by the environmental variables alone. As the data are grouped into periods of more equal sample coverage, it has a stronger basis for inclusion of the coordinates without fitting the survey effort too close in comparison to model 4.

4)   A mixed GAM (GAMM) including a spatio-temporal term (a three-way interaction between X and Y coordinates and Year) and a variable describing transects as closely as possible (survey, vessel and day). The thinking behind this modelling method is to account for yearly variation in the survey data and also accounting for the non-independence within survey transects. However, the interaction with year is difficult to justify as many years have almost no effort. This modelling method fits the survey effort 'most closely'.

2.7   Determination of persistent high-density areas

The distribution models were used for predicting average density surfaces (density rasters for the whole model extent of each management unit) during each of the eighteen years under scrutiny. Different methods were evaluated for determination of predicted yearly high-density areas, including alpha hulls, localised convex hulls (Pateiro-Lopez & Rodrguez-Casal 2010), local Getis-Ord Gi statistic (Kober *et al.* 2010), kernel methods (Sveegaard *et al.* 2011) and maximum curvature (O'Brien *et al.* 2011). Alpha hulls, localised convex hulls and kernel methods are useful home-range estimators, yet they are all of limited value as estimators of the spatial structure and density patterns as reflected by survey data. In addition, they introduce a degree of subjectivity with respect to the choice of the number of data points contained in the isopleths. Application of the local Getis-Ord Gi statistic would require an upper threshold of Getis-Ord Gi values to be defined. This would also introduce an unnecessary degree of subjectivity into the selection process. Maximum curvature and 90th percentile methods are similar as they both attempt to optimise density in the relationship between number of animals and the size of the area selected. The maximum curvature achieves this by choosing the density at which the greatest rate of increase in density is found, whereas the 90th percentile is defined solely on the basis of the statistical distribution of densities.

It was decided to use the 90th percentile for outlining the high density areas in the annual density surfaces due to the robustness and transparency of this method, and as it widely established as a useful upper threshold. The use of the 90th percentile is in line with Embling *et al.* (2010), who investigated the use of a range of percentiles for selection of candidate areas for protection of harbour porpoises off western Scotland, and found the lowest degree of variation of selected areas when using the 90th percentile.

Based on outlined yearly high density areas a selection of persistent high-density areas was made by evaluating both the number of years when high densities were predicted and the degree to which high densities were predicted to occur recently. As these two sets of evaluations are 'soft' and both reflect a gradient of scoring rather than a fixed threshold fuzzy logic membership functions were used to score both characteristics. As the number of years and degree of recent high densities may trade off each other (e.g. in cases with recent high densities over few years or historical high densities over a larger range of years) the scores were combined into a final persistency index by simple averaging. The scoring of both characteristics was made on a scale from 0 to 1 using a function with the following deflection points:

i.   Number of years: 0=0; 1=10
ii.   Most recent year: 0=1994; 1=2009

The use of a function made it possible to define gradients from low persistency (non-acceptance; fewer than six years, most recent occurrence of high densities before 2000) to

high persistency (acceptance; more than five years, most recent occurrence after 1999) without the need to define sharp thresholds between the two classifications. Based on the combined classification score from 0 to 1 areas with a score equal to or higher than 0.5 were selected. As the selected persistent high-density areas are model predictions, a second analysis was used to filter out areas of insufficient evidence in terms of years of survey effort. This filter masked out areas with survey effort of less than three years, and was applied at the scale of 10km. Finally, to filter out noise in the resulting maps following each set of analyses identified high-density areas smaller than 100km^2 were removed.

3   Results

3.1   Spatio-temporal characteristics in observed densities of porpoises

In Figure 10 the observation effort in the North Sea in summer have been aggregated into 25 km grid cells for the three different 6-year periods used in the distribution models. Over the course of the three periods the effort in the southern part of the North Sea has increased markedly, and the effort south of 57° N reached a very high level during the period between 2006 and 2011. The areas to the east of Shetland and Orkney were surveyed less during the period 2000-2005. During the period 2006-2011 the whole northern part of the North Sea received much less effort than during the periods before 2000.

The changes in the latitudinal trends in the observed densities of porpoises in the North Sea to some degree follow the trends in the effort with lower densities being observed in the northern parts after 2000 (Figures 11 and 12). In the south densities have increased slightly during the period 2006-2011, however, the tendency for high densities at the latitude around Dogger Bank is seen in all three periods (Figure 12). The same changes are seen in the observed presences (Figure 13).
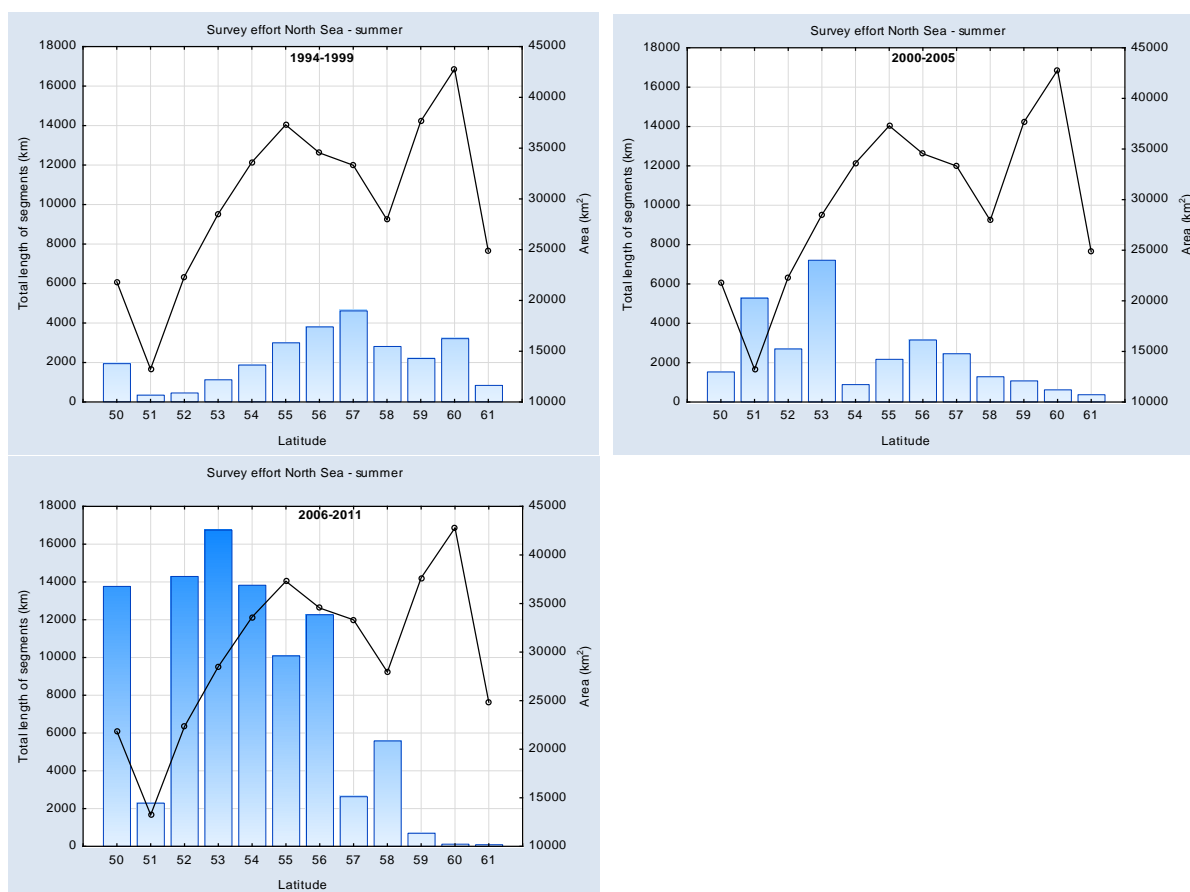
Figure 10. Total survey effort (km, shown as bars) and area of available sea (line) for surveying in the North Sea during summer split per period. Effort and area is shown per degrees latitude.
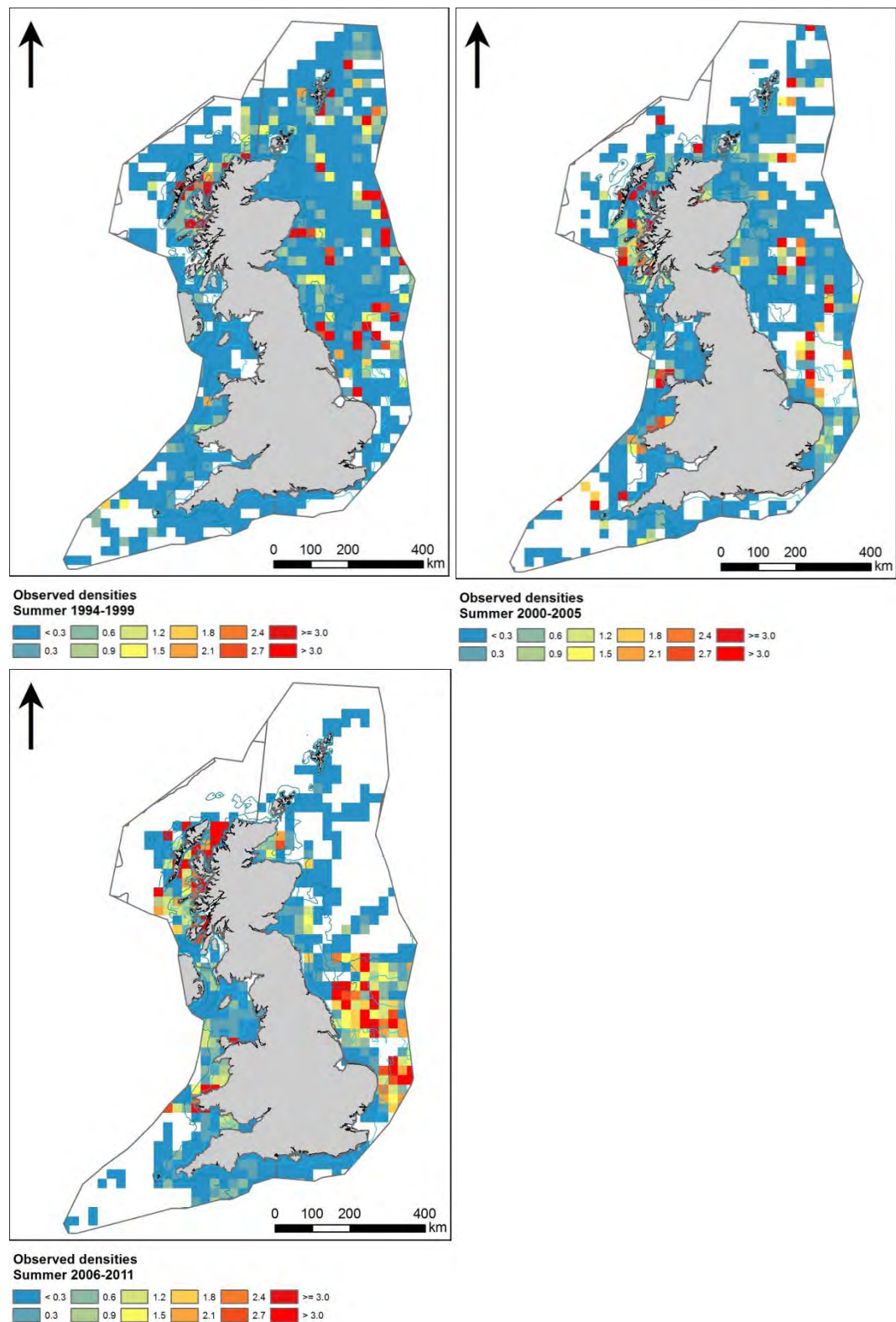
Figure 11. Maps of mean observed densities (n/km^2) of harbour porpoise in summer during three 6 year periods. Densities are shown for grid cells of 25km. White squares indicate no effort.
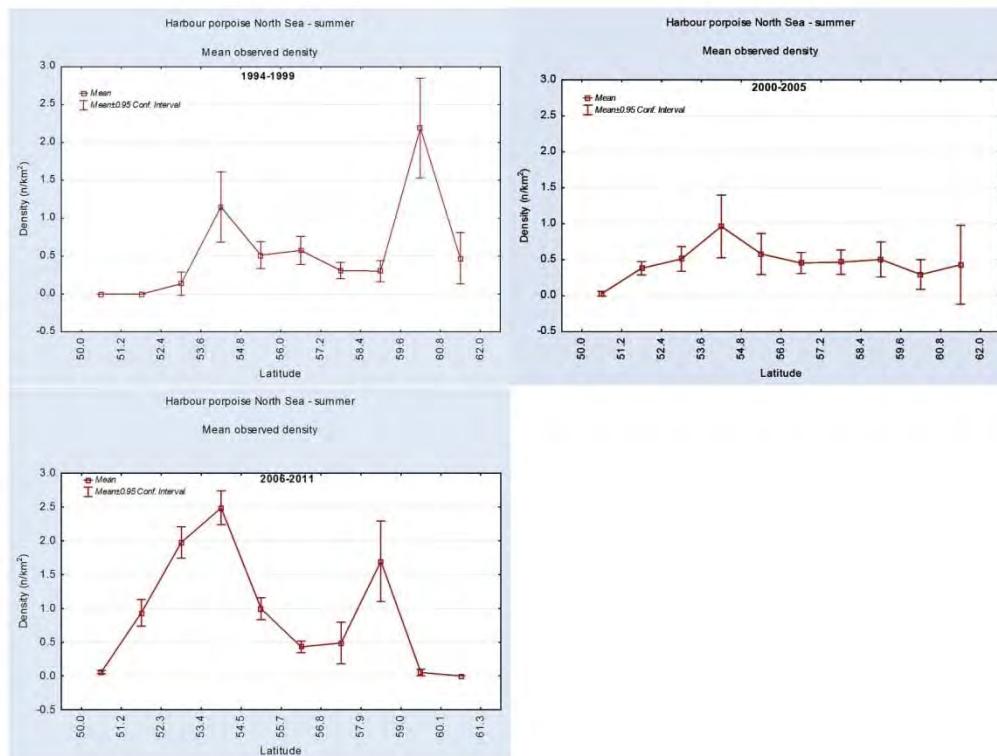
Figure 12. Graphs of mean observed densities of harbour porpoise in summer during three 6 year periods. Densities are shown for per degrees latitude.
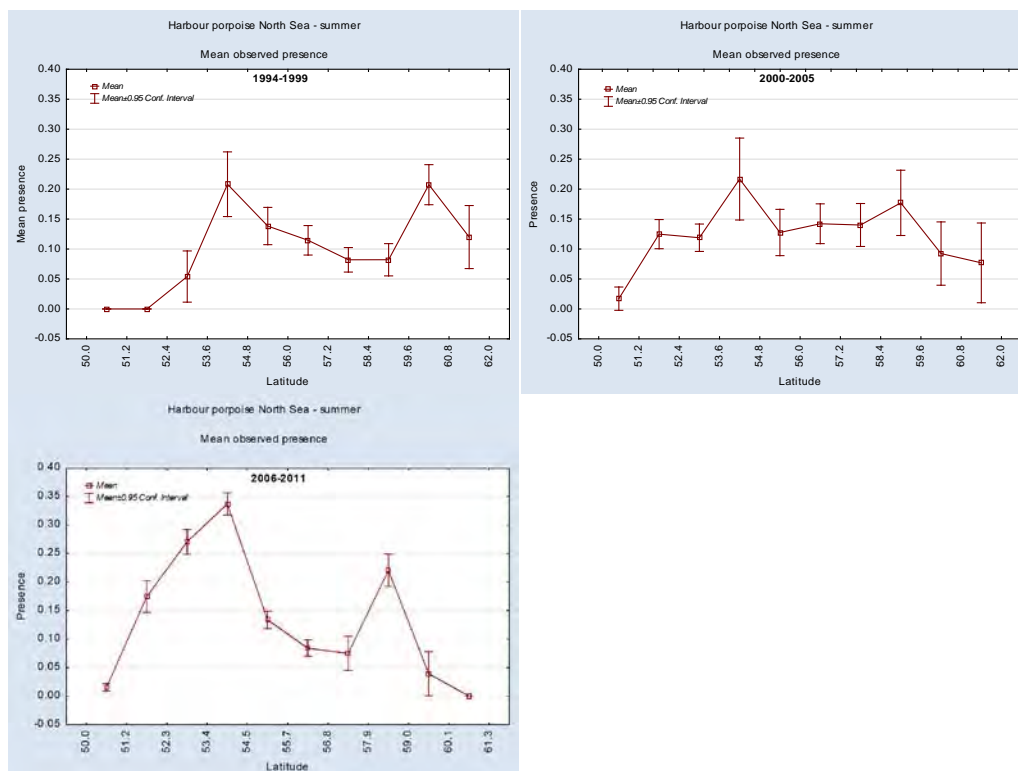
Figure 13. Graphs of mean observed presences of harbour porpoise in summer during three 6 year periods. Presences are shown for per degrees latitude.

3.2   Evaluation of model approaches

The evaluation results for each of the four approaches to distribution modelling are summarised in Table 2. The evaluation results for method 4 (see Section 2.6) could not be completed for all management units, as the GAMMs were too unstable to produce k-fold cross validations. Evaluation results for method 4 are based on a split-sample approach (70% used for model fitting, 30% used for testing), and are only reported for the North Sea MU.

The four methods produce different results, yet similarities in patterns can also be observed. All methods have strengths and weaknesses. Method 1 and 2 probably explain the distribution best from an ecological point of view; they explain where the best habitats are, purely based on the environmental variables. If looking at predictive accuracy which is measured on semi-independent data it seems that method 3 using information on period as an interaction term is most accurate.

Methods 1 and 2 might be better at extrapolating to un-surveyed areas as they are not geographically constrained. Method 4, the mixed model, is unstable, as the model did not converge during 10-fold cross validation. It seems also to be inappropriate to fit the data with a 'yearly smoother' as there is very little effort in many years. It should also be pointed out that there is little evidence of spatial autocorrelation in model residuals, thus it is considered correct to use a GAM model instead of GAMM.

On the basis of the model evaluations method 3 is preferred on account of its combination of environmental space with geographic space (while not overfitting due to uneven coverage) and its ability to produce relatively accurate predictions when evaluated using a 10-fold cross validation.

Table 2.
The explanation degree by each model part (P/A = presence/absence and positive = positive model part) is indicated by deviance explained (Dev. Exp.). In Method 4 the values for explanation degree (indicated by a *) are adjusted R^2. Evaluation statistics (AUC and Spearman's Rank correlation) for the four models based on 10-fold cross validation is a measure of the predictive ability by each model part. AUC indicates the predictive ability of the presence/absence model part, and the Spearman Rank correlation indicates the agreement between observed densities and the final predicted densities (combined predictions of presence/absence and positive model parts).

		Dev. Exp. P/A	Dev. Exp. positive	AUC	Spearman Rank correlation
Method 1	Celtic/Irish Sea MU	7.1	30.3	0.692	0.192
	North Sea MU	8.1	7.63	0.7	0.254
	NW Scottish Waters MU	11	8.9	0.726	0.262
Method 2 period 1	Celtic/Irish Sea MU	7.5	39.7	0.668	0.107
	North Sea MU	8.69	21.6	0.697	0.212
	NW Scottish Waters MU	12.8	14.5	0.719	0.303
Method 2 period2	Celtic/Irish Sea MU	11.5	23.2	0.732	0.272
	North Sea MU	5.3	15.2	0.651	0.138
	NW Scottish Waters MU	16.4	13.2	0.77	0.299
Method 2 period 3	Celtic/Irish Sea MU	5.85	39.2	0.673	0.169
	North Sea MU	12.4	5.7	0.74	0.323
	NW Scottish Waters MU	8.19	8.98	0.694	0.223
Method 3	Celtic/Irish Sea MU	10	39.4	0.723	0.218
	North Sea MU	14.2	21.5	0.758	0.319
	NW Scottish Waters MU	13.7	30.5	0.737	0.256
Method 4	Celtic/Irish Sea MU				
	North Sea MU	10.7*	4.0*	0.758	did not converge
	NW Scottish Waters MU				

3.3   Celtic Sea/Irish Sea MU

The model results for the summer season in the Celtic and Irish Seas indicate that water depth, surface sediments, current speed and eddy potential all play a major role as determinants of the distribution of harbour porpoises in this management unit (Table 3). In the winter season, water depth and current speed are the major determinants with some influence from surface salinity (Table 4). At the same time, the number of ships also has a significant effect on the density (summer) of the animals. The interaction terms with survey period share a strong effect on the presence of animals, but less effect on the density. Additionally, the

segment length has an important effect on the probability of presence with higher probabilities associated with high levels of effort.

The most important factors for probability of presence in this management unit in summer are current speed and eddy potential which displays increasing probabilities with increasing current speeds up to 0.4m/s and with increasing eddy activity (Figure 14). In winter, the same response to current speed is observed, yet with a tendency for lower probabilities with high current speeds (Figure 15).

The responses to water depth indicate that high densities of harbour porpoise are associated with the shallowest areas (areas shallower than 40m) in summer and high probability of presence in the same areas in winter. During summer, high densities are associated with areas of high eddy activity and degree of coarseness of sediments also plays an important role; the latter shows a positive dome shaped response to particle size of surface sediments with peak densities in sandy-gravelly sediments, and rather low densities in muddy areas. Responses to number of ships per year indicate markedly lower densities with increasing levels of traffic in summer. A threshold level in terms of impact seems to be a traffic density of approximately 15,000 ships/year (approx. 50/day).

Table 3. Smooth terms, deviance explained and evaluation statistics for summer model Celtic Sea/Irish Sea MU. The z-values and significance for the parametric terms are shown and for the smooth terms the approximate significance and chi-square/F statistics. Variables not included in either the binomial or positive model part are indicated with a dash.

Smooth terms	Presence/absence		Positive density	
	chi-sqr	p	F	p
Current speed	21.06	< 0.001	-	-
Eddy potential	17.86	< 0.001	7.302	< 0.001
Current gradient	-	-	-	-
Surface salinity	-	-	-	-
Vertical temp. Gradient	-	-	-	-
Water depth	-	-	19.326	< 0.001
Slope of seafloor	-	-	-	-
Surface sediments	-	-	5.314	< 0.001
Shipping density	-	-	9.612	< 0.001
Length survey segment	135.21	< 0.001	-	-
Spatio-temporal Period1	72.60	< 0.001	4.281	< 0.001
Spatio-temporal Period2	68.71	< 0.001	2.695	< 0.05
Spatio-temporal Period3	502.94	< 0.001	10.296	< 0.001
Spatio-temporal Period4	450.80	< 0.001	9.212	< 0.001
Spatio-temporal Period5	80.14	< 0.001	7.214	< 0.001
Sample size (n)	18934		2015	
Dev. Exp.	10.8		39.8	
AUC	0.730			
Spearman's corr.		0.226		

Table 4. Smooth terms deviance explained and evaluation statistics for winter model Management Unit 0 (Celtic Sea/Irish Sea). The z-values and significance for the parametric terms are shown and for the smooth terms the approximate significance and chi-square/F statistics. Variables not included in either the binomial or positive model part are indicated with a dash.

Smooth terms	Presence/absence		Positive density	
	chi-sqr	p	F	p
Current speed	19.76	< 0.001	1.780	0.14
Eddy potential				
Current gradient	-	-	-	-
Surface salinity	-	-	2.542	<0.05
Vertical temp. Gradient	-	-	-	-
Water depth	11.61	< 0.05	1.116	0.33
Slope of seafloor	-	-	-	-
Surface sediments	-	-		
Shipping density	-	-		
Length survey segment	43.00	< 0.001	-	-
Spatio-temporal Period1	190.44	< 0.001	5.550	< 0.001
Spatio-temporal Period2	162.35	< 0.001	3.683	< 0.001
Spatio-temporal Period3	198.35	< 0.001	2.942	< 0.001
Sample size (n)	11409		1096	
Dev. Exp.	12.3		26.6	
AUC	0.731			
Spearman's corr.	0.238			
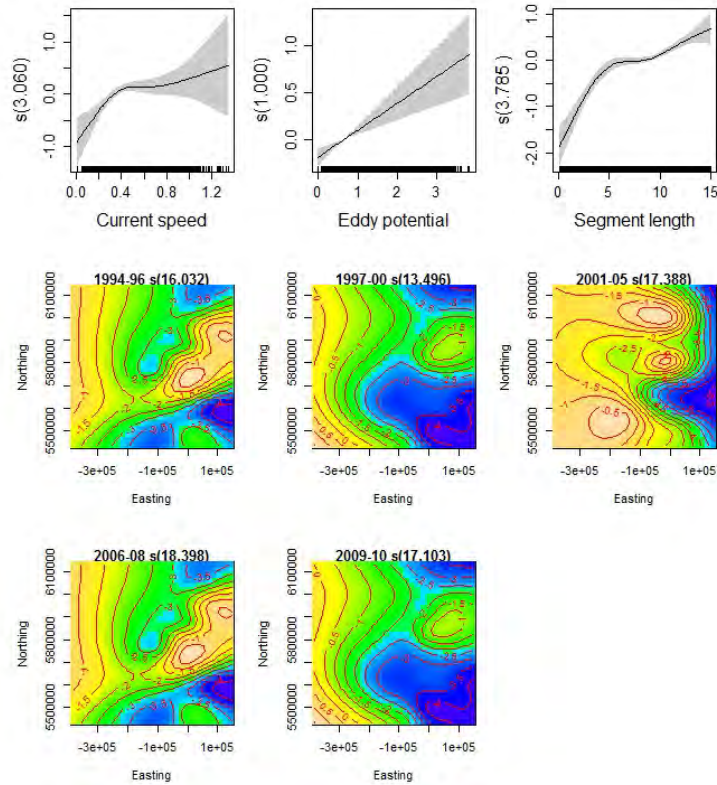
Presence/absence

Density
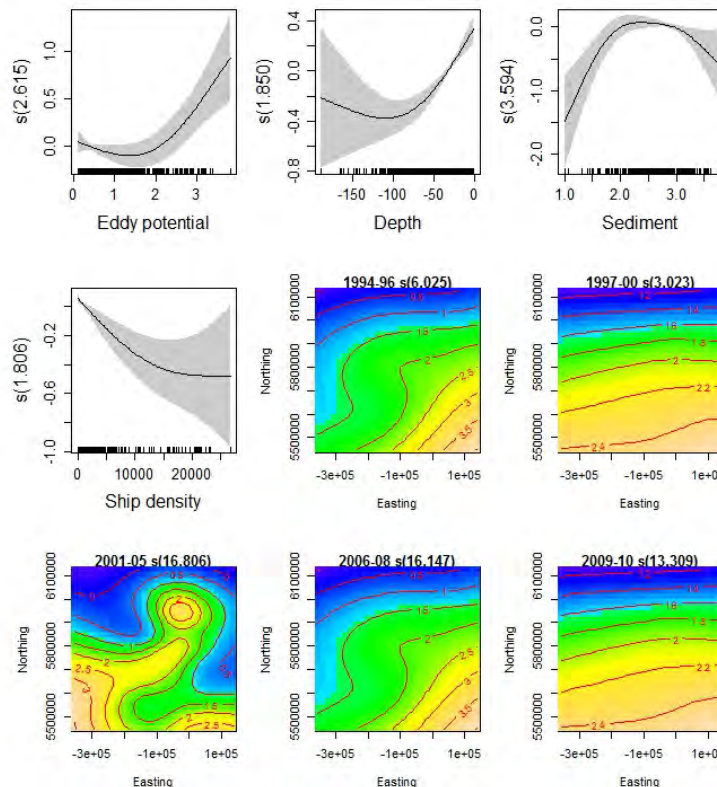
Figure 14. Partial GAM plots for presence/absence (upper panel) and positive (lower panel) parts for the summer model Celtic Sea/Irish Sea MU. The values of the environmental variables are shown on the X-axis and the probability on the Y-axis in the scale of the linear predictor. The grey shaded areas and the dotted lines show the 95% Bayesian confidence intervals. The degree of smoothing is indicated in the legend of the Y-axis and for the interaction terms (Easting, Northing) in the heading.
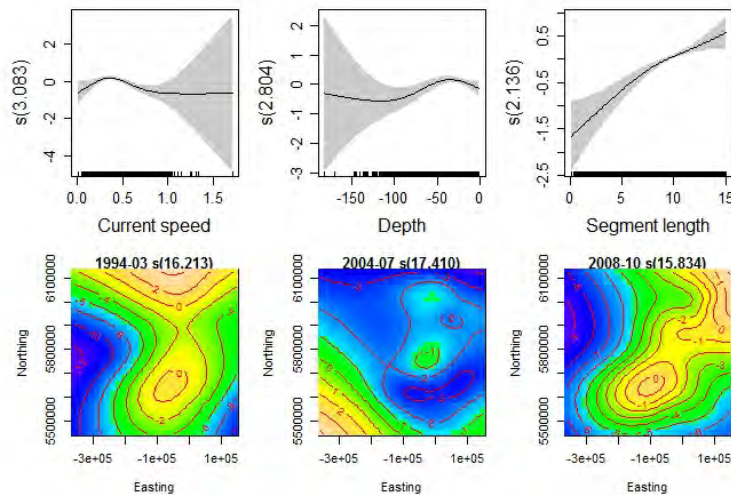
Presence/absence

Density
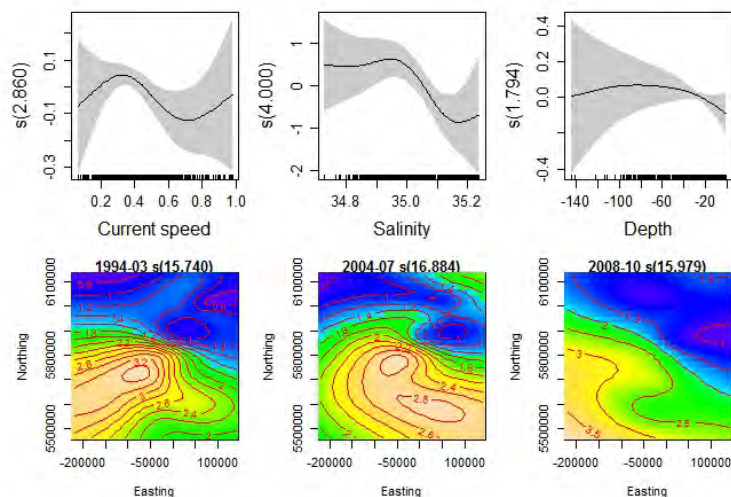
Figure 15. Partial GAM plots for presence/absence (upper panel) and positive (lower panel) parts for the winter model Management Unit 0 (Celtic Sea/Irish Sea). The values of the environmental variables are shown on the X-axis and the probability on the Y-axis in the scale of the linear predictor. The grey shaded areas and the dotted lines show the 95% Bayesian confidence intervals. The degree of smoothing is indicated in the legend of the Y-axis and for the interaction terms (Easting, Northing) in heading.

3.3.1   Predicted distributions and persistency of estimated patterns

The predicted densities of harbour porpoise during the summer and winter seasons in the Celtic and Irish Seas show considerable variation between periods in offshore waters and more persistent patterns in coastal areas. In the offshore waters a large area of high densities is predicted at the shelf edge and another area south of Cornwall in some years both during summer and winter (Figures 16, 17). These predictions are extrapolations of high densities observed from ferries centrally in the western Channel, and have relatively high levels of uncertainty (Figures 18, 19). The uncertainty of the modelled density estimates as visualised by the patterns of relative standard errors indicate robust model predictions in most coastal parts of St. George's Channel, Irish Sea and Welsh coastal waters (Figure 18, 19). The estimates for the offshore waters have high standard errors.

26

Coherent zones of high densities of porpoises are estimated off the north-west and west coasts of Wales during summer, predictions which reflect well the observed densities (Figure 20). Predictions indicate that the western Bristol Channel supports high densities, as does the area north of the Isle of Man during the first period in winter. The predictions for the Bristol Channel are mainly extrapolations from a limited survey effort in the central part of the Channel (Figure 21).

When accounting for the number of years when survey effort has been undertaken the high density area in the western Channel are removed and the high density zones west (Pembrokeshire and Cardigan Bay) and north-west (Anglesey, Lleyn Peninsula) off Wales are reduced by approximately 30% during summer (Figures 22, 23). During winter, large reductions are seen in the area of high densities predicted for northern Irish Sea and Cardigan Bay. The high density area predicted south of Cornwall during summer is reduced by 30%.

In spite of the wide distributions the high-density areas as indicated by the 90th percentiles comprise less than 25% of the management unit during summer and less than 10% during winter (Figures 22, 23).
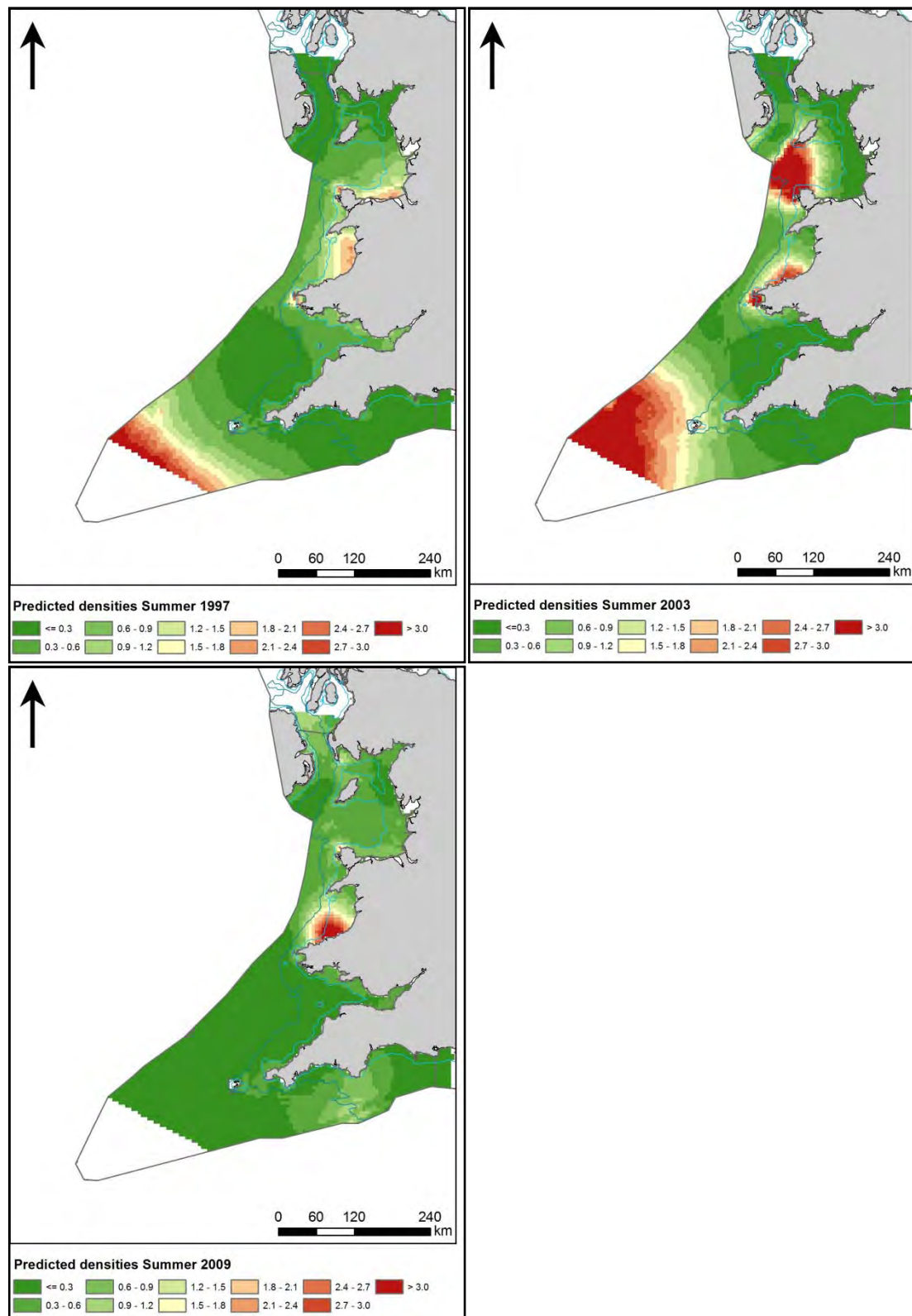
Figure 16. Predicted densities (number/km^2) during summer in management unit 0 for three different years in each model period. Predicted densities for all years are shown in Appendix 2.
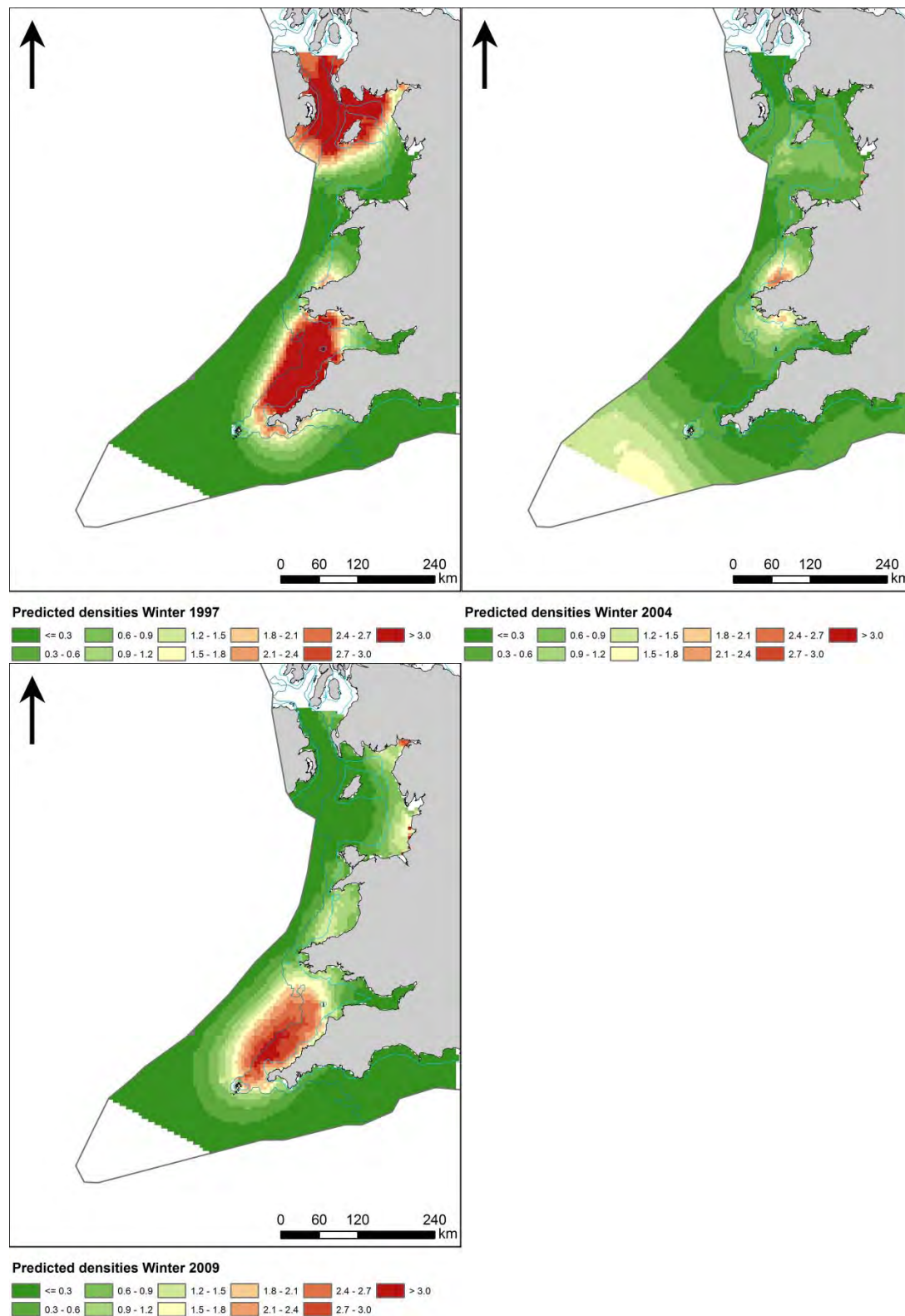
Figure 17. Predicted densities (number/km^2) during winter in management unit 0 for three different years in each model period. Predicted densities for all years are shown in Appendix 3.
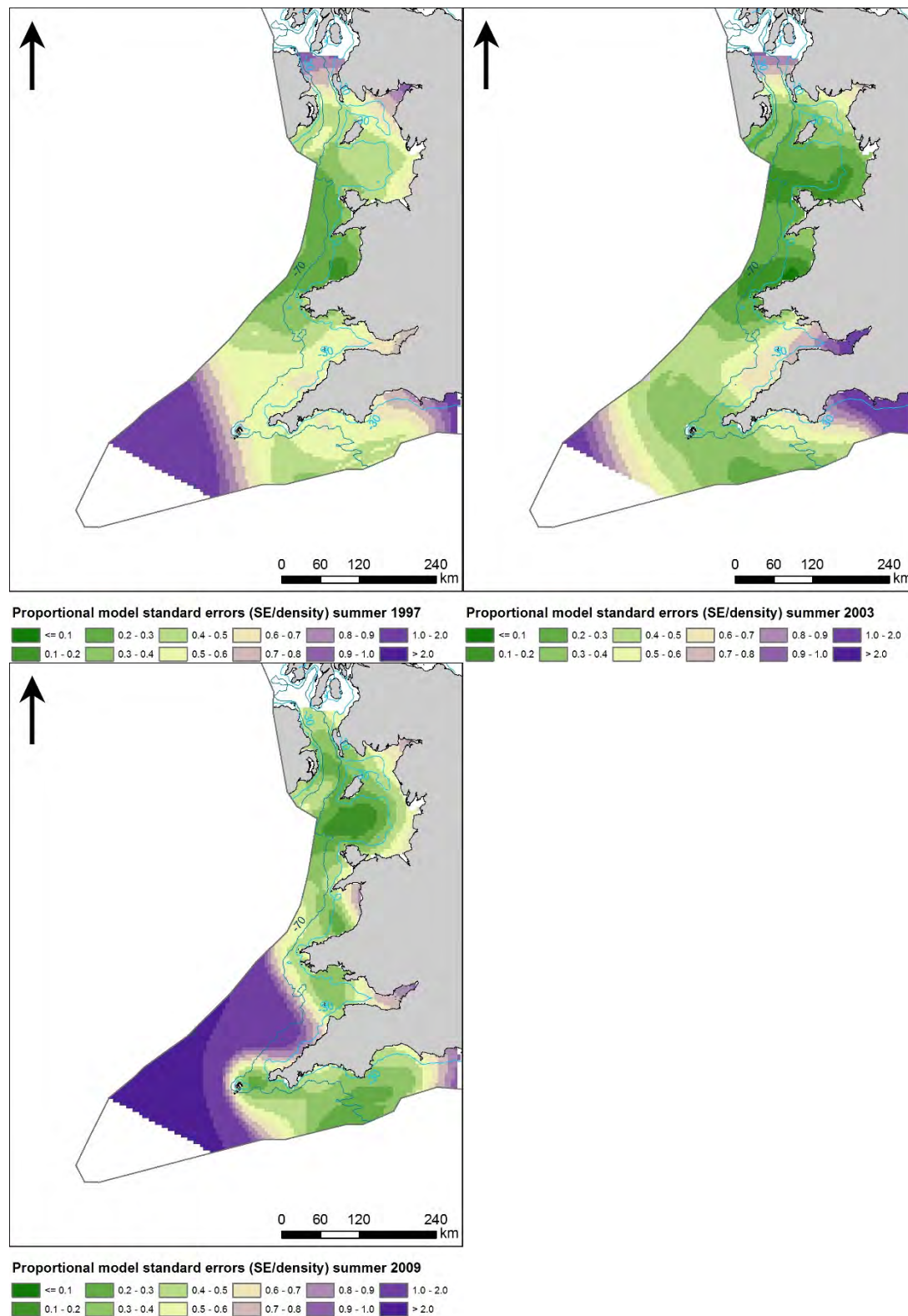
Figure 18. Model uncertainty. Proportional model standard errors for the summer models in management unit 0 (three selected years). Proportional model standard errors for all years are shown in Appendix 4.
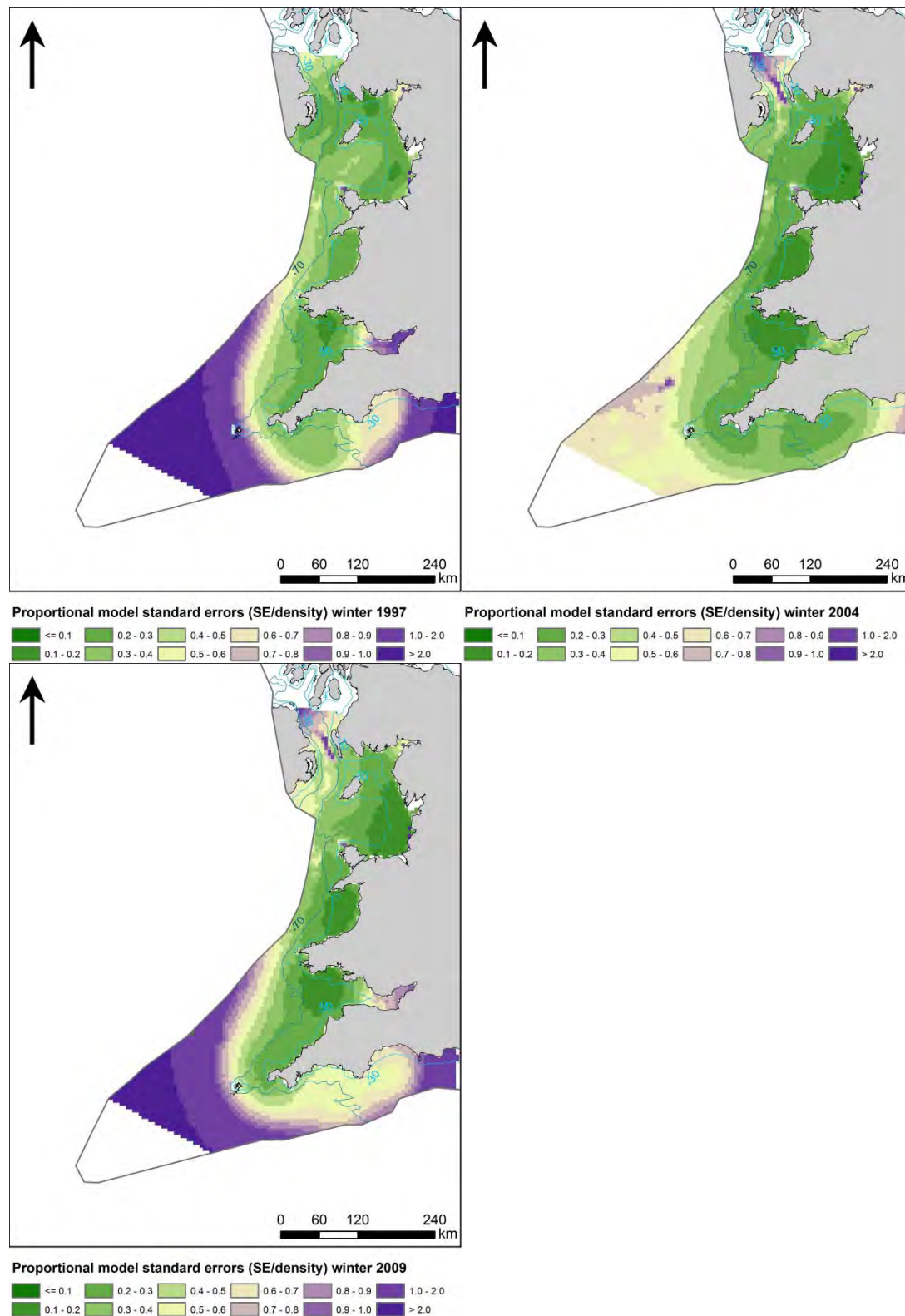
Figure 19. Model uncertainty. Proportional model standard errors for the winter models in management unit 0 (three selected years). Proportional model standard errors for all years are shown in Appendix 4.
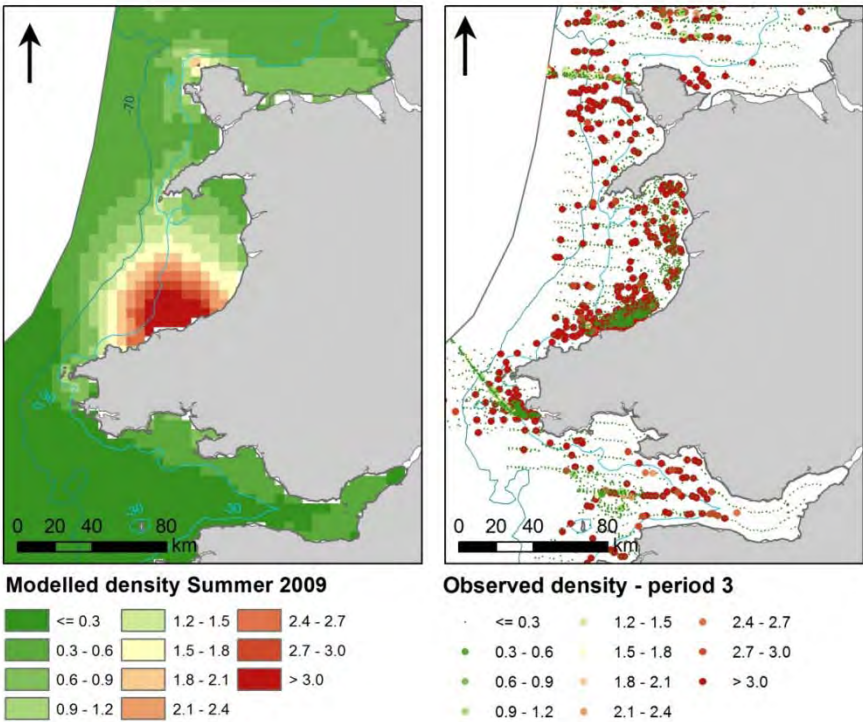
Figure 20. Close-up of high density (number/km^2) areas during summer in management unit 0 showing predicted and observed densities. Observed densities are indicated by dots using the same colour range as used for the predicted densities.
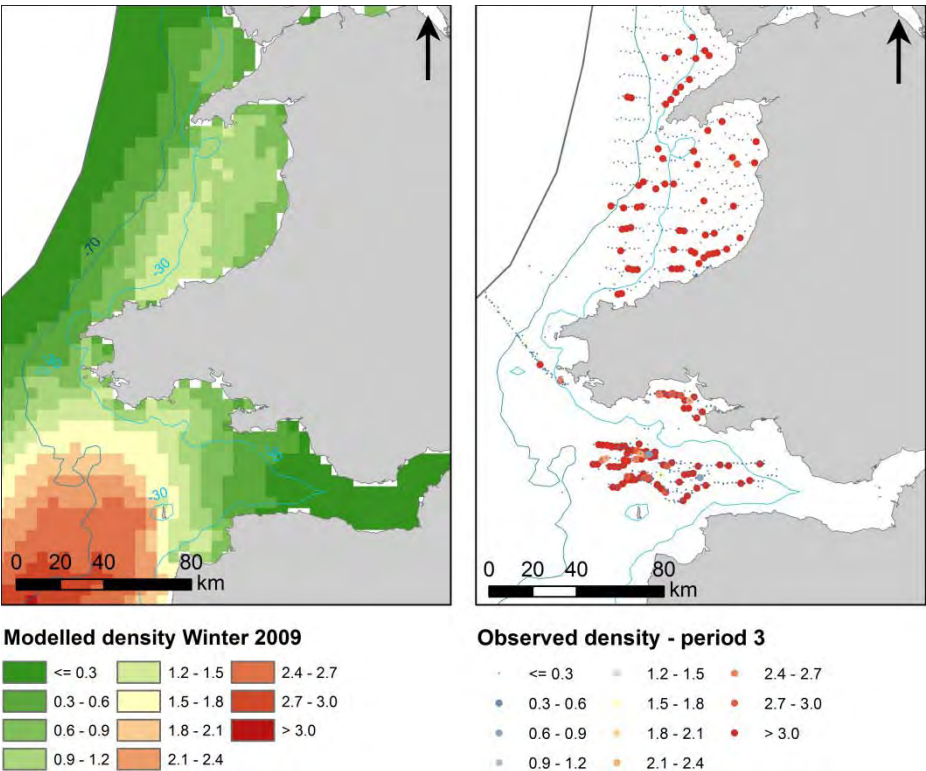
Figure 21. Close-up of high density areas during winter in management unit 0 showing predicted and observed densities. Observed densities are indicated by dots using the same colour range as used for the predicted densities.
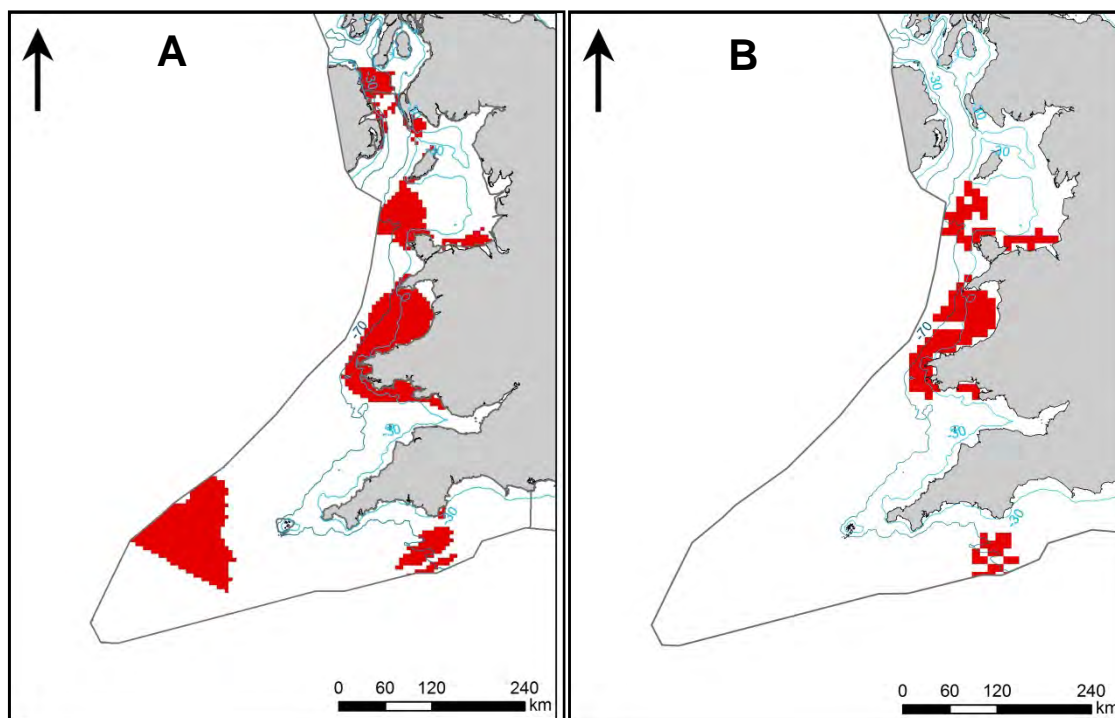
Figure 22. Persistent high-density areas identified and selected in management unit 0 during summer. In map A the red colours mark areas with where persistent high densities as defined by the upper 90th percentile have been identified. In the map B the red colours mark persistent high-density areas with survey effort from three or more years.
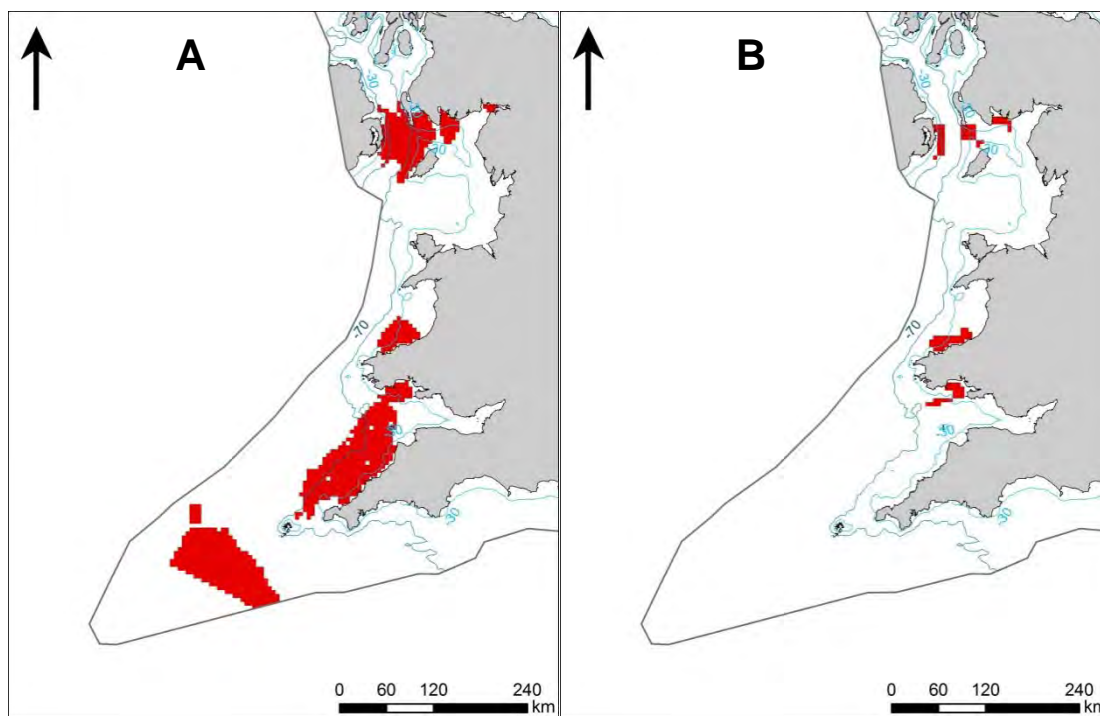
Figure 23. Persistent high-density areas identified and selected in management unit 0 during winter. In map A the red colours mark areas with where persistent high densities as defined by the upper 90 percentile have been identified. In map B the red colours mark persistent high-density areas with survey effort from three or more years.

3.4   North Sea MU

For the North Sea the model results for both the summer and winter seasons show water depth and hydrodynamic variables as the most important factors both for the probability of presence and density of harbour porpoise in this management unit (Tables 5 and 6). The interaction terms with survey period share a strong effect on the presence of animals, but less effect on the density. During summer, surface salinity and eddy potential are the most important hydrodynamic determinants of presence, while stability (vertical temperature gradient) is the most important dynamic determinant of density. During winter, eddy activity is still very important for the presence of animals, while current speed has some influence on observed densities. Additionally, degree of coarseness of surface sediments plays an important role in the presence of animals and current speed and slope of seafloor (summer) in the density part. The number of ships represents a relatively important pressure determining the density of animals in this management unit during both seasons. The segment length has an important effect on the probability of presence with higher probabilities associated with high levels of observational effort.

In terms of water mass characteristics during summer, the animals seem to avoid well-mixed areas, and prefer more stable areas with the density showing a peak on the lower gradient at the interface between mixed and stratified waters, and another peak at high values of stratification (Figure 24). Responses to surface salinity indicate both lower presence and density levels with decreasing practical salinity units (psu) values, hence reflecting an avoidance of estuarine water masses.

Both probability of presence and densities peak at the lower gradient of eddy activity, and the animals seem to avoid areas with high current speeds.

The responses to water depth during summer indicate two peaks in the presence/absence part with high values over the inner shelf (30- 50m depth) and in areas of approximately 200m depth, and a peak in densities on the inner shelf. During winter, only a peak in the presence/absence part at 30-40m depth is seen (Figure 25).

In the presence part the animals display a strong dome-shaped response to particle size of surface sediments during summer, thus avoiding muddy and hard bottom areas (Figure 25). During winter, the response to particle size indicates avoidance of muddy areas. Responses to number of ships per year indicate markedly lower densities with increasing levels of traffic (Figures 24, 25). A threshold level in terms of impact seems to be approximately 20,000 ships/year (approx. 80/day).

Table 5. Smooth terms, deviance explained (Dev. Exp.) and evaluation statistics for summer model North Sea MU. The z-values and significance for the parametric terms are shown and for the smooth terms the approximate significance and chi-square/F statistics. Variables not included in either the binomial or positive model part are indicated with a dash.

Smooth terms	Presence/absence		Positive density	
	chi-sqr	p	F	p
Current speed	-	-	5.78	< 0.05
Eddy potential	33.80	< 0.001	3.92	< 0.01
Current gradient	-	-		-
Surface salinity	26.55	< 0.001	2.30	-
Vertical temp. Gradient	-	-	5.51	< 0.001
Water depth	59.74	< 0.001	5.79	< 0.001
Slope of seafloor	-	-	4.46	< 0.01
Surface sediments	13.03	< 0.01	-	-
Shipping density	-	-	7.03	< 0.01
Length survey segment	176.11	< 0.01	-	-
Spatio-temporal Period1	219.87	< 0.001	6.11	< 0.001
Spatio-temporal Period2	149.93	< 0.001	7.38	< 0.001
Spatio-temporal Period3	506.92	< 0.001	10.05	< 0.001
Sample size (n)	17236		2730	
Dev. Exp.	14.2		21.5	
AUC	0.758			
Spearman's corr.	0.319			

Table 6. Smooth terms, deviance explained and evaluation statistics for winter model North Sea MU. The z-values and significance for the parametric terms are shown and for the smooth terms the approximate significance and chi-square/F statistics. Variables not included in either the binomial or positive model part are indicated with a dash.

Smooth terms	Presence/absence		Positive density	
	chi-sqr	p	F	p
Current speed	-	-	4.73	< 0.01
Eddy potential	33.91	< 0.001		
Current gradient	-	-	-	-
Surface salinity	-	-	-	-
Vertical temp. Gradient	-	-	-	-
Water depth	43.01	< 0.001	1.116	0.33
Slope of seafloor	-	-	-	-
Surface sediments	26.34	< 0.001	-	-
Shipping density	-	-	6.28	< 0.05
Length survey segment	36.45	< 0.001	-	-
Spatio-temporal Period1	249.61	< 0.001	6.621	< 0.001
Spatio-temporal Period2	296.92	< 0.001	6.609	< 0.001
Spatio-temporal Period3	456.24	< 0.001	8.418	< 0.001
Sample size (n)	11530		1738	
Dev. Exp.	32.9		24.4	
AUC	0.862			
Spearman's corr.	0.446			

Presence/absence
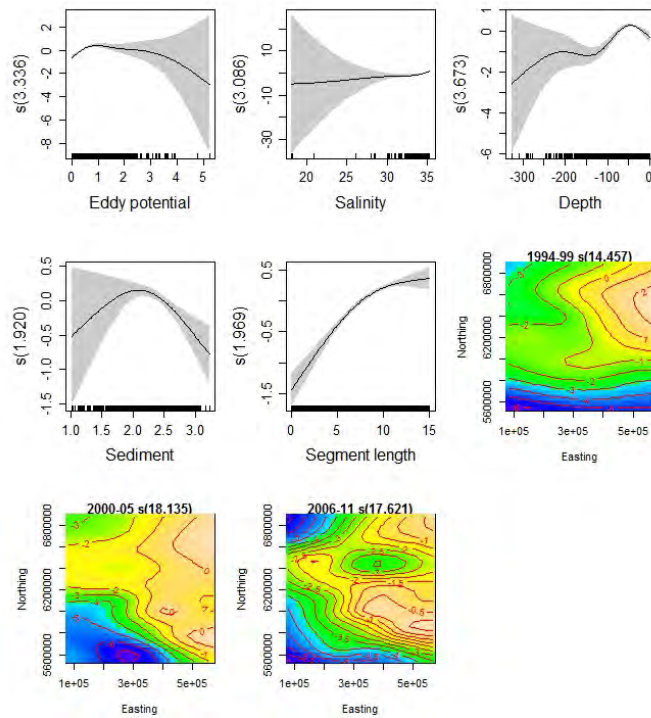
Density
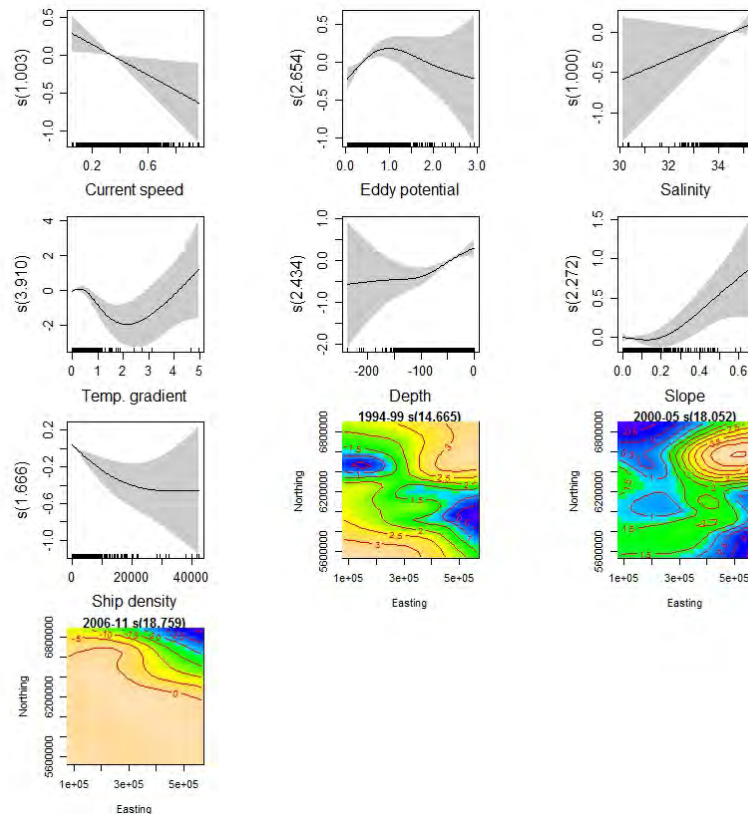
Figure 24. Partial GAM plots for presence/absence (upper panel) and positive (lower panel) parts for the summer model Management Unit 1 (North Sea). The values of the environmental variables are shown on the X-axis and the probability on the Y-axis in the scale of the linear predictor. The grey shaded areas and the dotted lines show the 95% Bayesian confidence intervals. The degree of smoothing is indicated in the legend of the Y-axis and for the interaction terms (Easting, Northing) in the heading.
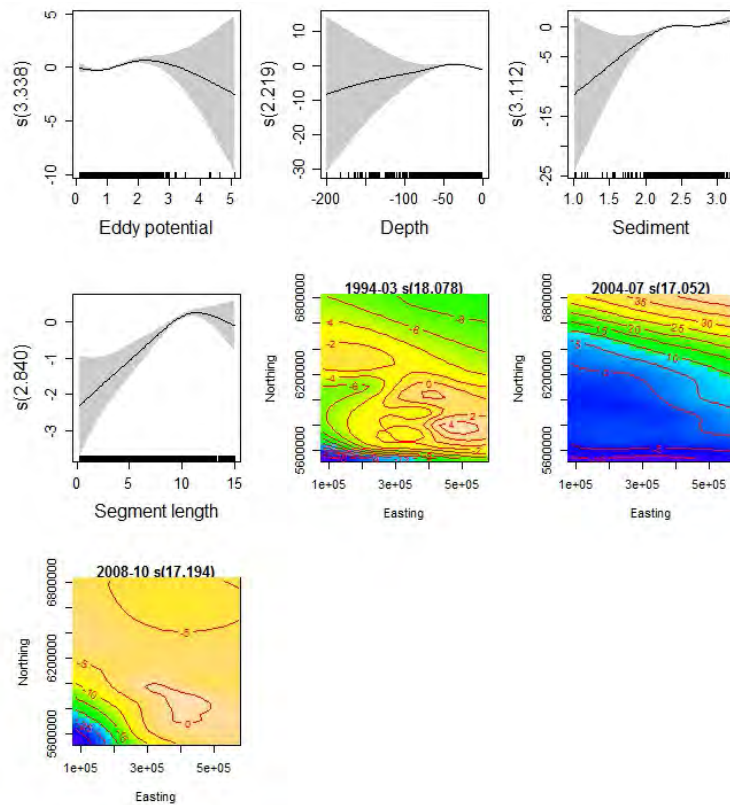
Presence/absence

Density
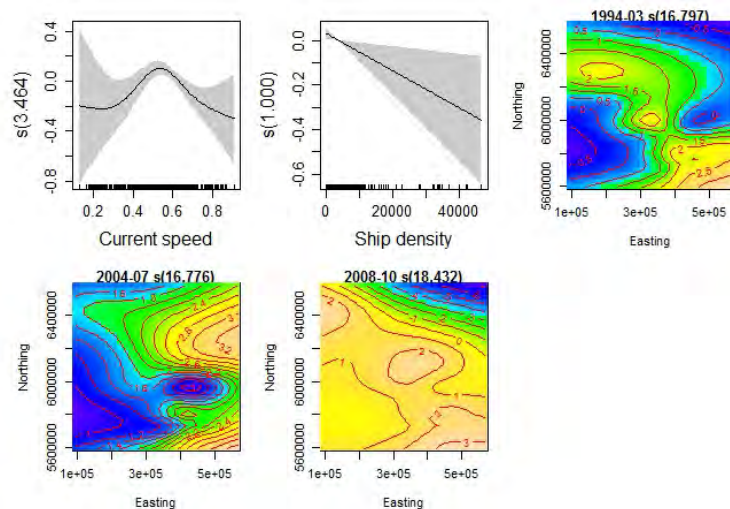
Figure 25. Partial GAM plots for presence/absence (upper panel) and positive (lower panel) parts for the winter model North Sea MU. The values of the environmental variables are shown on the X-axis and the probability on the Y-axis in the scale of the linear predictor. The grey shaded areas and the dotted lines show the 95% Bayesian confidence intervals. The degree of smoothing is indicated in the legend of the Y-axis and for the interaction terms (Easting, Northing) in the heading.

3.4.1   Predicted distributions and persistency of estimated patterns

The predicted densities of harbour porpoise in the North Sea during the summer season show some large-scale variations in certain aspects, and similarities in others between the three model periods (Figure 26). The depicted patterns in summer show much higher dispersion during the first period, slightly less so during the second period and a more-contracted distribution during the third period. As shown in Figure 10 the coverage of the survey effort in the North Sea, especially in the northern part, has declined between period 1 and 3. High densities (approximately 10 times background levels) were estimated off the northern Scottish coast and Shetland during the first period, but not during the second and third periods when effort declined in the northern parts. Localised high densities were also estimated in the northern part during the first period at Wee Bankie and during the first two periods along the edges of the Norwegian Trench.

In the southern part of the North Sea, high densities were estimated during summer at the western slopes of the Dogger Bank during all three periods. During the period 2006-2011, the estimated high density zone stretched southwards to include an area off Norfolk. All of the identified high-density areas and their variation over time reflect well the patterns of observed densities (Figure 30). The uncertainty of the modelled density estimates as visualised by the patterns of relative standard errors indicate robust model predictions in all shelf waters north of the Channel (Figure 28). The estimates for the Channel have high standard errors during the first two periods, and the northern North Sea during the last period.

The density predictions during winter indicate high densities in the southern parts of the North Sea during the first and third periods, and high densities in a large sector of the north-eastern North Sea during the second period (Figure 27). However, the uncertainty of the model predictions during winter are generally very high in the northern 2/3 of this management unit (Figure 29), which means that the predicted high densities only between Flamborough Head and the outer Thames Estuary reflect the observations well (Figure 31).

In spite of the wide distributions the high-density areas as indicated by the 90th percentiles comprise less than 15% of the management unit during both seasons (Figures 32, 33).

During summer, one large coherent offshore zone of persistent high densities is estimated from the western slopes of the Dogger Bank southwards along the 30m depth contour to the area off Norfolk. In addition, smaller areas of persistent high densities are estimated in the outer Moray Firth, north of Shetland and at the edge of the Norwegian Trench. When accounting for the number of years when survey effort has been undertaken, a smaller proportion of the large offshore zone remains, and the zone is now broken up into two areas of persistent high densities; Silver Pit and the north western slopes of the Dogger Bank (Figure 32). All other areas except for parts of the outer Moray Firth are removed when level of effort is taken into account. During winter, after accounting for areas of low survey effort persistent high density areas are retained off the Norfolk coast and the outer Thames Estuary as well as the inner Silver Pit, south-east of Flamborough Head (Figure 33).
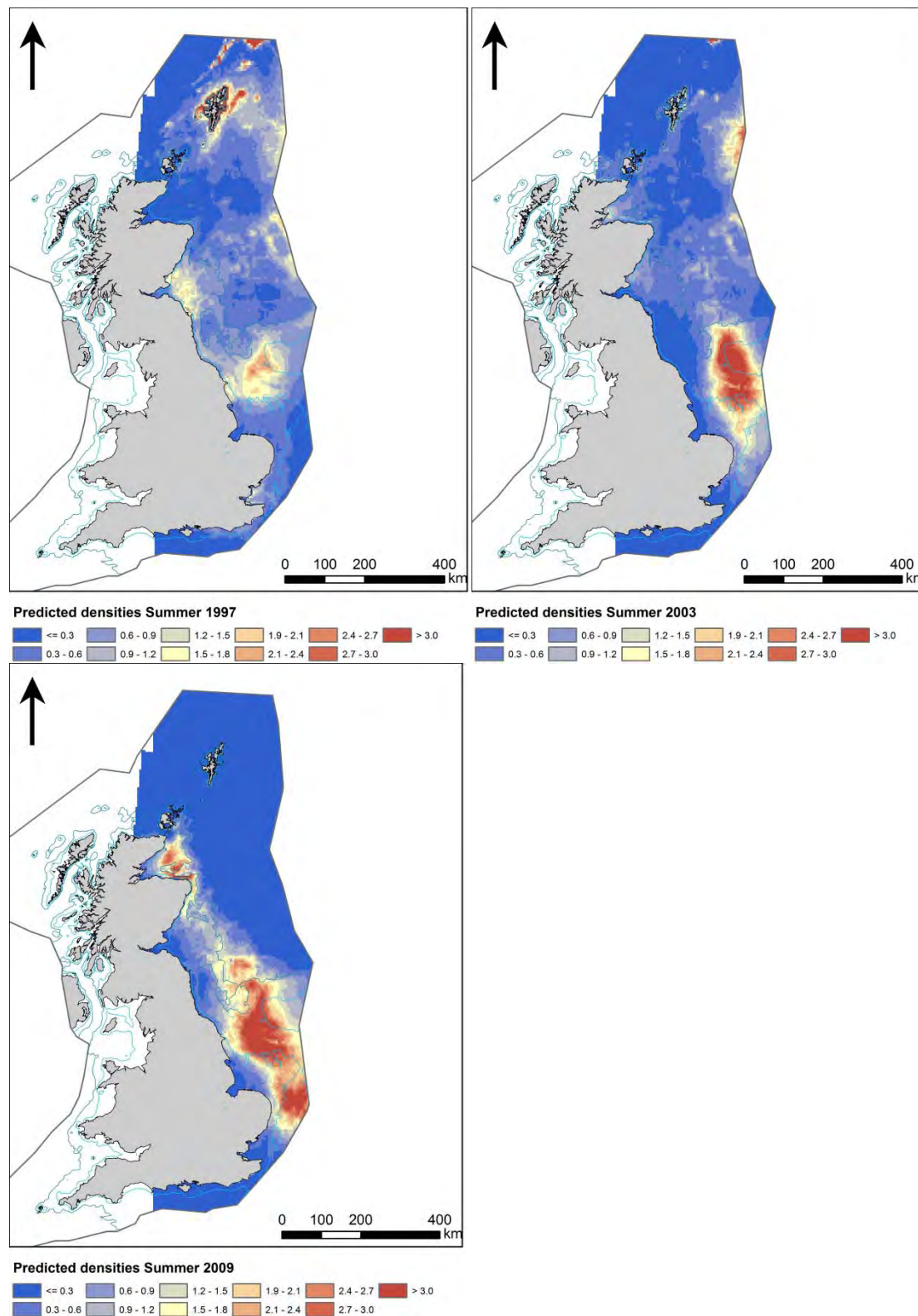
Figure 26. Predicted densities (number/km^2) during summer in management unit 1 for three different years in each model period. Predicted densities for all years are shown in Appendix 3.
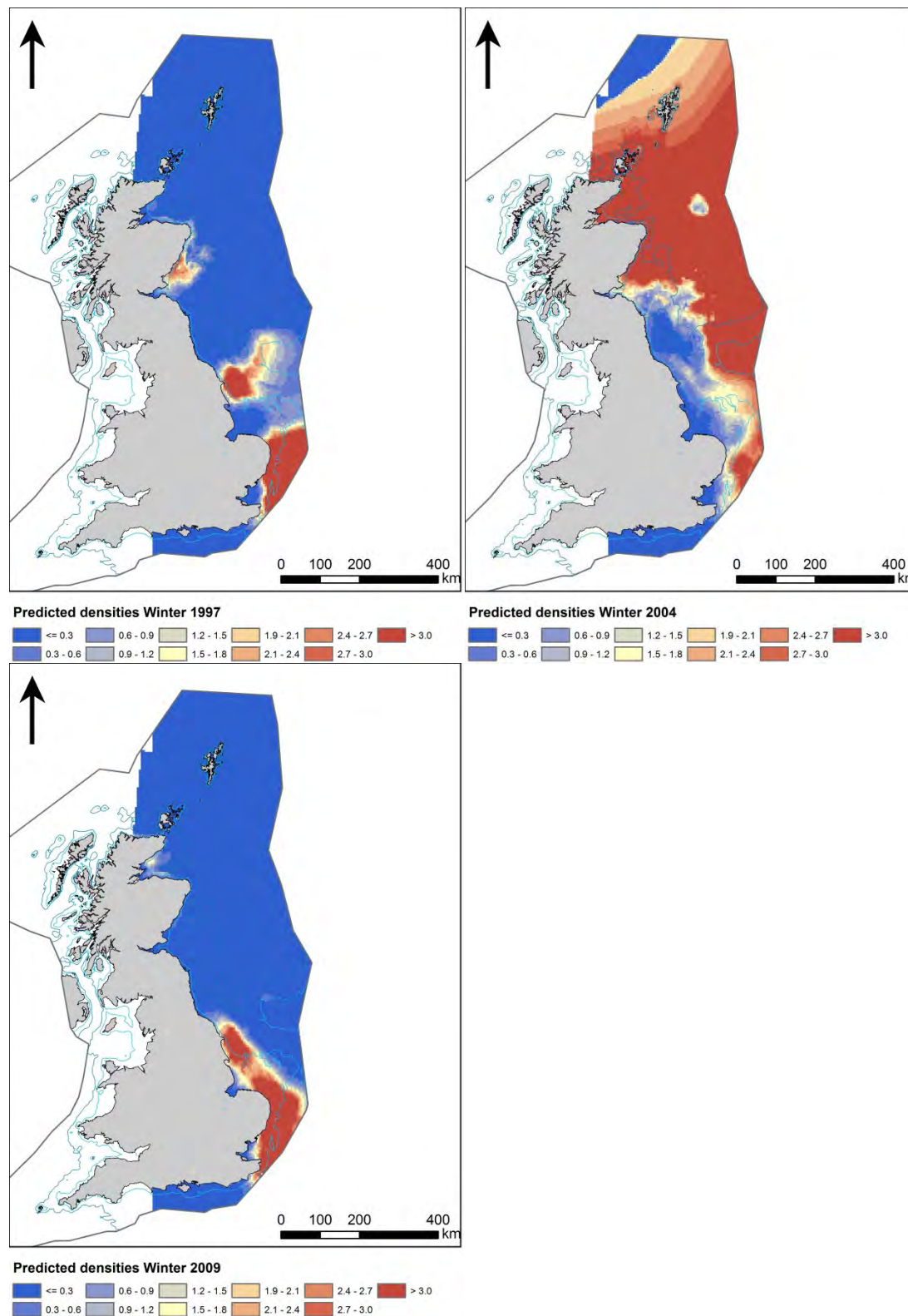
Figure 27. Predicted densities (number/km^2) during winter in management unit 1 for three different years in each model period. Predicted densities for all years are shown in Appendix 3.
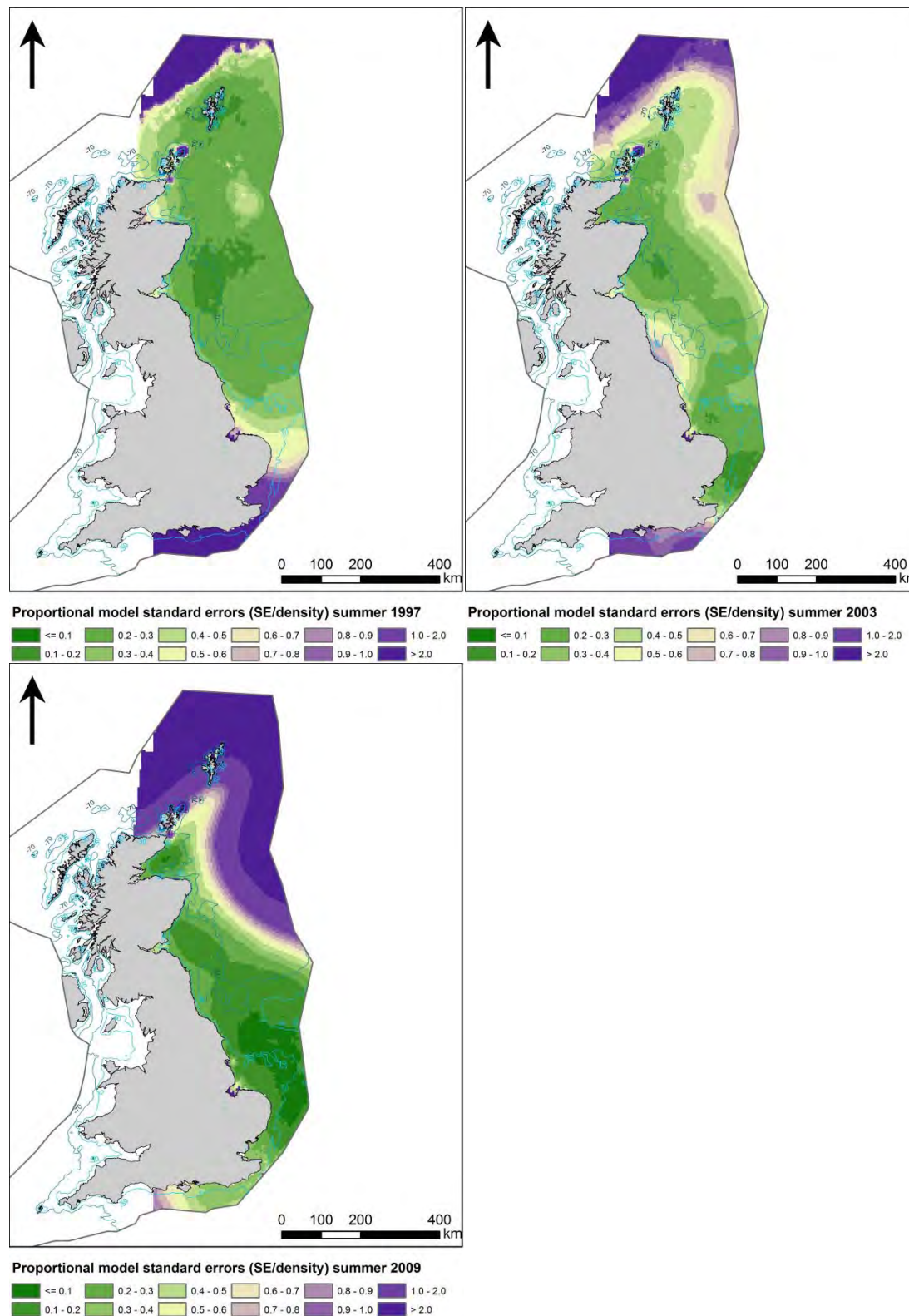
Figure 28. Model uncertainty. Proportional model standard errors for the summer models in management unit 1 (three selected years). Proportional model standard errors for all years are shown in Appendix 4.
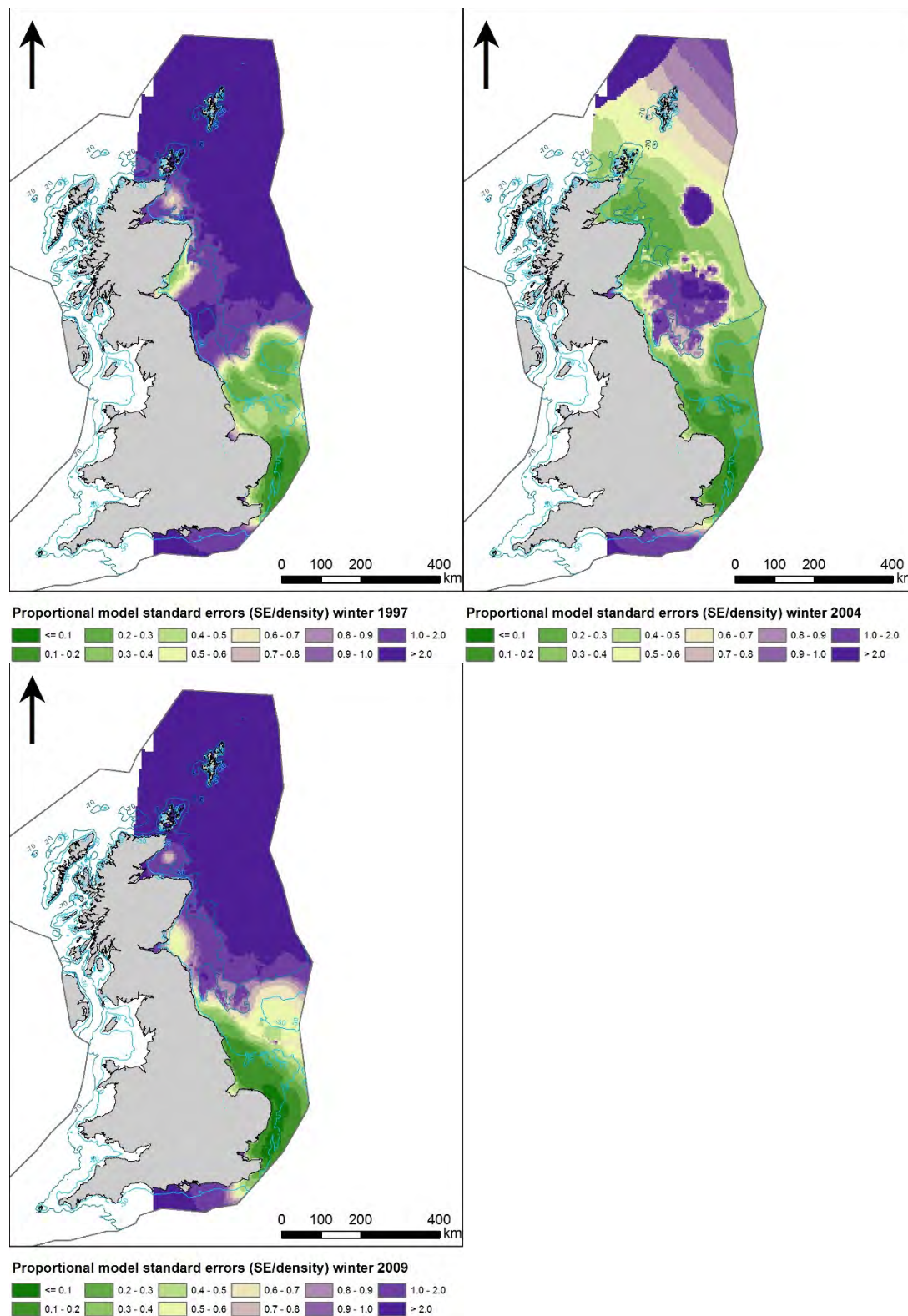
Figure 29. Model uncertainty. Proportional model standard errors for the winter models in management unit 1 (three selected years). Proportional model standard errors for all years are shown in Appendix 4.

Modelled density Summer 2009

<= 0.3	1.2 - 1.5	2.4 - 2.7
0.3 - 0.6	1.5 - 1.8	2.7 - 3.0
0.6 - 0.9	1.9 - 2.1	> 3.0
0.9 - 1.2	2.1 - 2.4	

Observed density - period 3

<= 0.3	1.2 - 1.5	2.4 - 2.7
0.3 - 0.6	1.5 - 1.8	2.7 - 3.0
0.6 - 0.9	1.8 - 2.1	> 3.0
0.9 - 1.2	2.1 - 2.4	
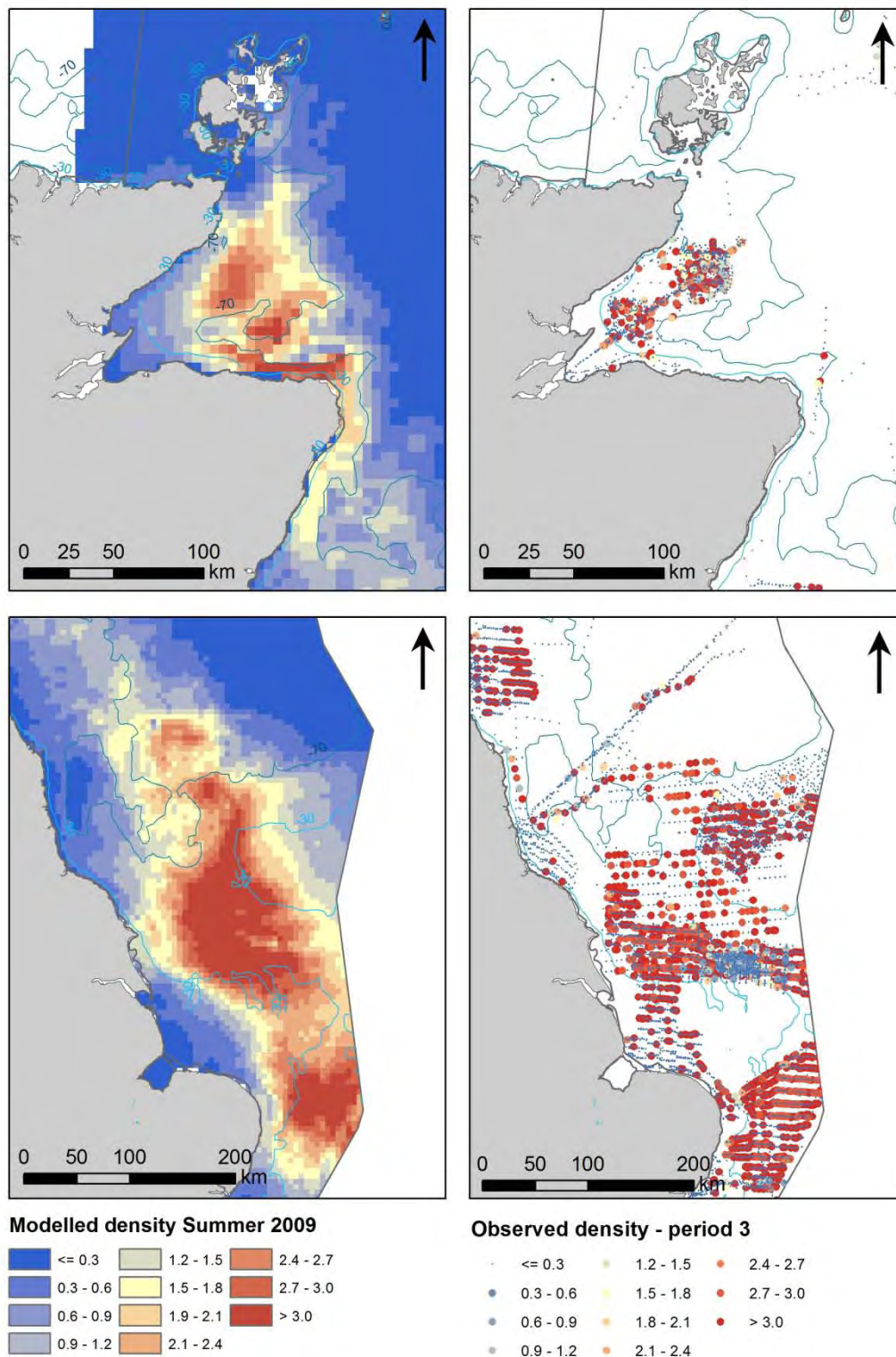
Figure 30. Close-up of high density (number/km^2) areas during summer in management unit 1 showing predicted and observed densities. Observed densities are indicated by dots using the same colour range as used for the predicted densities.

44

Modelled density Winter 2009

<= 0.3	1.2 - 1.5	2.4 - 2.7
0.3 - 0.6	1.5 - 1.8	2.7 - 3.0
0.6 - 0.9	1.9 - 2.1	> 3.0
0.9 - 1.2	2.1 - 2.4	

Observed density - period 3

<= 0.3	1.2 - 1.5	2.4 - 2.7
0.3 - 0.6	1.5 - 1.8	2.7 - 3.0
0.6 - 0.9	1.8 - 2.1	> 3.0
0.9 - 1.2	2.1 - 2.4	
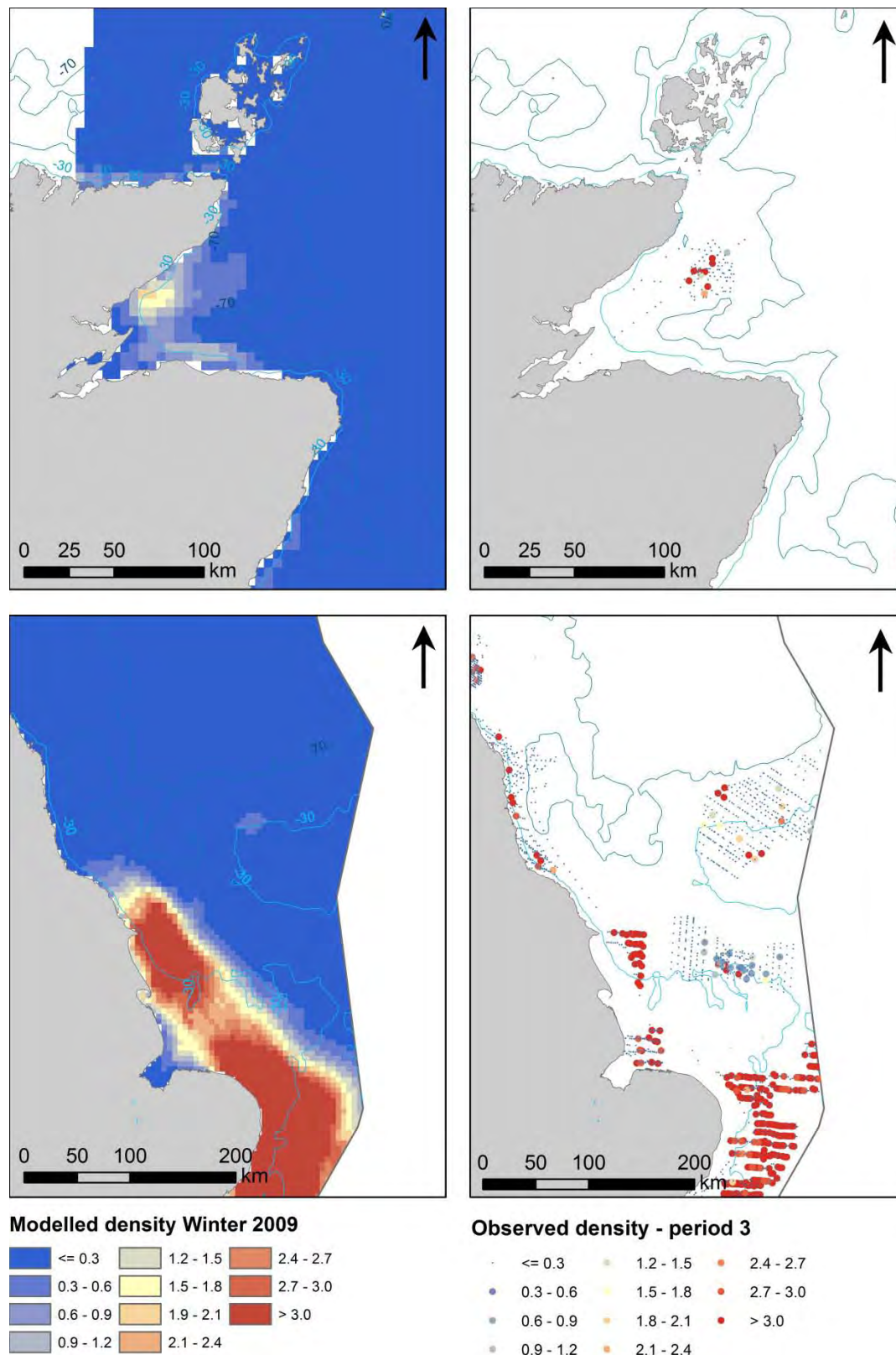
Figure 31. Close-up of high density (number/km^2) areas during winter in management unit 1 showing predicted and observed densities. Observed densities are indicated by dots using the same colour range as used for the predicted densities.

45
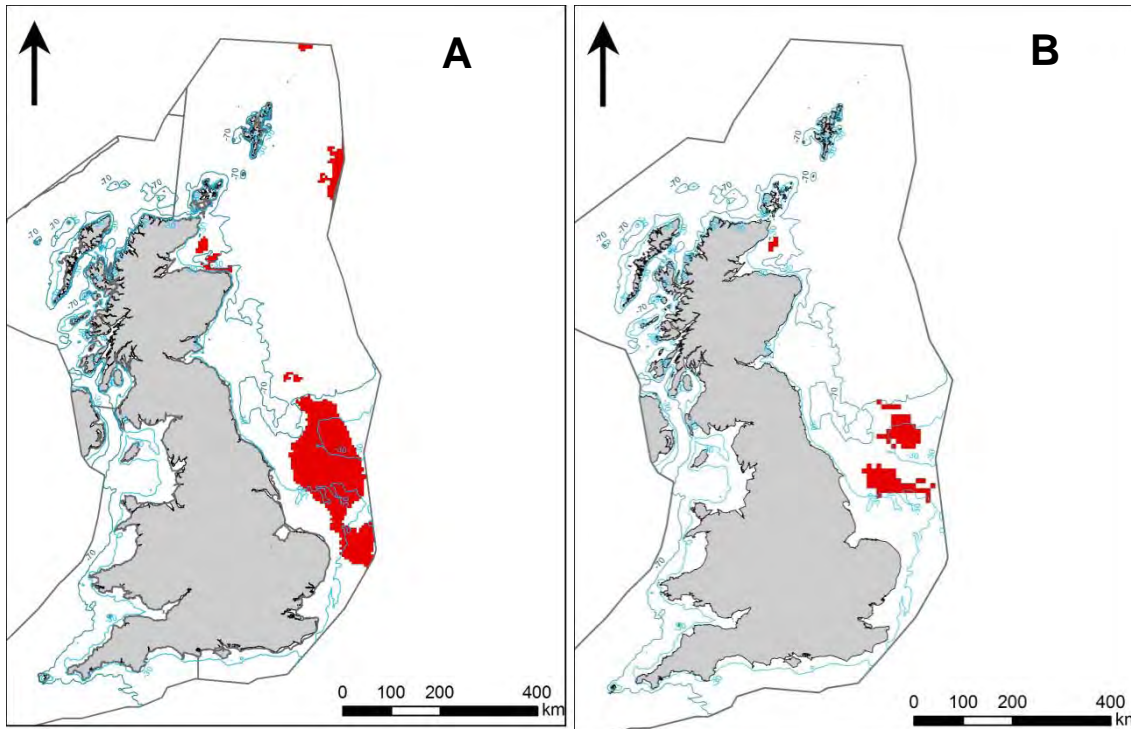
Figure 32. Persistent high-density areas identified and selected in management unit 1 during summer. In map A the red colours mark areas with where persistent high densities as defined by the upper 90th percentile have been identified. In map B the red colours mark persistent high-density areas with survey effort from three or more years.
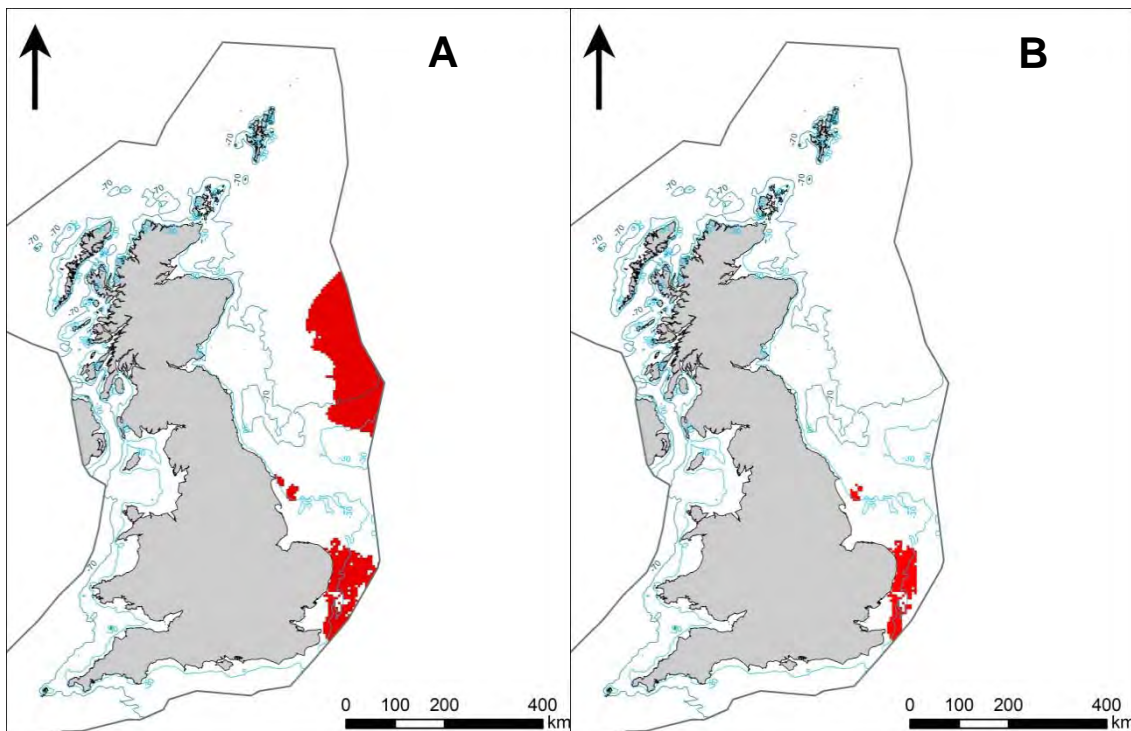
Figure 33. Persistent high-density areas identified and selected in management unit 1 during winter. In map A the red colours mark areas with where persistent high densities as defined by the upper 90th percentile have been identified. In map B the red colours mark persistent high-density areas with survey effort from three or more years.

3.5   NW Scottish Waters MU

The model results for the summer season for the area north-west of Scotland indicate that particle size of surface sediments is the most important determinant of the distribution of harbour porpoises in this management unit (Table 7). The low sample of available density data for the winter season in the NW Scottish Waters MU did not allow for development of distribution models during this season. The interaction terms with survey period share a strong effect on the presence of animals, but less effect on the density.

Surface salinity also plays a relatively important role in this region, whereas water depth and number of ships have little effect on porpoise distribution. As is the case for the other two management units described above, the segment length also has an important effect on the probability of presence in the management unit.

Both the presence and abundance part of the model have a dome-shaped response to particle size of surface sediments with peak presence/abundance at values between 2.5 and 3, i.e. in areas of rather coarse sand or gravel (Figure 34). The response curves indicate an avoidance of areas of high surface salinity (≥ 35 psu).

Table 7. Smooth terms, deviance explained and evaluation statistics for summer model NW Scottish Waters MU. The z-values and significance for the parametric terms are shown and for the smooth terms the approximate significance and chi-square/F statistics. Variables not included in either the binomial or positive model part are indicated with a dash.

Smooth terms	Presence/absence		Positive density	
	chi-sqr	p	F	p
Current speed	-	-	-	-
Eddy potential	-	-	-	-
Current gradient	-	-	-	-
Surface salinity	12.844	< 0.01	2.319	0.09
Vertical temp. Gradient	-	-	-	-
Water depth	2.685	0.25	0.341	0.61
Slope of seafloor	-	-	-	-
Surface sediments	20.099	< 0.001	3.954	< 0.01
Shipping density	-	-	-	-
Length survey segment	203.163	< 0.001	-	-
Spatio-temporal Period1	94.682	< 0.001	3.391	< 0.001
Spatio-temporal Period2	41.670	< 0.001	9.094	< 0.001
Spatio-temporal Period3	56.122	< 0.001	5.641	< 0.001
Sample size (n)	7332		1169	
Dev. Exp.	12.4		27.5	
AUC	0.732			
Spearman's corr.	0.252			

Presence/absence
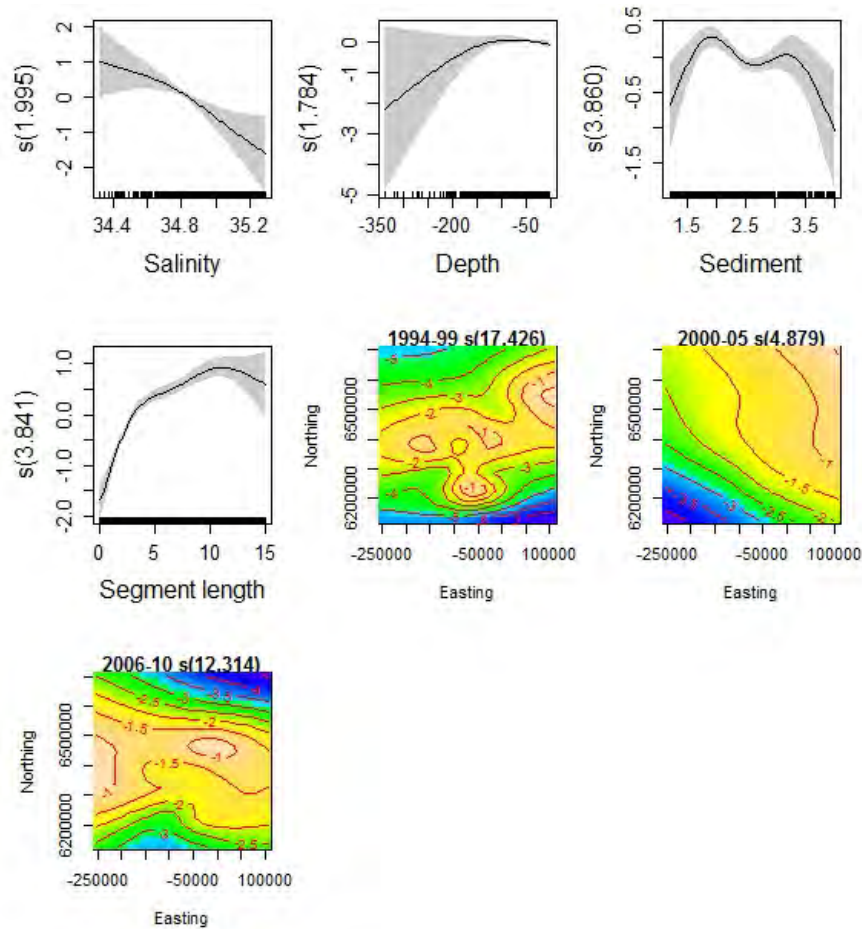
Density
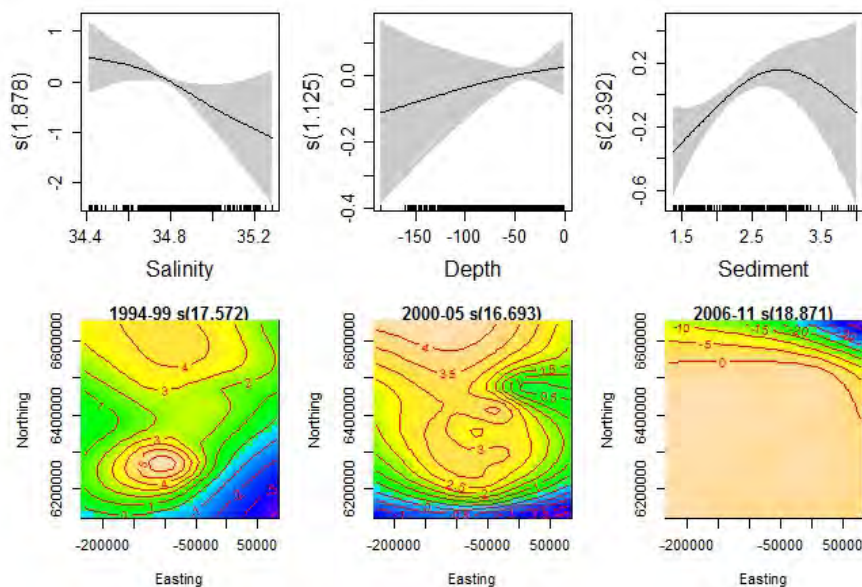
Figure 34. Partial GAM plots for presence/absence (upper panel) and positive (lower panel) parts for the summer model NW Scottish Waters MU. The values of the environmental variables are shown on the X-axis and the probability on the Y-axis in the scale of the linear predictor. The grey shaded areas and the dotted lines show the 95% Bayesian confidence intervals. The degree of smoothing is indicated in the legend of the Y-axis and for the interaction terms (Easting, Northing) in the heading.

3.5.1 Predicted distributions and persistency of estimated patterns

The predicted densities of harbour porpoise during the summer season display a high degree of variations in density levels between periods; especially the predicted densities west of the Hebrides during the period 2006-2011 which were clearly higher in the entire management unit as compared to the first two periods (Figure 35). The uncertainty of the modelled density estimates as visualised by the patterns of relative standard errors indicate robust model predictions in most parts along the north-west coast (Figure 36). During the last period the estimates for the coastal areas north of Scotland have high standard errors. The predicted densities in the offshore waters in this management unit have high errors in all three periods.

High densities of harbour porpoises are predicted during summer along almost the entire north-west coast of Scotland. The close-up on the coastal area during the period 2006-2011 shows a satisfactory degree of correspondence between the predicted and observed densities (Figure 37). In combination with the moderate level of uncertainty associated with the model predictions for the coastal area it indicates that the large size of the area with high densities of harbour porpoise has been confidently determined. When judged from the calculation of the 90th percentiles, the relative variation in the location of the highest densities is rather stabile between periods, and the area shows as a coherent zone stretching along the north-western coast of Scotland and through the Minches and eastern parts of the Sea of Hebrides (Figure 38). The densities predicted along the north coast of Scotland during the first period were quite high but fell below the 90th percentile threshold.

The coastal areas of this management unit have received a relatively even effort across the three model periods. Thus, the major part of the high-density zone along the north-west coast remains after taking the level of observational effort into account (Figure 38).

In spite of the wide distributions, the high-density areas as indicated by the 90th percentiles comprise less than 10% of the management unit during summer. However, the high density areas comprise more than 50% of the offshore area as marked by the 70m depth contour.
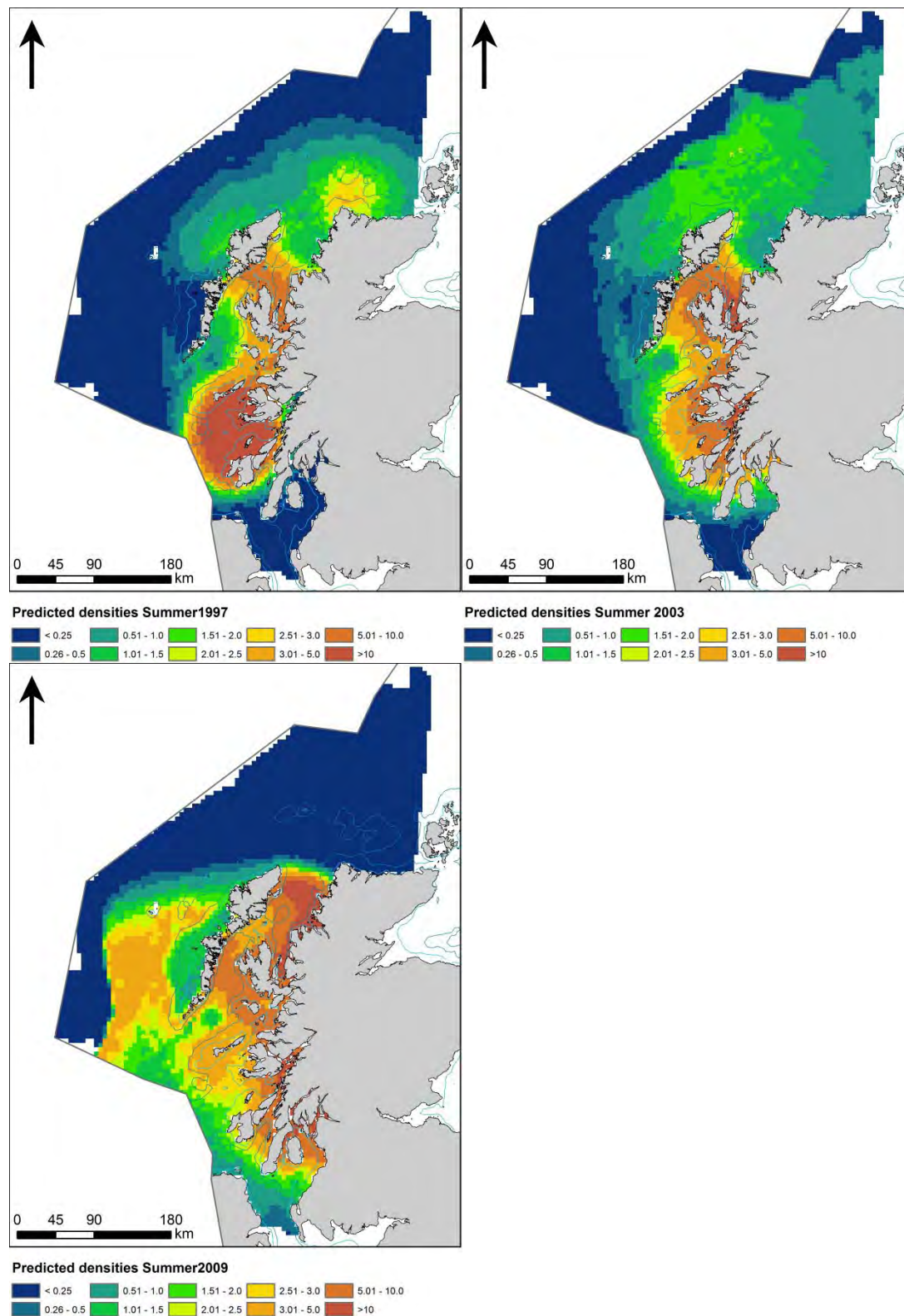
Figure 35. Predicted densities (number/km^2) during summer in NW Scottish Waters MU for three different years in each model period. Predicted densities for all years are shown in Appendix 3.
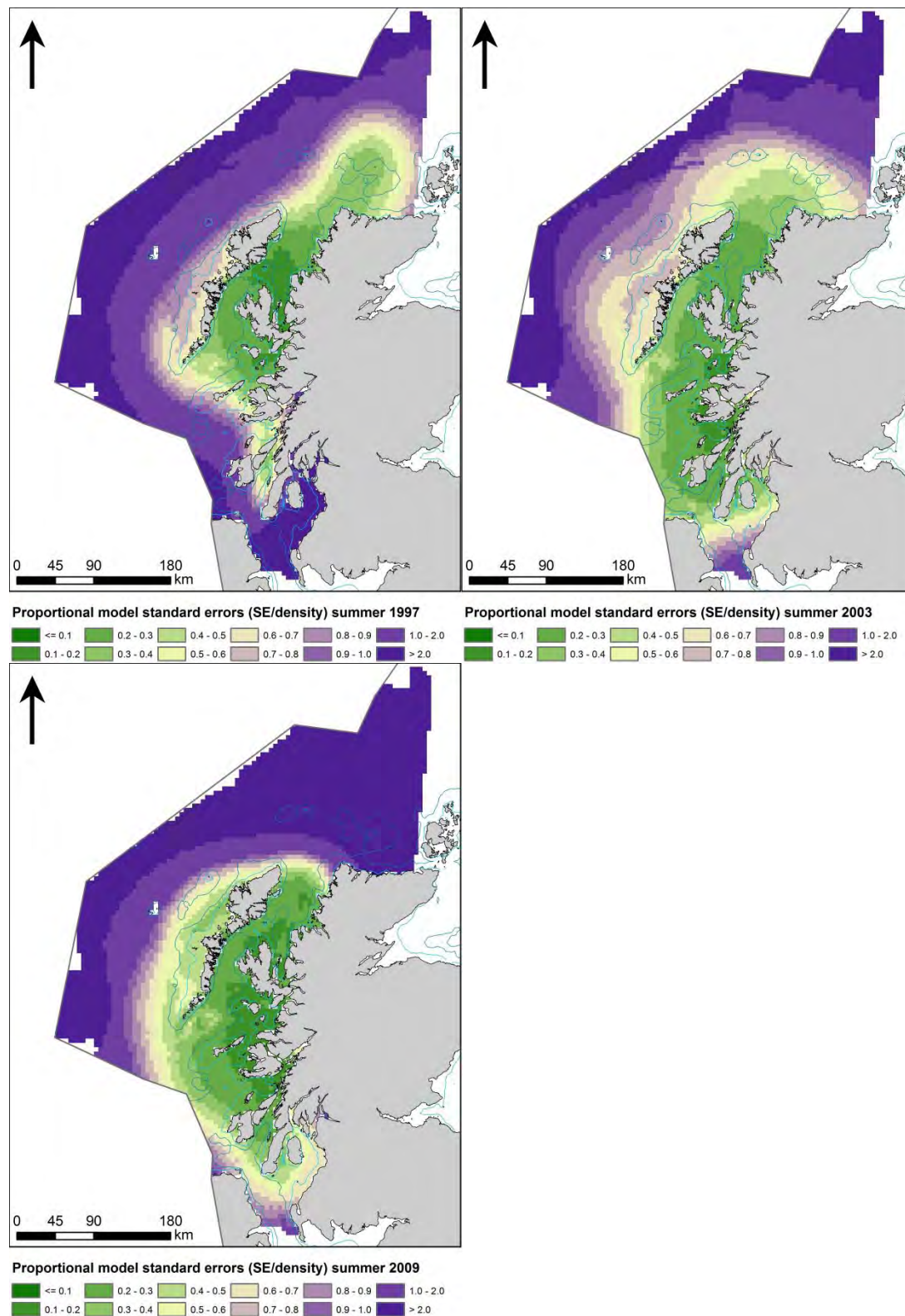
50

Figure 36. Model uncertainty. Proportional model standard errors for the summer models in NW Scottish Waters MU (three selected years). Proportional model standard errors for all years are shown in Appendix 4.
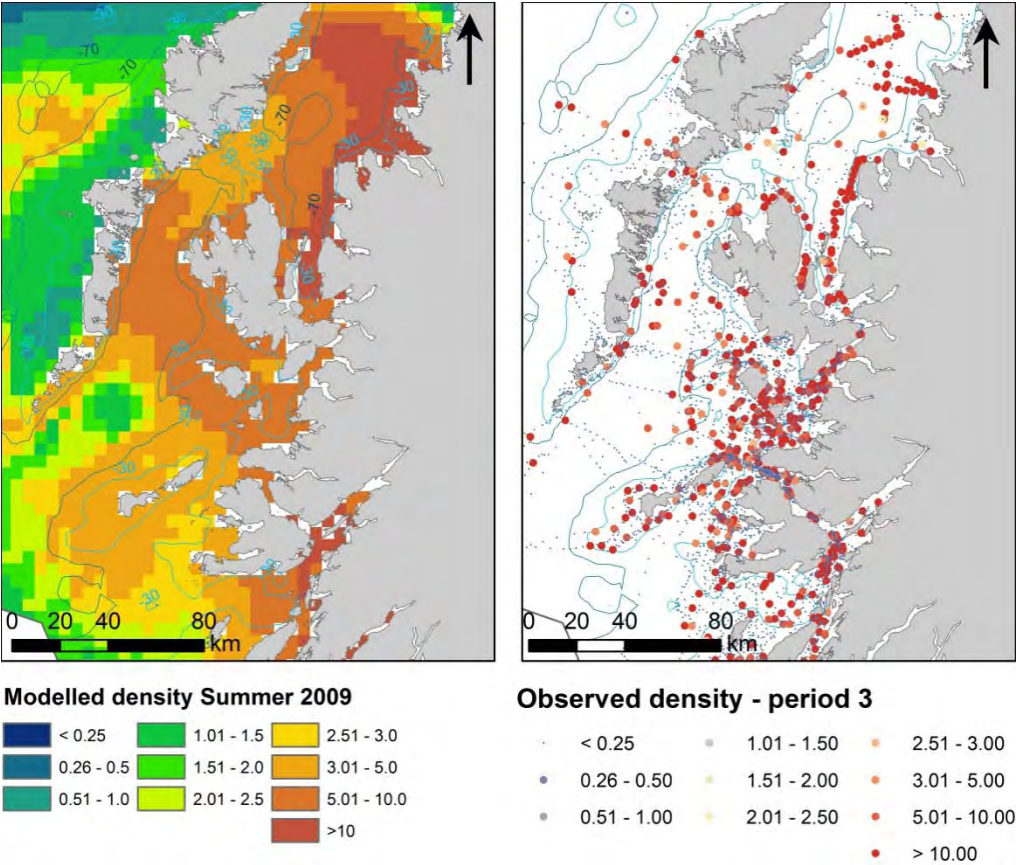
Figure 37. Close-up of high density (number/km^2) areas during summer in NW Scottish Waters MU showing predicted and observed densities. Observed densities are indicated by dots using the same colour range as used for the predicted densities.
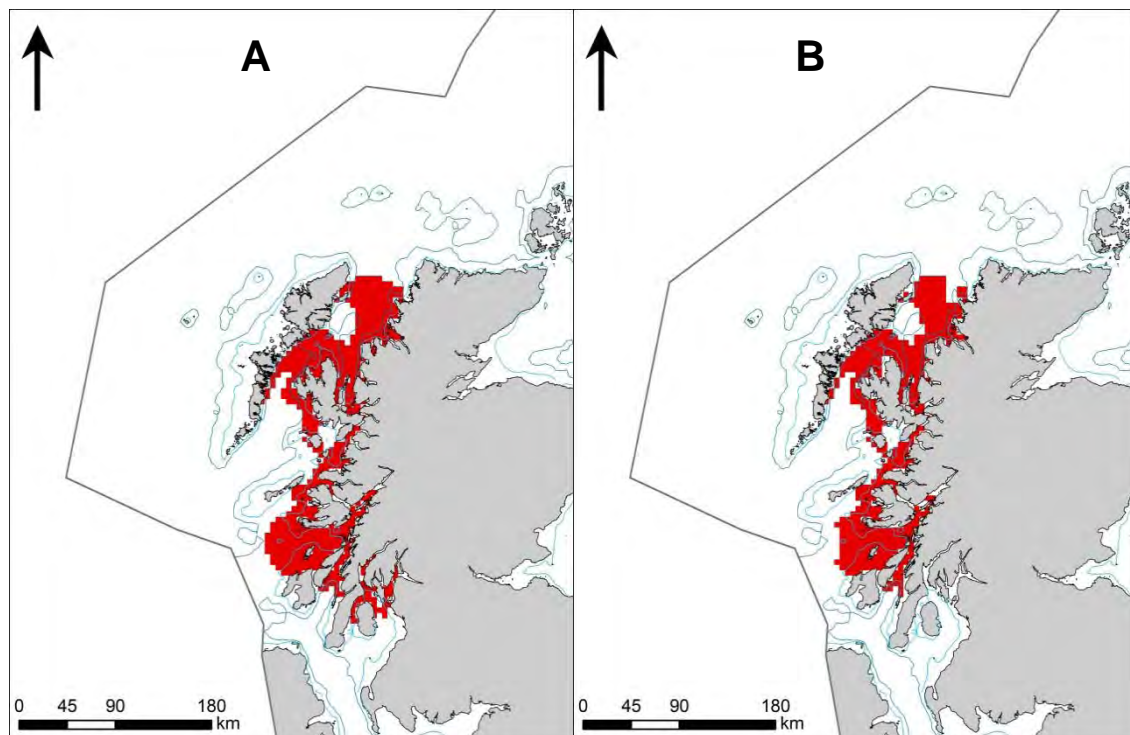
Figure 38. Persistent high-density areas identified and selected in NW Scottish Waters MU during summer. In map A the red colours mark areas with where persistent high densities as defined by the upper 90th percentile have been identified. In map B the red colours mark persistent high-density areas with survey effort from three or more years.

4   Discussion

4.1   Assumptions of the JCP data

It is important to stress that while the JCP data comprise an unprecedented volume of effort corrected density data for standardised units of transect length on harbour porpoises in UK waters; the data rest on assumptions, which, if invalid, would compromise the ability to make inferences and draw conclusions. The JCP data are potentially appropriate for exploring large-scale trends in space and time in the relative abundance of porpoises, but are not appropriate for estimating abundance at small spatial and temporal scales. Despite having large quantities of data, survey effort is distributed very patchily over space and time, and there are significant spatio-temporal gaps (particularly in autumn and winter seasons) and confounding between survey type and location/time. Thus, the generation and presentation of estimates of abundance in *small areas over discrete periods of time* is not supportable.

Since the patchiness of the survey coverage manifests itself as a change from complete lack of coverage in an area one part in one year followed by an intensive survey effort in the next, following year analyses of densities of harbour porpoises using the JCP data are most appropriately done by merging data across several years. However, even when analyses of densities are undertaken by combining based on periods of multiple years, as in this study, differences in survey coverage may still influence mean densities, especially in areas of repeated surveys. In areas of repeated surveys, such as areas subjected to baseline studies investigations in relation to offshore wind development schemes, this effort-related bias is potentially influential, and may cause differences in mean densities which are mainly related to differences in survey effort. Thus, users of the results of this study should be cautious to assess the influence of the location of such monitoring activities on identified areas.

One of the key assumptions in the JCP data is that surveys that collected distance-sampling data have the same detection probabilities as surveys that did not record distances, and that detection probabilities within survey type do not change with time (Paxton *et al.* 2012). Further, it is assumed that distances are accurately recorded and detection probabilities are the same across survey types (i.e. dedicated survey compared to platform of opportunity). These assumptions may not be correct. The JCP includes a relatively large amount of data collected during seabird surveys. Although a lot of observations of harbour porpoises have been made from these seabird surveys, detection probabilities may be influenced to an unknown degree by the level of seabird densities. Comparisons of detection probabilities between the different survey and platform types are needed to assess the comparability of data within the JCP.

Further, it is worth mentioning the assumption that the variability in survey platform height is insignificant within the three classes of survey boats used in the detection functions: little boats (observer eye height < 5m above the water level), big boats (observer eye height between 5 and 10m above water level) and ferries (observer eye height > 10m above the water). Variability in survey platform height has been shown to be important in detection function modelling of SCANS-II data (Hammond *et al.* 2013).

4.2   Performance of distribution models

Predictive distribution models like the GAMs applied in this study are now commonplace in studies aiming at describing and understanding the distribution of species at various spatial scales (Guisan & Zimmermann 2000, Elith *et al.* 2006). In comparison, relatively few applications of predictive distribution models have been realised in the marine environment, and the vast majority have been made at a relatively coarse resolution and covering relatively large extents (Bailey & Thompson 2009; Maxwell *et al.* 2009). As the application of distribution models assume that the physical environment exerts a dominant control over the

natural distribution of a species, validation of marine distribution models and their assumptions and predictive performance have to take the unique physical properties of marine habitats into account (Robinson *et al.* 2011). This study explicitly aimed at resolving the distribution of harbour porpoises in UK waters by developing GAMs describing the dynamic coupling to their physical environment. The validation of the explanatory and predictive power of the distribution models applied in this study show that in spite of a moderate fit of the presence-absence part the density part of the models had relatively high deviance explained values. As indicated by the validation statistics and the proportional standard errors of model predictions the accuracy of predictions was acceptable in areas of good survey coverage. In these areas, as seen in the fine-scale maps, the predicted density of harbour porpoises agreed well with the observed values. These results indicate that the two-step model design including a spatio-temporal smoother produced useful results.

An important prerequisite for resolving the habitat features of porpoises was the possibility to assimilate post-processed oceanographic habitat variables from a calibrated hydrodynamic model as well as pressure variables from a database on ship density. The strong influence of both water mass, current characteristics and shipping density on the presence and abundance of harbour porpoises found in this study indicates that despite the uneven coverage of the JCP data model, predictions are parsimonious. Due to the patchiness of input data, predictions may often be extrapolations on the basis of the physical characteristics of the areas. Although such areas were excluded from the final identification of persistent high density areas the predictions outside areas of frequent survey effort may be used to indicate areas of potential important habitat. However, because the models included geographical coordinates as predictors, the extrapolations should be used with care, especially for the winter season.

Although the hydrodynamic models used describe well the mean seasonal patterns of water column structure, currents and hydrographic fronts in UK waters, the data do not describe tidal propagations and detailed interactions between currents and bathymetry in local areas. Fine-scale hydrodynamic modelling would be necessary to resolve oscillations in physical conditions at the local scale, and hence in the distribution of porpoises in response to the dynamics of fine-scale hydrodynamic features, especially hydrodynamic fronts and eddies. Such oscillations would be expected from the associations found in this study. Hence, it will be possible to increase the knowledge of the local habitats of harbour porpoises in the identified high density areas by downscaling the models.

The peak densities described by the model for the North Sea during summer at the lower gradient in the difference between surface and bottom temperature indicates an association with the location of tidal mixing fronts. This is not surprising given the reporting of ubiquitous concentrations of piscivorous species at these frontal features (Schneider 1982, Kinder *et al.* 1983). Similar positive responses between the distribution of porpoises and the location of tidal mixing fronts have been described in the eastern part of the North Sea (Skov *et al.* 2014). Another important association with frontal features described by the models was the positive response to eddy activity in MU 1 and 2. This association may be interpreted as an affinity to entrainment processes of eddies which enhance the probability of prey encounter, which greatly maximize the foraging success of piscivorous predators (Fauchald *et al.* 2011). In all three management units the presence of harbour porpoises was positively related to the coarseness of surface sediments. This relationship is probably a general feature in European waters, as indicated by similar habitat associations in the eastern part of the North Sea (Skov *et al.* 2014). Harbour porpoises are known to feed on sandeels (Ammodytidae; Benke & Siebert 1996, Santos 1998), which exhibit strong associations with surface sediments. Studies at the Shetland Isles demonstrated that the fine particle fraction effectively limits the distribution of the lesser sandeel (*Ammodytes marinus,* Wright *et al.* 2000). Thus, the general avoidance by harbour porpoises of areas with high silt/clay content may be directly related to the distribution of sandeels and other prey fish.

4.3 Robustness of persistence analyses

The methods employed during the different stages of the persistency analyses were developed following the requirements set out by the Interagency Marine Mammal Working Group. The persistence analyses ultimately represent the final step in the identification of areas for which sufficient evidence exist that they sustain long-term concentrations of harbour porpoises. The evaluation of the available evidence in the multi-year predictions of seasonal densities should be two-fold; an evaluation of degree of recent high densities and the number of years that high-densities were predicted. As this combined evaluation was based on modelled distributions of porpoises the final identification should seek to select predicted high density areas for which survey effort had been undertaken in at least three years.

The combined evaluation of the age and number of years of the evidence obviously needed to rely on soft criteria with scorings which in some cases may show opposite results for each component (e.g. high densities predicted in recent, but few years). Fuzzy logic membership functions were chosen as a means for both providing standardised and hence robust scorings on both components and enabling trade-offs between the two evaluations.

'Fuzzy logic is a widespread method applicable in situations when caution has to be taken using sharp boundaries between categories of acceptance/no acceptance. Fuzzy logic involves calculations of probability derived not merely from Boolean laws, but through a fuzzy membership function. The shape of this function is governed by control points (Robertson *et al.*, 2004), and both the shape and the values of the control points are defined by the user. As is often the case in nature, crisp criteria are not easily supported by the evidence, and despite the subjectivity in the choice of function and control points the use of fuzzy logic secures fuzzy limits around sharp boundaries to qualifying the uncertainty of their positions. Thus, the method has increased the confidence in the identification of persistent areas as it has made it possible to account for the lack of clear definitions of acceptance criteria for age and number of years of high densities.

It is not surprising that the use of a filter of data for minimum survey effort of three years had a large effect on the final identification in areas with limited survey effort. This was the case in offshore waters in the Celtic/Irish Sea MU and in the North Sea MU during winter. As the model predictions in these areas had relatively large standard errors the application of the filter ensured that the final identification was supported by both observed and predicted high densities of harbour porpoises.

References

AUSTIN, M.P. 2002. Spatial prediction of species distribution: an interface between ecological theory and statistical modelling. *Ecological Modelling* **157**: 101-118.

BAILEY, H. & THOMPSON, P.M. 2009. Using marine mammal habitat modelling to identify priority conservation zones within amarine protected area. *Marine Ecology Progress Series* **378**: 279–287

BENKE, H. & SIEBERT, U. 1996. *The current status of harbour porpoises (Phocoena phocoena) in German waters*. Reports of the International Whaling Commission, SC/47/SM49.

CAMERON, A. & ASKEW, N. (EDS.). 2011. EUSeaMap - Preparatory Action for development and assessment of a European broad-scale seabed habitat map final report. *Available at http://jncc.gov.uk/euseamap*

CAMPHUYSEN, C.J., SCOTT, B.E., & WANLESS, S. 2006. Distribution and foraging interactions of seabirds and marine mammals in the North Sea: multispecies foraging assemblages and habitat-specific feeding strategies. In: Boyd, I.; Wanless, S.; Camphuysen, C. J., (eds.) *Top predators in marine ecosystems: their role in monitoring and management*. Cambridge, Cambridge University Press, 82-97.

CLARK, C.J., POULSEN, J.R, MALONGA, R. & ELKAN, P.W. 2009. Logging concessions can extend the conservation estate for central African tropical forests. *Conservation Biology* **23**: 1281-1293

COOPER, R., GREEN, S., LONG, D. 2010. *User Guide for the British Geological Survey DiGSBS250K Dataset*. British Geological Survey Internal Report, IR/11/026. 17pp

ELITH, J., GRAHAM, C. H., ANDERSON, R. P., DUDÝ´K, M., FERRIER, S., GUISAN, A., HIJMANS, R. J., HUETTMANN, F., LEATHWICK, J. R., LEHMANN, A., LI, J., LOHMANN, L. G., LOISELLE, B. A., MANION, G., MORITZ, C., NAKAMURA, M., NAKAZAWA, Y., OVERTON, J. MCC., PETERSON, A. T., PHILLIPS, S. J., RICHARDSON, K., SCACHETTI-PEREIRA, R., SCHAPIRE, R. E., SOBERÓN, J., WILLIAMS, S., WISZ, M. S. & ZIMMERMANN, N. E. 2006. Novel methods improve prediction of species' distributions from occurrence data. *Ecography* **29**: 129-151.

ELITH, J. & LEATHWICK, J. R. 2009. Species distribution models: ecological explanation and prediction across space and time. *Annual Review of Ecology, Evolution, and Systematics* **40**: 677-697.

EMBLING, C.R., GILLIBRAND, P.R., GORDON, J., SHRIMPTON, J., STEVICK, P.T., HAMMOND, P.S. 2010. Using Habitat Models to Identify Suitable Sites for Marine Protected Areas for Harbour Porpoises (Phocoena phocoena). *Biological Conservation* **143**: 267 – 279.

FAUCHALD, P, SKOV H., SKERN-MAURITZEN, M., HAUSNER, VH., JOHNS, D. & TVERAA, T. 2011. Scale-dependent response diversity of seabirds to prey in the North Sea. *Ecology* **92**: 228–239.

FOLK, R.L. 1954. The distinction between grain size and mineral composition in sedimentary rock nomenclature. *Journal of Geology* **62** (4), 344-359.

FRANKLIN, J. 2009. Mapping species distributions: spatial inference and prediction. *Cambridge University Press, Cambridge*.

GILLES,A., SCHEIDAT, M. & SIEBERT, U. (2009) Seasonal distribution of harbour porpoises and possible interference of offshore wind farms in the German North Sea. *Mar Ecol Prog Ser* **383**: 295–307.

GOODMAN, L.A. 1960. On the exact variance of products. *Journal of the American Statistical Association* **55**, 708-713.

GRAHAM, M. H. 2003. Confronting multicollinearity in ecological multiple regression. *Ecology* **84**: 2809-2815.

GRANADEIRO, J.P., ANDRADE, J. & PALMEIRIM, J.M. 2004. Modelling distribution of shorebirds in estuarine areas using generalized additive models. *Journal of Sea Research* **52**, 227-240.

GUISAN, A. & ZIMMERMANN, N.E. 2000. Predictive habitat distribution models in ecology. *Ecological Modelling* **135**: 147-86.

GUISAN, A., EDWARDS, T. C. & HASTIE, T. 2002. Generalized linear and generalized additive models in studies of species distributions: setting the scene. *Ecological Modelling* **157**: 89-100.

HAMMOND, P.S., BERGGREN, P., BENKE, H., BORCHERS, D.L., COLLET, A., HEIDE-JØRGENSEN, M.P., HEIMLICH, S., HIBY, A.R., LEOPOLD, M.F. & ØIEN, N., 2002. Abundance of harbour porpoises and other cetaceans in the North Sea and adjacent waters. *J. Appl. Ecol.* **39**: 361–376.

HAMMOND, P.S., MACLEOD, K., BERGGREN, P., BORCHERS, D.L., BURT, M.L., CAÑADAS, A., DESPORTES, G., DONOVAN, G.P., GILLES, A., GILLESPIE, D., GORDON, J., HIBY, L., KUKLIK, I., LEAPER, R., LEHNERT, K., LEOPOLD, M., LOVELL, P., ØIEN, N., PAXTON, C.G.M., RIDOUX, V., ROGAN, E., SAMARRA, F., SCHEIDAT, M., SEQUEIRA, M., SIEBERT, U., SKOV, H., SWIFT, R., TASKER, M.L., TEILMANN, J., VAN CANNEYT, O. & VÁZQUEZ, J.A. 2013. Cetacean abundance and distribution in European Atlantic shelf waters to inform conservation and management. *Biological Conservation* **164**: 107-122.

HASTIE, T. & TIBSHIRANI, R. 1990. Generalized additive models. *Chapman & Hall, London.*

HEIKKINEN, R. K., LUOTO, M., ARAÚJO, M. B., VIRKKALA, R., THUILLER, W. & SYKES, M. T. 2006. Methods and uncertainties in bioclimatic envelope modelling under climate change. *Progress in Physical Geography* **30**: 751-777.

HEINÄNEN, S., RÖNKÄ, M. & von NUMERS, M. 2008. Modelling the occurrence and abundance of a colonial species, the arctic tern Sterna paradisaea in the archipelago of SW Finland. *Ecography* **31**:601-611.

KINDER, T.H., HUNT, G.L. JR., SCHNEIDER, D. & SCHUMACHER, J.D. 1983. Correlations between seabirds and oceanic fronts around the Pribilof Islands, Alaska. Est. Coast. *Shelf Sci.* **16**: 309-319.

KOBER, K., WEBB, A., WIN, I., LEWIS, M., O'BRIEN, S., WILSON, L.J., REID, J.B. 2010. An analysis of the numbers and distribution of seabirds within the British Fishery Limit aimed at identifying areas that qualify as possible marine SPAs. *JNCC report No. 431.*

LE PAPE, O., GUÉRAULT, D. & DÉSAUNAY, Y. 2004. Effect of an invasive mollusc, American slipper limpet Crepidula fornicata, on habitat suitability for juvenile common sole Solea solea in the Bay of Biscay. *Mar. Ecol. Prog. Ser.* **277**: 107-115.

Mann, K.H. & Lazier, J.R.N. 1991. *Dynamics of marine ecosystems*. Blackwell Scientific Publications. Boston.

MARTIN, T.G., WINTLE, B. A., RHODES, J.R., KUHNERT, P.M., FIELD, S.A., LOW-CHOY, J., TYRE, A. J.& POSSINGHAM, P. 2005. Zero tolerance ecology: improving ecological inference by modelling the source of zero observations. *Ecology Letters* **8**: 1235-1246.

MAXWELL, D. L., STELZENMÜLLER, V., EASTWOOD, P.D. & S. ROGERS, I. 2009. Modelling the spatial distribution of plaice (Pleuronectes platessa), sole (Solea solea) and thornback ray (Raja clavata) in UK waters for marine management and planning. *Journal of Sea Research* **61**: 258-267.

MOISEN, G. G. & FRESCINO, T. S. 2002. Comparing five modelling techniques for predicting forest characteristics. *Ecological modelling* **157**: 209-225.

NIELSEN, T.G., LØKKEGAARD, B., RICHARDSON, K., PEDERSEN, F.B. & HANSEN, L. 1993. Structure of plankton communities in the Dogger Bank area (North Sea) during a stratified situation. *Mar. Ecol. Prog. Ser.* **95**: 115-131.

O'BRIEN, S., WEBB, A., BREWER, M.J. & REID, J.B. 2011. Use of kernel density estimation and maximum curvature to set Marine Protected Area boundaries: Identifying a Special Protection Area for wintering red-throated divers in the UK. *Biol. Conservation* **156**: 15-21.

PATEIRO-LOPEZ, B. & RODRGUEZ-CASAL, A., 2010. Generalizing the Convex Hull of a Sample: The R Package alphahull. *Journal of Statistical Software* **34**: 1-28.

PAXTON, C.G.M., SCOTT-HAYWARD, L., MACKENZIE, M., REXSTAD, E. & L. THOMAS. 2012. Revised Phase III Data Analysis of Joint Cetacean Protocol Data Resource. *Centre for Research into Ecological and Environmental Modelling, University of St Andrews*

PEARCE, J. & FERRIER, S. 2000. Evaluating the predictive performance of habitat models developed using logistic regression. *Ecological Modelling* **133**: 225-245.

PEDERSEN, F.B. 1994. The Oceanographic and Biological Tidal Cycle Succession in Shallow Sea Fronts in the North Sea and the English Channel. *Est. Coast.Shelf Science* **38**: 249-269.

PINGREE, R.D. & GRIFFITHS, D.K. 1978. Tidal fronts on the shelf seas around the British Isles. *J. Geophys. Res.* **83**: 4615-4622.

POTTS, J. M. & ELITH, J. 2006. Comparing species abundance models. *Ecological Modelling* **199**: 153-163.

R CORE TEAM. 2013. R: A Language and Environment for Statistical Computing. R *Foundation for Statistical Computing, Vienna*. http://www.R-project.org.

ROBERTSON, M. P., VILLET, M. H. & PALMER, A. R. 2004. A fuzzy classification technique for predicting species' distributions: applications using invasive alien plants and indigenous insects. *Diversity and Distributions* **10**: 461–474. doi: 10.1111/j.1366-9516.2004.00108.

ROBINSON, L.M., ELITH, J., HOBDAY, A.J., PEARSON, R.G., KENDALL, B.E., POSSINGHAM, H.P. & A. J. RICHARDSON. 2011. Pushing the limits in marine species distribution modelling: lessons from the land present challenges and opportunities. *Global Ecol. Biogeogr.* **20**: 789–802.

SANTOS, M. B. 1998. *Feeding ecology of harbour porpoises, common and bottlenosed dolphins and sperm whales in the northeast and Atlantic.* PhD thesis, School of Biology, University of Aberdeen, Scotland.

SCHNEIDER & HUNT 1982: Carbon flux to seabirds in waters with different mixing regimes in the southeastern Bering Sea. *Mar.Biol.* **67**: 337-344.

SCHNEIDER, D.C. 1982. Fronts and seabird aggregations in the southeastern Bering Sea. *Mar. Ecol. Prog. Ser.* **10**: 101-103.

SKOV, H. & PRINS, E. 2001. Impact of estuarine fronts on the dispersal of piscivorous birds in the German Bight. *Mar. Ecol. Prog. Ser.* **214**: 279-287.

SKOV, H. & THOMSEN, F., 2008. Resolving fine-scale spatio-temporal dynamics in the harbour porpoise Phocoena phocoena. *Marine Ecology Progress Series* **373**: 173-186

SKOV, H., HEINÄNEN, S., HANSEN, D.A., LADAGE, F., SCHLENZ, B., ZYDELIS, R. & THOMSEN, F. Habitat Modelling. 2014. Pp 102-112 in: BSH & BMU (2014). Ecological Research at the Offshore Windfarm alpha ventus - Challenges, Results and Perspectives. *Federal Maritime and Hydrographic Agency (BSH), Ministry for the Environment, Nature Conservation and Nuclear Safety (BMU). Springer Spektrum. 180 pp.*.

STEFÁNSSON, G. 1996. Analysis of groundfish survey abundance data: combining the GLM and delta approaches. *ICES Journal of Marine Science* **53**: 577-588.

SVEEGARD, S., TEILMANN, J., TOUGAARD, J., DIETZ, R., MOURITZEN, K. N., DESPORTES, G. & SIEBERT, U. 2011. High-density areas for harbor porpoises (Phocoena phocoena) identified by satellite tracking. *Marine Mammal Science* **1**: 230-246.

SWEET, K. 1988. Measuring the accuracy of diagnostic systems. *Science* **240**: 1285-1293.

WEBLEY, J.A.C., MAYER, D.G. & TAYLOR, S.M. 2011. Investigating confidence intervals generated by zero-inflated count models: Implications for fisheries management. *Fisheries Research* **110**: 177-182.

WINTLE, B.A., ELITH, J. & POTTS, J.M. 2005. Fauna habitat modelling and mapping: A review and case study in the Lower Central Coast Region of NSW. *Austral Ecology* **30**: 719–738.
WOOD, S. N. 2006. Generalized Additive Models: An Introduction with R. Chapman and Hall, London.

WOOD, S. N. & AUGUSTIN, N. H. 2002. Gams with integrated model selection using penalized regression splines and applications to environmental modeling. *Ecological Modelling* **157**: 157-177.

WRIGHT, P.J., JENSEN, H. & TUCK, I. 2000. The influence of sediment type on the distribution of the lesser sandeel, Ammodytes marinus. *Journal of Sea Research* **44**: 243-256.

ZUUR, A. F., IENO, E. N., WALKER, N. J., SAVELIEV, A. A. & SMITH, G. M. 2009. Mixed effect models and extensions in ecology. *Springer, New York.*

ZUUR, A. F., SAVELIEV, A. A. & IENO, E. N. 2012. Zero inflated models and generalized linear mixed models with R. Highland Statistics Ltd.

APPENDIX 1 – Hydrodynamic models

Hydrodynamic models

Two dedicated hydrodynamic models were designed for resolving currents and mixing regimes at the highest possible resolution achievable within the time constraints of the project. An eighteen year time-series of current patterns was developed using an integrated 2-dimensional model set-up in DHI's MIKE 21 model system, while 3-dimensional density patterns were computed on the basis of four years (2009-2012) of model runs using a baroclinic model set up in DHI's MIKE 3 model system. Both models were developed using finite-element grids with increasing spatial resolution in shallower areas.

UK 2D flow model

Based on experience from other regions (Skov *et al.* 2014), currents were expected to represent important predictor variables for the distribution of harbour porpoises at medium and fine spatial scales. Thus, the dedicated UK 2D flow model was set up with the purpose of describing fine-scale patterns of currents, including resolution of eddies and fronts. MIKE 21 FM HD computes on a flexible mesh the depth-integrated currents, driven by a combined forcing, which may comprise forces induced by tide, wind and waves. This model solves the depth-averaged shallow-water equations of continuity and momentum and can reproduce temporal and spatial variations of water levels and currents. The applied driving forces can consist of wave forces (radiation stresses), water-level differences or fluxes at the boundaries (tidal and river flow), wind and atmospheric pressure forces and Coriolis force. The MIKE 21 Flow Model used for the present study was Release 2012, Service Pack 1.

The model system is based on the numerical solution of the two dimensional incompressible Reynolds averaged Navier-Stokes equations subject to the assumptions of Bousssines and of hydrostatic pressure. The model is applicable for the simulation of hydraulic and environmental phenomena in estuaries, bays, coastal areas, and seas wherever stratification can be neglected. The model can be used to simulate a wide range of hydraulic and related items, including tidal exchange and currents, storm surges, and water quality.

Set-up and specifications

Bathymetry, domain and mesh

The model uses a flexible mesh (FM) based on unstructured triangular or quadrangular elements and applies a finite volume numerical solution technique. The extent of the model domain is seen in the figure below. The model bathymetry, taken from a previous study carried out by DHI, is based on a combination of interpolated GEBCO_08[4] and C-map[5] data. Shorelines were adopted from the Global Self-consistent, Hierarchical, High-resolution Shoreline Database (GSHHS), version 2.2.2 provided by NOAA[6].

The horizontal reference system used is longitude/latitude (WGS-84). The vertical reference system is mean sea level (MSL).

The mesh resolution is displayed in the graph below. The spatial resolution of the mesh varies from approximately 30-50km off the shelf to 10-30km over the slope and shelf edge to 5-10km on the larger depths (>100m) on the shelf, 3-5km on the smaller depths (<100m) on the shelf and between 1 and 3km in the coastal areas.

---

[4] http://www.gebco.net
[5] http://ww1.jeppesen.com/marine/lightmarine/index.jsp
[6] http://www.ngdc.noaa.gov/mgg/shorelines/gshhs.html
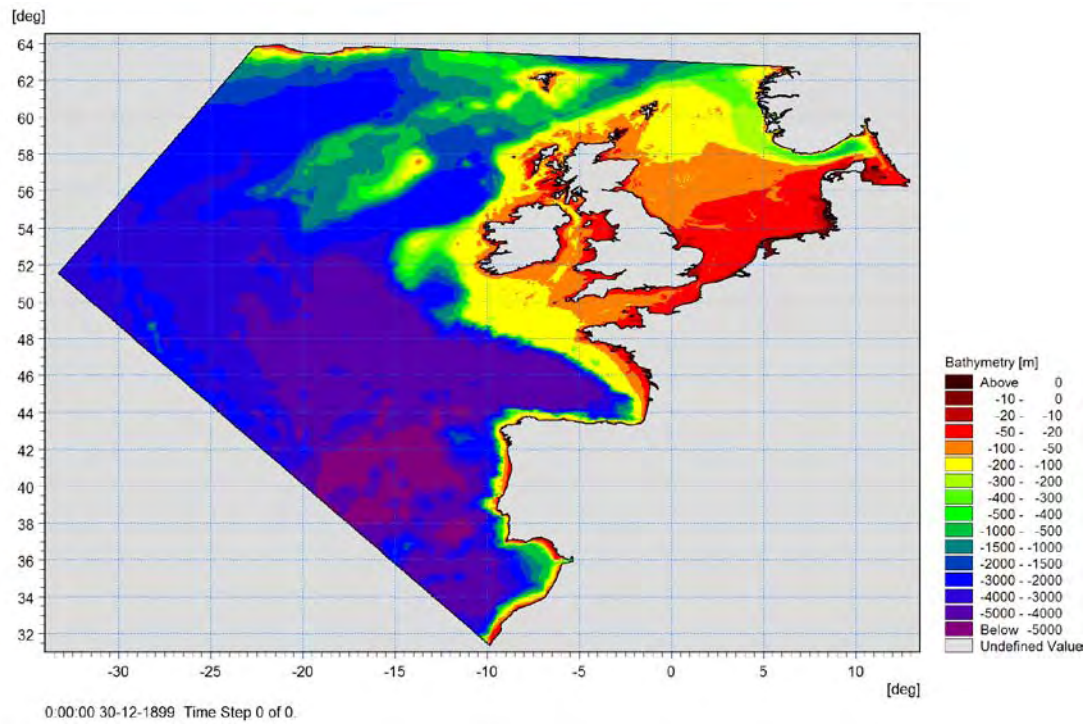
Figure A1.1. Model domain
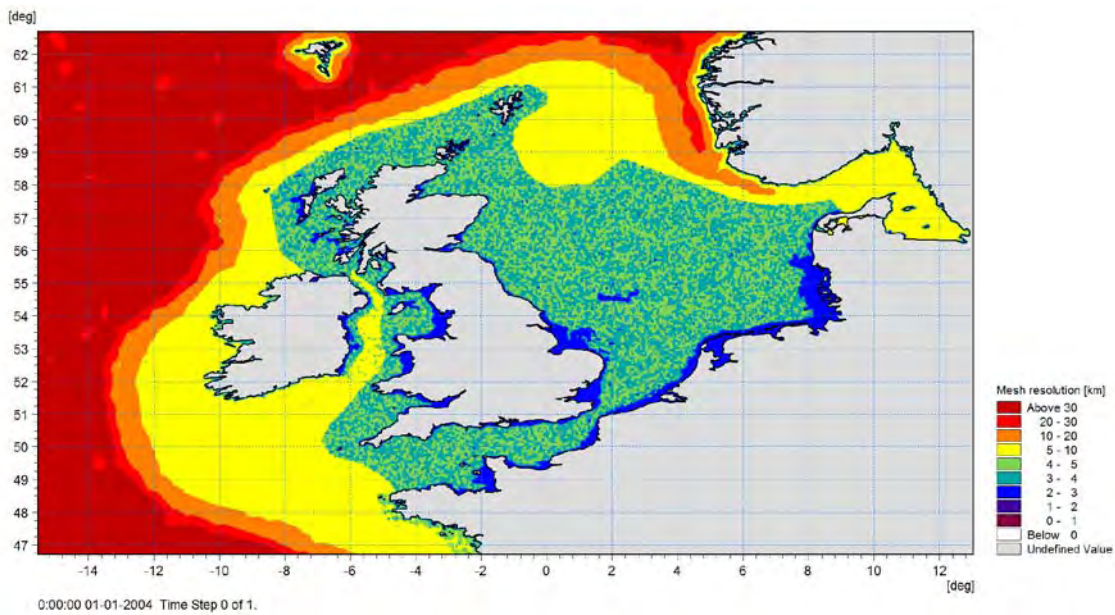
Figure A1.2. Mesh resolution

Boundary conditions

Spatial (1D) and time varying water level data were extracted from the global tide model (KMS) and applied to all four boundaries. The global tide model had obtained its tidal constituents from primarily satellite altimetry observations. The global tide model included 8 constituents (M2, S2, K1, O1, N2, P1, K2 and Q1) and had a spatial resolution of 0.25 degrees. Boundary data was extracted with a temporal resolution of 15min.

Meteorological forcing

The wind forcing and atmospheric pressure at MSL applied in the model were adopted from the Climate Forecast System Reanalysis (CFSR) numerical model provided by NOAA[7]. The CFSR data set was established by the National Centers for Environmental Prediction (NCEP). The data are available on an hourly basis from 1 January 1979 to present. The data set consists of Climate Forecast System Reanalysis (CFSR), covering the 31 year period from 1979 to 2009 and since then the operational data (CFSR2). The underlying model in CFSR2 is the same as for CFSR. In the following 'CSFR' will refer to the combined data of CFSR and CSFR2.

Table A1.1. Spatial resolution of the applied meteorological data.

Parameter	Temporal resolution	Spatial resolution CFSR	Spatial resolution CFSR2
Wind (U,V)	1 h	0.30°	0.30°
Air pressure reduced to MSL	1 h	0.50°	0.50°

The wind data included parameters of wind speed and wind direction (or wind velocity vectors, U and V) at height 10mMSL. The model values may be interpreted as representative of a 10 minute averaging period. The value in between the hourly values may attain a higher or lower value. However, the models produce a fairly smooth variation of the atmosphere, and the fluctuations within each time step are usually much smaller compared to what may be measured.

General model specifications

Based on sensitivity studies (see Sectionon validation below and calibration experience from previous studies, the model was set up with the following model specifications:

- Horizontal eddy viscosity: Smagorinsky formulation with constant = 0.28
- Bed resistance: Depth-dependent Manning map
- < 30m: 38m$^{1/3}$/s
- 30-100m: 42m$^{1/3}$/s
- > 100m: 45m$^{1/3}$/s
- The wind stress τ_s is defined by $\vec{\tau_s} = \rho_a c_f |U| \vec{U}$, where ρ_a is the density of the air, c_d represents the drag coefficient of the air and $\vec{U} = (U, V)$ are the wind components specified by in the CFSR data.
- Wind drag (empirical factors): $C_A = 1.255 \cdot 10^{-3}$, $C_B = 2.425 \cdot 10^{-3}$, $W_A = 7\ m/s$, $W_B = 25\ m/s$ (C_A, C_B, W_A, and W_B are used to calculate the empirical drag coefficient of air.)

$$c_d = \begin{cases} c_a \\ c_a + \frac{c_b - c_a}{w_b - w_a} \cdot (w_{10} - w_a) \\ c_b \end{cases}$$

- Direct tidal potential from 11 constituents (M2, O1, S1, K2, N2, K1, P1, Q1, MF, MM, SSA)
- Boundary conditions: Tides from the global tidal model (8 constituents)

Discharges from rivers were not included. They were considered to have an insignificant influence on the water level and current in a 2D regional model where no baroclinic conditions were included.

---

[7] http://journals.ametsoc.org/doi/pdf/10.1175/2010BAMS3001.1

Data assimilation

Data assimilation is a methodology that applies observed measurements in order to improve the skill and accuracy of the flow model. In this project, we considered only assimilation of in situ water level data.

The observations were used to update the model such that, broadly speaking, the model was used as an advanced interpolation and extrapolation tool. This allowed the model accuracy to be greatly improved also at non-observed positions and for additional variables such as the depth-averaged velocity.

The data assimilation scheme considered for this project was the Steady Kalman Filter approach based on the so-called Ensemble Kalman Filter. A time-varying temporally smoothed and distance regularized Ensemble Kalman Filter was used with a 8 ensemble member. The assimilation scheme assumes uncertainty in the open water level boundary conditions and wind forcing. The Ensemble Kalman Filter was used to construct a long-term averaged Kalman gain matrix based for January 2005. The Steady Kalman Filter then applies this time constant Kalman gain matrix, which has the advantage of reducing the computational cost significantly, while preserving good assimilation skills.

The data coverage from 1994-2011 for the 26 assimilation stations used is shown in the figure below. All measurements were corrected such that the datum approximately represents the model datum in order to allow proper comparison of observations and the model. The model datum was determined by the open boundary levels and a long-term average dynamical balance from a 1 year simulation without data assimilation. Note that the measurement-model difference could have a yearly mean variation. However, this was assumed to be insignificant.

A number of parameters need to be specified in the filter schemes. The assimilation system is very complex; hence, the parameters were based on experience and iterations (simulation tests). The standard deviation for most of the water level observations was in the range of 0.04-0.07. A lower value of the standard deviation for a measurement station implies that more trust was put on the observation data and hence the model was pulled more towards it.
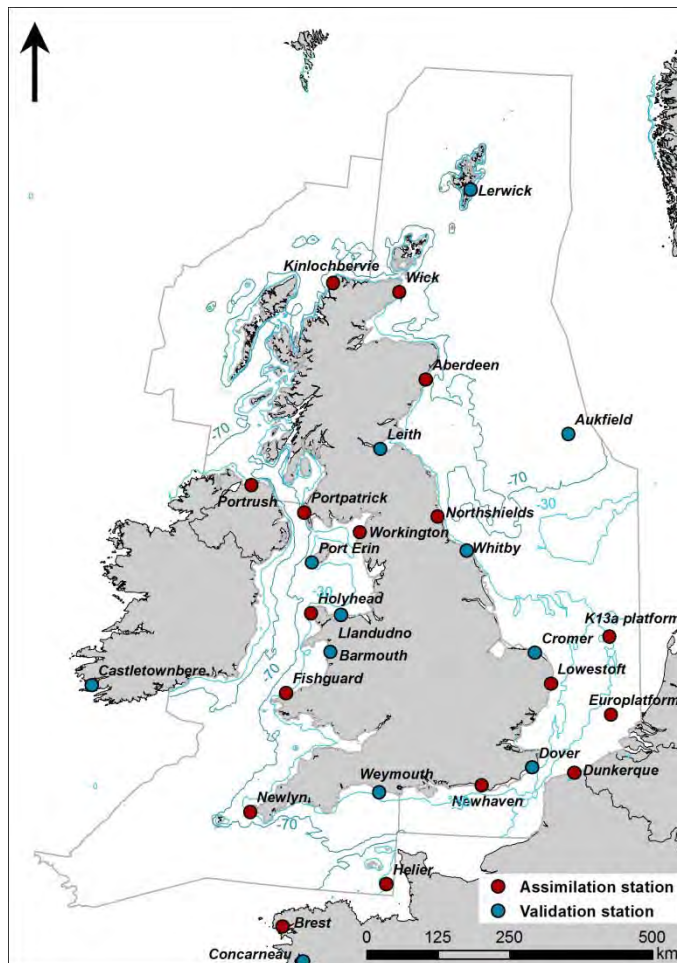
Figure A1.3. Stations used for assimilation and validation of the 2D flow model.

Validation

Quality indices

To obtain an objective and quantitative measure of how well the modelled water levels compared to the observed measurements, a number of statistical parameters, so-called quality indices (QIs), were calculated. Prior to the comparisons, the model data were synchronized to the time stamps of the observations so that both time series had equal length and overlapping time stamps. For each valid observation, measured at time t, the corresponding model value was found using linear interpolation between the model time steps before and after t. Only observed values that had model values within +/- the representative sampling or averaging period of the observations were included (e.g. for 10min observed wind speeds measured every 10min compared to modelled values every 1 hour, only the observed value every hour was included in the comparison).

The quality indices are described and defined below. Most of the quality indices are based on the entire data set, and hence the quality indices should be considered averaged measures and may not be representative of the accuracy during rare conditions.

The BIAS is the mean difference between the modelled and observed data and AME is the mean of the absolute difference. RMSE is the root mean square of the difference.

The scatter index (SI) is a non-dimensional measure of the difference calculated as the unbiased root-mean-square difference relative to the mean absolute value of the observations. In open water, an SI below 0.2 is usually considered a small difference

(excellent agreement) for significant wave heights. In confined areas, where mean significant wave heights are generally lower, a slightly higher SI may be acceptable.

The correlation coefficient (CC) is a non-dimensional measure reflecting the degree to which the variation of the first variable is reflected in the variation of the second variable. A value close to 0 indicates very limited or no correlation between the two data sets, while a value close to 1 indicates a very high or perfect correlation. Typically, a CC above 0.9 is considered a high correlation (good agreement) for wave heights.

The hit rate (HR) quantifies how often (in percent) the modelled value is within +/- a given threshold of the observed value.

The Q-Q line slope and intercept are found from a linear fit to the data quantiles in a least square sense. The lower and uppermost quantiles are not included on the fit. A regression line slope different from 1 may indicate a trend in the difference.

The peak ratio (PR) is the average of the Npeak highest model values divided by the average of the Npeak highest observations. The peaks are found individually for each data set through the peak-over-threshold (POT) method applying an average annual number of exceedance of 4 and an inter event time of 36 hours. A general underestimation of the modelled peak events results in PR below 1, while an overestimation results in a PR above 1.

In the peak event plot, 'X' is representing the observed peaks, while 'Y' is representing the modelled peaks, based on the POT method. Joint peaks are defined as any X and Y peaks within +/-36 hours of each other.

Table A1.2 Definition of quality indices (OBS = Observation, MOD = Model)

Abbreviation	Description	Definition
N	Number of valid and applied observations	–
MEAN	Mean of model data	$\frac{1}{N}\sum_{i=1}^{N} MOD_i$
BIAS	Mean of difference	$\frac{1}{N}\sum_{i=1}^{N} (MOD - OBS)_i$
AME	Mean of absolute difference	$\frac{1}{N}\sum_{i=1}^{N} (|MOD - OBS|)_i$
RMSE	Root mean square of difference	$\sqrt{\frac{1}{N}\sum_{i=1}^{N} (MOD - OBS)_i^{\,2}}$
SI	Scatter index (unbiased)	$\dfrac{\sqrt{\frac{1}{N}\sum_{i=1}^{N}(MOD - OBS - BIAS)_i^{\,2}}}{MEAN(\text{of absolute values})}$
CC	Correlation coefficient	$\dfrac{\sum_{i=1}^{N}(OBS_i - MEAN)(MOD_i - \overline{MOD})}{\sqrt{\sum_{i=1}^{N}(OBS_i - MEAN)^2 \sum_{i=1}^{N}(MOD_i - \overline{MOD})^2}}$
HR(threshold)	Hit rate (threshold)	Percentage data points within +/- threshold
Q-Q line	Quantile-Quantile line	Linear least square fit to quantiles
PR(Npeak)	Peak ratio of Npeak events	$PR(N_{peak}) = \dfrac{\sum_{i=1}^{N_{peak}} MOD_i}{\sum_{i=1}^{N_{peak}} OBS_i}$

Validation results
The modelled water levels are reasonably predicted in terms of phase and amplitude. The RMSE is less than 0.25m at all stations. The figure below gives examples of QIs computed for the validation stations at Dover and Port Erin. The vast majority of QIs indicate good correspondence between modelled and observed values.

From the above table it can be concluded that the predictive power of the hydrodynamic model complex is strong, and accurate hydrodynamic parameters have been supplied to the harbour porpoise distribution models.
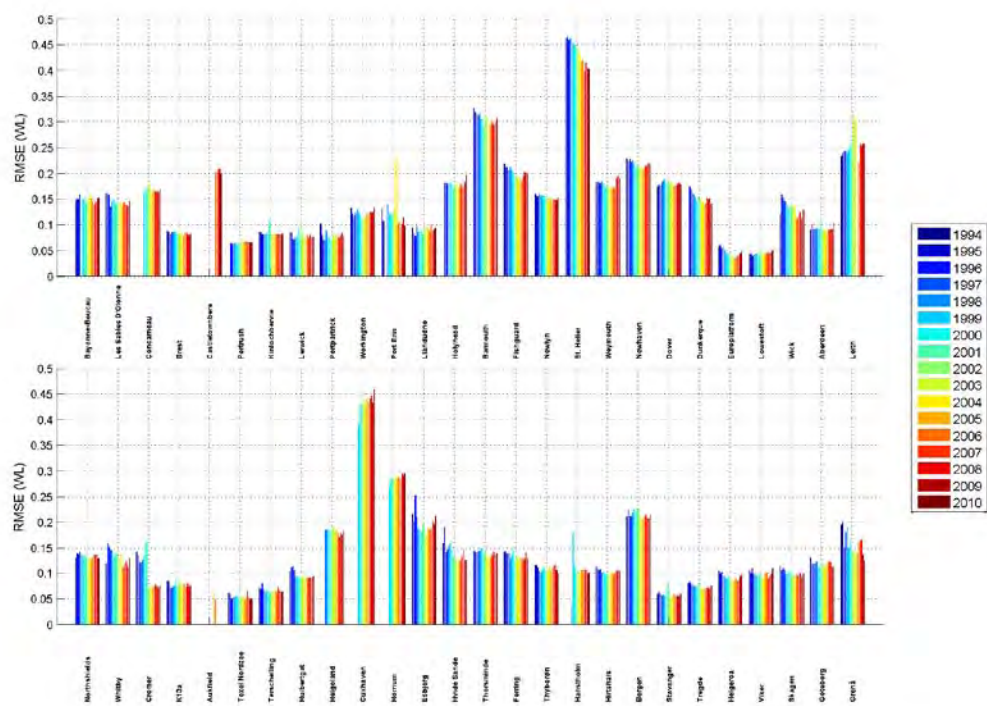
Figure A1.4. Annual RMSE values for modelled water levels (total) at all stations.
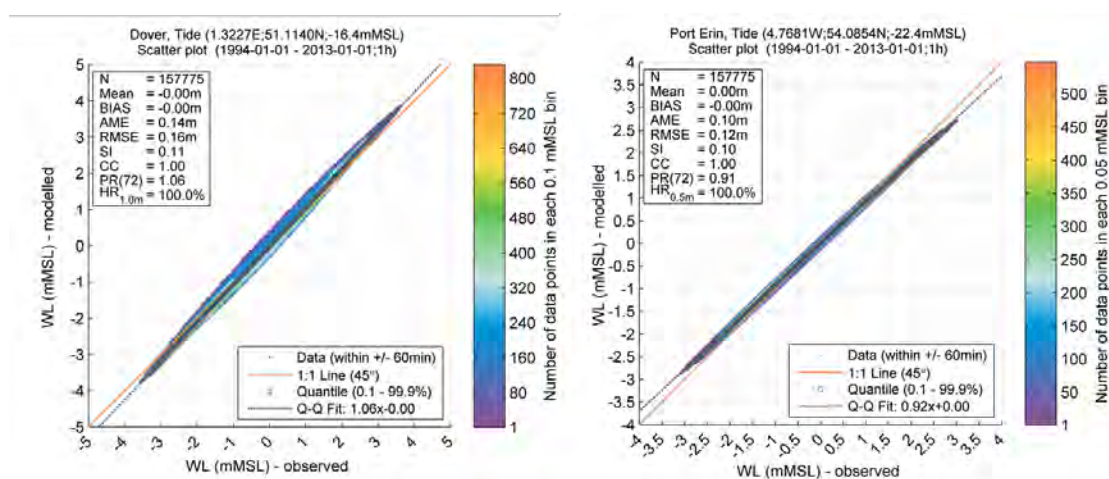
Figure A1.5. Example of validations of modelled water levels (tide) for the stations at Dover and Port Erin.

UK 3D flow model

The purpose of the dedicated UK 3D flow model was to provide information on changes in mixing regimes across the UK shelf, including determination of mean extent of estuarine water masses and location of tidal mixing fronts. As these features are expected to reflect coarse-scale structures with limited inter-annual variation the model was only run for a period of four years (2009-2012).

The 3D baroclinic hydrodynamic model was set up with MIKE 3 Flexible Mesh (FM) HD. MIKE 3 FM is DHI's general 3D simulation engine. MIKE 3 HD describing elevations, current profiles and turbulence statistic and is applicable for the study of a wide range of phenomena, including:

- Tidal exchange and currents, including stratified flows
- Heat and salt recirculation
- Mass budgets of different categories of solutes and other components such as particulate matter

MIKE 3 FM solves the time-dependent conservation equations of mass and momentum in three dimensions, the so-called Reynolds-averaged Navier-Stokes equations. The flow field and pressure variation are computed in response to a variety of forcing functions, when provided with the bathymetry, bed resistance, wind field, hydrographic boundary conditions, etc. The conservation equations for heat and salt are also included and provide among others the water temperature. MIKE 3 uses the UNESCO equation for the state of seawater (1980) as the relation between salinity, temperature and density. Hence, the model includes temperature and salinity such that baroclinic effects on the flow can be described.

MIKE 3 FM is based on an unstructured flexible mesh and uses a finite volume solution technique. The meshes are based on linear triangular elements. This approach allows for a variation of the horizontal resolution of the model grid mesh within the model area to allow for a finer resolution of selected sub-areas. The vertical discretization can be based on a combined sigma-z grid.

The numerical solution uses a finite-volume method, with a second order spatial representation, both in vertical and horizontal directions. The time marching is explicit, thus there is a strict Courant number criterion for stability. The relatively short time step enforced is balanced by a very efficient solution and ensures an accurate numerical solution.

Set-up and specifications

Bathymetry, domain and mesh

The North Sea model domain extends from Irish Sea around the Faroe Islands and the Shetland Islands into the central part of the Kattegat. The figures below show the extension of the entire model area with the bathymetry including mesh, and close-ups of the model bathymetry and mesh around the UK.

The model bathymetry is based on a modified version of DHI's bathymetry for the North Atlantic using all available depth measurements. The spatial resolution of the mesh varies from approximately 10km off the shelf to 6km on the shelf and 1.5km in the coastal areas. The vertical resolution is 2m, and the temporal resolution 1 hour.
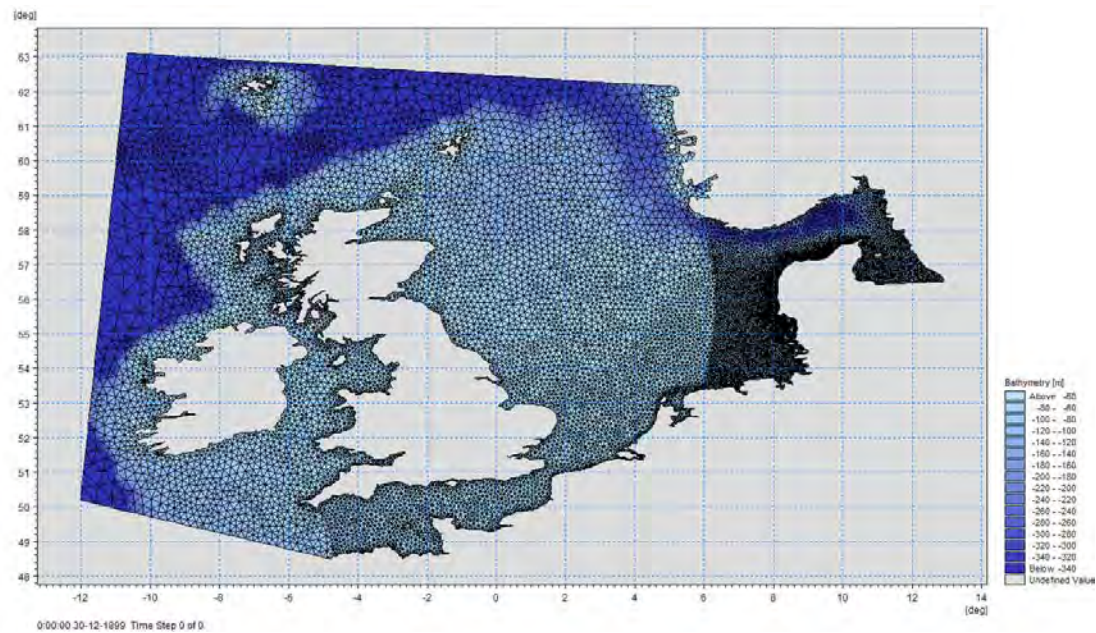
Figure A1.6. North Sea model domain and bathymetry for the MIKE 3 FM model
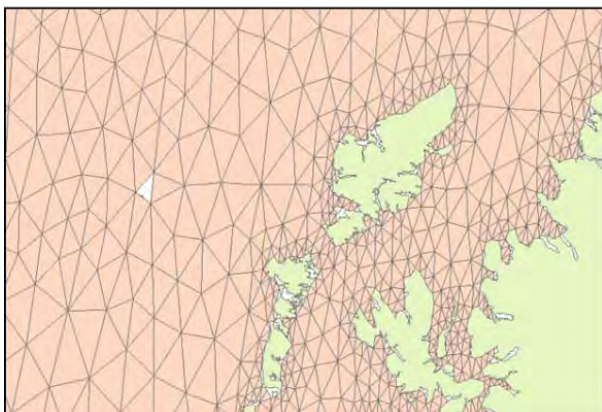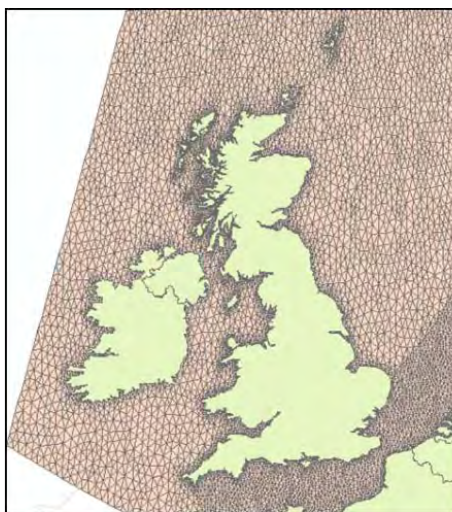
Figure A1.7. Mesh of the UK 3D flow model with a close-up of the area around the Hebrides.

Meteorology and Runoff

The main weather model used as a basis for the UK 3D flow model is the regional WRF model run routinely by StormGeo for DHI. It is based on the global weather model run by ECMWF as illustrated in the figure below.
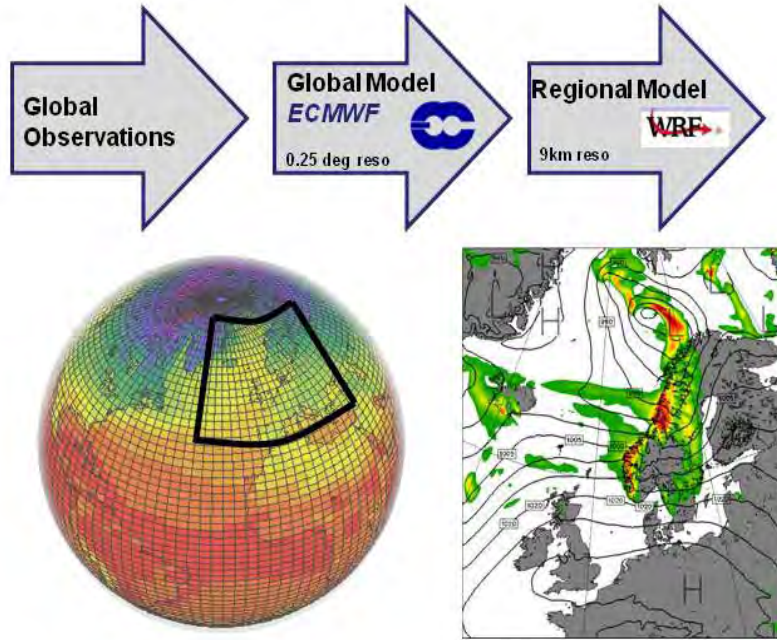
Figure A1.8. Global and regional weather model applied in the UK 3D flow model

Runoff data from rivers have been included as daily or weekly values for British, German and Dutch rivers and as monthly values of flow for Danish, Swedish and Norwegian rivers.

Open boundaries

The open boundaries for the 3D flow model were obtained from the Hybrid Coordinate Ocean Model (Hycom). Hycom is part of the multi-national Global Ocean Data Assimilation Experiment (GODAE) aiming for demonstrating real-time global ocean products in a way that will promote wide utility and availability for maximum benefit to the community. Hycom is designed as a generalized (hybrid isopycnal/ /z) coordinate ocean model. It is isopycnal in the open stratified ocean, but reverts to a terrain-following coordinate in shallow coastal regions, and to z-level coordinates near the surface in the mixed layer. The global model has 1/12° equatorial resolution and latitudinal resolution of 1/12° cos(lat) or 7km for each variable at mid-latitudes. It has 32 coordinate surfaces in the vertical.

The data assimilation is performed using the Navy Coupled Ocean Data Assimilation (NCODA) system with a model forecast as the first guess. NCODA assimilates available satellite altimeter observations (along track obtained via the NAVOCEANO Altimeter Data Fusion Center), satellite and in situ sea surface temperature (SST) as well as available in situ vertical temperature and salinity profiles from XBTs, ARGO floats and moored buoys.

The Hycom global ocean prediction system is designed to provide an advance over the existing operational global ocean prediction systems, since it overcomes design limitations of the present systems as well as limitations in vertical and horizontal resolution. The result should be a more-streamlined system with improved performance and an extended range of applicability, especially for shallow water and in handling the transition from deep to shallow water.

As the boundaries from the Hycom model does not include tides and tide generated flows the boundaries for this North Sea model needs to be superimposed with tides and flows at the boundaries generated from the 2D flow model (see section 3.3.1 of the main report). The data generated with the 2D flow model was used together with the data obtained from the Hycom model and added to construct the best possible boundaries for the 3D flow model.

Water level data and assimilation
The 3D model includes assimilation of real-time water levels at the 22 stations listed below. This assimilation plays a major factor in the high accuracy of the water levels and currents produced by the 3D model.

Profile data were available from ten hydrographic stations. Predicted temperature and salinity profiles were extracted from the model at the 10 locations shown in the figure below. The model period was 01-02-2009 to 31-12-2012. Any observed profile within a 0.25 degree radius of the predicted profiles was identified. The timestamp of the observed profile was rounded to the nearest hour (consistent with the model time step).
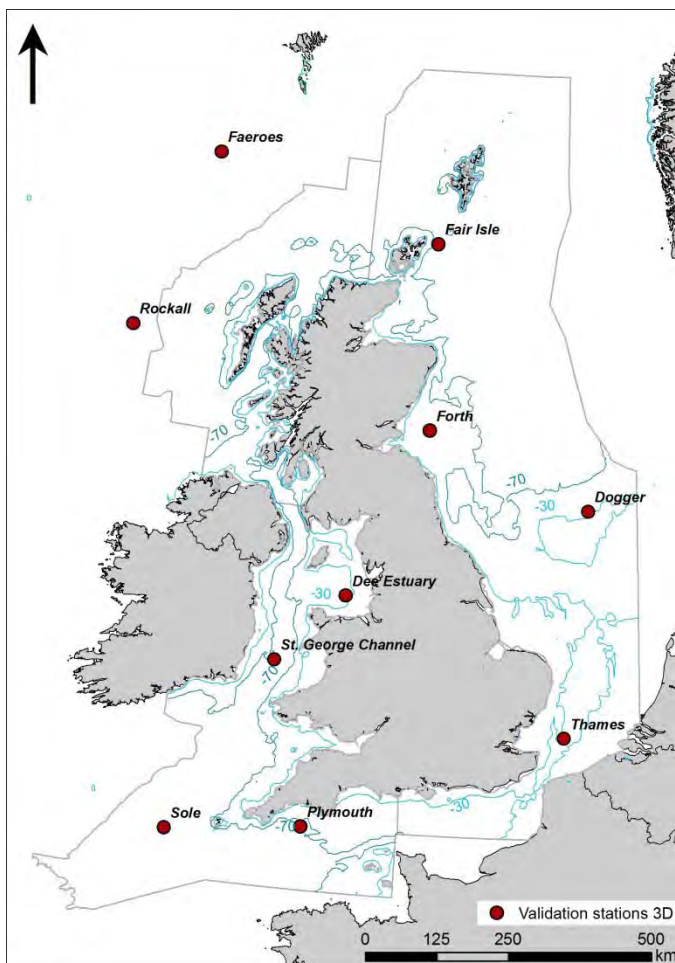
Figure A1.9. Validation stations used for the UK 3D flow model.

Table A1.3 Stations with online water level data

Station	Longitude (deg E)	Latitude (deg N)	Country	Source
Aberdeen	-2.0833	57.15	UK	DMI
Bournemouth	-1.87486	50.714333	UK	BODC
Cromer	1.30164	52.93419	UK	BODC
Devonport	-4.18525	50.36839	UK	BODC
Dover *	1.3167	51.117	UK	DMI
Esbjerg	8.45	55.467	Denmark	DMI
Felixstowe *	1.34655	51.95769	UK	BODC
Grenå	10.933	56.4	Denmark	DMI
Hanstholm	8.6	57.133	Denmark	DMI
Helgoland	7.883	54.183	Germany	DMI
Hirtshals	9.96	57.6	Denmark	DMI
Hornbæk	12.4667	56.1	Denmark	DMI
IJmuiden buitenhaven	4.555085	52.463335	The Netherlands	Rijkswaterstaat
Immingham	-0.187528	53.630417	UK	BODC
Lerwick	-1.14031	60.15403	Shetland Isles	BODC
Lowestoft *	1.75	52.467	UK	DMI
Måløy	5.116667	61.933333	Norway	IOC
Newhaven	0.05703	50.78178	UK	BODC
North Shields	-1.433	55.017	UK	DMI
Ostende	2.933	51.233	Belgium	DMI
Smögen	11.217	58.367	Sweden	DMI
Stavanger	5.733	58.967	Norway	DMI
Tredge	7.566667	58	Norway	IOC
Wick	-3.0833	58.433	UK	DMI
Wierumergronden	5.95882	53.51696	The Netherlands	Rijkswaterstaat

*: Station not used for data assimilation.

Validation

Comparisons of water levels from the regional 3D model are shown in the figure below.
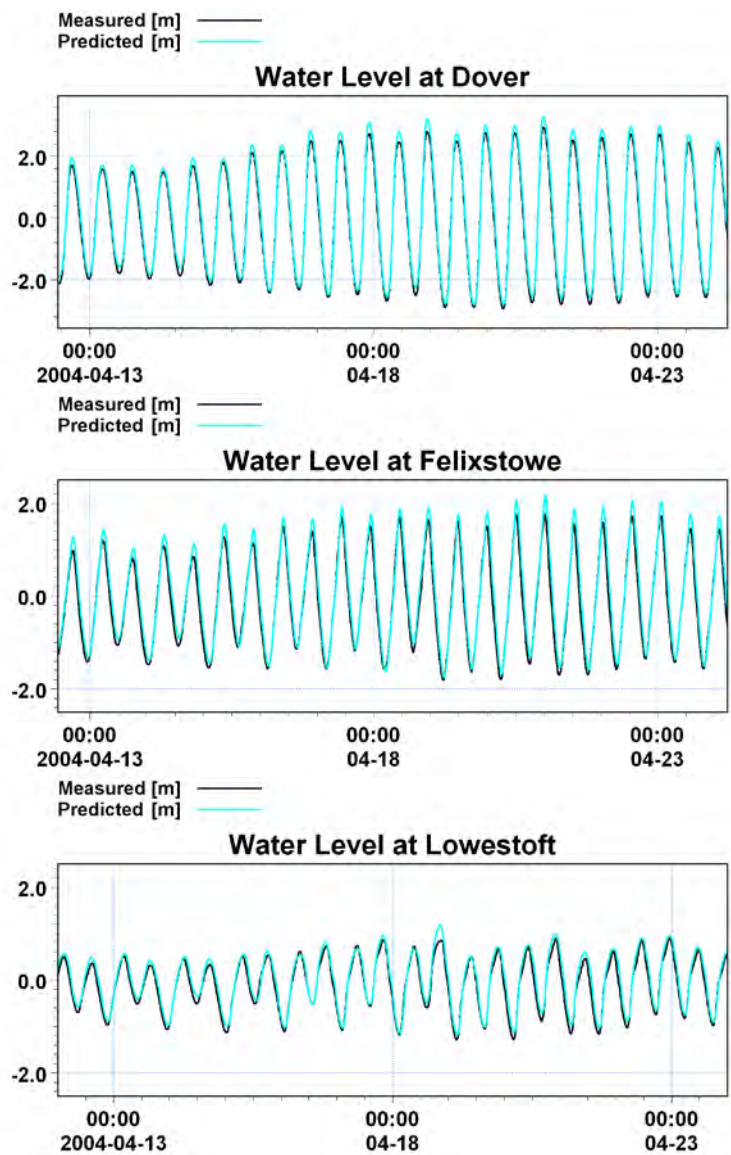
Table A1.10. Comparison of measured (black line) and predicted (blue line) water levels during validation period. Predicted data taken from the regional 3D hydrodynamic model.

Statistical parameters quantifying the accuracy of the hydrodynamic model complex have been computed for three stations and are listed below, while a comparison of the accuracy of the 2D regional model in relation to other 2D hydrodynamic models is illustrated in the figure below.

Table A1.4. Performance of hydrodynamic model system during validation period for water levels.

Station	Mean, measured (m)	Bias (m)	RMS (m)	Standard Deviation (m)	Correlation Coefficient	Explained Variance
Felixstowe	-0.014	0.139	0.228	0.181	0.984	0.965
Lowestoft	0.016	0.081	0.132	0.104	0.983	0.967
Dover	0.005	0.141	0.2	0.142	0.997	0.993
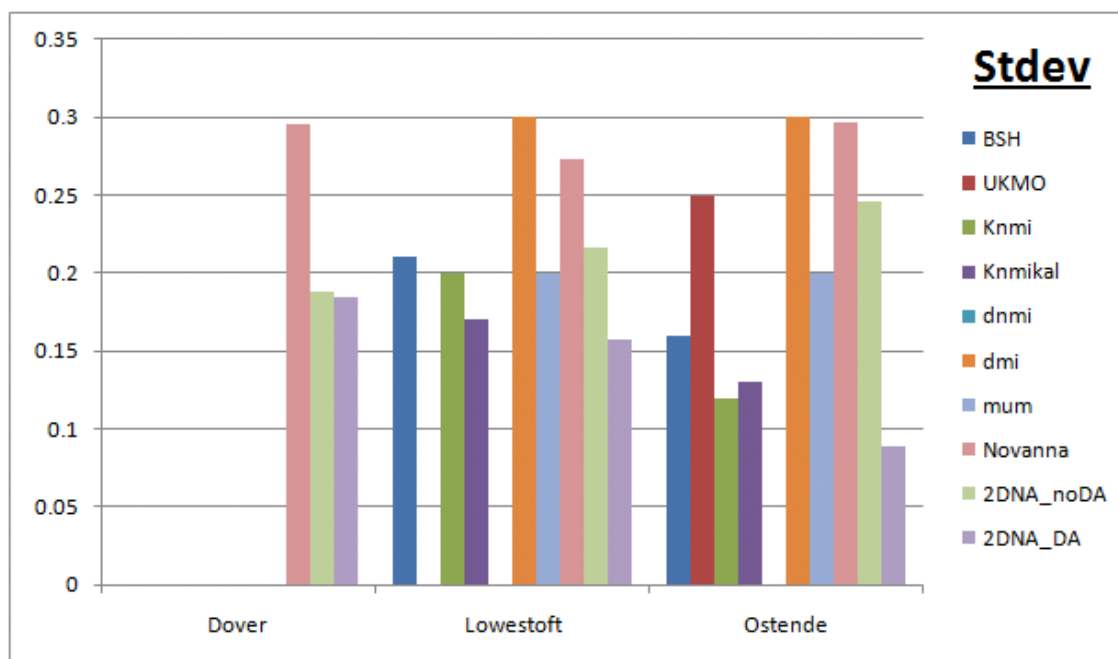
Figure A1.11. Comparison of accuracy (standard deviation in m) between DHI's hydrodynamic model including data assimilation (denoted 2DNA_DA) and without data assimilation (denoted 2DNA_noDA) as well as other models from BSH (Germany) UKMO (UK), KNMI (Netherland) DNMI (Norway), DMI (Denmark), MUM (Belgium) and Novana (Denmark).

The comparisons between measurements and predicted (modeled) data shown both as time series and as profiles and in relation to other hydrodynamic models are satisfactory.
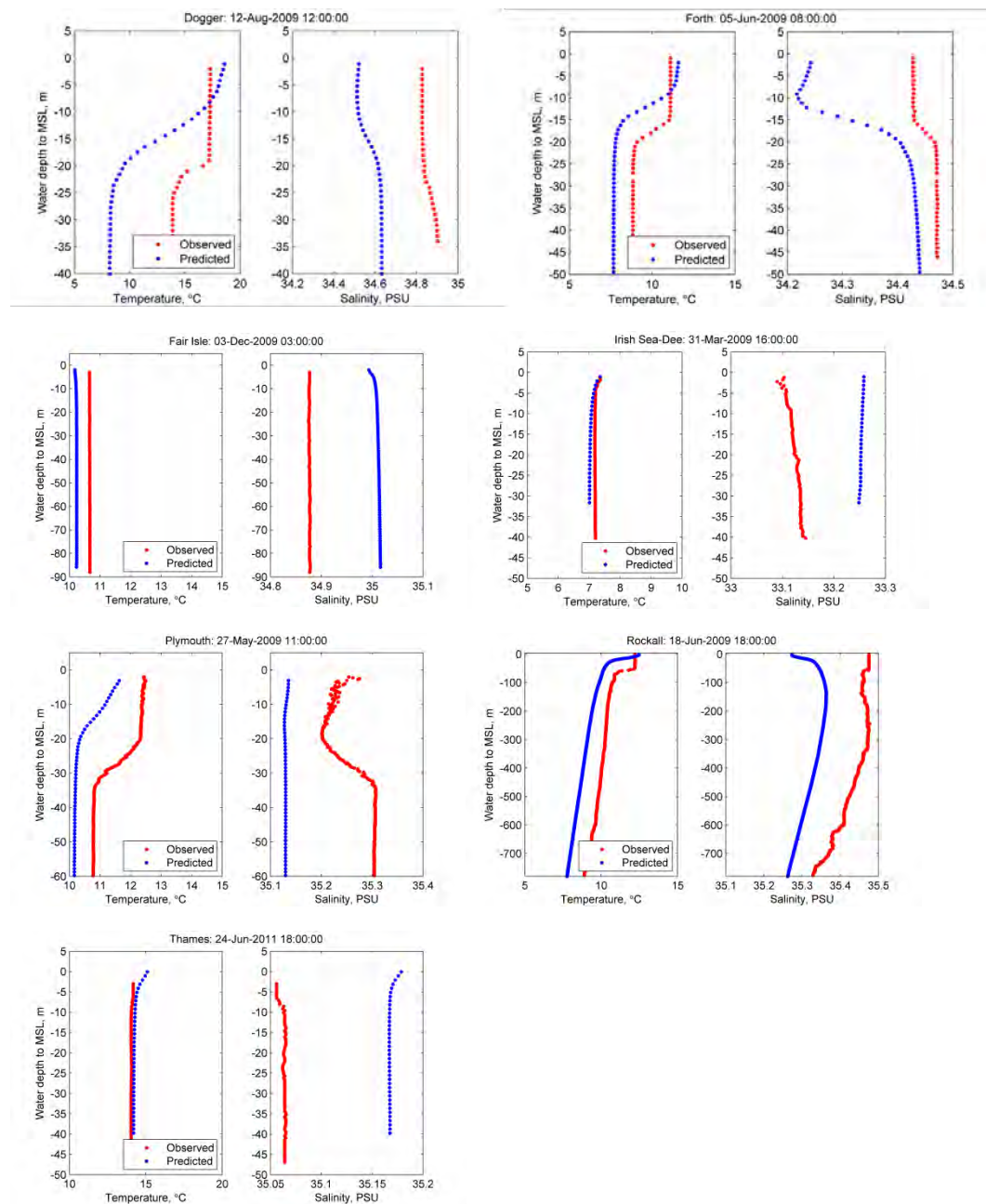
Figure A1.12. Comparison between observed and modeled profiles of salinity and temperature at selected stations.

APPENDIX 2 – Survey effort
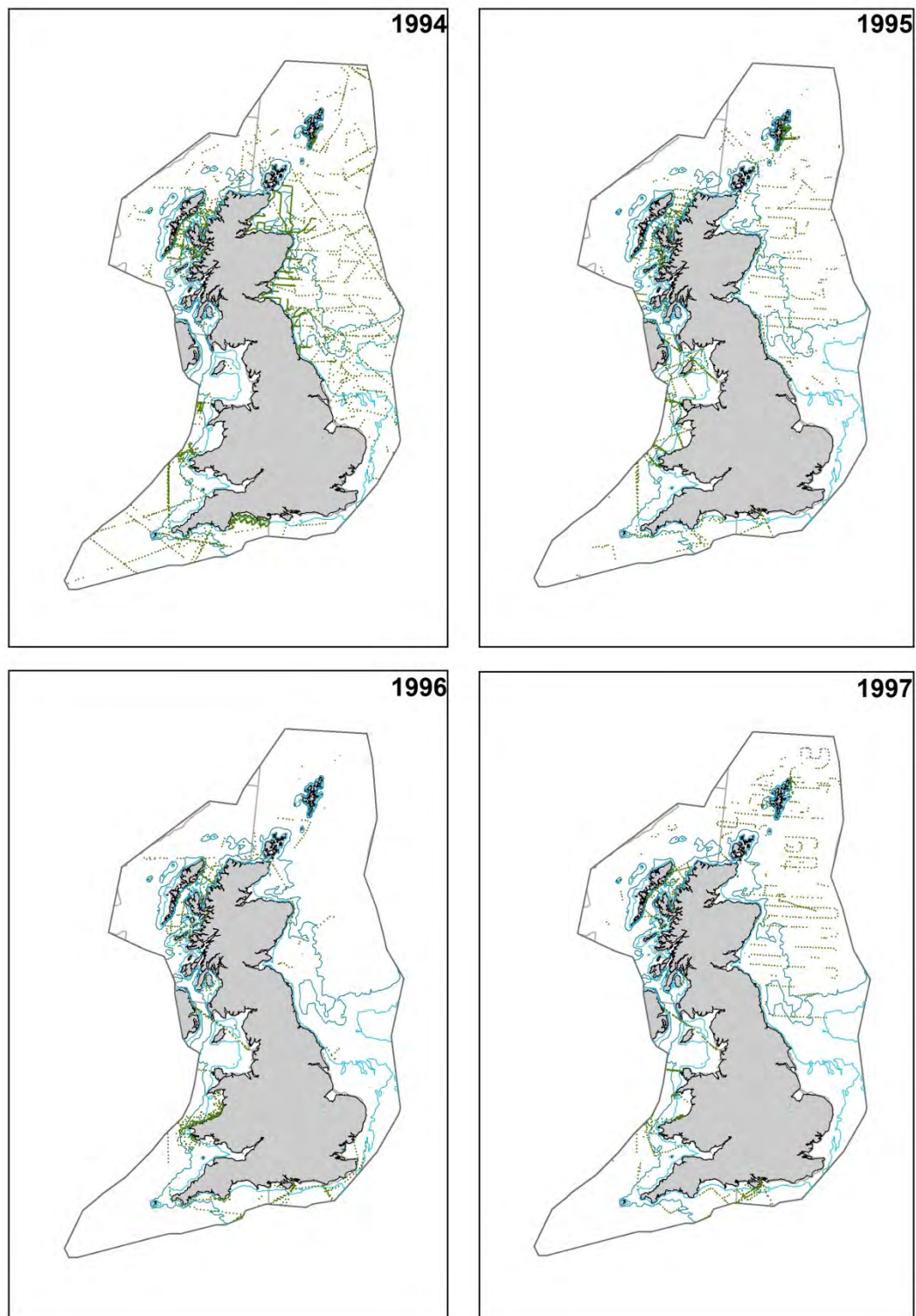
Figure A2.1. Survey effort 1994-1997
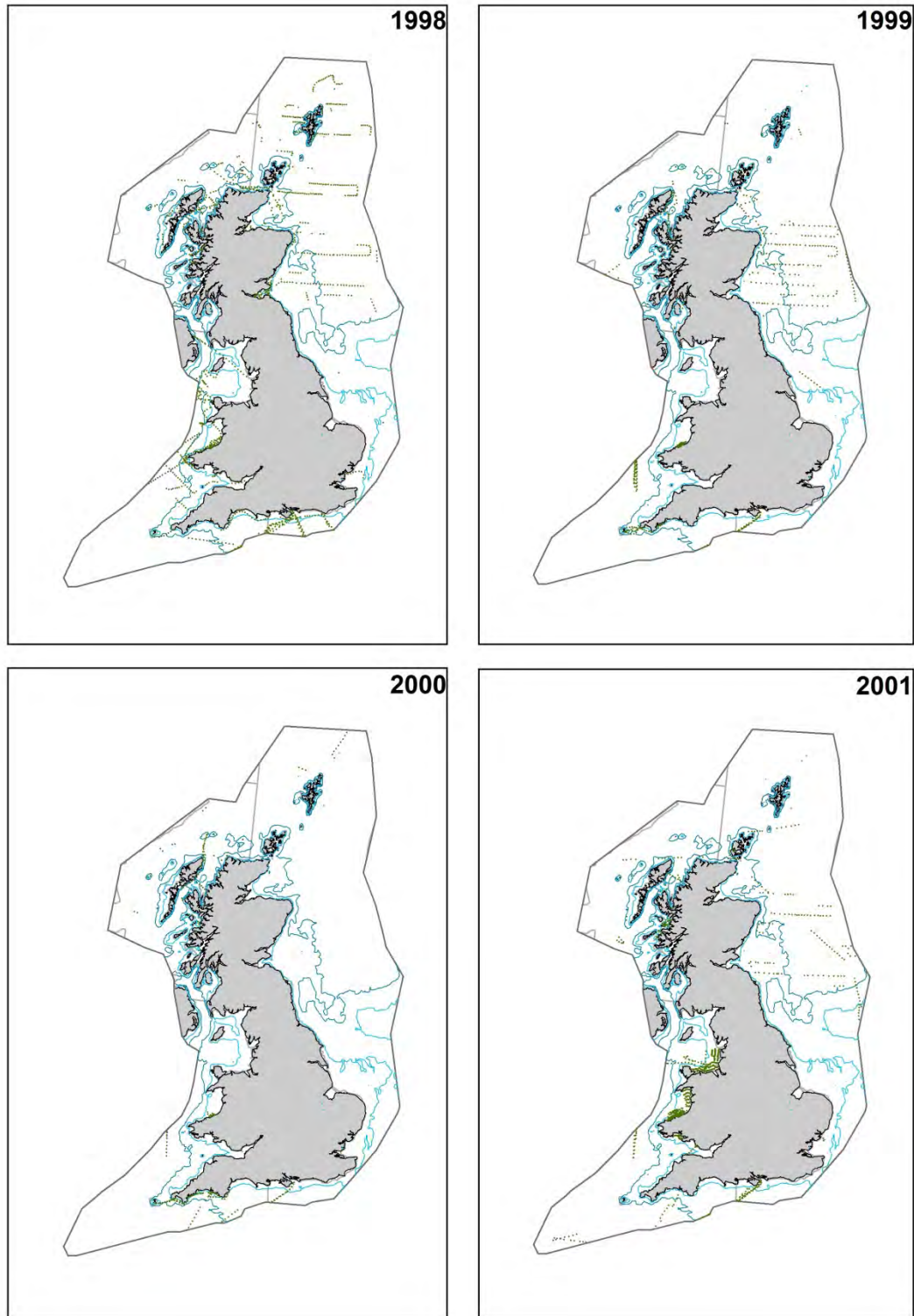
Figure A2.2. Survey effort 1998-2001
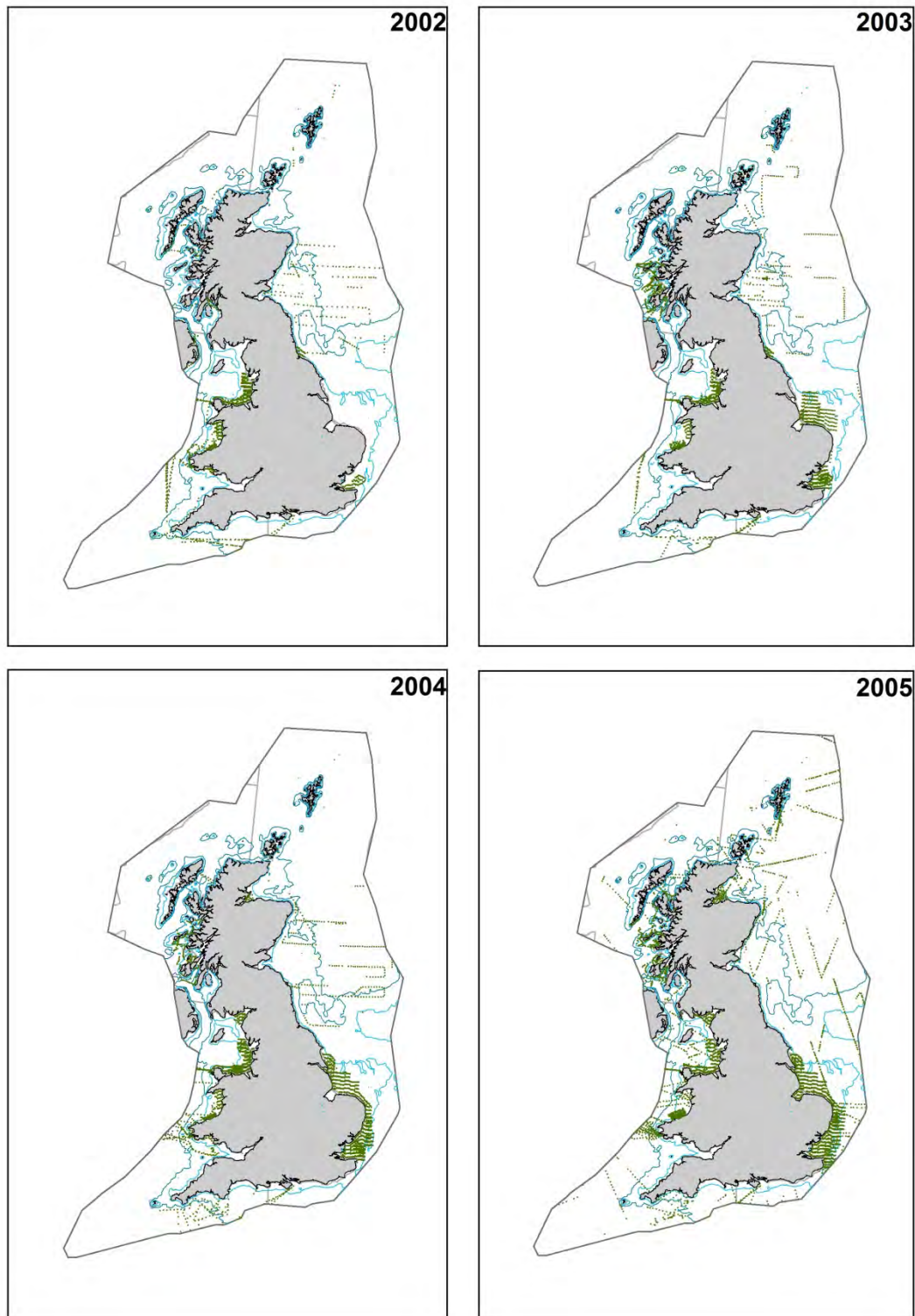
Figure A2.3. Survey effort 2002-2005
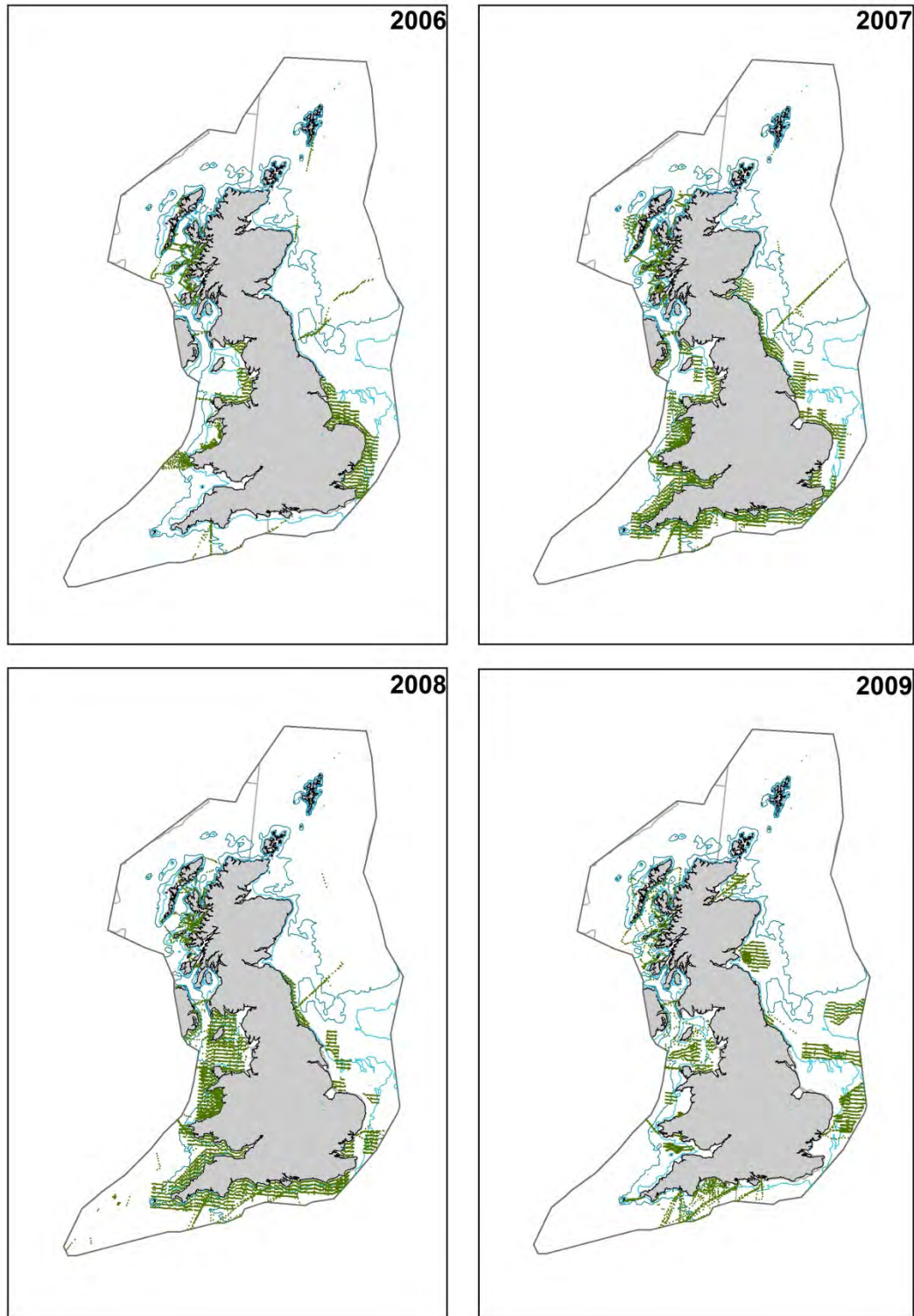
Figure A2.4. Survey effort 2006-2009
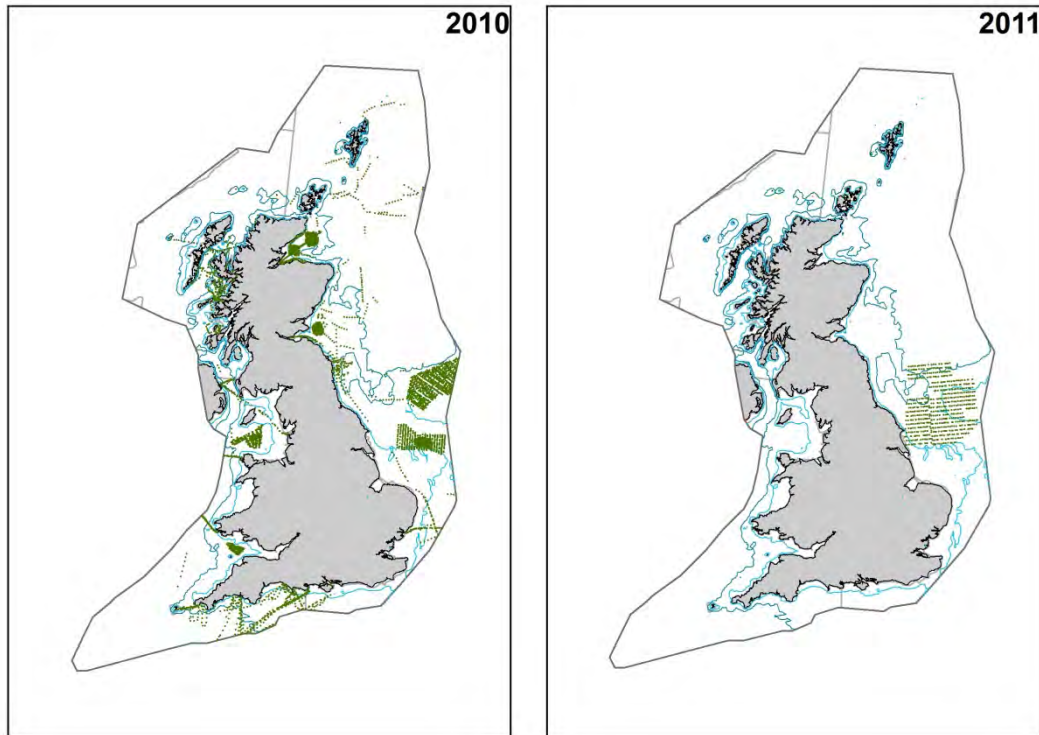
Figure A2.5. Survey effort 2010-2011

APPENDIX 3 – Yearly predictions of the mean density of harbour porpoise
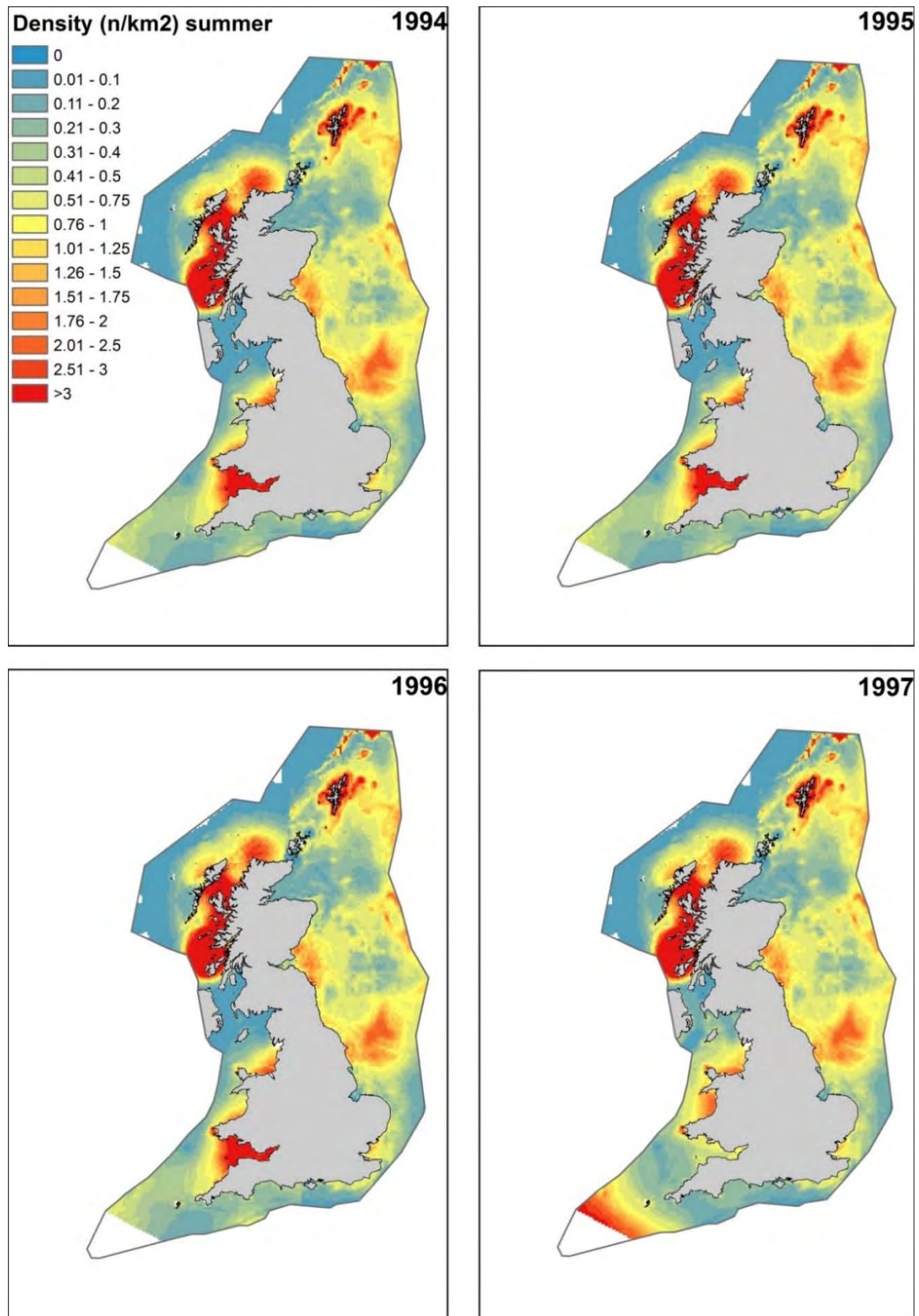
Figure A3.1. Predicted mean densities 1994-1997 (summer).
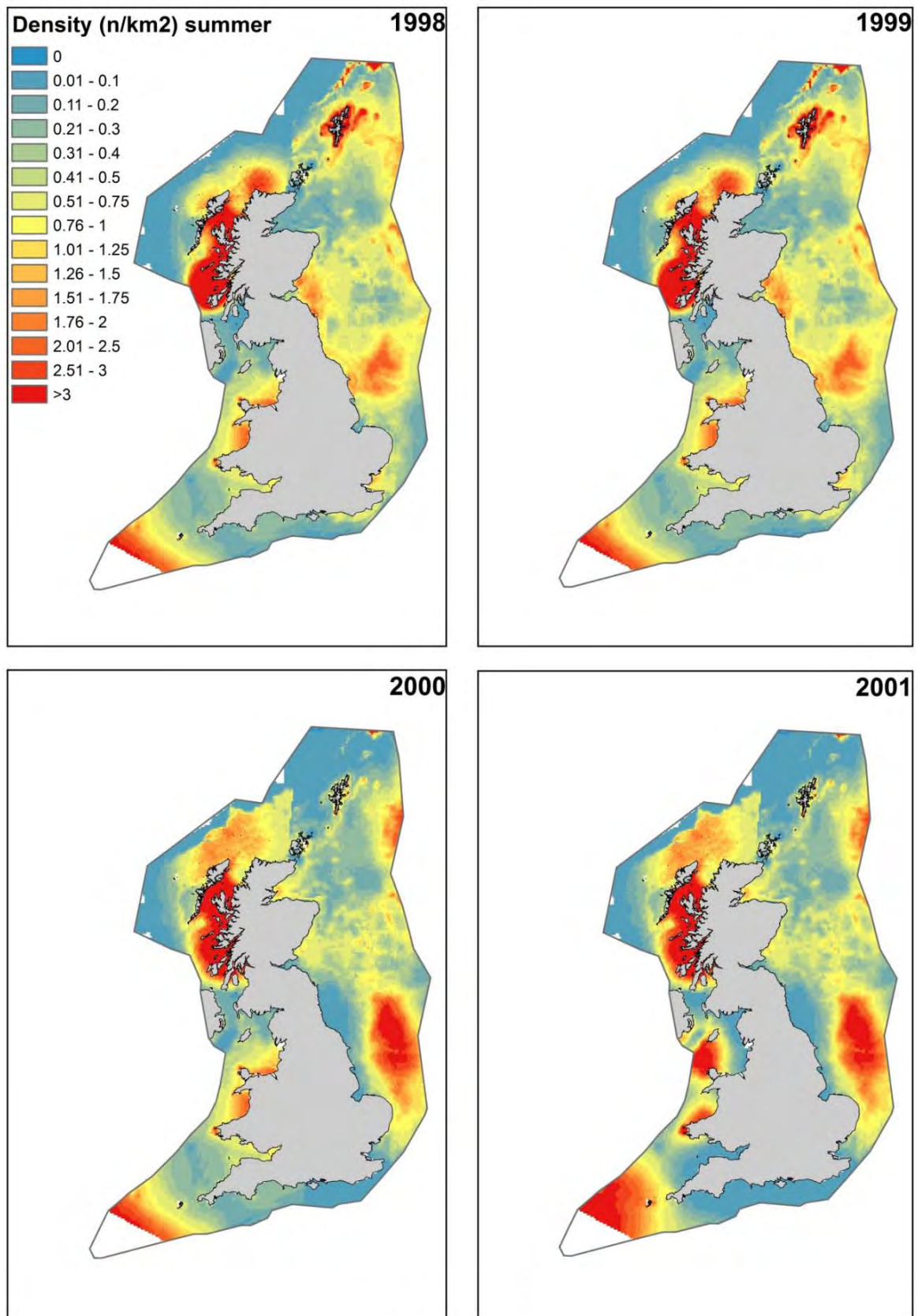
Figure A3.2. Predicted mean densities 1998-2001 (summer).
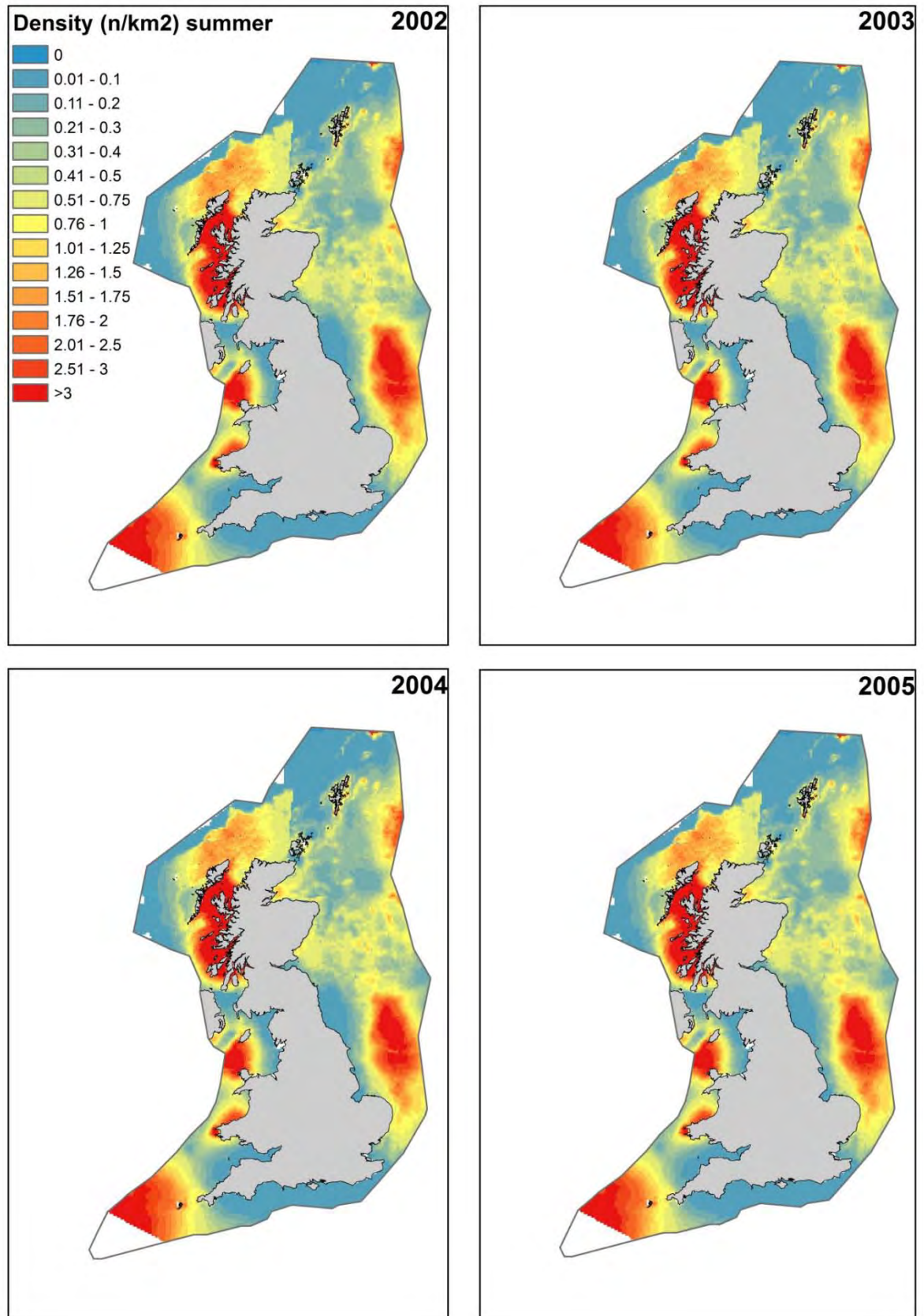
Figure A3.3. Predicted mean densities 2002-2005 (summer).
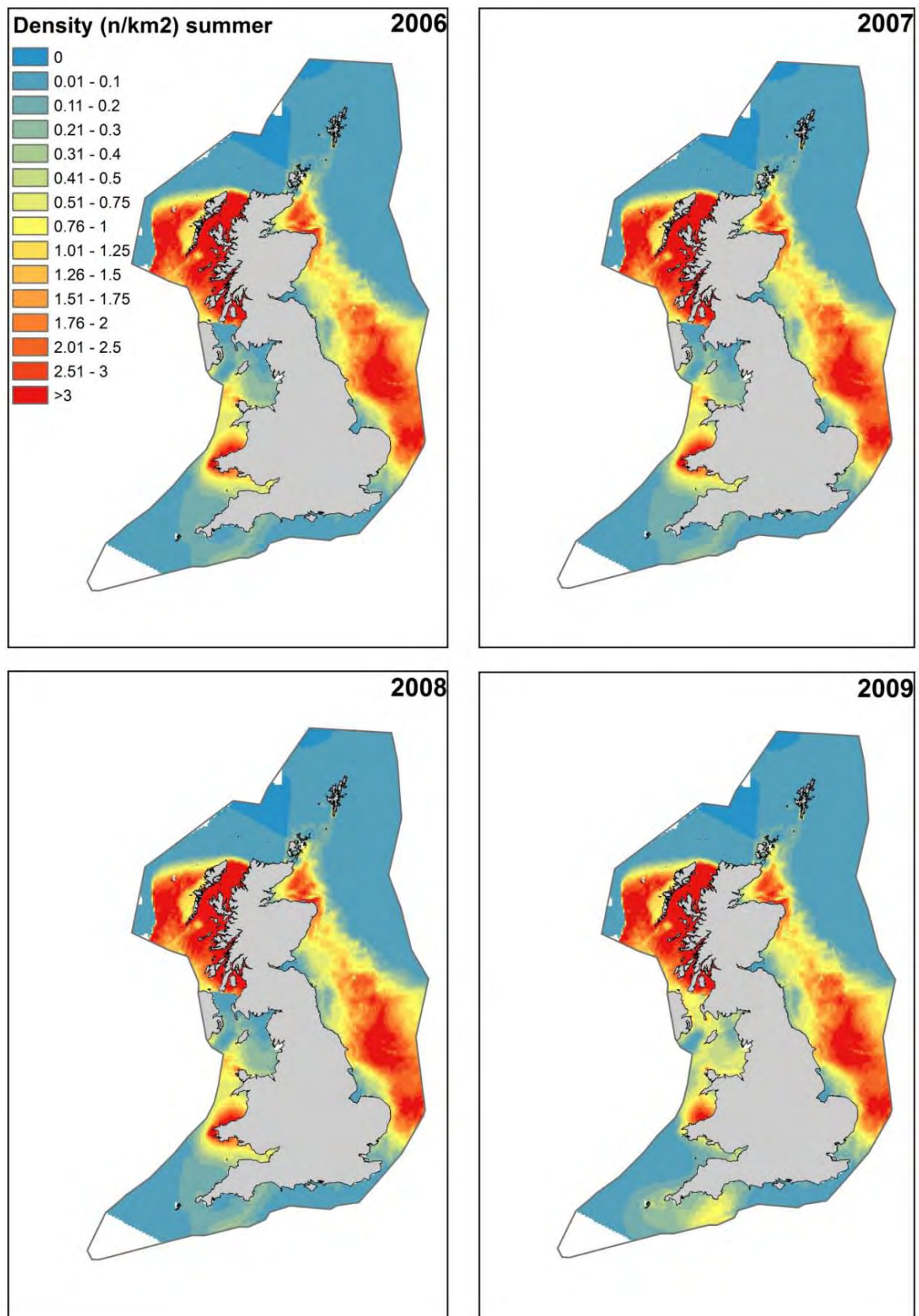
Figure A3.4. Predicted mean densities 2006-2009 (summer).
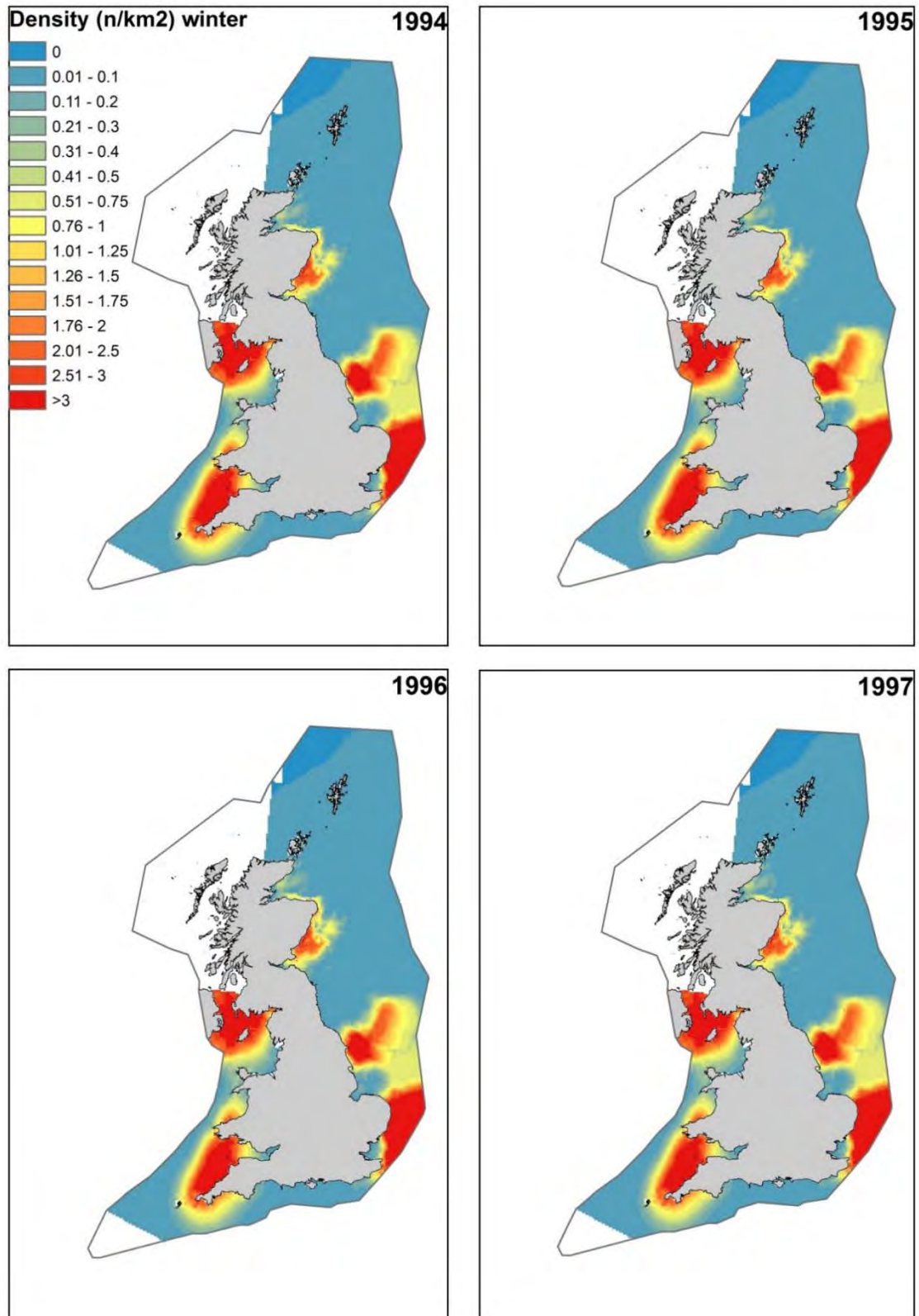
Figure A3.5. Predicted mean densities 1994-1997 (winter).
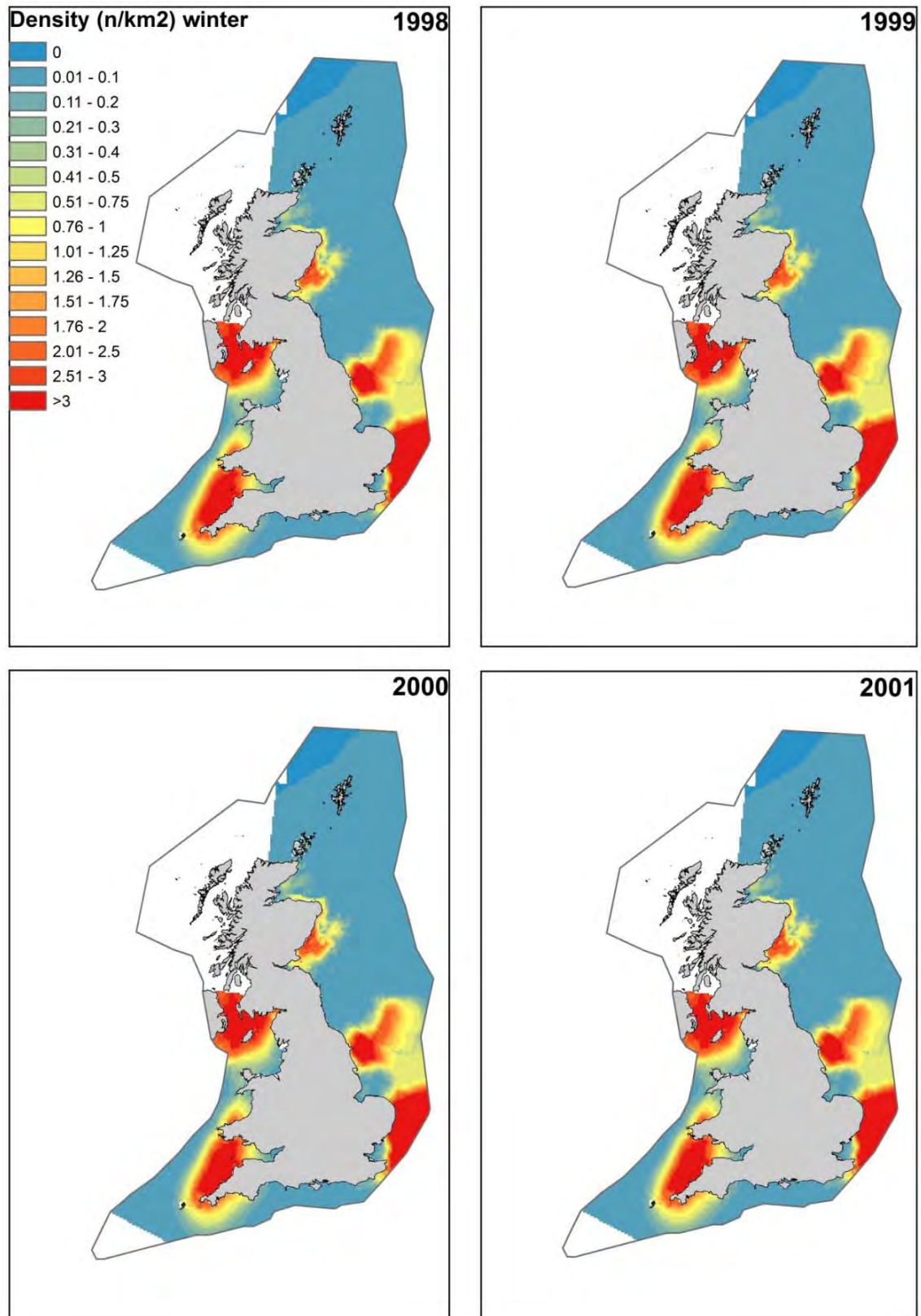
Figure A3.6. Predicted mean densities 1998-2001 (winter).
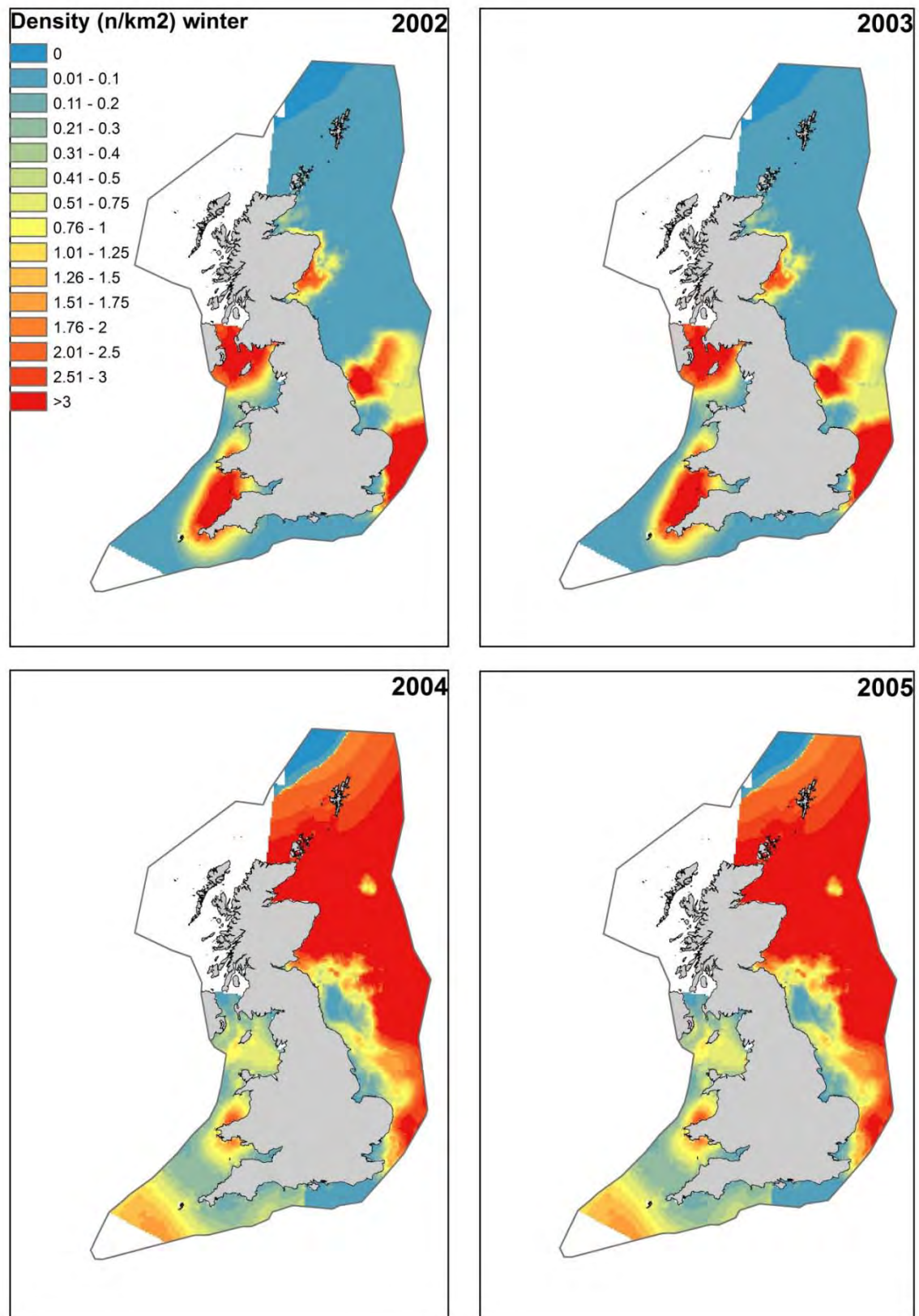
Figure A3.7. Predicted mean densities 2002-2005 (winter).
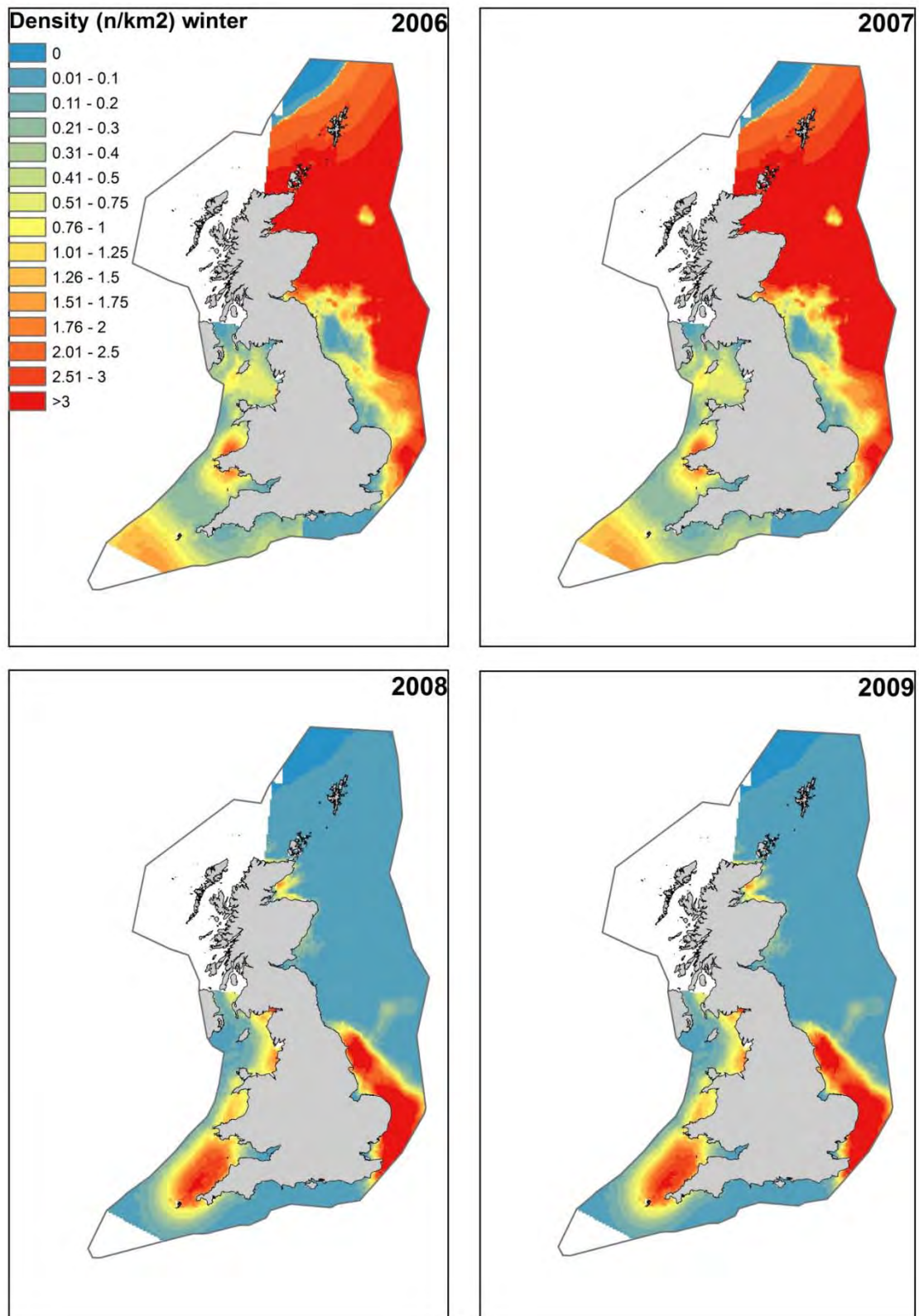
Figure A3.8. Predicted mean densities 2006-2009 (winter).

APPENDIX 4 – Model standard errors of predictions of the mean density of harbour porpoise
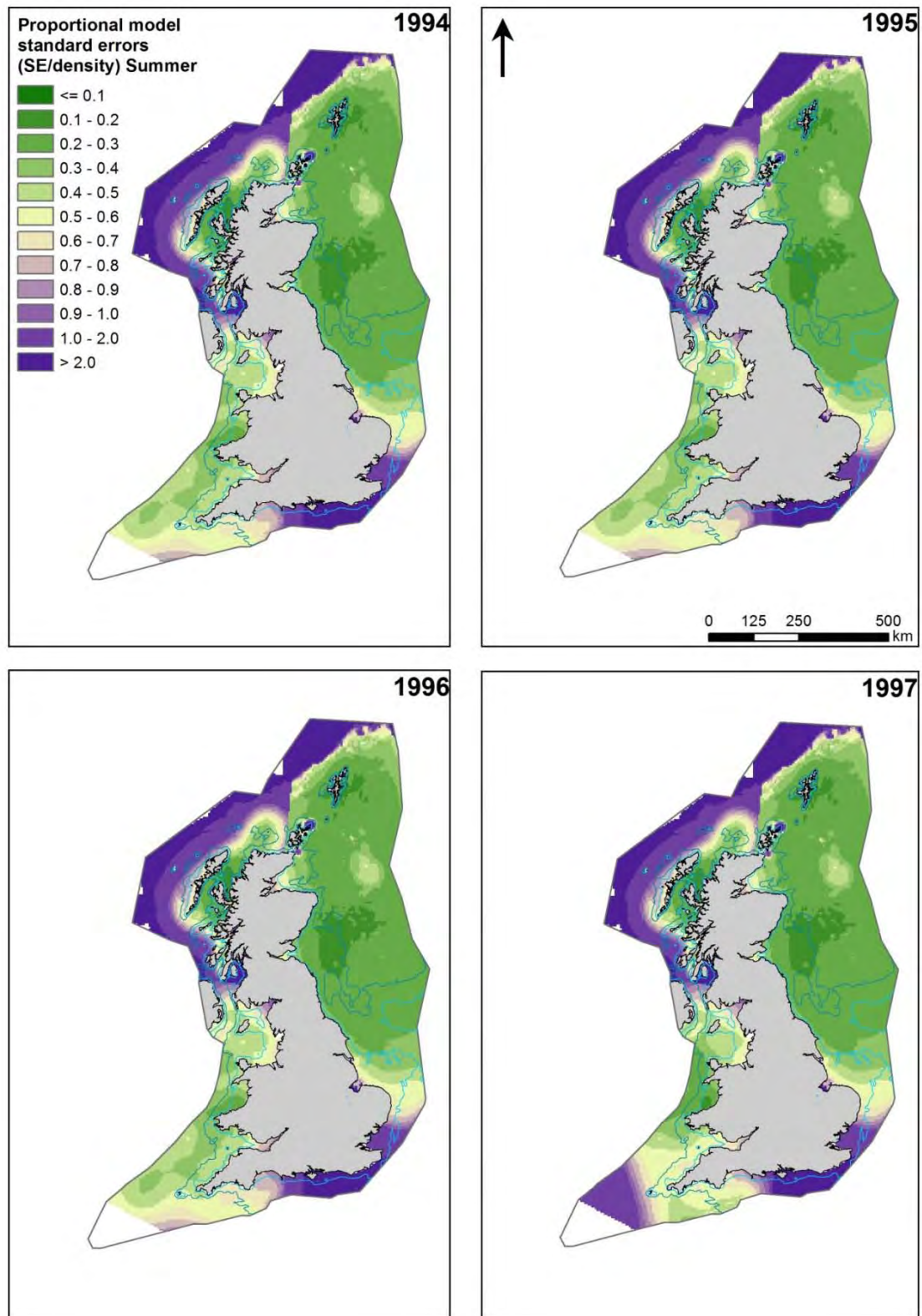
Figure A4.1. Standard errors on predicted mean densities 1994-1997 (summer)
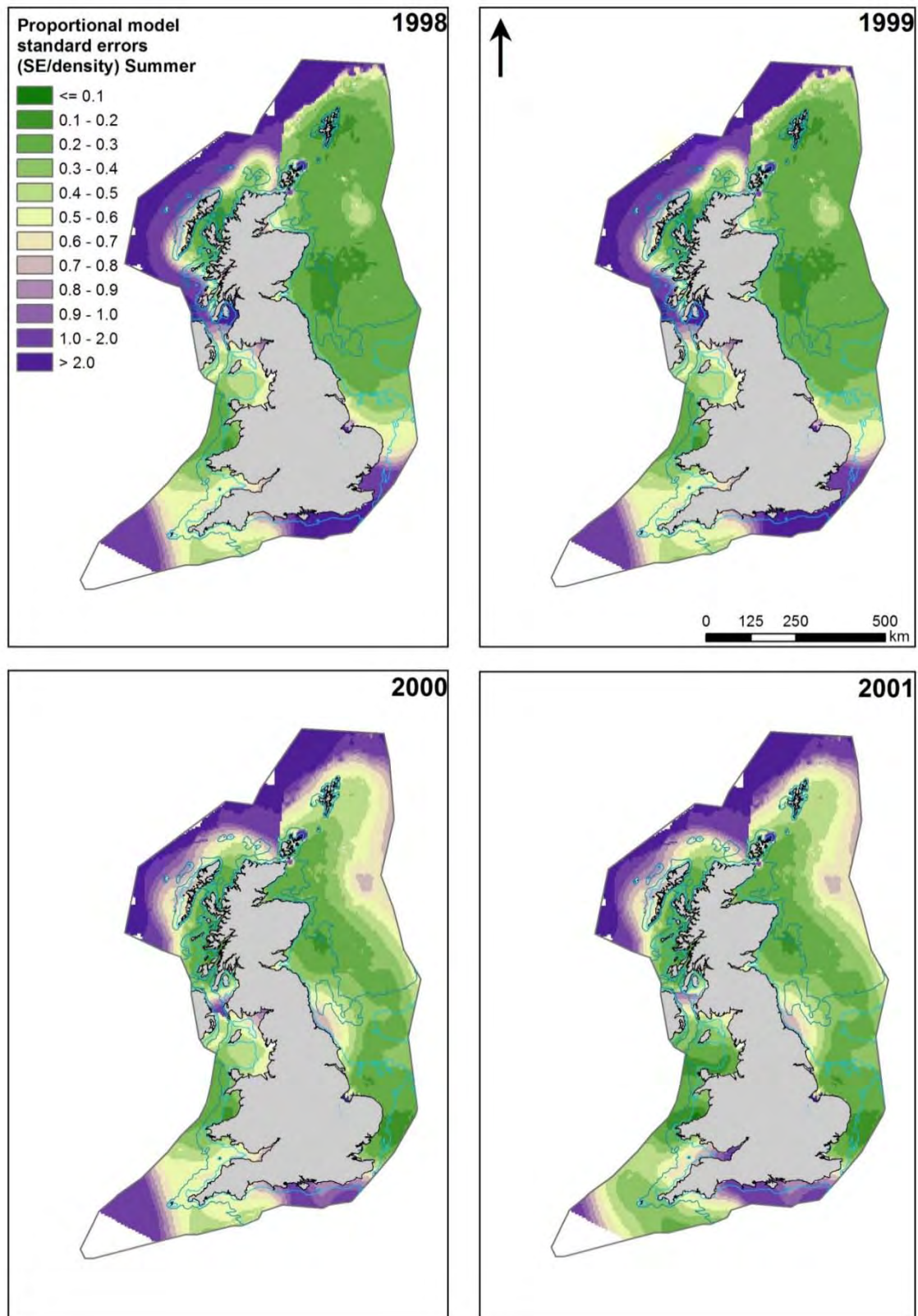
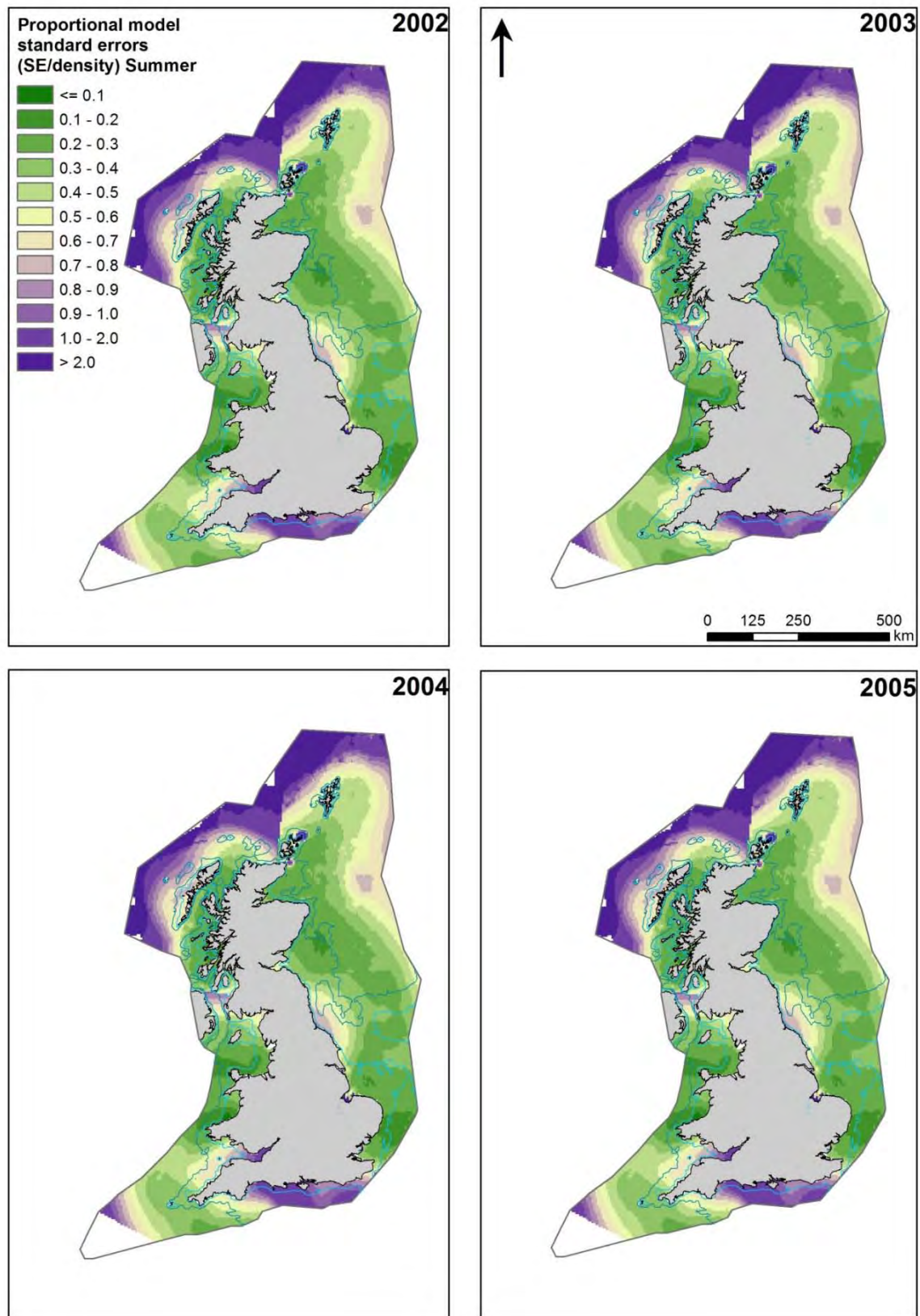**Figure A4.2.** Standard errors on predicted mean densities 1998-2001 (summer)

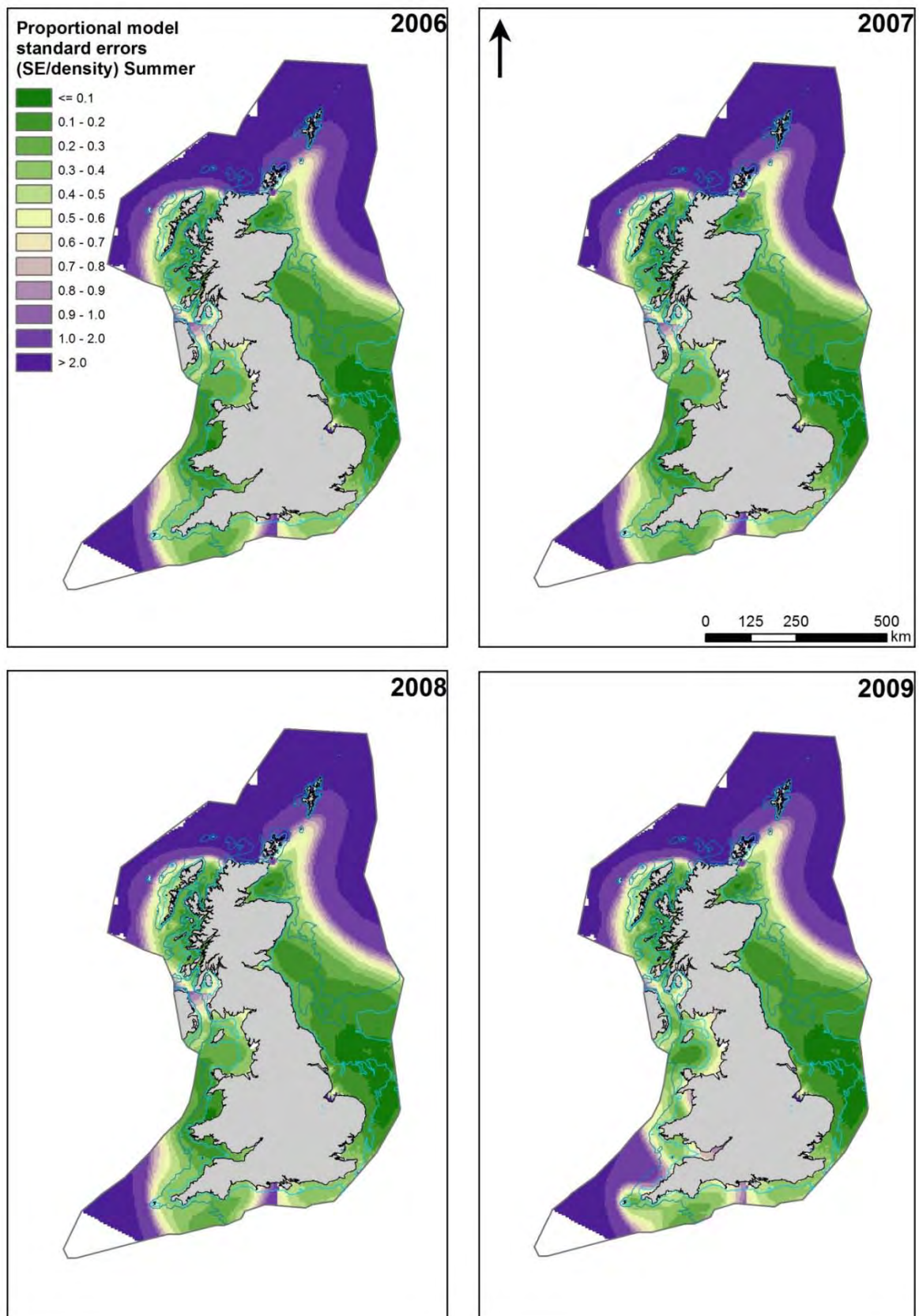**Figure A4.3.** Standard errors on predicted mean densities 2002-2005 (summer)

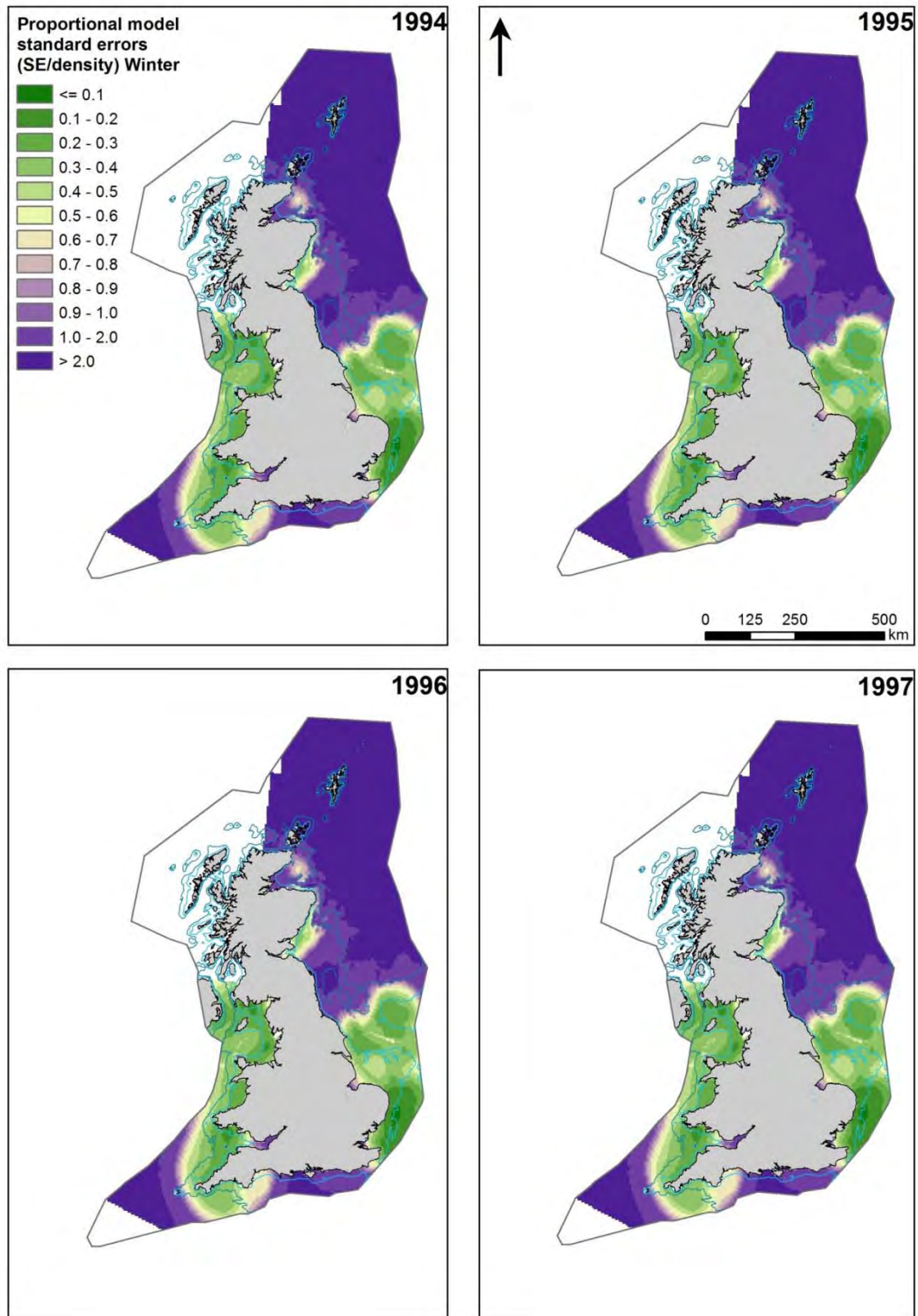**Figure A4.4.** Standard errors on predicted mean densities 2006-2009 (summer)

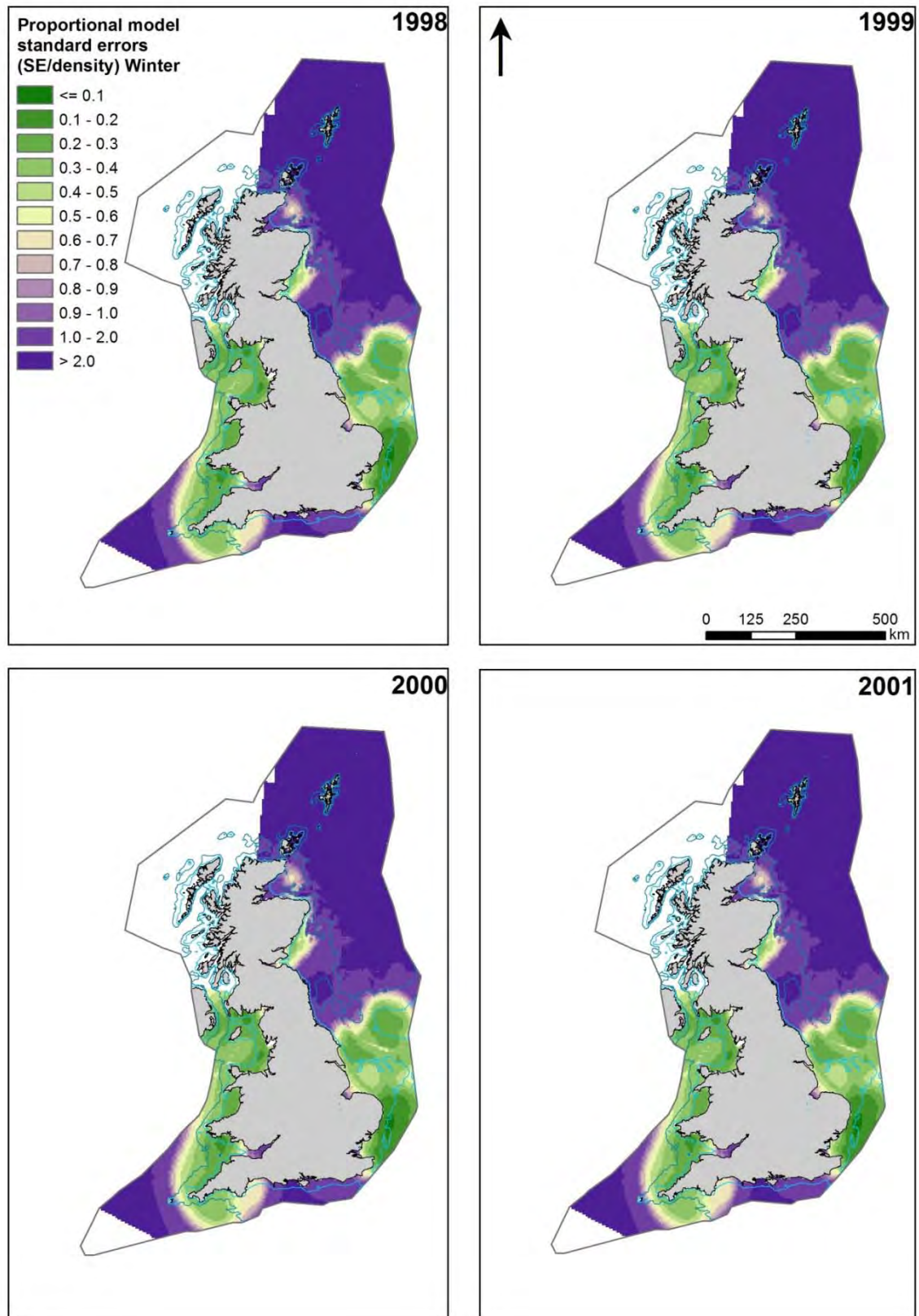**Figure A4.5.** Standard errors on predicted mean densities 1994-1997 (winter)

Figure A4.6. Standard errors on predicted mean densities 1998-2001 (winter)
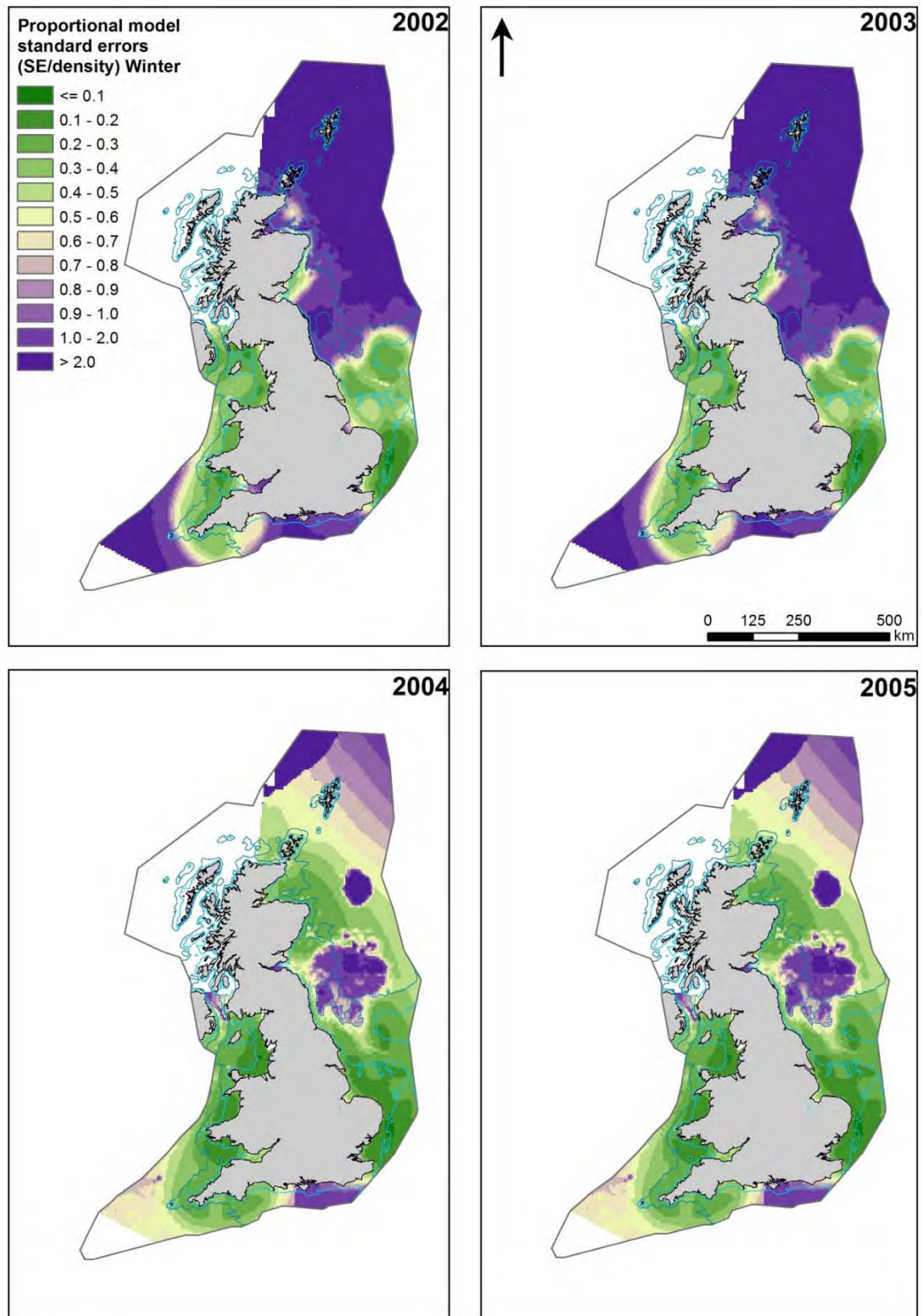
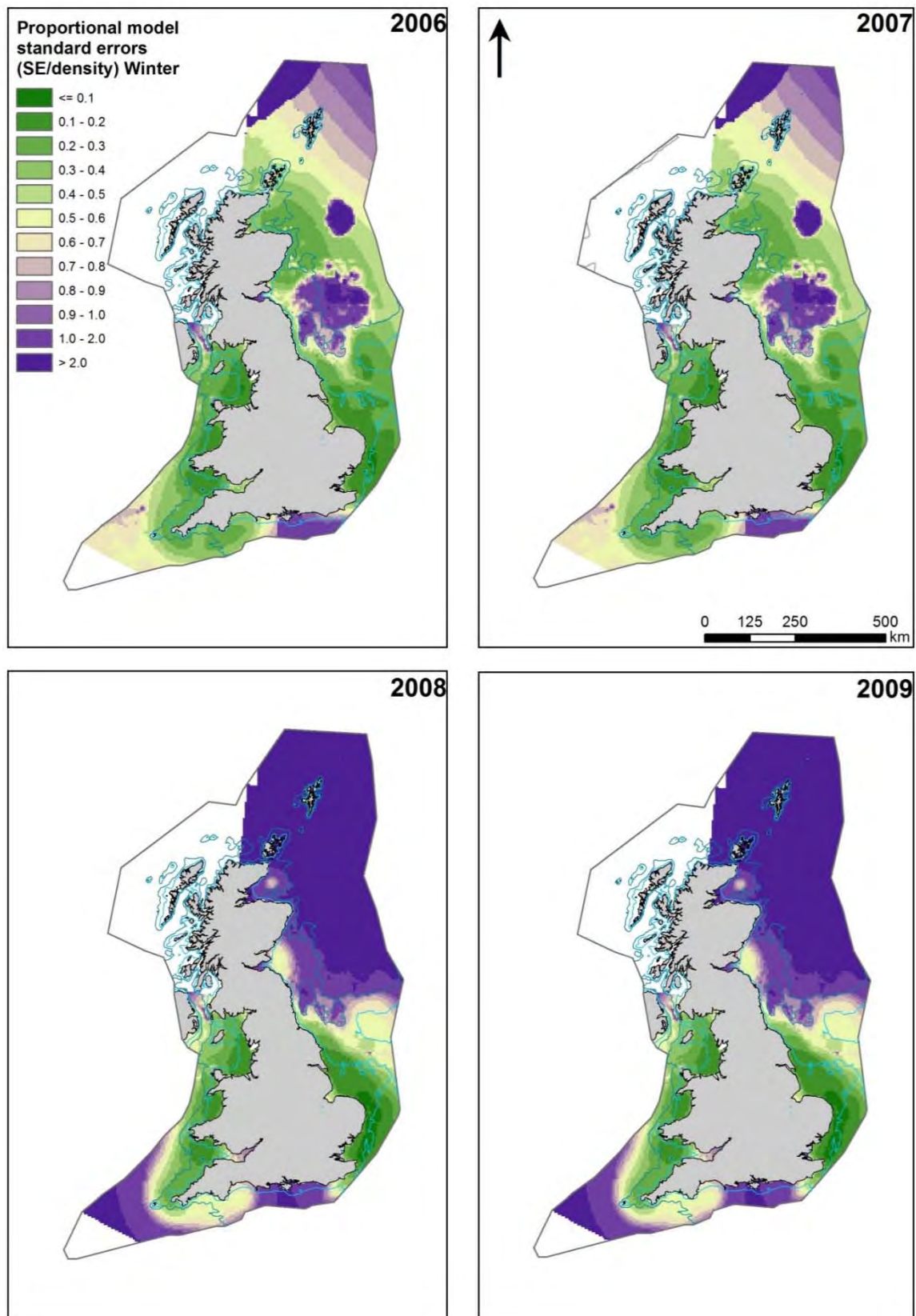**Figure A4.7.** Standard errors on predicted mean densities 2002-2005 (winter)

Figure A4.8. Standard errors on predicted mean densities 2006-2009 (winter)

APPENDIX 5 – Observed presences
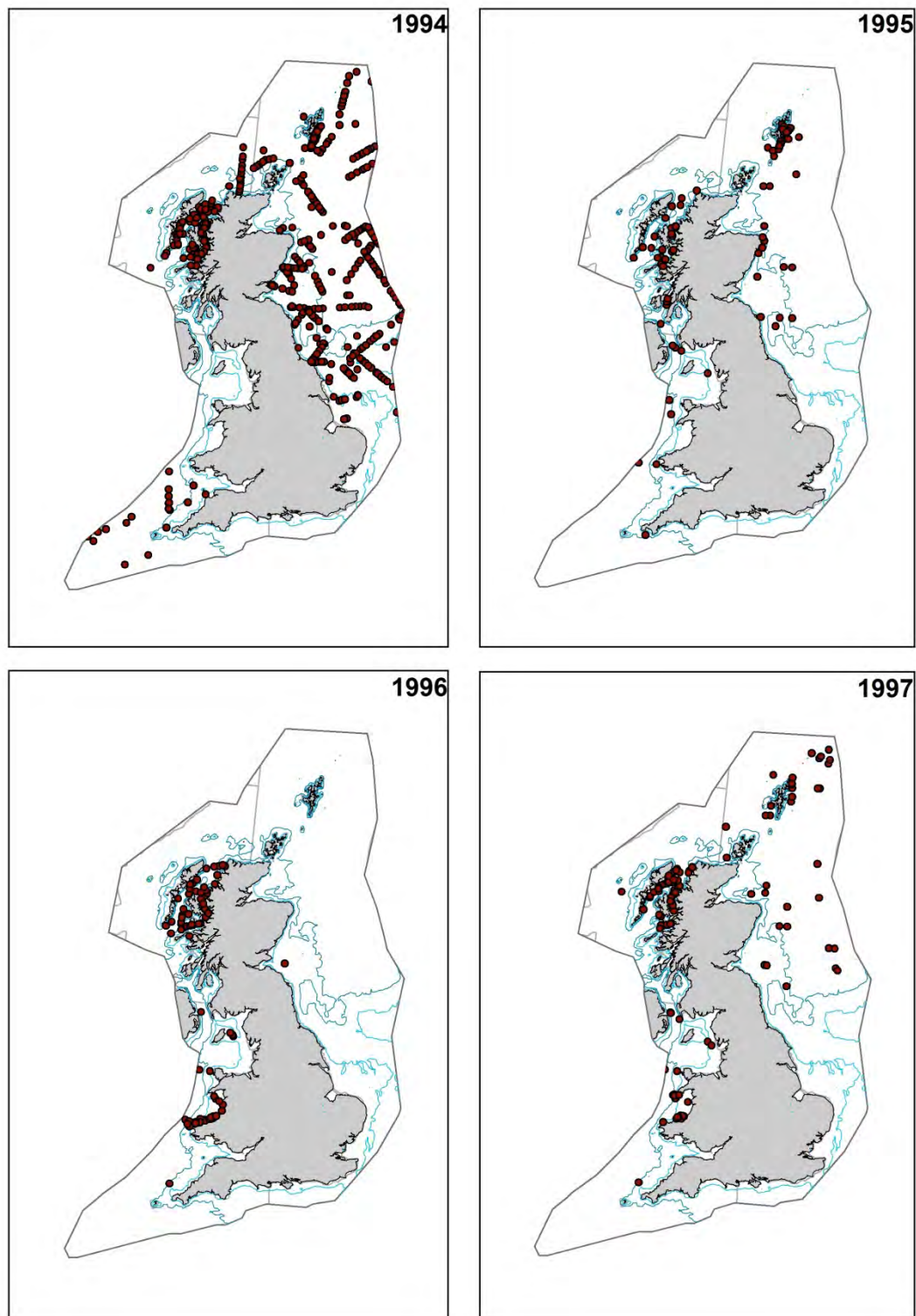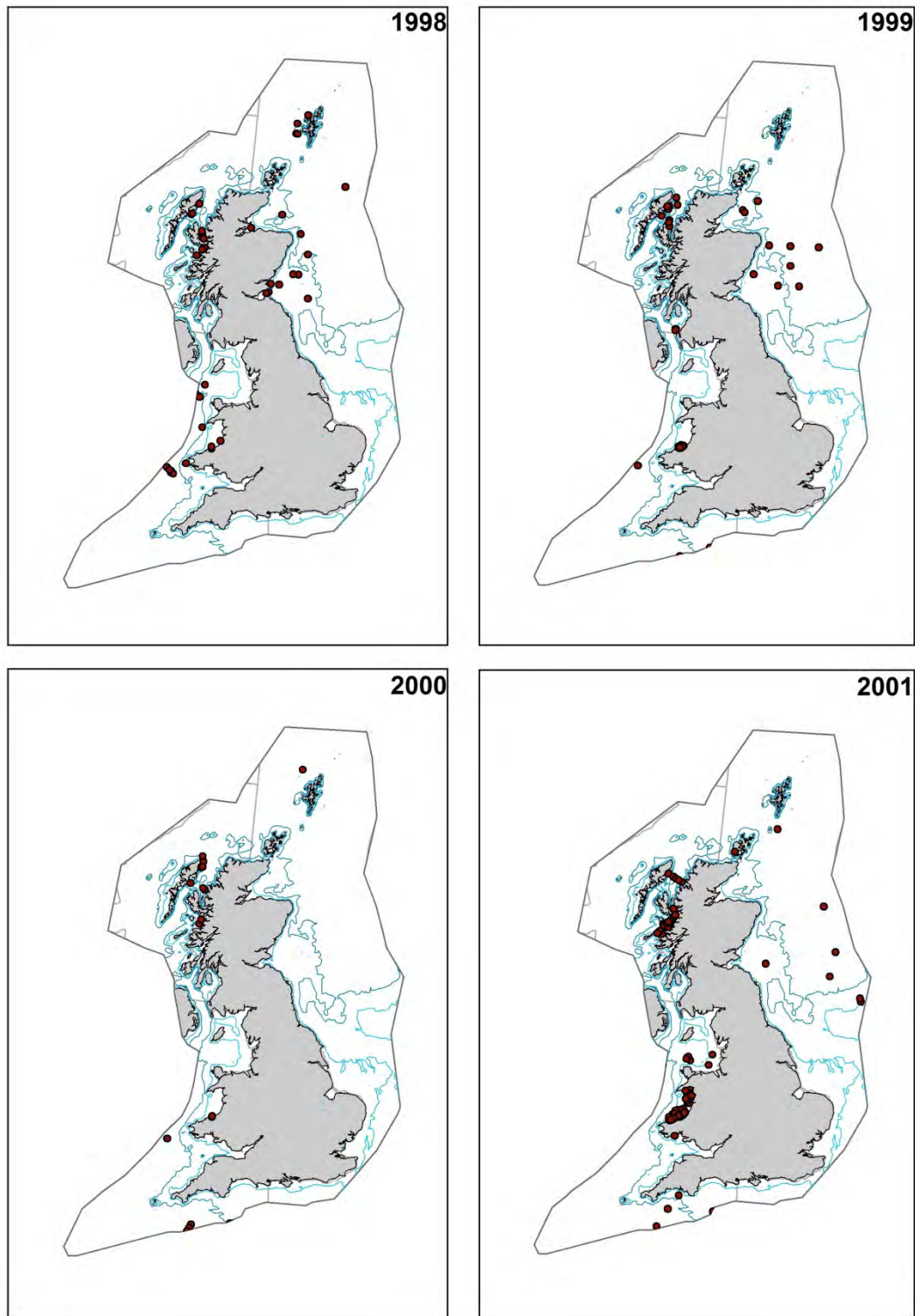

Figure A5.1. Observed presences 1994-1997
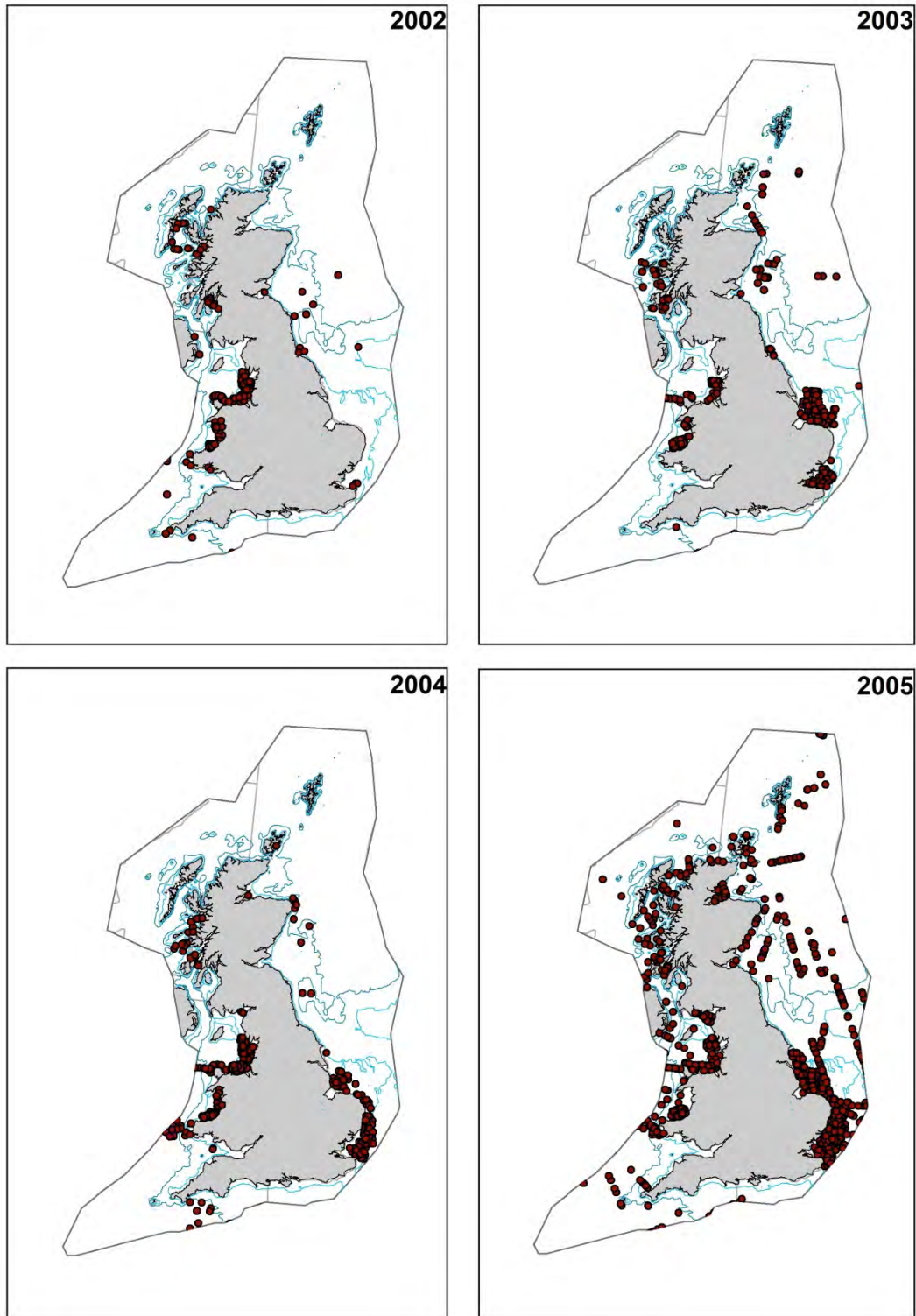
Figure A5.2. Observed presences 1998-2001

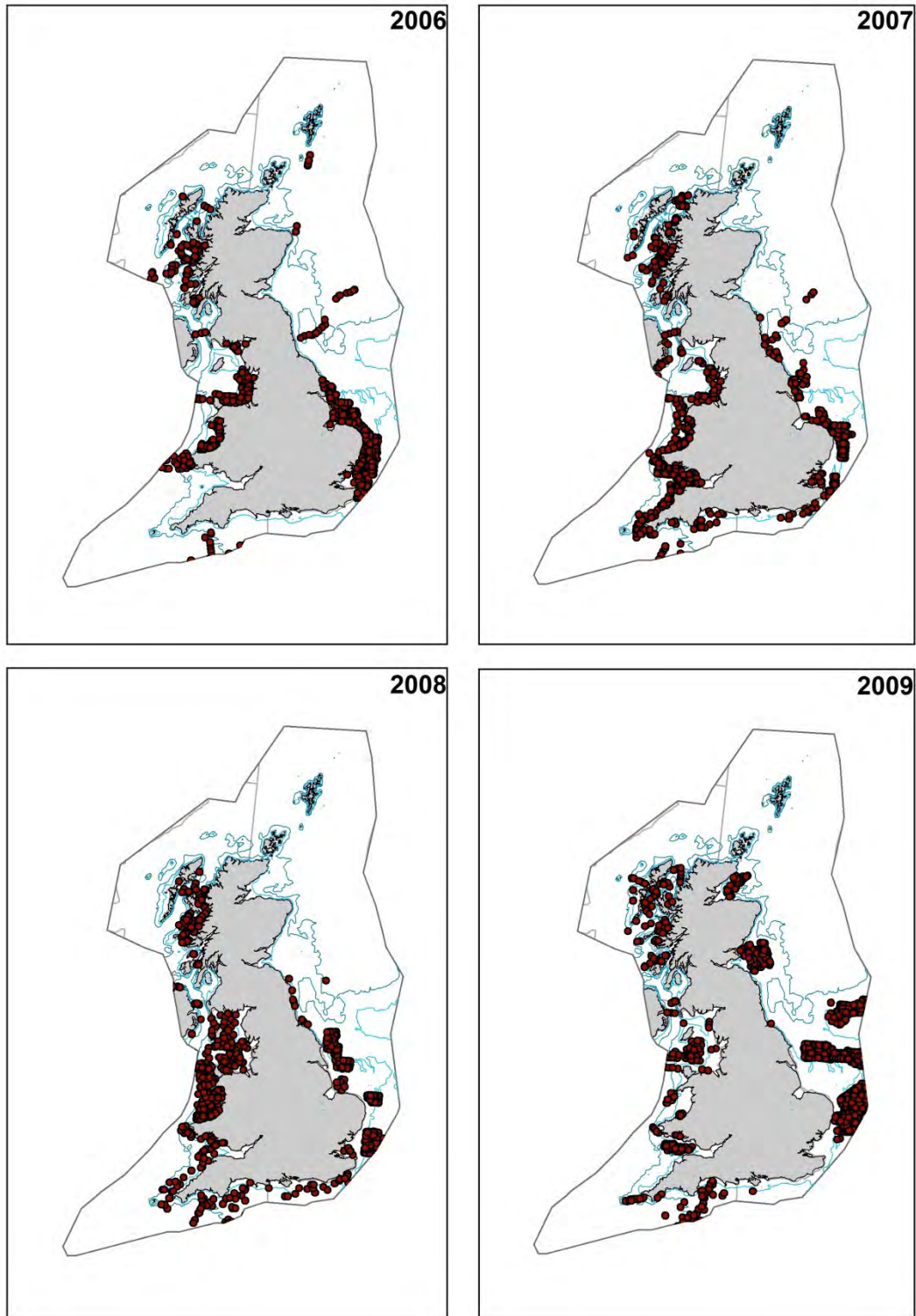**Figure A5.3.** Observed presences 2002-2005
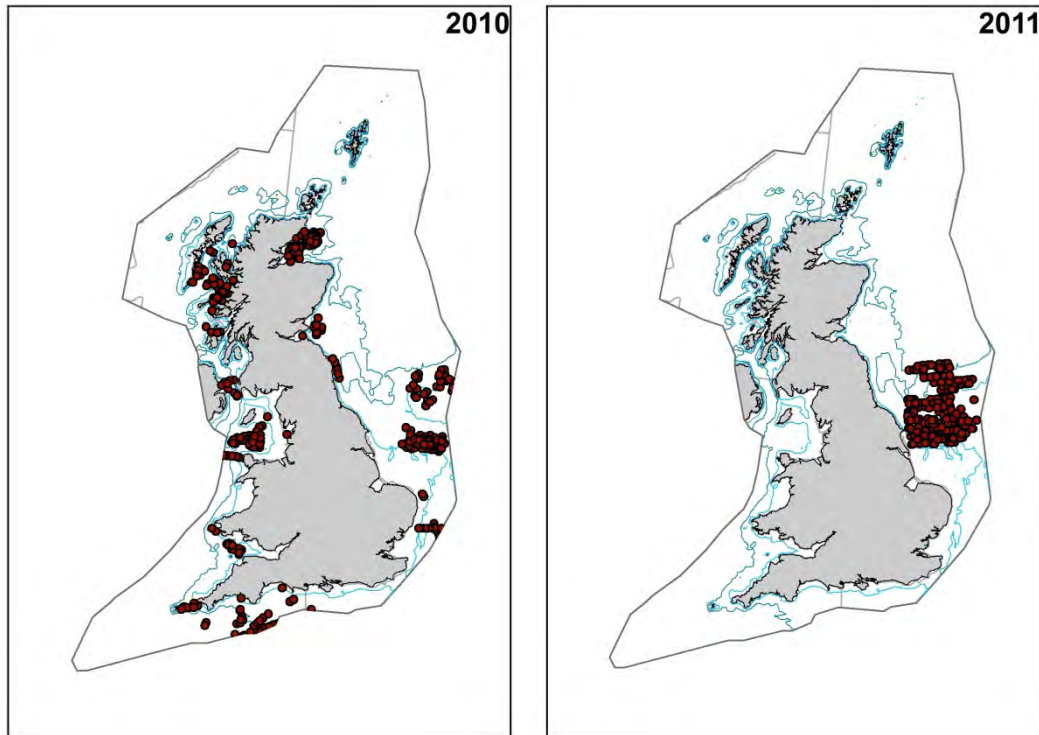
Figure A5.4. Observed presences 2006-2009

Figure A5.5. Observed presences 2010-2011

APPENDIX 6 – R code for annual-seasonal prediction model (example Northwest Scottish waters)

```
#####################################################
##    GAM Harbour Porpoise distribution modelling      ###
##    Region 2 NW Scotland                             ###
#####################################################

# Load data
Data<-read.csv("HP_extracted25jan_all4modelling.csv",header=TRUE, sep=",")
#load yearly prediction files
DeployS94reg2<-read.csv("Deploy_reg2_S94.csv",header=TRUE, sep=",")
DeployS95reg2<-read.csv("Deploy_reg2_S95.csv",header=TRUE, sep=",")
DeployS96reg2<-read.csv("Deploy_reg2_S96.csv",header=TRUE, sep=",")
DeployS97reg2<-read.csv("Deploy_reg2_S97.csv",header=TRUE, sep=",")
DeployS98reg2<-read.csv("Deploy_reg2_S98.csv",header=TRUE, sep=",")
DeployS99reg2<-read.csv("Deploy_reg2_S99.csv",header=TRUE, sep=",")
DeployS00reg2<-read.csv("Deploy_reg2_S00.csv",header=TRUE, sep=",")
DeployS01reg2<-read.csv("Deploy_reg2_S01.csv",header=TRUE, sep=",")
DeployS02reg2<-read.csv("Deploy_reg2_S02.csv",header=TRUE, sep=",")
DeployS03reg2<-read.csv("Deploy_reg2_S03.csv",header=TRUE, sep=",")
DeployS04reg2<-read.csv("Deploy_reg2_S04.csv",header=TRUE, sep=",")
DeployS05reg2<-read.csv("Deploy_reg2_S05.csv",header=TRUE, sep=",")
DeployS06reg2<-read.csv("Deploy_reg2_S06.csv",header=TRUE, sep=",")
DeployS07reg2<-read.csv("Deploy_reg2_S07.csv",header=TRUE, sep=",")
DeployS08reg2<-read.csv("Deploy_reg2_S08.csv",header=TRUE, sep=",")
DeployS09reg2<-read.csv("Deploy_reg2_S09.csv",header=TRUE, sep=",")
DeployS10reg2<-read.csv("Deploy_reg2_S10.csv",header=TRUE, sep=",")
#Check data
dim(Data)
head(Data)

####Extract regional data############################

Data_region2<-subset(Data,subset=Data$Region==2)
Data_region2S<-subset(Data_region2,subset=Data_region2$Season2==1)
Data_region2W<-subset(Data_region2,subset=Data_region2$Season2==0)

##Extract the positive data
Data_reg2_pos<-subset(Data_region2,subset=Data_region2$PA>0)
Data_reg2S_pos<-subset(Data_region2S,subset=Data_region2S$PA>0)
Data_reg2W_pos<-subset(Data_region2W,subset=Data_region2W$PA>0)
hist(Data_reg2_pos$cor_EstDen,breaks =100)
hist(Data_reg2S_pos$cor_EstDen,breaks =100)
hist(Data_reg2W_pos$cor_EstDen,breaks =100)

#######Explore data###########
#Visualise the correlation between variables using a "correlodendrogram"
require(Hmisc)
names(Data)
v<-
varclus(~CG_SM+CS_SM+VortSfoc15+T_s+S_s+Depth5km+Sed5foc15+Ships5km+Slope5
km+Easting+Northing,
```

```
similarity="pearson",data=Data_region2S)
plot(v)

###Have a look at yearly data
library(lattice)
xyplot(Northing ~ Easting | as.factor(Year_),
        data=Data_region2S,
        ylab="latitude", xlab="longitude",
        pch=".",col=1,
        layout=c(5,4),
        par.strip.text = list(cex = 0.75),
        aspect="iso")

xyplot(Northing ~ Easting | as.factor(Year_),
        data=Data_region2W,
        ylab="latitude", xlab="longitude",
        pch=".",col=1,
        layout=c(5,4),
        par.strip.text = list(cex = 0.75))

##-> -> Not enough data for modelling the winter season in region 2
sum(Data_reg2W_pos$PA)

#################################################
####    MODEL FITTING      #####################
####Presence/absence part #####################
#################################################

#Load the mgcv package
require(mgcv)

#############################################
###REGION2#################################
#############################################

#Model including all potentially important predictor variables is first fitted.

Reg2S_PATall3_full<-
gam(PA~s(CG_SM,k=5)+s(VortSfoc15,k=5)+s(CS_SM,k=5)+s(S_s,k=5)+s(T_s,k=5)+s(Dept
h5km,k=5)
        +s(Sed5foc15,k=5)+s(Slope5km,k=5)+s(Ships5km,k=5)+s(SegLenKm,k=5)+s(Eastin
g,Northing,
by=as.factor(Groups3),k=20), family=binomial,data=Data_region2S)
summary(Reg2S_PATall3_full)

#Reduced final model: uninfluential and ecologically unreliable variables dropped. In this
model water depth was #retained as it was regarded as an important variable for predictive
purposes, see more information about #modelling approach in the main report.

Reg2S_PATall3<-gam(PA~s(S_s,k=5)+s(Depth5km,k=3)
        +s(Sed5foc15,k=5)+s(SegLenKm,k=5)+s(Easting,Northing,by=as.factor(Groups3),k=
20),
        family=binomial,data=Data_region2S)
names(Data_region2S)
summary(Reg2S_PATall3)
```

```
plot(Reg2S_PATall3,pers=T,scale=0,all.terms=T,shade=T,page=1)



######################################
########POSITIVE MODEL##############
######################################

names(Data_reg2S_pos)
#Model including all potentially important predictor variables was first fitted.
Reg2S_POSTall3_full<-
gam(cor_EstDen~s(CG_SM,k=5)+s(VortSfoc15,k=5)+s(CS_SM,k=5)+s(S_s,k=5)+s(T_s,k=5
)+s(Depth5km,k=5)
        +s(Sed5foc15,k=5)+s(Slope5km,k=5)+s(Ships5km,k=5)+s(Easting,Northing,by=as.fa
ctor(Groups3),k=20),
        family=Gamma(log),data=Data_reg2S_pos)
summary(Reg2S_POSTall3_full)
plot(Reg2S_POSTall3_full,scale=0,all.terms=T,shade=T,page=1)

#Reduced final model: uninfluential and ecologically unreliable variables dropped.
Reg2S_POSTall3<-gam(cor_EstDen~s(S_s,k=5)+s(Depth5km,k=5)
        +s(Sed5foc15,k=5)+s(Easting,Northing,by=as.factor(Groups3),k=20),
        family=Gamma(log),data=Data_reg2S_pos)

plot(Reg2S_POSTall3,scale=0,all.terms=T,shade=T,page=1)
summary(Reg2S_POSTall3)
gam.check(Reg2S_POSTall3)

######################################
###   GAM PLOT LAYOUT      #############
######################################

require(mgcv)
summary(Reg2S_PATall3)
summary(Reg2S_POSTall3)

#Plot layout
x11(width=7, height=8)
par(mfrow=c(3,3), oma=c(1,1,1,1),pty="s",mar=c(4.5,4.5,1,1))
plot.gam(Reg2S_PATall3,select=1,scale=0,pers=TRUE,all.terms=T,shade=T,xlab="Salinity",
ylab="s(1.995)",cex.lab=1.5, cex.axis=1.3)
plot.gam(Reg2S_PATall3,select=2,scale=0,pers=TRUE,all.terms=T,shade=T,xlab="Depth",y
lab="s(1.784)",cex.lab=1.5, cex.axis=1.3)
plot.gam(Reg2S_PATall3,select=3,scale=0,pers=TRUE,all.terms=T,shade=T,xlab="Sedime
nt",ylab="s(3.860)",cex.lab=1.5, cex.axis=1.3)
plot.gam(Reg2S_PATall3,select=4,scale=0,pers=TRUE,all.terms=T,shade=T,xlab="Segmen
t length",ylab="s(3.841)",cex.lab=1.5, cex.axis=1.3,)
vis.gam(Reg2S_PATall3,view=c("Easting","Northing"),cond=list(Groups3=1),color="topo",ma
in="1994-99 s(17.426)",plot.type="contour")
vis.gam(Reg2S_PATall3,view=c("Easting","Northing"),cond=list(Groups3=2),color="topo",ma
in="2000-05 s(4.879)",plot.type="contour")
vis.gam(Reg2S_PATall3,view=c("Easting","Northing"),cond=list(Groups3=3),color="topo",ma
in="2006-10 s(12.314)",plot.type="contour")

x11(width=7, height=5)
par(mfrow=c(2,3), oma=c(1,1,1,1),pty="s",mar=c(4.5,4.5,1,1))
```

```
plot.gam(Reg2S_POSTall3,select=1,scale=0,pers=TRUE,all.terms=T,shade=T,xlab="Salinit
y",ylab="s(1.878)",cex.lab=1.5, cex.axis=1.3)
plot.gam(Reg2S_POSTall3,select=2,scale=0,pers=TRUE,all.terms=T,shade=T,xlab="Depth"
,ylab="s(1.125)",cex.lab=1.5, cex.axis=1.3)
plot.gam(Reg2S_POSTall3,select=3,scale=0,pers=TRUE,all.terms=T,shade=T,xlab="Sedim
ent",ylab="s(2.392)",cex.lab=1.5, cex.axis=1.3,)
vis.gam(Reg2S_POSTall3,view=c("Easting","Northing"),cond=list(Groups3=1),color="topo",
main="1994-99 s(17.572)",plot.type="contour")
vis.gam(Reg2S_POSTall3,view=c("Easting","Northing"),cond=list(Groups3=2),color="topo",
main="2000-05 s(16.693)",plot.type="contour")
vis.gam(Reg2S_POSTall3,view=c("Easting","Northing"),cond=list(Groups3=3),color="topo",
main="2006-10 s(18.871)",plot.type="contour")


############################################################
##################### EVALUATION SCRIPT###################
############################################################

#####K-FOLD CROSS VALIDATION OF HURDLE MODEL

summary(Reg2S_PATall3)
summary(Reg2S_POSTall3)

#load AUC fuction, by Wintle et al. 2005, available online
source("C:\\Data\\model_functions.R")
require(mgcv)
require(dismo)
set.seed(10)
k<-10
group<-kfold(Data_region2S,k)
group[1:10]
unique(group)
e<-list()
e2<-list()
for (i in 1:k){
        train<-Data_region2S[group !=i,]
        test<-Data_region2S[group ==i,]

                #binomial model
                model1<-gam(PA ~ s(S_s, k = 5) + s(Depth5km, k = 3) + s(Sed5foc15, k = 5)
+
                 s(SegLenKm, k = 5) + s(Easting, Northing, by = as.factor(Groups3),
                k = 20)
                ,family=binomial,data=train)

                #positive model
                model2<-gam(cor_EstDen ~ s(S_s, k = 5) + s(Depth5km, k = 5) +
s(Sed5foc15,
                k = 5) + s(Easting, Northing, by = as.factor(Groups3), k = 20)
                ,family=Gamma(log),data=subset(train,subset=train$cor_EstDen>0))

                #predictions
                preds<-
(predict(model1,test,type="response"))*(predict(model2,test,type="response"))
                preds2<-predict(model1,test,type="response")
                e[[i]]<-cor(test$cor_EstDen, c(preds,recursive=TRUE),method="spearman")
```

```
                    e2[[i]]<-roc(test$PA, c(preds2,recursive=TRUE))
                    }

e
mean(unlist(e))
e2
mean(unlist(e2))

#########################################################################
### Check SPATIAL AUTOCORRELATION IN RESIDUALS using a variogram ###
#########################################################################

library(gstat)
library(spdep)
#presence/absence part
resid<-residuals(Reg2S_PATall3,type="p")
mydata_pa<-data.frame(resid,Data_region2S$Easting,Data_region2S$Northing)
names(mydata_pa)
coordinates(mydata_pa)<-c("Data_region2S.Easting","Data_region2S.Northing")
Vario_pa<-variogram(resid~1,mydata_pa,width=10000)
plot(Vario_pa)

#positive part
resid_pos<-residuals(Reg2S_POSTall3,type="p")
mydata_pos<-data.frame(resid_pos,Data_reg2S_pos$Easting,Data_reg2S_pos$Northing)
coordinates(mydata_pos)<-c("Data_reg2S_pos.Easting","Data_reg2S_pos.Northing")
Vario_pos<-variogram(resid_pos~1,cutoff=100000,mydata_pos)
plot(Vario_pos)

##########################
#########PREDICTIONS#####
##########################

#function for combining predictions and SEs from presence/absence and positive model
parts and export as csv

export.gam.pred<- function(PAmodel,POSmodel,deploy_file,outfile) {
        PA_pred<-predict(PAmodel,deploy_file,type="response",se.fit=TRUE)
        Pos_pred<-predict(POSmodel,deploy_file,type="response",se.fit=TRUE)
        Comb_pred<-PA_pred$fit*Pos_pred$fit
        Comb_var<-sqrt(PA_pred$fit^2*Pos_pred$se.fit^2+
        Pos_pred$fit^2*PA_pred$se.fit^2+PA_pred$se.fit^2*Pos_pred$se.fit^2)
        deploy_file$p_dens<-Comb_pred
        deploy_file$p_densSE<-Comb_var
        deploy_file$DpropSE<-Comb_var/Comb_pred
        deploy_file$prob<-PA_pred$fit
        deploy_file$probSE<-PA_pred$se.fit
        deploy_file$PpropSE<-PA_pred$se.fit/PA_pred$fit
        write.csv(deploy_file,outfile,row.names=FALSE)
        }
#Add factor variable defining time period
DeployS94reg2$Groups3<-1
DeployS95reg2$Groups3<-1
DeployS96reg2$Groups3<-1
DeployS97reg2$Groups3<-1
```

```
DeployS98reg2$Groups3<-1
DeployS99reg2$Groups3<-1
DeployS00reg2$Groups3<-2
DeployS01reg2$Groups3<-2
DeployS02reg2$Groups3<-2
DeployS03reg2$Groups3<-2
DeployS04reg2$Groups3<-2
DeployS05reg2$Groups3<-2
DeployS06reg2$Groups3<-3
DeployS07reg2$Groups3<-3
DeployS08reg2$Groups3<-3
DeployS09reg2$Groups3<-3
DeployS10reg2$Groups3<-3
```

```
#Execute the prediction function for each year
export.gam.pred(Reg2S_PATall3,Reg2S_POSTall3,DeployS94reg2,outfile="preds94S_gamT1all_reg2.csv")
export.gam.pred(Reg2S_PATall3,Reg2S_POSTall3,DeployS95reg2,outfile="preds95S_gamT1all_reg2.csv")
export.gam.pred(Reg2S_PATall3,Reg2S_POSTall3,DeployS96reg2,outfile="preds96S_gamT2all_reg2.csv")
export.gam.pred(Reg2S_PATall3,Reg2S_POSTall3,DeployS97reg2,outfile="preds97S_gamT2all_reg2.csv")
export.gam.pred(Reg2S_PATall3,Reg2S_POSTall3,DeployS98reg2,outfile="preds98S_gamT2all_reg2.csv")
export.gam.pred(Reg2S_PATall3,Reg2S_POSTall3,DeployS99reg2,outfile="preds99S_gamT2all_reg2.csv")
export.gam.pred(Reg2S_PATall3,Reg2S_POSTall3,DeployS00reg2,outfile="preds00S_gamT3all_reg2.csv")
export.gam.pred(Reg2S_PATall3,Reg2S_POSTall3,DeployS01reg2,outfile="preds01S_gamT3all_reg2.csv")
export.gam.pred(Reg2S_PATall3,Reg2S_POSTall3,DeployS02reg2,outfile="preds02S_gamT3all_reg2.csv")
export.gam.pred(Reg2S_PATall3,Reg2S_POSTall3,DeployS03reg2,outfile="preds03S_gamT3all_reg2.csv")
export.gam.pred(Reg2S_PATall3,Reg2S_POSTall3,DeployS04reg2,outfile="preds04S_gamT3all_reg2.csv")
export.gam.pred(Reg2S_PATall3,Reg2S_POSTall3,DeployS05reg2,outfile="preds05S_gamT3all_reg2.csv")
export.gam.pred(Reg2S_PATall3,Reg2S_POSTall3,DeployS06reg2,outfile="preds06S_gamT4all_reg2.csv")
export.gam.pred(Reg2S_PATall3,Reg2S_POSTall3,DeployS07reg2,outfile="preds07S_gamT4all_reg2.csv")
export.gam.pred(Reg2S_PATall3,Reg2S_POSTall3,DeployS08reg2,outfile="preds08S_gamT5all_reg2.csv")
export.gam.pred(Reg2S_PATall3,Reg2S_POSTall3,DeployS09reg2,outfile="preds09S_gamT5all_reg2.csv")
export.gam.pred(Reg2S_PATall3,Reg2S_POSTall3,DeployS10reg2,outfile="preds10S_gamT5all_reg2.csv")
```